PhD Dissertation

Transformation of CO_2 into High Performance Polyhydroxyurethane Adhesives and Coatings

Satyannarayana PANCHIREDDY

PhD. Dissertation

Transformation of CO_2 into High Performance Polyhydroxyurethane Adhesives and Coatings

Submitted by

Satyannarayana PANCHIREDDY

Under the supervision of

Prof. Christine JÉRÔME, Promoter

Dr. Christophe DETREMBLEUR, Co-Promoter

This Dissertation has been Approved by the Promoters and Board of Jury Members is as Follows:

Prof. Christine JÉRÔME	University of Liege (*Promoter*)
Dr. Christophe DETREMBLEUR	University of Liege (*Co-promoter*)
Dr. Sylvain CAILLOL	University of Montpellier
Prof. Jean-Marie RAQUEZ	University of Mons
Dr. Kevin MATHIEU	CRM Group, Liege
Dr. Jean-Michel THOMASSIN	University of Liege (*Secretary*)
Prof. Anne-Sophie DUWEZ	University of Liege (*President*)

DECLARATION

I hereby declare that the content of the thesis "***Transformation of CO_2 into high performance polyhydroxyurethane adhesives and coatings***" is my own research work done under supervision of Prof. Christine Jérôme (promoter) and Dr. Christophe Detrembleur (co-promoter) at University of Liége, Belgium. I further declare that this work has not been previously submitted at any other University for any other degree. I have exercised reasonable care to ensure that the work is original, not been taken from the work of others and not copied from the published source (except the references, standard mathematical equations/formulations, protocols etc). The university may take action if the information provided is found inaccurate at any stage.

Faculty of Sciences
University of Liege
Belgium
Date: 30-08-2018

Satyannarayana PANCHIREDDY
Reg No: s147379

Verified by

Dr. Bruno GRIGNARD
Dr. Jean-Michel THOMASSIN
Dr. Christophe DETREMBLEUR
Prof. Christine JÉRÔME

SUMMARY

Today, adhesive bonding is a widespread technology many fields including automotive, aeronautic, surgery, packaging, electronic devices or in the building sector. It enables designing novel (lightweight) materials/products with performances comparable to the ones of systems fixed by mechanical adhesion. Glues, adhesives exist as a large variety of compositions such as cyanoacrylates (superglue ®), (meth)acrylate or epoxy resins, polyesters, polyurethanes… that fit on-demand to the specificity of the glued assembly (nature of the substrate, the thermo-mechanical performances, the resistance against water, acids, bases or solvents…). Due to their easy tunable and versatile properties (soft and flexible to rigid materials, high bonding adhesion, compatibility with numerous substrates…) polyurethanes (PUs) are reference systems. PUs are produced from toxic isocyanates that cause severe health concerns (asthma, skin irritation, DNA mutation). To surpass these issues, the quest for novel isocyanate-free PUs glues and adhesives formulations is essential. This thesis responds to this current trend which aims to develop well-designed innovative sustainable PU adhesives (and coatings) free of isocyanates. It explores the potential of poly(hydroxyurethane)s (PHU) made by step-growth polymerization of CO_2-sourced bis- or multi-functional cyclic carbonates with di- or polyamines to construct novel PU glues/adhesives for various substrates (metals, wood, glass, plastics). Three main research axes were investigated and focused i) on the establishment of solvent-free petro-based PHU formulations and their corresponding nanocomposites thermoset PHUs (native or functional silica or ZnO fillers) to tailor high performance adhesives for various substrates; ii) on the increase of the sustainability of the PHU nanocomposites glues by incorporation of renewable monomers (vegetable oils) within the formulations and iii) the development of biomimetic PHU glues inspired from mussels (incorporation of dopamine). All formulations were benchmarked with commercial Terpmix-6700 and Araldite®2000 PU glues and results highlight that these PHU glues represent promising and competitive alternatives to conventional PU glues prepared from the toxic isocyanate chemistry. We believe that this work opens a realistic route to the next generation of PU adhesives.

RESUME

Aujourd'hui, le collage est une technologie largement répandue dans notre quotidien dans divers secteurs comme l'automobile, l'aéronautique, la chirurgie, l'emballage, l'électronique ou le bâtiment… Il permet de concevoir des matériaux / produits innovants avec des performances comparables à celles de systèmes fixés mécaniquement (vis, soudure…). Les colles/adhésifs existent sous une grande variété de compositions (cyanoacrylates (superglue ®), résines (méth)acrylates ou époxydes, les polyesters, les polyuréthanes...) qui répondent aux spécificités de l'assemblage collé (performances mécaniques, résistance à l'eau, aux acides, aux bases ou aux solvants ...). Grâce à leurs propriétés facilement modulables (matériaux souples à rigides, adhérence élevée, compatibilité avec de nombreux substrats ...), les polyuréthanes (PU) sont des systèmes de référence. Les PU sont produits à partir d'isocyanates toxiques qui causent de graves problèmes de santé (asthme, irritation cutanée, mutation de l'ADN). Pour dépasser ces problèmes, la recherche de nouvelles formulations de colles et d'adhésifs sans isocyanate est essentielle. Cette thèse répond à cette tendance actuelle qui vise à développer des adhésifs PU (et revêtements) durables, innovants et exempts d'isocyanates. Elle explore le potentiel des poly(hydroxyuréthanes)s (PHU) obtenus par polymérisation par étape de carbonates cycliques di- ou multifonctionnels dérivés du CO_2 avec des di- ou polyamines pour construire de nouvelles colles/adhésifs PU pour divers substrats (métaux, bois, verre, plastiques). Trois axes de recherche principaux ont été étudiés et se sont focalisés sur: i) la mise au point de formulations de PHU sans solvant et de leurs nanocomposites (charges de silice ou de ZnO natives ou fonctionnelles) pour élaborer des adhésifs à hautes performances pour différents substrats; ii) l'accroissement de la durabilité des colles PHU nanocomposites par incorporation de monomères issus de ressources renouvelables (huiles végétales) dans les formulations et iii) le développement de colles PHU biomimétiques inspirées des moules (incorporation de dopamine). Toutes les formulations ont été comparées avec des colles PU commerciales (Terpmix-6700 et Araldite®2000) et les résultats soulignent que ces colles PHU représentent des alternatives prometteuses et compétitives aux colles PU classiques préparées à partir de la chimie des isocyanates toxiques. Nous pensons que ce travail ouvre une voie réaliste à la conception de la prochaine génération d'adhésifs PU.

ACKNOWLEDGEMENTS

I would like to express my heartfelt gratitude to all the people who have helped me in various manners during this project and without whom I would not have been able to finish this thesis in that form. I earnestly thank each and every one of them for supporting me throughout.

I would like to express my special appreciation and thanks to Prof. Christine Jérôme and Dr. Christophe Detrembleur for accepting me as PhD student, supervising and supporting me during my thesis. First and foremost, the financial supports, FLYCOAT Excellence PhD program and University of Liege for the completion of my thesis are greatly appreciated. I could not have imagined having a better promoter and co-promoter for my PhD thesis.

I would like to express my deepest gratitude to my co-promoter Dr. Christophe Detrembleur for his valuable suggestions, unwavering support, inspiration and comments that helped in improving quality of work, writing skills, encouraging my research to develop state-of-the-art materials. He gave me the unique opportunity to realize my thesis work by putting them into a realistic frame.

I would like to extend my appreciation to Prof. Christine Jérôme for her support, taking care, encouragement and patience. Thanks for guiding me towards right path. You are fantastic mentor that is worthy of emulation. Thank you also for inviting me out for the Christmas celebration at your place, it was my first time to celebrate in my life.

Special thanks to Bruno Grignard for guiding in a good direction, sharing ideas, available for discussions, improving research environment, correcting my articles and took care of my thesis more than mentor, even though you had very tight schedule. Without your support it would have been difficult for me to frame my thesis on time. You are real inspiration for me, to write projects, leading multiple projects while collaborating with others. I'm also thankful to Jean-Michel Thomassin who involved during analysis, concerning rheology and correcting my articles.

I am very much glad for being a part of the CERM family! I have spent more time with the CERM members than my family. This work would never be possible without help from a great people in the CERM. The lovely and always cooperative atmosphere in our lab was certainly inspired by Sophie, Enza, Valérie, Martine, Laetitia, Charlotte, Grégory. Always-ready to help mentality of yours will remain in my heart forever and will be respected incessantly. Many, thanks to Philip.L, Antoine, Raphael, Bruno, Jean Michel, Abdel, Farid, Cedric, Zyenep, Stephanie, Daniela, Mathilde, Thomas, Kevin, Jeremy[1], Sandro, Walid, Philip.S, Stephan, Hirotaka, Mohammed, Rahmet, Assala, Maxime, Jamal, Vidya, Pierre, Jeremy[2] for an excellent working environment, help in practical and personal matter, and many interesting discussions about all the possible topics. Finally, thanks to Urmil for being special, helping me during my work, coffee breaks, sharing funny memories. All of you are truly unique, and it is hard to find people like you in some other places. It was nice memory of playing volleyball with positive working energy.

Thanks to Nagaraj, it was nice memories from IISER-K. Unexpectedly we met in Belgium. I never felt that I'm far away from home. We had a great time being here, helping me out in experiments, sharing ideas, happiness and sadness, travelling, funny moments. I am happy for you, eventually you got good opportunity in Spain.

I would to like to acknowledge my deepest appreciation to my best friends ever from Leuven: Remi, Veysi, and Nithya. If I could speak out about our times then I need to write one full book chapter. Thanks for being special, sharing happiness and sadness, organizing activities, unforgettable Italian, Turkish and Indian cuisine. Thanks to Remi family, always it feels like my home, best food ever, barbecue under rain, cooking pasta with fish bones, hiking in dolomites, eating food for hours then think about next meal…

Thanks for being so special!! Satya.CM, I must be very lucky to have a friend like you. You know very well when I face a problem and helped with them, cares, scolds and teases.

Thanks to Indians in liege, Anil, Ravi family, JoJo, Satya[b], Kishore, Vinayak, bikram...I am particularly thankful to Srikanth, Keerthana, Nakshitha being a part of family. I really miss you all.

I am very thankful to Prof. Raja Shunmugam and IISER-K friends and colleagues: Vijay, Naidu, Shiva, Santhu, Pawan, Amar, Kamal, Sunirmal, Saswati, brammi, Ramesh, Ramakrishna[1,2], Ramesh, Pavan.V, Kishore, for sharing workplace, having fun during my stay in Kolkata.

I would like to thank to Prof. Ashwini nangia, Prof. Mariappan Periasamy and University of Hyderabad, School chemistry friends and colleagues. Special thanks to Mahesh, Daya, Praveen, Sada, Rafi, Baskar, Siddu, Sampat…..I'm looking forward to see you all.

Thanks for giving me freedom, being support and encouragement from my parents though they're not educated but they know much better than educated people. I cannot express my gratefulness in words to them. Thanks to my brother, always being special and understanding my situations.

Last but not least, I would like to thank the jury members *Prof. Christine JÉRÔME, Dr. Christophe DETREMBLEUR, Dr. Sylvain CAILLOL, Prof. Jean-Marie RAQUEZ, Dr. Kevin MATHIEU Dr. Jean-Michel THOMASSIN, Prof. Anne-Sophie DUWEZ,* for accepting to examine and evaluate my thesis and being a part of my defense.

Thank you all.

Merci Beaucoup

आप सभी को धन्यवाद।

అందరికి ధన్యవాదాలు

"Thesis is Dedicated to My Beloved Parents

Grandparents (Late)

For Their Love, Support and Freedom for My Studies"

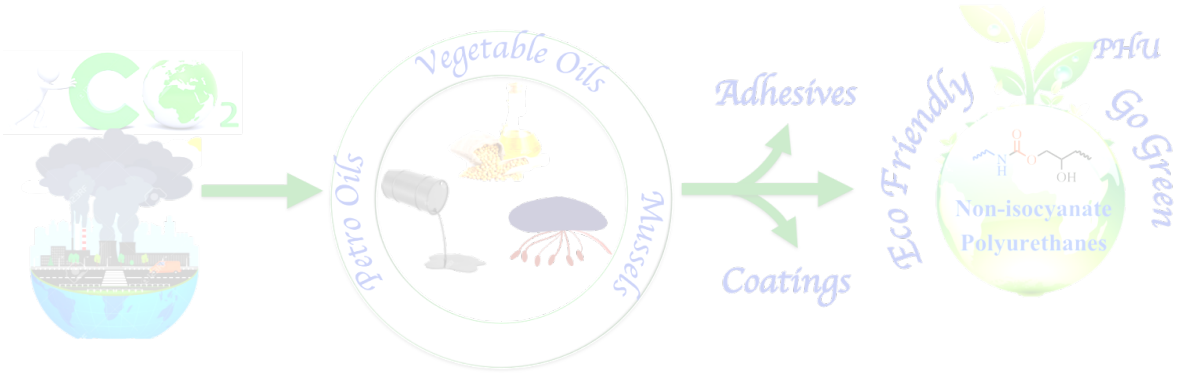
CO2
Vegetable Oils
Petro Oils
Mussels
Adhesives
Coatings
Eco Friendly
PHU
Go Green
Non-isocyanate
Polyurethanes

PUBLICATIONS[1–3]

(1) Satyannarayana Panchireddy; Thomassin, J.-M.; Grignard, B.; Damblon, C.; Tatton, A.; Jerome, C.; Detrembleur, C. Reinforced Poly(Hydroxyurethane) Thermosets as High Performance Adhesives for Aluminum Substrates. ***Polym. Chem.*** **2017**, *8* (38), 5897–5909.

(2) Satyannarayana Panchireddy; Grignard, B.; Thomassin, J.-M.; Jerome, C.; Detrembleur, C. Bio-Based Poly(Hydroxyurethane) Glues for Metal Substrates. ***Polym. Chem.*** **2018**, *9* (19), 2650–2659.

(3) Satyannarayana Panchireddy.; Grignard, B.; Thomassin, J.-M.; Jerome, C.; Detrembleur, C. Catechol Containing Polyhydroxyurethanes as High Performance Coatings and Adhesives. ***ACS Sustain. Chem. Eng.*** **2018,** acssuschemeng.8b03429.

AWARDS

(1) Received "**Young Researcher Award**" for the *design, Innovation and Sustainability of polyhydroxyurethane adhesives from renewable resources* at the Euro Green Chemistry 2018, Dublin, Ireland.

(2) Received "**Best Poster award"** for the presentation of "*Sustainable polyhydroxyurethane thermoset adhesives for affixing metals*" at the Euro Green Chemistry 2018, Ireland.

ORAL COMMUNICATIONS

- S.Panchireddy, B.Grignard, J-M.Thomassin, C.Jerome, C.Detrembleur* ***"Sustainable poly(hydroxyurethane)s thermoset adhesives for affixing metals"*** June-2018, Green chemistry and technology, Dublin, Ireland.

- S.Panchireddy, B.Grignard, J-M.Thomassin, C.Jerome, C.Detrembleur* ***"High performance poly(hydroxyurethane)s thermoset adhesives"*** June-2018, Polymers and Organic Chemistry (POC), France.

- S.Panchireddy, B.Grignard, J-M.Thomassin, C.Jerome, C.Detrembleur ***"From CO2 to high-performance adhesives for affixing metal substrates"*** May-2018, Belgian Polymer Group (BPG), Belgium.

- S.Panchireddy, B.Grignard, J-M.Thomassin, C.Jerome, C.Detrembleur "From ***CO2 to high performance urethane adhesives"*** **July-2017,** Department day, University of liege.

POSTER PRESENTATIONS

- S.Panchireddy, B.Grignard, J-M.Thomassin, C.Jerome, C.Detrembleur* ***"High performance poly(hydroxyurethane)s thermoset adhesives"*** June-2018, Polymers and Organic Chemistry (POC), France.

- S.Panchireddy, B.Grignard, J-M.Thomassin, C.Jerome, C.Detrembleur* ***"Sustainable poly(hydroxyurethane)s thermoset adhesives for affixing metals"*** June-2018, Green chemistry and technology, Ireland.

- S.Panchireddy, B.Grignard, J.-M.Thomassin, CJérôme, C.Detrembleur ***"Reinforced poly(hydroxyurethane) coatings and high performance adhesives"*** May-2017: Belgian Polymer Group (BPG), Belgium.

- S.Gennen, S.Panchireddy, B.Grignard, J.-M.Thomassin, C.Jérôme, C.Detrembleur ***"Bio- and CO_2 sourced polyhydroxyurethanes for hydrogels, coatings, foams and high-performance adhesives"*** June-2017, CESAM, Liege.

- S.Panchireddy[a], B.Grignard[a], J-M Thomassin[a], A.renaud[b], M.Olivier[b], M.Poorteman[b], C.Detrembleur[a], C.Jérôme[a] ***"Non-isocyanate polyurethanes (NIPUs) coatings for corrosion protection of metal surfaces"*** May-2016: Belgian Polymer Group (BPG), Belgium.

- S.Panchireddy[a], B.Grignard[a], J-M Thomassin[a], A.renaud[b], M.Olivier[b], M.Poorteman[b], C.Detrembleur[a], C.Jérôme[a] ***"Novel promising way to synthesise Non-isocyanate polyurethanes (NIPUs) for innovative coating applications against corrosion protection of metal surfaces"*** *October-2016: Société Royale de Chimie (SRC)*

- S.Panchireddy[a], B.Grignard[a], J-M Thomassin[a], A.renaud[b], M.Poorteman[b], C.Detrembleur[a], C.Jérôme[a] ***"Efficiently crosslinkined non-isocyanate polyurethane (NIPU) coatings for corrosion protection of metal surfaces"*** July-2016: Department day, Liege.

- S.Panchireddy[a], B.Grignard[a], J-M Thomassin[a], A.renaud[b], M.Olivier[b], M.Poorteman[b], C.Detrembleur[a], C.Jérôme[a] ***"Environmentally friendly bio-based non-isocyanate polyurethane (NIPU) coatings for corrosion protection of metal surfaces"*** September-2016: IAP meeting, Liege.

- S.Panchireddy, S.Gennen, B.Grignard, J-M.Thomassin, C.Detrembleur, C.Jérôme ***"Synthesis and characterization of novel bio and CO_2 sourced polymers for innovative coating applications"*** June-2015: University of Mons.

List of Abbreviations and Symbols

Abbreviation	: Name
Acronyms	
NIPU	: Non-isocyanate polyurethane
PHU	: Poly(hydroxyurethane)
PU	: Polyurethane
REACH	: Registration, Evaluation, Authorization and Restriction of chemicals
ROP	: Ring-opening polymerization
Catalysts	
DBCO	: 1,4-Diazabicyclo[2.2.2]octane
DBU	: 1,8-Diazabicyclo [5.4.0] undec-7-ene
HFIB	: 1,3-Bis(2-hydroxyhexafluroisopropyl) benzene
HFIP	: Hexafluroisopropanol
PTSA	: P-toluene sulphonic acid
TBAB	: Tetrabutylammonium bromide
TBAI	: Tetrabutylammonium iodide
TEA	: Triethylamine
Cyclic carbonates	
BACC	: 2,2-bis(1,3-dioxolane-2-one-4ylmethoxyphenyl)propane
BADGC	: Bisphenol-A diglycidyl cyclic carbonate
CBGPPO	: Bis-cyclic carbonate linked by a triphenylphosphine
CC-NC-514	: Cyclic carbonate based NC-514 (cardanol based CC)
C-GY	: Cyclic carbonate derivative bisphenol-A
CMPC	: (2-oxo-1,3-dioxolan-4-yl)methyl phenyl carbonate
CNSL	: Cashew nut shell liquid
CPPG	: Propylene glycol diglycidylcarbonate
CSBO	: Carbonated soybean oil
CTEFA	: Cyclic carbonated tris-2-hydroxy ethyl isocyanurate ester of fatty acid
DPA-BisCC	: Diphenolic acid-based bis(cyclocarbonate)
GAC	: Gallic based cyclic carbonate
GGC	: Glycerol glycidyl ether based cyclic carbonate

LC	: Limonene dicyclocarbonate
PC	: Propylene carbonate
PGC	: Pentaerythritol glycidyl ether cyclic carbonate
RBC	: Rosin based cyclic carbonate
STC	: Sorbitol tricarbonate
TMPTC	: Trimethylol propane tricyclic carbonate
VEC	: Vinyl ethylene carbonate
VEC-VV9	: Vinyl ethylene carbonate-vinyl neodecanoate
VEC-VV10	: Vinyl ethylene carbonate- vinyl neononanoate
VOPC	: 3-(2-vinyloxyethoxy)1,2-propylene carbonate
VOPC-MI	: Poly[3-(2-vinyloxyethoxy)-1,2-propylene carbonate-*co*-*N*-phenyl-maleimide]

Amines

AEPP	: Aminoethylpiperazine
BAA	: Bis(2-aminoethyl)amine
BDA	: 1,4-Diaminobutane
CBMA	: 1,3-cyclohexanebis(methylamine)
DAP	: 1,5-Diaminopentane
DETA	: Diethylenetriamine
DDA	: 4,9-dioxa-1,12-dodecane diamine
DDDM	: 4,4’-diamino-3,3’-dimethyldiphenyl methane
DDM	: Diaminodiphenylmethane
DMDA	: 1,10-diaminodecane
D-230	: Jeffamine®D-230 polyetheramine
EDA	: 1,2-ethylene diamine
EDR-148	: Jeffamine®EDR-148 polyetheramine
ETA	: Ethanolamine
HMDA	: Hexamethylene diamine
IPDA	: Isophorone diamine
MPE	: 2-methyl-1,5-pentanediamine
MXDA	: m-Xylylenediamine

PEI	: Polyethylene imine
PDA	: 1,4-Diaminopropane
PDMS	: α,ω–(3-aminopropyl) polydimethylsiloxane, 3-(dimethyl-amino)-1-propylamine,
TEAE	: Tris(2-aminoethyl)amine
TMHMDA	Trimethyl hexamethylene diamine
T-403	: Jeffamine®T-403 polyetheramine
Acrylates	
AHM	: 3-acryloyloxy-2-hydroxypropyl methacrylate
TPGDA	: Tripropylene glycol diacrylate
Additives	
BADGE	: Bisphenol A diglycidylether
BGPPO	: Bis(4-glycidyloxy phenyl)phenyl phosphine oxide
CC-ZnO	: Cyclic carbonate functionalized ZnO
CC-SiO2	: Cyclic carbonate functionalized SiO_2
C-GPTMS	: (4-((3-(trimethoxysilyl)propoxy)methyl)-1,3-dioxolan-2-one
C-POSS	: Cyclic carbonate-functionalized polyhedral oligomeric silsesquioxanes
DER®324	: Monofunctional epoxide reactive diluent
DOP	: 3,4-dihydroxyphenyl-L-alanine
EPON®828	: Bisphenol-A diglycidyl ether epoxy precursors
E-POSS	: Epoxy-functionalized polyhedral oligomeric silsesquioxanes
GPTMS	: (3-Glycidyloxypropyl)trimethoxysilane
NC-514	: Di-epoxidized cardanol
PGTE	: Phloroglucinol tri-epoxy
PMI	: N-phenylmalemide
POSS-8GC	: Octaglycidyldimethylsilyl POSS cyclic carbonate
PPG-DGE	: Polypropylene glycol diglycidylether
TEOS	: Tetraethyl orthosilicate
Solvents	
$CDCl_3$	: Deuterium chloroform
$CHCl_3$	: Chloroform
CO_2	: Carbon dioxide

DCM : Dichloromethane

D_2O : Deuterium oxide

DMF : N,N-dimethylformamide

DMSO-d_6 : Deuterated dimethylsulfoxide

EtOAC : Ethyl acetate

MEK Methyl ethyl ketone (Butanone)

MeOD Deuterated methanol

MeOH : Methanol

THF : Tetrahydrofuran

Substrates

Al : Aluminum

Gl : Glass

PE : Polyethylene

PET : Polyester textile

PP : Polypropylene

SS : Stainless steel

W : Wood

Analytical techniques

ARES Advanced Rheometric Expansion System

CA : Contact angle

CAT : Crosscut adhesion test (ASTM D3359)

DSC : Differential scanning calorimetry

FTIR : Fourier transform infrared spectroscopy

LST : Lap shear test (Instron 5594)

MEK : Methyl ethyl ketone double rub test (ASTM D4752)

NMR : Nuclear magnetic resonance spectroscopy

TGA : Thermo-gravimetric analysis

TEM : Transmission electron microscopy

TT : Tensile tests-Instron 5594

SEM : Scanning electron microscopy

Name	***Symbol***	***Unit***
Absolute temperature	T	^{0}C
Angular frequency	ω	Hz
Contact angle	CA	^{0}
Degradation temperature	T_d	^{0}C
Displacement	Δs	mm
Equilibrium water absorption	EWA	%
Equilibrium water content	EWC	%
Elongation at break (Strain)	ε_{break}	%
Frequency	f	Hz
Force	F	N
Gel content	GC	%
Gel time	GT	min
Glass transition temperature	T_g	^{0}C
Lap shear strength	LSS	N mm^{-2} (MPa)
Number average molar mass	Mn	g mol^{-1}
Stress	σ	MPa
Storage and loss Moduli	G′, G″	Pa
Tensile strength	σ_{yield}	MPa
Thickness	μ	μm
Weight average molar mass	Mw	g mol^{-1}
Young's modulus	E	MPa

TABLE OF CONTENTS

Chapter-I: Recent Advances in Polyhydroxyurethane Applications in Coatings and Adhesives

Chapter-II: Reinforced poly(hydroxyurethane) thermosets as high-performance adhesives for aluminum substrates

Chapter-III: Bio-Based Polyhydroxyurethanes Glues for Metal Substrates

Chapter-I

Recent Advances in Polyhydroxyurethane Applications in Coatings and Adhesives

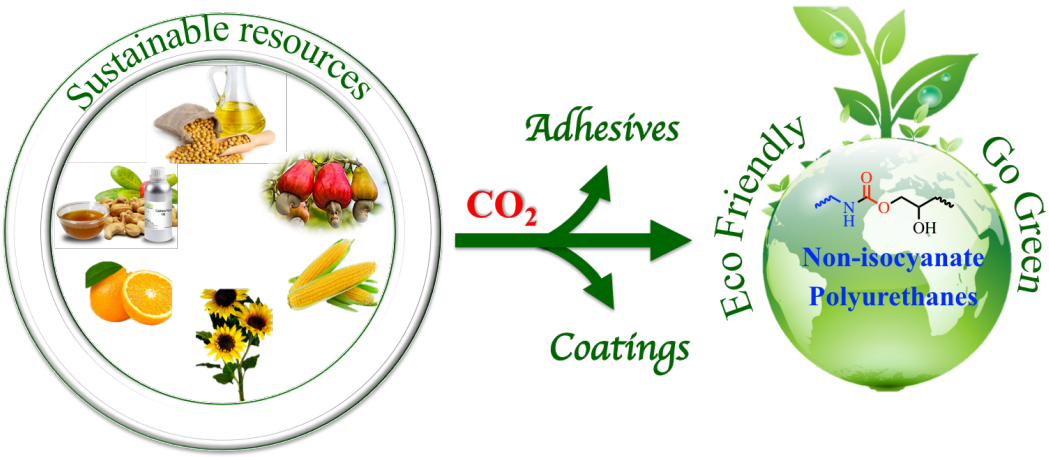

Table of Contents

I.1 General Introduction and Motivation

Polymer adhesives and coatings are found in multiple industrial and everyday-life applications in automotive,[1–3] aerospace,[4–8] engineering[9–11] and biomedical,[12–14] textile,[15–17] packaging,[18–20] building and construction etc.[21–25] Adhesives are classified according to their strength. Structural adhesives typically show high strength and durability while the non-structural ones are characterized by low strength and durability (pressure sensitive materials, elastomers and sealants...).[26–28] Adhesives and coatings are commercially available in the form of pastes, viscous liquids, paints, films and tapes. They are generally made of UV-curable or thermoset epoxy, phenolics, (meth)acrylics or urethane resins combined to adhesion promotors and additives such as inorganic fillers (SiO_2, TiO_2…)**.** Dual cure systems consisting of a mixture of various precursors (epoxides, (meth)acrylates, urethane and polyesters etc) and hardener pre-cured by exposure to UV-light followed by a second thermal curing vice versa have also been designed.

Epoxy adhesives or coatings[29–33] (one & two-component systems) consist of mixtures of a multi-functional epoxy precursors and a hardener (amines, acids, acid anhydrides, phenols, alcohols and thiols) that can be cured from room temperature to temperatures till 120-150 ^{0}C, Figure 1a. To fit the requirement of the envisioned applications, the curing rate is improved by adding accelerators. These formulations are generally preferred when properties such as gap filling ability, long term durability, high resistance to temperature, chemicals, impact or flame… are searched for.

Phenolic adhesives and coatings[34–38] (one & two-component systems) are prepared from chemically reactive phenol and formaldehyde resins, Figure 1b. The formulations (vinyl-phenolics, epoxy-phenolics, nitrile-phenolics, neoprene-phenolics) can be cured in presence of heat (at 150-260 ^{0}C) and pressure up to 14 bar. These formulations have been dominated the wood adhesive market and bonding metals due to resistance to degradation, chemical, water, oil, salt and weathering. However, they present limitations such as low impact strength, high shrinkage stress lead to brittleness, limited shelf life and not corrosion resistant.

Acrylic adhesives and coatings[39–44] exist as one component formulations of appropriate viscosity that cure *via* exposure to UV-light, Figure 1c. These materials are optically transparent and resistant to high temperature, solvents, chemicals and acids. Well-known (meth)acrylic-derived formations are trademarked under the name of "super glue" (cyanoacrylate-based system) or Loctite® (methacrylates-based systems).

Polyurethanes[45–54] (one & two-component systems) such as commercial Araldite, Teromix® are produced by catalyst driven polyaddition of di- or polyisocyanates and di- or polyols, Figure 1d. These viscous formulations can be cured in a broad range of temperature, i.e. from room temperature to 120-150 ^{0}C. They are preferred for gap filling uses or for adhesives and coatings applications where high strength, resistance to chemicals, abrasion and impact or flexibility are required.

Thanks to this large pallet of formulations, cost-effective, protective and durable coatings and adhesives with good flexibility, ability to bind similar and dissimilar substrates, high shear and tensile strength, improved load bearing capacity and vibration absorption (compared to conventional metal joints such as welding, bolting and screwing …) can be designed.[55]

Adhesive (joints), glues and paints/coatings also present some limitations. In most of the cases, the adhesive strength decreases rapidly with a rise in temperature. Formulations do not have the ability to build up immediately materials with a maximal adhesion strength, which means that long curing times are needed for achieving optimal performances. To adjust the formulations viscosity, facilitate the accelerator diffusion and/or the components reactivity, the use of environmentally harmful organic solvent requiring special handling and disposal is often needed. Last but not the least, none of the adhesives can adhere to all surfaces. The adhesion is strongly dependent on the substrate nature and is governed by a complex interplay of phenomena, forces and intermolecular interactions described in the "mechanisms of adhesion".

(a) Epoxy Adhesives/Coatings

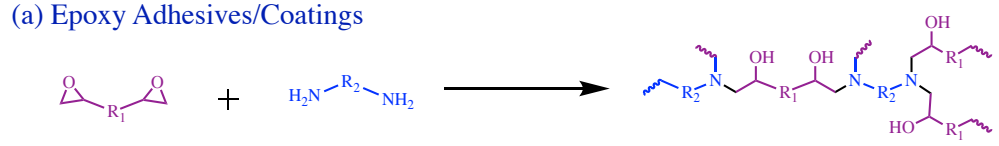

Di- or polyepoxide Di- or polyamines Epoxy resin

(b) Phenolic Adhesives/Coatings

Phenol Formaldehyde Phenolic resin

(c) Acrylic Adhesives/Coatings

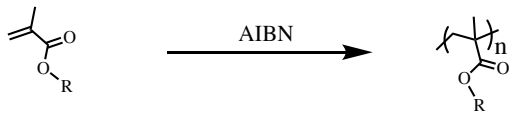

Methyl Methacrylate Poly (Methyl Methacrylate)

(d) Polyurethane Adhesives/Coatings

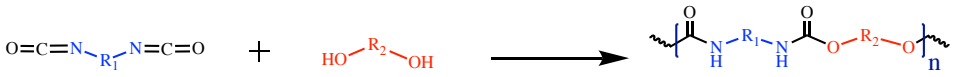

Di- or polyisocyanate Di- or polyol Polyurethane (PU)

Figure 1. Schematic representation of synthesis of conventional (a) epoxy resins, (d) Phenolic resins, (c) Acrylic and (d) Polyurethane adhesives and coatings.

I.2 Mechanisms of Adhesion

Different mechanisms of adhesions have been described in the literature[56–63] and can be classified between a chemical approach (chemisorption model) and a physical approach (mechanical, adsorption, diffusion, and electrostatic laws). However, the adhesion of a coating and/or adhesive to a substrate is generally more complex and the result of two or more of these mechanisms, Figure 2.

In the ***chemisorption theory***,[64,65] the good wettability combined with the formation of chemical bonds across the interface between the adhesive/coating and the substrate is responsible for the adhesion.[66,67]

In the ***mechanical theory***,[68,69] the adhesion of the glue/coating is induced by the porosity and the surface roughness of the substrate. At the microscopic level, the surface presents irregularities that allow the formulations to penetrate and fill the voids generating adhesive anchoring points by mechanical interlocking and entanglements. [70] In this mechanism, good performances can be achieved with adhesives that possess appropriate "adhesive filling power" which is directly linked to its formulation viscosity and its capability to wet the substrate surface.

In the ***adsorption theory***, the adhesion phenomenon is closely related to the contact angle, the surface wettability and surface tension. Unlike the mechanical model, the adsorption theory suggests that the adhesion is only generated by the contact between the adhesive and substrate without penetration in the voids/pores of the surface. When the adhesive/coating shows a lower surface tension than the substrate surface energy, it is capable of wetting the substrate, the presence of synergistic intermolecular or Van der Waals forces, dipole-dipole interactions or hydrogen bonds, favouring its adhesion.

In the ***electrostatic theory***, the adhesion strength is triggered by the creation of an electrical double layer at the interface between the adhesive/coating and the substrate via the transfer of electron and/or positive charges. This model requires an intimate contact between the coating/adhesive and the substrate and sufficient difference in electronegativity between the two "layers".

In the ***diffusion theory***, only valid for "plastics", the interdiffusion and the mixing of mobile chains from both polymers creates anchorage areas and adhesion points (autocohesion). The mobility and degree of penetration of the adhesive/coating is dictated by the molar mass/viscosity of the polymers and their compatibility.

The description of these different mechanisms demonstrates why resin-based adhesives are so efficient. Indeed, the low viscosity of their precursor formulation favours the wettability (chemisorption and adsorption theory), the pore penetration (mechanical theory) and the interdiffusion (diffusion theory) on a surface while the cured polymer network ensures good mechanical interlocking (mechanical theory) and good cohesion of the adhesive. The high reactivity of the resin precursor can also lead to the formation of chemical bond (chemisorption theory) with the substrate leading to good adhesive performances.

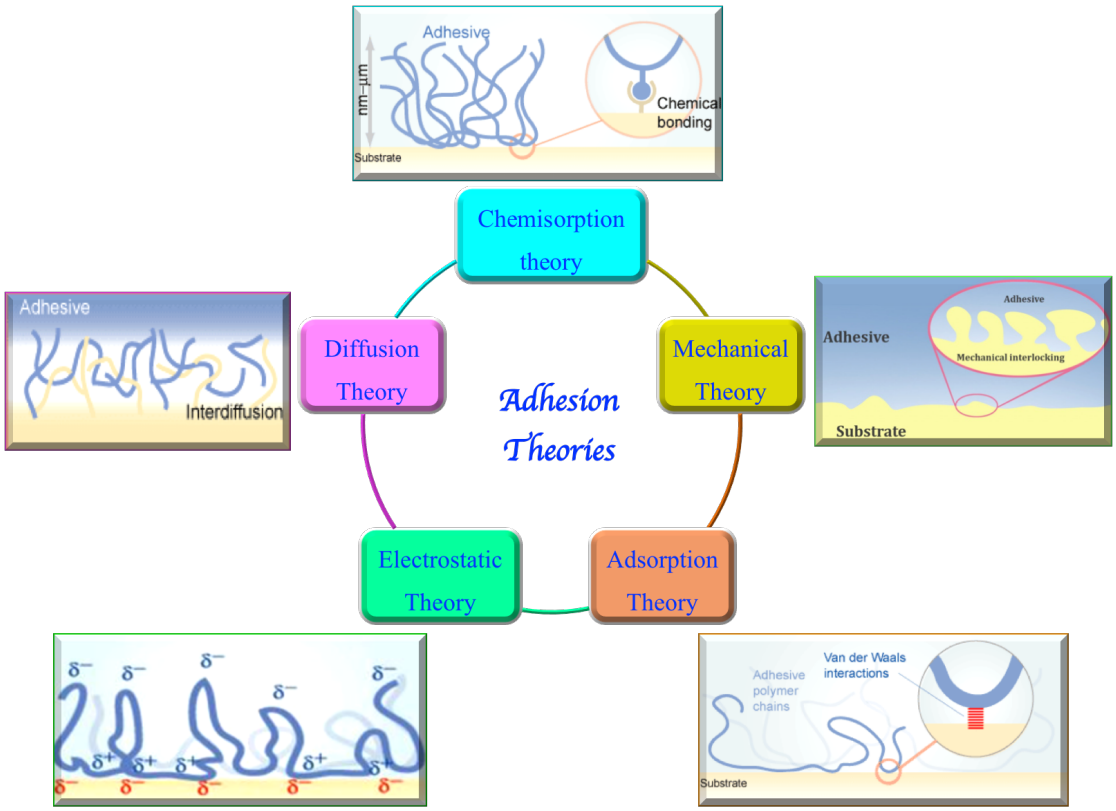

Figure 2. Schematic representation of adhesion theories

I.2.1 *Adhesion and Cohesion*

Adhesion and cohesion determine the overall bonding performance adhesive joints.

Adhesion is the force acting between the adhesive and the surface of the materials. The adhesive force is the result of the mechanical interlocking (mechanical adhesion), as well as the physical and/or chemical interaction (specific adhesion) between the adhesive and substrate, Figure 3a.[71–73]

Cohesion is the internal strength of adhesive. This is a result of the chemical bonds, intermolecular interactions, mechanical entangling and interlocking of the adhesive molecules and their physical and/or chemical affinity for each other, Figure 3b.

Optimal strength of the bond is achieved when adhesion rather than the cohesive strength of the adhesive determines the overall strength of the bond.[71–75]

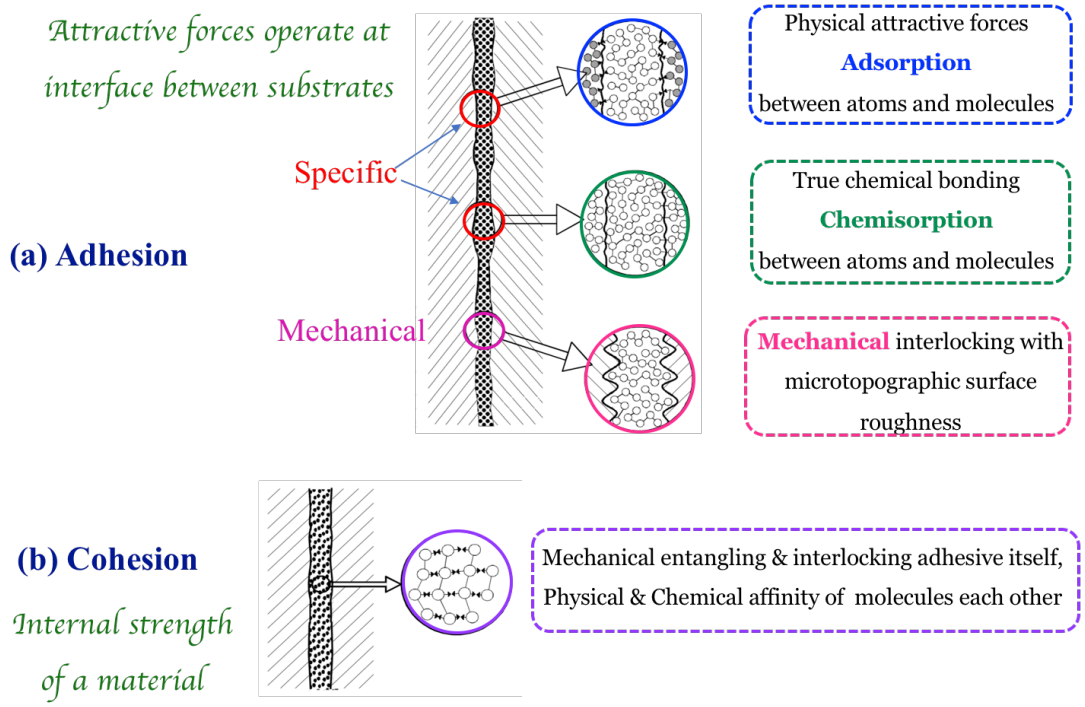

Figure 3. Schematic representation of (a) adhesion and (b) cohesion.

I.2.2 Surface Treatment of Substrates

From the fundamental adhesion theory, it is obvious that the surface state and chemistry of the substrate plays a key role in the design of durable adhesives/coatings with high adhesion properties. To achieve these performances, appropriate surface preparations and operations by chemical or physical methods are required (Figure 4).[76–79] These treatments enables i) to remove or prevent the formation of weak layer; ii) to maximize the degree of interactions and optimize the adhesion forces between the substrate and the adhesive/coating and iii) modify the surface microstructure. In plastics bonding, surface treatments increase the surface polarity and wettability, creating sites for the adhesive/coating bonding. Metal substrates are covered by oxide layers, rendering the surface polar and making them generally suitable for the adhesion. Additional metal surface treatment helps enhancing the bonding strength durability especially under humid environments.

Typically, an efficient surface treatment follows a well-established procedure including:

- The **pre-treatment** by mean of solvents (ex: acetone, isopropanol, water etc) for cleaning and/or degreasing the surface from contaminants (dust, dirt, grease, oil and moisture).

- The properly said **surface treatment** to remove strongly absorbed weak boundary layers and modify the surface chemistry and roughness by mean of 3 approaches:

- ***the mechanical treatment or abrasion*** through grinding, jet cleaning... increasing the specific surface area of substrate
- ***the chemical treatment,*** generally by mean of acids, changing the chemistry and the surface roughness. This treatment varies with the type of substrate. Chromic-sulfuric acid or phosphoric acid etchings are preferred for Al while sulphuric acid etching is commonly used for stainless steel. For low energy polymeric surfaces, the surface treatment consists of acid etching with chromic acid, potassium iodate, sulfuric acid or mixture of different acids.
- ***the physical treatment*** providing more reactive surfaces by oxidation trough plasma, corona discharge, UV light, laser and flame methods.

Those two operations may be complemented by a final **post-treatment** either for favouring the adhesion of the top layer/coating/adhesive by covering the surface by an adhesion promotor/primer or to impart additional functionalities such as corrosion resistance by immersing the substrates in chromate solutions for instance.

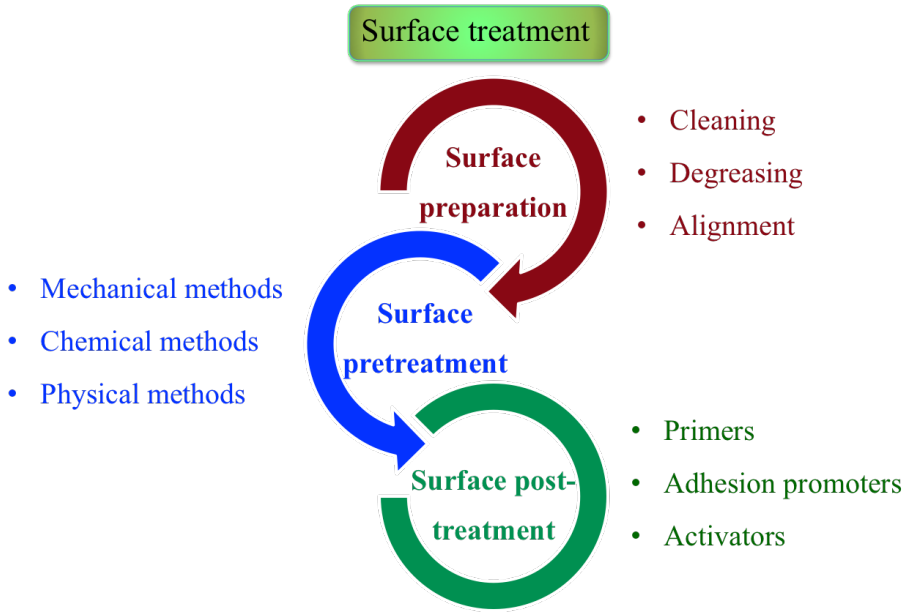

Figure 4. General strategy for the surface treatment of substrates.[76–79]

I.4 Characterization of the Coatings/Adhesives

Coating and adhesives are widely used in industrial sectors such as automotive, construction, pharmaceutical, aerospace… for which the quality of the products is crucial and must fulfil very demanding specifications. For instance, the precursor formulation must be stable in storing condition (pot life) and have an appropriate curing and drying time. The coatings and/or adhesives must have appropriate dimension and appearance, good mechanical properties (resistance to impact, abrasion, wear…), important chemical resistance (water, solvent…) and good adhesion properties. All these important characteristics are evaluated through ASTM standardised methods as listed in, Figure 5 and Figure 6.

I.4.1 Tests Specific to Coatings

Table 1. Standardised ASTM methods to evaluate the coatings/adhesives performance

Coating properties	**ASTM standards**
Formulation and curing properties	
Pot life (time evolution of the viscosity) or gel time	: ASTM D3056
Rheological properties of non-Newtonian materials	: ASTM D2196
Volatiles content of the coatings	: ASTM D2369
Drying time (time for a dry touch, hard dray and full cure)	: ASTM D1640
Cure time (for UV-cured coatings)	: ASTM D3732-82
Dimension and appearance	
Thickness (wet film)	: ASTM D4414
Thickness (dry film)	: ASTM D7091
Specular gloss	: ASTM D523
Apparent density of rigid cellular plastics	: ASTM D1622
Mechanical properties	
Flexibility	: ASTM D522
Degree of blistering	: ASTM D714-02
Film hardness by Pencil test	: ASTM D3363
Abrasion resistance by Taber Abraser	: ASTM D4060
Impact resistance	: ASTM D2794
Wear resistance (testing with pin-on-disc)	: ASTM G99-17
Chemical resistance	
Water resistance using water immersion	: ASTM D870-15
Water resistance using water fog apparatus	: ASTM D1735-14
Water resistance in 100% relative humidity	: ASTM D2247-15
Solvent resistance (rub test)	: ASTM D5402-06
Hydrolytic stability	: ASTM B1308
Corrosion resistance of organic coatings	: ASTM D2803-09
Corrosion resistance by salts spray test	: ASTM B117
Adhesion performances	
Adhesion by tape test (cross-cut adhesion)	: ASTM D3359
Adhesion by pull off strength of the coatings	: ASTM D4541
Adhesion by single lap-shear joint strength	: ASTM D1002

(a) Coating Performances:

Thickness
ASTM D7091

Pencil hardness
ASTM 3363

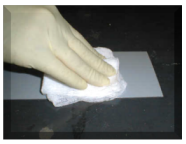

MEK Rub test
ASTM D5402-06

Salts spray test
ASTM B117

Abrasion resistance
ASTM D4060

Glossmeter
ASTM D523

Flexibility
ASTM D522

Impact resistance
ASTM D2794

(b) Adhesion Performances:

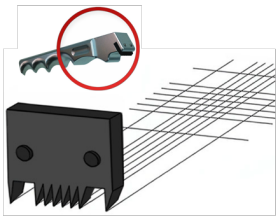

Cross-cut adhesion
ASTM 3359

Pull-off strength
ASTM D4541

lap-shear joint strength
ASTM D1002

Figure 5. Images of techniques used for coating and adhesion performances.

(a) Pencil hardness test (ASTM D3363)

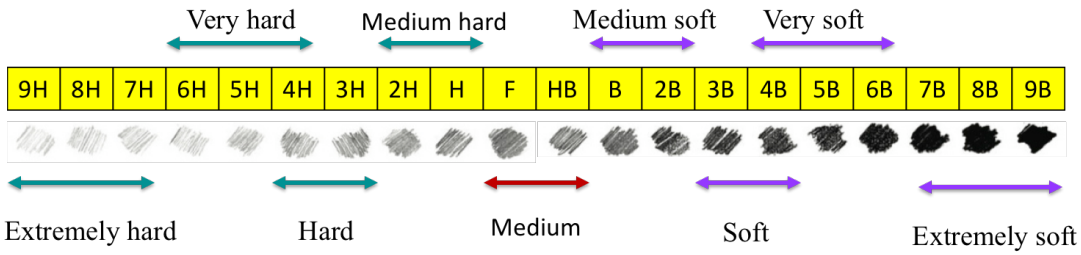

(b) Gloss measurements (ASTM D523)

ASTM D523	20^0	60^0	85^0	45^0	75^0
	High gloss	Medium gloss	Low gloss	Medium gloss	Low gloss
	Coatings, Plastics, Related Materials			Ceramics	Paper

0-100 GU: The scaling is suitable for most non-metallic coatings and materials (paints and plastics).

100-2000 GU: For the highly reflective appearance (transparent materials, mirrors, plated/raw material components)

(c) Cross-cut adhesion test (ASTM D3359)

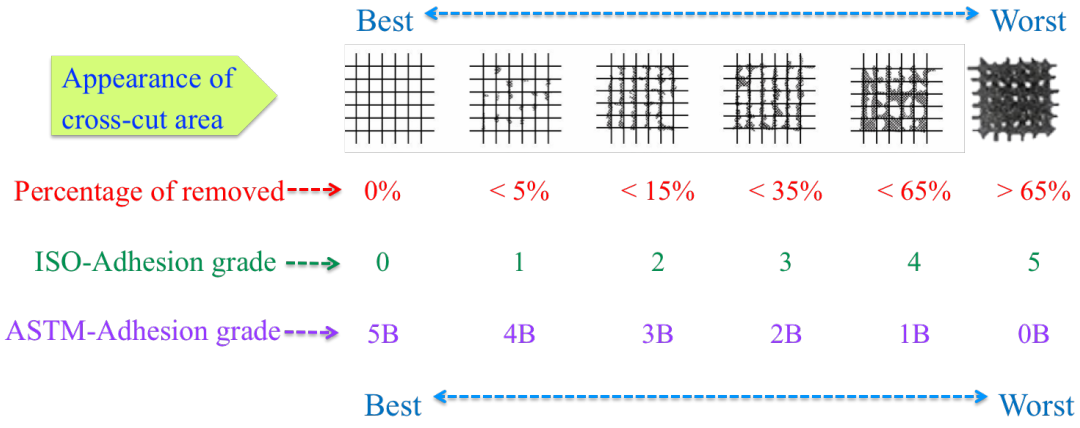

Figure 6. Characteristics of adhesion grade of the coatings (a) Pencil hardness, (b) Gloss measurements and (c) Cross-cut adhesion tests.

I.4.2 Tests Specific to Adhesives

The interaction energy between a polymeric adhesive and a substrate is known as the adhesive strength while the cohesive strength is related to the interactions between the chains among the polymeric networks. Typically, the bonding strength of the adhesively bonded joints may be evaluated by tensile, peel and cleavage tests. However, the ASTM D1002 lap shear test is one of most commonly used standardised method to evaluate the shear strength of adhesives. This test imposes a uniform stress across the joints of the bonded area by pulling apart along the plane of adhesion and measures the force required to brake the adhesive as well as its failure mode. The ***lap shear adhesion*** strength can be calculated by using equation-1.

$$\tau = \frac{P}{A} \qquad (1)$$

Where, τ is lap shear strength (N mm^{-2} or MPa), P is the force to remove the adhesive or load (N) and A is the overlapped or gluing area (100 mm^2).

The ***failure pattern of adhesives*** also gives a clear indication of the phenomenon responsible for the breaking of the adhesive. Four failure mode mechanisms (Figure 7) can be identified from the fraction of the adhesive remaining in contact with the substrate surface and are classified as:[80–83]

1. *The **cohesive failure*** for which the failure takes place within the adhesives (Cohesive strength < Interfacial strength). After failure of adhesive joint, both substrates remain covered by adhesive layer.
2. *The **adhesive failure*** for which the failure occurs at the interface between adhesive layer and the substrate meaning that the adhesive detaches from the surface. (Cohesive strength > Interfacial strength)
3. *The **adhesive/cohesive failure*** for which only part of the adhesive is detached from the substrate (Cohesive strength = Interfacial strength)
4. *The **substrate failure*** for which the adhesive bond strength is higher than the cohesive strength of the substrate

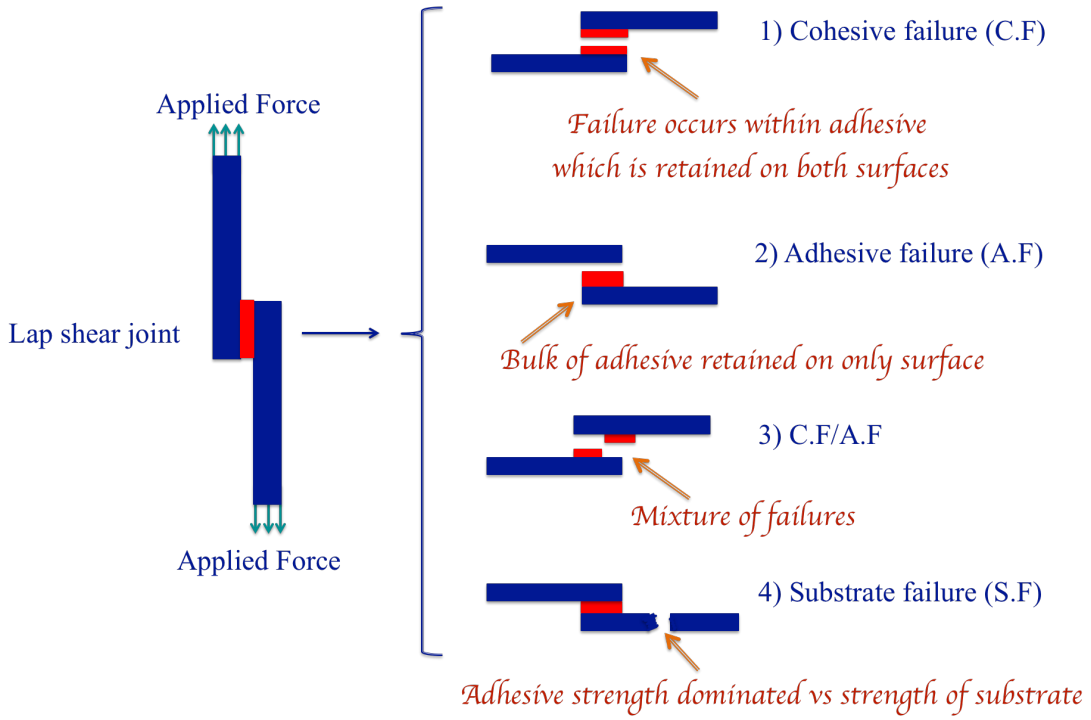

Figure 7. Schematic representation of the failure mode of adhesive, 1) cohesive failure, 2) adhesive failure, 3) cohesive and adhesive failure and 4) substrate failure.

I.5 Isocyanate-Free PUs (PHUs) In Coatings and Adhesives

Due to their intrinsic and easy tuneable properties polyurethane (PU) is a polymer of choice for designing coatings and adhesives, Figure 8a.[84–90] However, the toxicity of isocyanates has pushed the chemists to develop novel and green isocyanates-free pathways to PUs.[86,91–96] If various strategies including the CO_2/aziridine ring-opening copolymerization,[97–99] the cationic ring opening of 6-membered cyclic urethanes[100] or transurethanization[101–103] methods have been proposed, the most promising approach relies on the polyaddition of di- or multicyclic carbonates with di- or polyamines.[86,89,111–120,92,121–123,104–110] The resulting polymer, named polyhydroxyurethane (PHU) structurally differs from conventional PUs by the presence of additional pendant primary and secondary hydroxyl groups (Figure 8b) and have already found applications as thermoset materials,[124–131] foams,[107,132,133] hydrogels,[134] latexes,[135,136] coatings[114,115,145,146,137–144] and adhesives.[110,147–149]

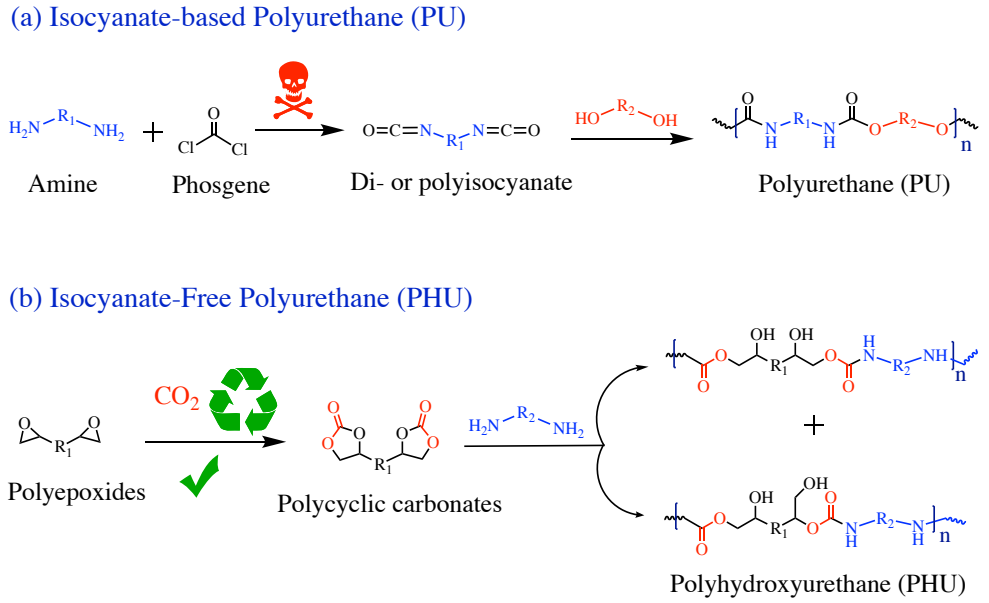

Figure 8. (a) Synthesis conventional PUs by polyaddition of di- or polyisocyanates and di- or polyols and (b) PHUs by polyaddition between di- or polycyclic carbonates and di- or polyamines.

The presence of the –OH groups in PHUs may be exploited advantageously for designing the next generation of novel high-performance polyurethane-based adhesives and coatings. As previously mentioned, the presence of additional functional groups along the polymer chain could play a major role in the improvement of the cohesive and adhesive strength compared to conventional PUs thanks to the additional hydrogen bonding and Van der Waals interactions (of the chemisorption theory, Figure 9).[32] To the best of our knowledge, up to now, no specific studies on the adhesion mechanism of PHUs onto substrates have been reported making this explanation still hypothetic.

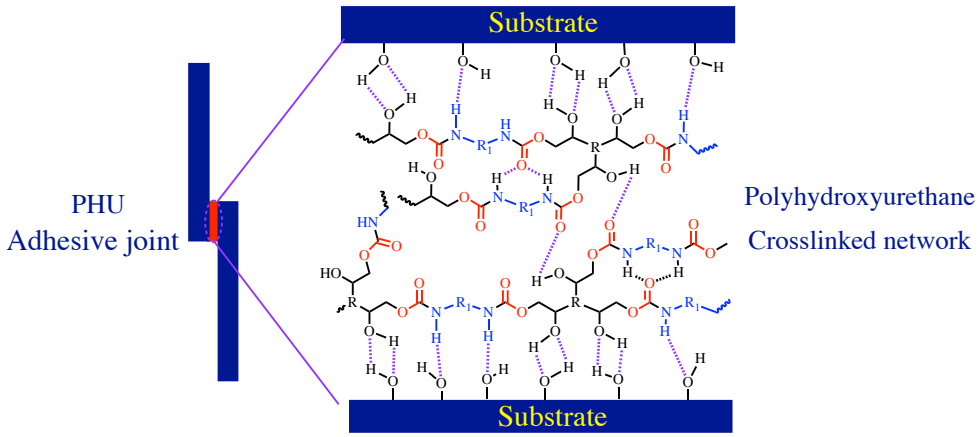

Figure 9. Schematic representation of a PHU network and the expected interfacial interactions with the substrates.

In the next part of the introduction, a literature survey of the adhesive and coating performances of PHUs material is proposed with special emphasis on strategies and formulations exploiting the chemistry of cyclic carbonate and amine.

I.5.1 Solvent-Based PHU Coatings

Kathalewar *et al.*[150,151] investigated the structure-properties relationship of various solvent-based isocyanate-free PU coatings made of polyols[150] (Figure 10, route 1) or bis-cyclic carbonates[151] (Figure 10, route 2) derived from cashew nut shell liquids, mainly containing cardanol analogues.

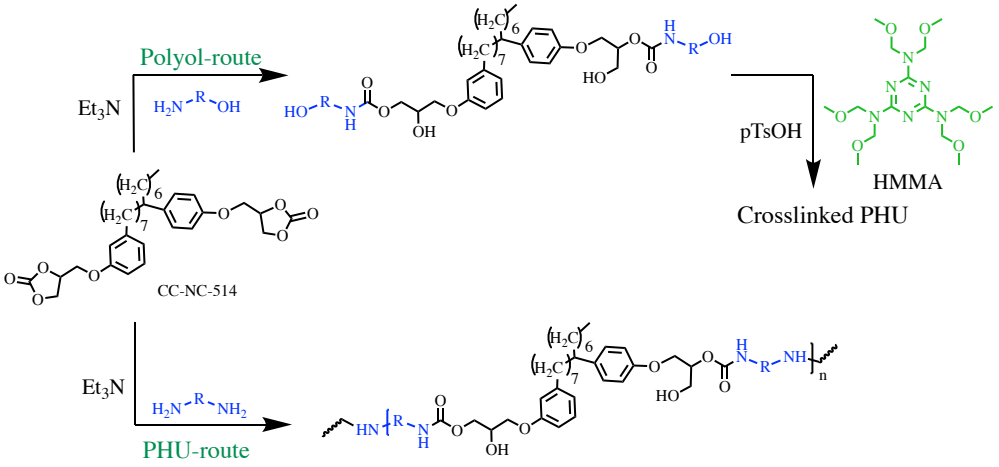

Figure 10. Schematic representation of synthetic routes to produce of linear and crosslinked PHUs using polyol with primary and secondary hydroxyl groups.[150,151]

In the first approach, a polyol with hydroxyurethane moieties was synthesized by the ring-opening of the bis-cyclic carbonate derived from the diglycidyl ether of cardanol in the presence of an aminoalcohol. Then, the so-produced building block was cured at 150 °C for 5 min with hexamethoxy methylene melamine (HMMM) as hardener using *para*-toluene sulfonic acid (3 mol%, PTS) as a catalyst. To adjust the viscosity and ensure the solubility/miscibility of all reactants, a mixture of solvent, i.e. xylene/methyl ethyl ketone/*N,N*-dimethylformamide (50:20:20 on volume basis) was used prior to the deposition of the formulation onto a pre-treated steel panel choose as model substrate. After curing, clear, glossy and light red coatings (thickness of 40-60 µm) were formed. But they showed poor adhesion performance at a HMMM/hydroxyl 1:1 equivalent ratio due to the brittleness of the crystalline films and the absence of residual hydroxyl

groups known to promote/favour the interactions with the substrate. Coatings with the optimum performances were designed by decreasing the HMMM content to 70%. Such formulation offered the best compromise between the cross-linking density of the films and their flexibility induced by the presence of the β-hydroxyurethane moieties while maintaining a sufficient concentration of hydroxyl groups to promote good adhesion. The negative effect of the excessive crystallinity was further confirmed by measuring the surface hardness properties of the cured structure. The maximum scratch hardness, impact resistance value (70.2 lbs.inch) and abrasion resistance (marginal weight loss after 1000 abrasion cycles) were obtained for a HMMM loading of 70%. Thanks to pull-off tests, the adhesive strength between the coating and the substrate was estimated to 4.9 MPa and resulted in cohesive failure. Finally, the chemical resistance of the optimized coating formulations against acidic, or alkali treatment and solvents was studied, respectively by the immersion method and by the rubber test. Both the alkali and acidic tests did not produce any visible damages other than loss in gloss after a 5 days immersion and were found resistant above 200 rubs to polar (methyl ethyl ketone) and non-polar (xylene) solvents.

In the second route, Kathalewar *et al.*[151] reported on CNSL based PHU coatings with insight on the effects of the amine, i.e. hexamethylene (HMDA) or isophorone diamine (IPDA) and the curing conditions (time and temperature) on their mechanical, adhesion and chemical performances. Various formulations of bis-cyclic carbonates and diamines or blends of HMDA and IPDA were prepared using triethylamine (0.5% w/w, TEA) as catalyst and a 70:30 (v/v) xylene/MEK mixture and deposited onto steel substrates. The curing was performed at 120 ^{0}C and 150 ^{0}C for 10-30 min. HMDA-based coatings displayed a soft and rubbery behaviour with a poor adhesion of 2.02 MPa (adhesive failure) onto the metal substrate while IPDA-based materials were hard and brittle with a 50% higher adhesion strength of 3.03 MPa (cohesive failure). Optimum formulations were designed from ternary mixtures made of the bis-cyclic carbonate derived from cardanol and a HMDA/IPDA blend as hardening system. The impact resistance of the so-produced coatings reached a value of 70 lbs.inch while the abrasion resistance increased with the increase of the HMDA content. However, the

introduction of HMDA within the formulation slightly softened the coating and reduced both its adhesion strength (between 2.83 and 2.37 MPa, adhesive failure) and its scratch hardness compared to PHU systems made of IPDA as sole hardener. Similarly, to the polyol route, no visible damages were detected after immersion into water, acidic or alkali media and coatings were found resistant above 200 rubs to polar (methyl ethyl ketone) and non-polar solvents (xylene). Interestingly, for both approaches, the PHU coating performances were benchmarked with the ones of analogues epoxy systems. Clearly, crosslinked PHU displayed better adhesion strength, comparable mechanical properties and improved chemical resistance thanks to the presence of the OH groups along the crosslinked polymer backbone favouring the coating/substrate and the inter-chain interactions by hydrogen bonding. However, their thermal stability was ~20 °C lower than the ones of the epoxy coatings.

Kalinina[152] and Webster[153] reported on thermosetting PHUs derived from polymeric multifunctional cyclic carbonates and di- or polyamines form metals coating. In their similar conceptual approaches, both authors designed reactive random copolymers made of vinyl monomers bearing 5-membered cyclic carbonates moieties (such as 3-(2-vinyloxyethoxy)-1,2 propylene carbonate or vinyl ethylene carbonate), VOPC and *N*-phenyl-maleimide or vinyl esters as comonomers. DMF-based PHU formulations made of poly[3-(2-vinyloxyethoxy)-1,2-propylene carbonate-*co*-*N*-phenyl-maleimide], VOPC-MI and ethylene or hexamethylene diamine crosslinker showed poor substrate adhesion and mechanical resistance after curing at 150 °C for 3h (Figure 11, route 1). The coating performance, i.e. the resistance against chemicals, acids and alkalis, was improved by replacing the EDA and HMDA by 4,4'-diamino-3,3'-dimethyldiphenyl methane (DDDM) but the adhesion onto steel sheets and the impact strength remained very low. No further discussion on the coating performances was detailed by Kalinina.

In a rational study, Webster synthesized series of copolymers of vinyl ethylene carbonate (VEC) and vinyl neodecanoate (VV9) or vinyl neononanoate (VV10) with molar masses between 1800 and 14000 g/mol that were used as multicyclic carbonates in the formulation of clear PHU coatings for iron substrates (Figure 11, route 2). The effects of the amine structure on aminolysis rate, and of the copolymer composition,

the variation of the cyclic carbonate/amine stoichiometry and the solvent on the coating performances and properties were deeply investigated. Primary diamines such as tris(2-aminoethyl)amine (TAEA), diethylenetriamine (DETA), aminoethylpiperazine (AEPP), 2-methyl-1,5-pentanediamine (MPE) or 1,3-cyclohexanebis(methylamine) (CBMA), were identified as the most efficient cross-linkers enabling a fast ring-opening of the cyclic carbonate ring. Then, PHU coated iron panels (with a film thickness of 0.8-1.0 mils) were prepared by deposition of multicyclic carbonate/diamine formulations in propylene glycol monomethyl onto the substrate and cured at 80 °C for 45 min followed by an additional treatment for 7 days under ambient conditions prior testing. Coatings derived from a polymer of VEC and VV9 with a 40/60 [VEC]/[VV9] weight composition and tris(2-aminoethyl)amine or diethylenetriamine (cyclic carbonate/amine) stoichiometric molar ratio) were found glossy and resistant to the MEK solvent. However, they showed poor impact resistance as a result of the too high crosslinking density (at least in the tested experimental conditions). Replacing propylene glycol monomethyl ether by butyl acetate, tetrahydrofuran or xylene had no significant effect on the adhesion properties as attest by MEK double rubs higher than 300. Finally, lowering the VEC content or replacing vinyl neodecanoate (VV9) by vinyl neononanoate (VV10) had a detrimental effect on the coating resistance against solvents when cured in the presence of diethylenetriamine. However, all coatings kept good pendulum hardness and were correlated to the Tg and crosslinking densities of the materials that increased with the VEC content.

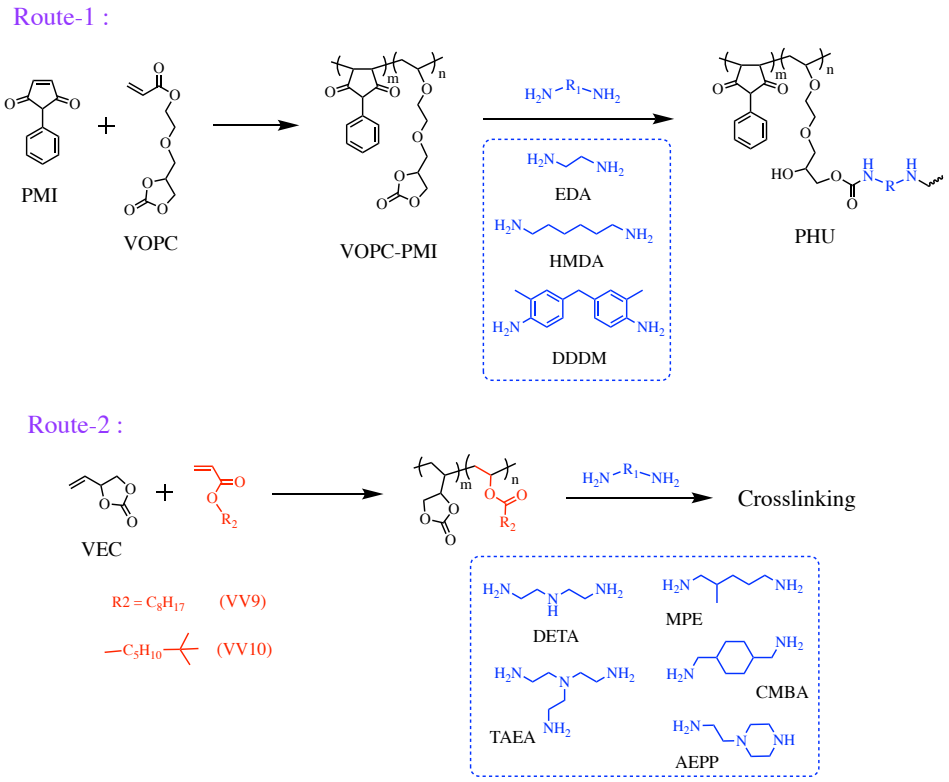

Figure 11. PHU coatings from polycyclic carbonate/diamines formulations.[152,153]

I.5.2 Solvent-Free PHU Coatings

Because most of the polycyclic carbonates are high melting point solids, examples of solvent-free PHU formulations for coating applications are still limited. In 2016, Schmidt *et al.*[154] tailored viscous liquid PHU oligomers by a 1 min pre-mixing at room temperature of high purity sorbitol tricarbonate (STC) with Priamine 1074 (i.e. a long chain non-polar fatty acid diamine), or a blend of Priamine 1074 and isophorone diamine in a 60/40% molar ratio (Figure 12). As amines were immiscible to sorbitol carbonate, the liquid prepolymers were synthesized by using a three-roll mill allowing for the breaking of the STC crystallites and facilitate the formation of hydroxyurethane moieties. Unlike usual PHU chemistry, kinetic insights revealed that the internal cyclic carbonate groups of STC were 3.2 times more reactive than the terminal ones owing to the electron withdrawing effect of the latters. Then, after mixing of the reactive PHU oligomers with a diamine curing agent, the liquid two-component mixture was casted onto glass, degassed at 60 ^{0}C for 5 min and then crosslinked at 80 ^{0}C for 14 h. The resultant coatings were colourless, optically transparent and scratch resistant.

Moreover, they showed a hydrophobic character as attested by a contact angle value of 101^0. Their film properties varied from highly flexible and soft (Tg of 29 ^{0}C and Young's modulus of 12 MPa) by using Priamine 1074 as sole amine (at high STC content) to stiff (Tg of 60 ^{0}C and Young's modulus of 630 MPa) by blending Priamine 1074 with more rigid IPDA. No further details on the coating properties were provided by the authors.

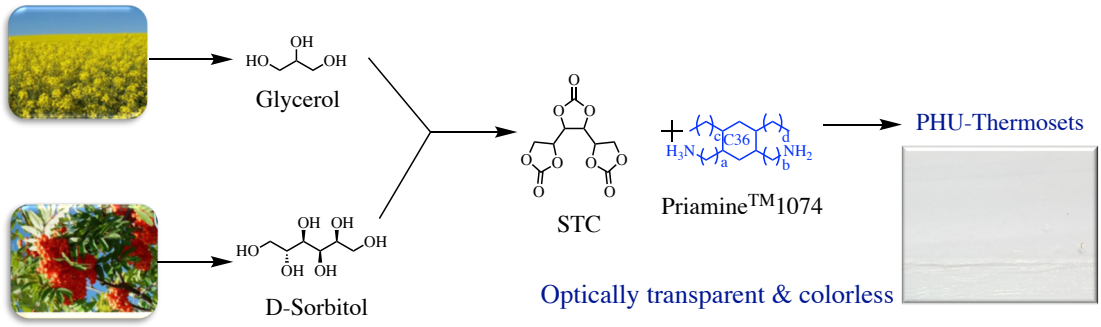

Figure 12. Synthesis of sorbitol-derived poly(carbohydrate-urethane) for optically transparent and colorless coatings.[154]

In his study illustrating the importance of the purity of limonene dicarbonate (LC) on the thermo-mechanical properties of the resulting sustainable PHU thermosets and thermoplastics materials, Schimpf.[130] tested LC/Lupersol (i.e. a polyamine derived from poly(ethylene imine) (PEI)) formulations for coating applications on glass, Figure 13. Molten PEI was mixed with liquefied LC at 160 °C and stirred for 40s before deposition onto heated glass plates and adjustment of the film thickness to 500 µm using a doctor blade. After curing at 100 ^{0}C for 16 h, while the PHU coating containing impure LC was dark brownish, the one from purified LC was fully transparent, colourless with a high gloss of 140 ± 5 GU. In addition, PHU thermosets produced from the purified LC and PEI displayed increased thermo-mechanical properties compared to state-of-the-art analogues formulations made of non-purified LC. This was evidenced by an increase of the Tg from 55 to 94 ^{0}C, of the young's modulus from 2400 ± 700 to 4370 ± 1300 MPa and of the tensile strength from 7 to 53 MPa without sacrificing elongation at break, for formulations respectively produced from non-purified and purified limonene dicarbonate.

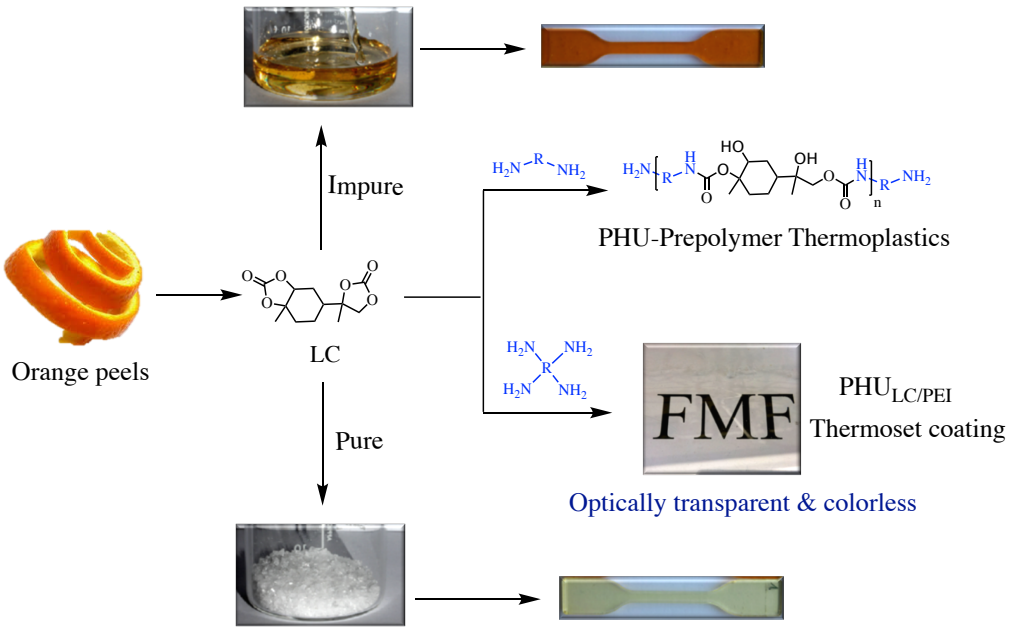

Figure 13. 100% biobased PHU coatings produced by melt phase polyaddition of high purity limonene carbonates and PEI coating (thickness of 500 µm) onto a glass substrate.[130]

I.5.3 UV-Curable PHU Coatings

Alike others types of UV-curable resins, UV-curable isocyanates-free PUs formulations exist as mono- or bicomponent systems composed of low molar masses viscous oligomers or organic molecules bearing photo-reactive (meth)acrylate groups, eventually blended with reactive diluents, and photo-initiators. Upon exposure to UV light of appropriate wavelength, at room temperature, the photo-initiator decomposes to generate radicals that promotes the polymerization of the (meth)acrylate moieties. UV-curable PHU formulations were first patented by Figovsky who exploited the cyclic carbonate/amine chemistry to design urethanediols that subsequently underwent a post-transformation with anhydride acrylic to afford photo-reactive urethanes.[155] Through a strategy sharing conceptual similarities to Figovsky's work, Wang evaluated the coating performances of three UV-curable isocyanate-free formulations designed by blending α,ω-acrylated polyesters of Mn = 3500 g/mol with 10 to 40 wt% of dimethacrylate reactive urethane diluents (Figure 14).[137] Three reactive diluents were synthesized by esterification of urethanediols (made from ethylene or propylene carbonate and aminoalcohols) with methacrylic anhydride. From the film properties, the author observed an increase of the tensile strength with the increase of the

dimethacrylate urethane diluent content that reached a maximum value of 22 MPa to 26-29.5 MPa at loadings of 30 wt% and 40 wt% of dimethacrylate urethane diluents respectively made from ethylene carbonate and ethanol- or propanolamine precursors or from propylene carbonate and ethanolamine. This trend reflected inter- and intramolecular reactions between the α,ω-acrylated polyesters and the reactive diluents as well as a concomitant increase of the cross-linking density. For all three dimethacrylate urethanes considered in the study, the Tg of the cured material was found dependent on the diluent content and evolved from –10 °C to ~ 4 °C in line with an increase of the crosslinking density at higher diluent content that restricted the chains mobility. All three polyester/dimethacrylate urethane cured formulations showed similar thermal stability that decreased from 291 °C to 256 °C with respectively 10 wt% to 40 wt% of the diluent. Such behavior is in line with the thermal sensitivity of the C–NH urethane bond that undergoes much more facile decomposition than the C–O bond of the polyester. Finally, the coating performances of 150 µm thick films casted onto glass and aluminum were evaluated for all three formulations by the pencil hardness, the impact and solvent (MEK) resistance. Whatever the diluent chemical structure, the pencil hardness evolved from 2B at 10 wt% loading to HB above 20 wt%. For all three isocyanates-free PU systems, the impact resistance was maximum at a diluent concentration of 20 wt% while the MEK resistance only surpass 200 double rubs at a diluent content above 30 wt%.

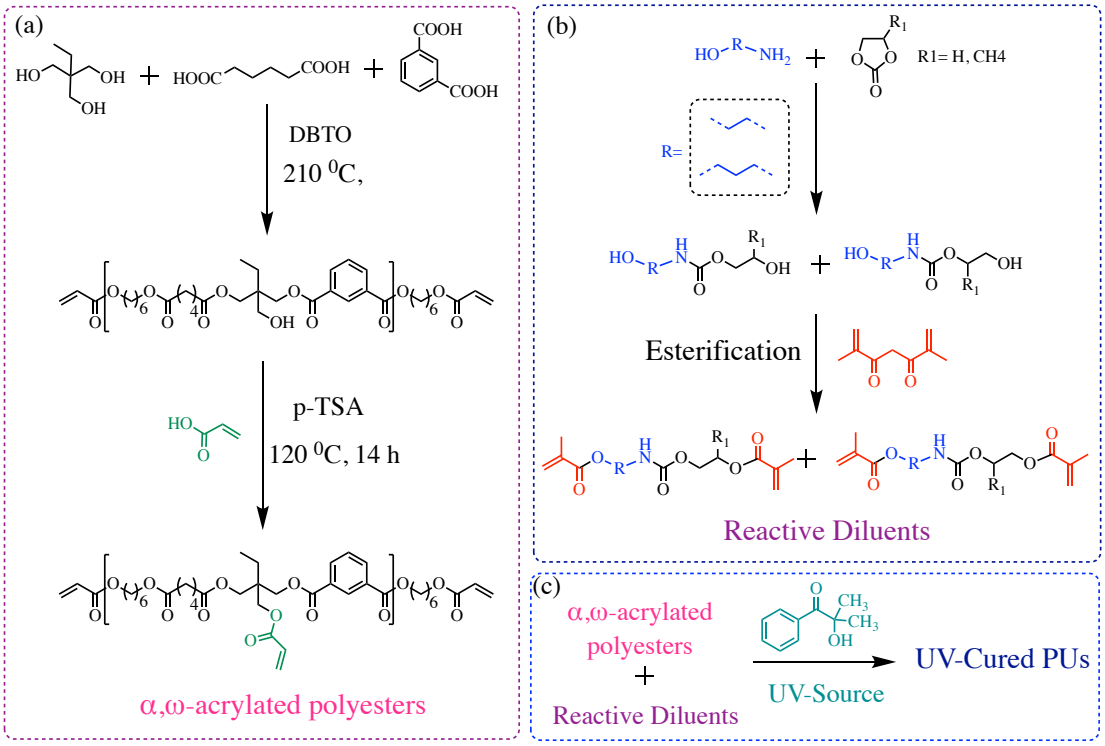

Figure 14. (a) Synthesis of acrylated polyester oligomer, (b) Synthesis of PHU-dimethacrylate diluents and (c) Preparation of UV-cured PUs from α,ω-acrylated polyesters and reactive diluents.[137]

In 2014, Han et al.[139] developed biobased UV-curable poly(ester-urethane)s for tin plate coating. Series of isocyanates-free urethanediols were first synthesized by room temperature aminolysis of ethylene carbonate with ethylene-, butane- or hexamethylene diamine, Figure 15. The so-produced urethanediols were then condensed with itaconic acid at 110 °C using para-toluene sulfonic acid affording oligomers that subsequently underwent chain extension under vacuum by using dibutyltindilaurate as a catalyst. This melt polycondensation approach left three different poly(ester-urethane)s of molar masses in the range of 750-1330 g/mol with reactive methacrylate moieties within the main polymer backbone. These oligomers were cured by exposure to UV radiations (power = 500 W, λ = 366 nm) in 30 min. at room temperature by using 2,2-dimethoxy-2-phenylacetophenone (DMPA) as free radical photo-initiator and triethanol amine (TEA) as curing promoter. Prior to testing the formulations for coating application, the thermo-mechanical properties of the cured materials were evaluated on thin films. The Tg of the cured PUs evolved from 28 °C to 8 °C when the ethylene spacer between the urethane bond is replaced by a hexamethylene group. If the three PU films showed

similar thermal stability with onset temperatures between 255 °C and 273 °C, the maximum tensile strength (up to 2.5 MPa) and young's modulus values (up to 51.9 MPa) were obtained for crosslinked polymers designed from urethanediols with a C_4 spacer between the 2 urethane groups. Such features were reflected in the PU coating performances. The pencil hardness evolved with the length of the aliphatic spacer of the urethanediols precursor in the order $C_4 > C_2 > C_6$ and were respectively determined to 2H, H and 2B (hard to medium hardness). The author correlated the better mechanical and hardness performances of the PUs containing a C_4 spacer to the highest crosslinking density of these materials. All coatings also showed good flexibility (from 0T to 1T, tight bend without gap) and good to excellent adhesion classified as 5B for coatings made of poly(ester-urethane)s derived from urethanediols with C_2 or C_6 spacers and as 4B for materials with a C_4 spacer.

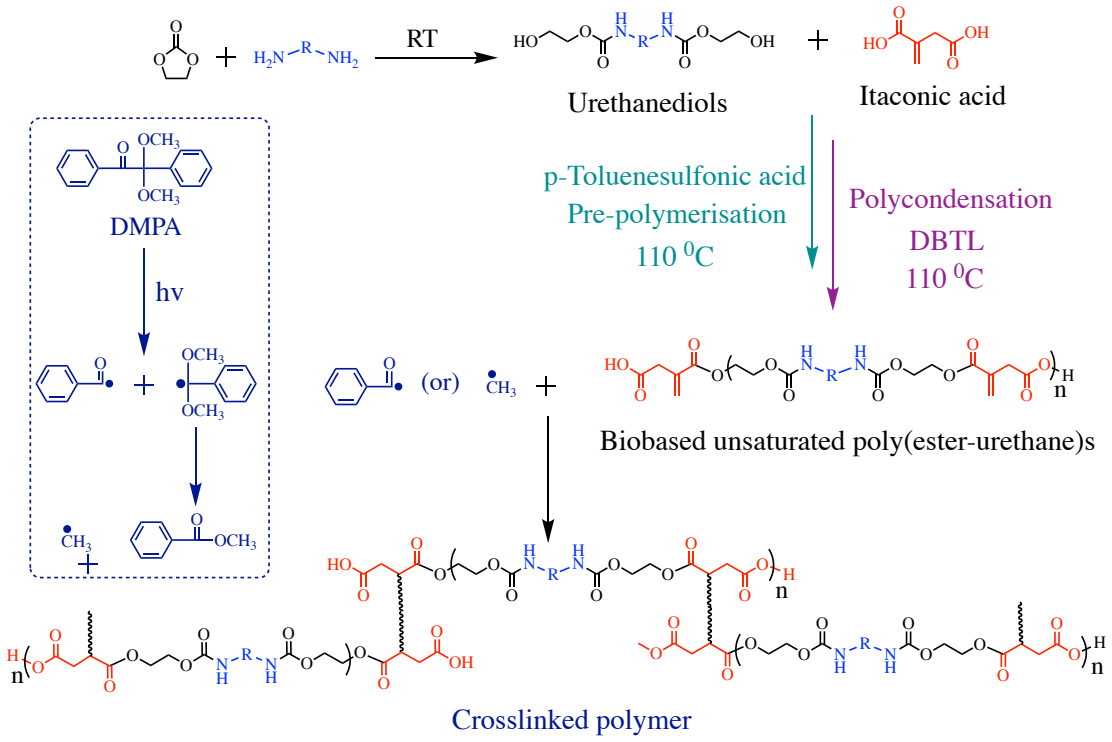

Figure 15. Synthesis of biobased poly(ester-urethane)s crosslinked UV-curable polymers.[139]

In 2012, Hwang *et al.*[156] developed long-lasting hydrophilic UV-curable polyhydroxyurethane resins for treating polyester (PET) tissues. UV-curable α,ω-methacrylate telechelic PHU oligomers were synthesised by a multistep approach,

Figure 16. First, a α,ω-amino-telechelic PHU prepolymer of molar masses of 20000 g/mol was synthesized by the polyaddition of bisphenol-A diglycidyl cyclic carbonate (BADGC) with an excess of Jeffamine D-2000. Then, the amine chain ends were converted in methacrylate moieties by chemoselective Michael addition with the acrylate group of 3-acryloyloxy-2-hydroxypropyl methacrylate (AHM). The prepolymers were blended with 0 to 5% of tripropylene glycol diacrylate (TPGDA) as reactive diluents and the formulations casted on glass plates or onto a polyester (PET) textile surfaces before curing by exposure to a medium-pressure mercury lamp using 1% of photoinitiator (Darocur 1173) (with no further informations on the curing time), Figure 16. Prior to testing the film and coatings performances of the PHUs, all samples were placed in an oven at 50 °C for 24h before conditioning under humid atmosphere at a 75% relative humidity. The thermal stability and the water absorption of the PHU networks were correlated to the content of reactive diluent. The thermal stability felt from 257 °C for a formulation made of pure PHUs to 201 °C for formulations containing 5% of TPGDA. Such evolution was assigned to an increase of the molar fraction of polyacrylate chains within the network at higher reactive diluent dosage, chains that undergoes thermal decomposition more easily than the aromatic skeleton of the main PHU chains. The water absorption decreases from 71.2% to 30.7%, with the addition of the reactive diluent in line with an increase of the crosslinking density of the PHU network limiting its swelling. Finally, the PHU/TPGDA treated textiles showed a long-lasting hydrophilic behaviour even after 30 washing cycles with water, highlighting a strong anchoring of the UV-cured PHU coating onto the PET substrate.

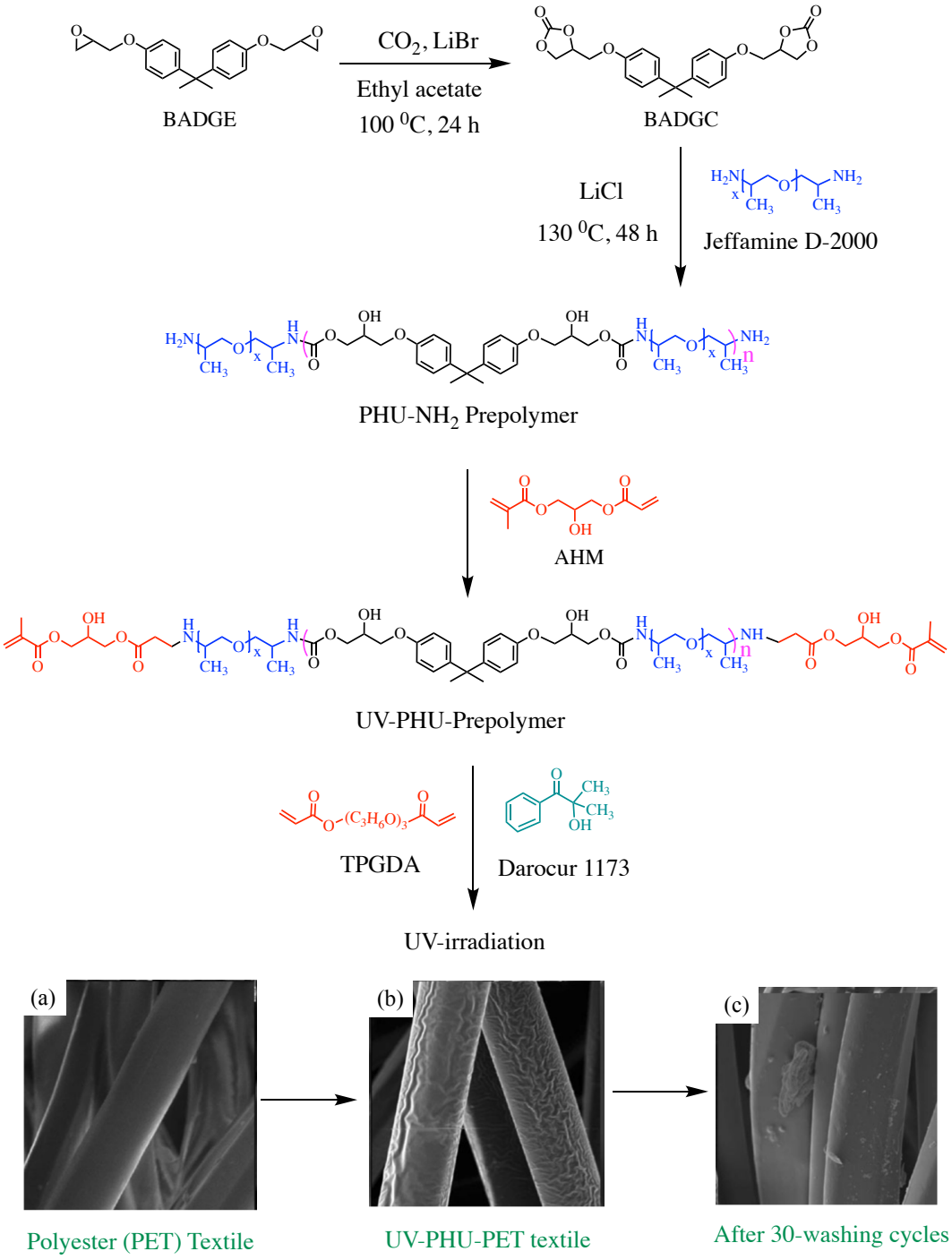

Figure 16. Synthesis of UV-curable poly(hydroxyurethane) prepolymers. SEM images (3000 x) of (a) Polyester (PET) textile surface, (b) UV-PHU-coated textile surface and (c) UV-PHU-coated textile after 30 washing cycles with water.[156]

I.5.4 Poly(Epoxy-Hydroxyurethane) Hybrid Coatings (HPHU)

In 2004, Figovsky et al.[93,155,157] promoted the development of chemically-resistant paints for industrial applications from hybrid Poly(epoxy-hydroxyurethane) resins. If his communication clearly lacks of informations (exact composition of the formulation, molar masses of the oligo- or PHU segments, curing time…), he justified the introduction of polyhydroxyurethane segments by the need to improve both the mechanical properties and the adhesion strength of such epoxy coatings, Figure 17. As a general strategy, hydroxyurethane adducts were synthesized by aminolysis of cyclic carbonate oligomers (chemical structure not specified) with aromatic or cycloaliphatic primary diamines and dissolved into a mixture of Aradur® 830 and 850, i.e. two aromatic polyamine hardeners. The application of the curing solution into a mixture of a bisphenol-A diglycidyl ether epoxy precursors (EPON®828) and a monofunctional epoxide reactive diluent (DER®324) led to the formation of hybrid isocyanate-free PU coatings. These HPHU formulations were cured in 5 to 8 days at 23 °C and gave clear smooth films with a pencil hardness 2H. The impact resistance increased from 10-15 kg/cm for epoxy resins to 50kg/cm for the hybrid coatings. The introduction of hydroxyurethane segments within the formulation also improve the adhesion of the coatings (from 2-3B for the epoxy resin to 4B for the HPHU) and the abrasion resistance (average weight loss of the film ~ twice lower after 1000 cycles for HPHU) while maintaining identical chemical resistance to acids, bases and saline solutions than epoxy resins. Later, the same author and others patented HPHU formulations to manufacture liquid leather materials[158,159] or floorings applications[160,161]. For further details on the impact of the introduction of PHU segments within a bisphenol A-derived epoxy resins on their thermo-mechanical properties, the reader is invited to refer to Cornille's work.[162] However, no discussion of the coating or adhesive performances of these materials was provided in this study.

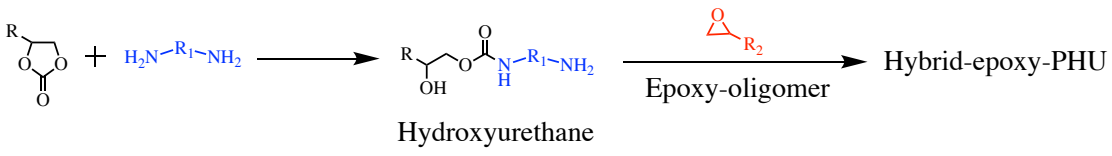

Figure 17. Model reaction of synthesis of hybrid (epoxy-hydroxyurethane)s.[155]

Recently, Anitha *et al.*[163] developed a novel concept to enhance the toughness, the transparency and the adhesion strength of epoxy resin by introducing hydroxyurethanes moieties within the polymeric material. Hybrid epoxy-hydroxyurethane resins were produced from tricomponent formulations made of bisphenol-A diglycidyl ether, Jeffamine-T403 and various content of monofunctional 5-membered cyclic carbonate bearing hydroxyl group, Figure 18. All formulations were cured at 30 ^{0}C for 18 h, 80 ^{0}C for 1 h and 100 ^{0}C for 2 h by using DABCO as organocatalyst and THF as a solvent for a homogeneous mixing of all components. Following this specific procedure, it was postulated that the epoxy rings underwent faster aminolysis at low temperature than cyclic carbonates, leaving amino terminated chains within the network able to react at higher temperature with the carbonate ring.

The covalent attachment of the cyclic carbonate modifier to the amine groups led to a hybrid network with hydroxyl-urethane linkages for which the –OH groups displayed a hydrogen bonding spacer capability affecting the properties of the hybrid material. While the neat epoxy resin was characterized by one Tg at 60 °C, two transitions existed in the hybrid network representing two different Brownian movements and network areas. As no phase separation was observed in the network, meaning that all chain had rather similar chemical structure, the origin of the second Tg was attributed to the presence of additional secondary forces that tightened the chains by hydrogen bonding and prevented their rotation. The benefits of the additional intra/intermolecular interaction was reflected in the mechanical properties of the network that evolved from brittle for neat epoxy resins to flexible by introduction of the urethane linkage. The tensile modulus decreased from 666 MPa to 123 MPa while the elongation at break increased from 20 to 67% by increasing the urethane linkage content. The adhesive strength of the hybrid network (up to 22 MPa for Al-Al sticking) surpassed the value of the neat epoxy material (17 MPa). Finally, by adding the monofunctional cyclic carbonate within the resin formulation, the transparency of the coatings increased from 68% to > 80% and the yellow color vanished. The absence of light yellow coloration and the high transparency was assigned i) to an increase of the groups in the hybrid coatings that did not absorb the light and ii) the proper dispersion

of hard domains within the soft segments. As the length of the hard domains was shorter that the visible light wavelength, all hybrid coatings were transparent.

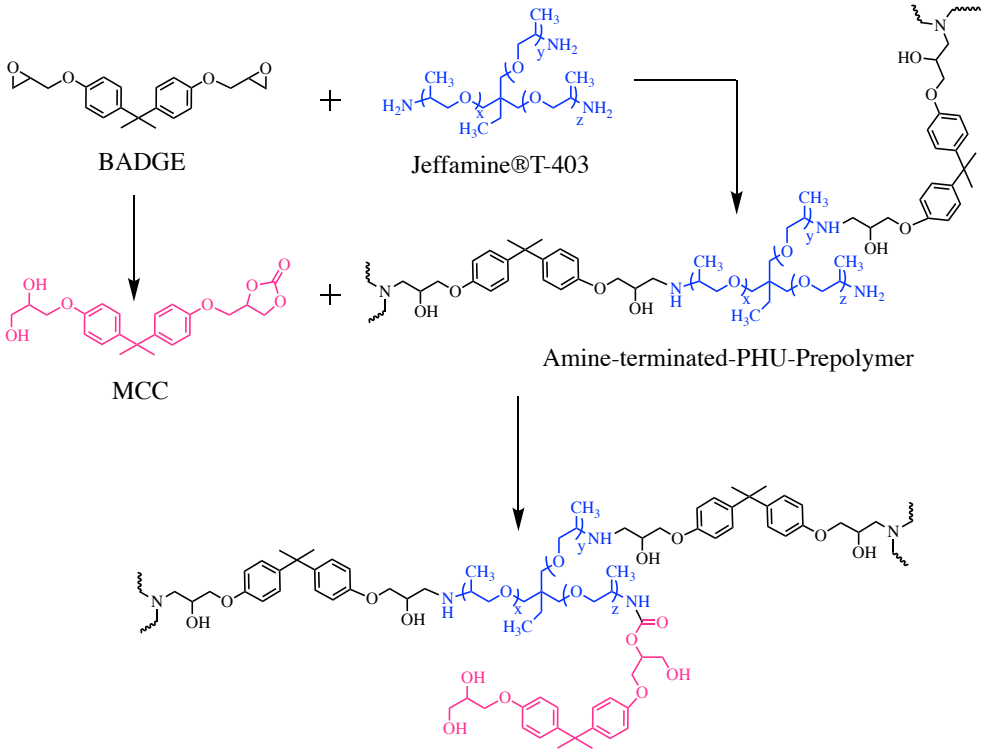

Figure 18. Possible reaction pathway for incorporation of the hydrogen bonding spacer into epoxy networks. The spacer unit is covalently attached to amine-terminated polymer chains from the epoxy-amine reaction.[163]

Ma *et al.*[114] developed sustainable, biobased acetone-borne hybrid coatings for aluminum, Figure 19, route-1. The solvent-based formulations were prepared from diphenolic acid-based bis(cyclocarbonate) (DPA-BisCC), bisphenol-A diglycidyl ethers as curing agent, and diamines (ethylene diamine, diethylenetriamine or isophorone diamine). After a progressive three-step curing at 60 ^{0}C for 2h followed by a 2 h treatment at 120 ^{0}C and finally at 160 ^{0}C for 2 h, the hybrid PU coatings exhibited Tg from 54 °C (for formulation made of ethylene diamine) to 116 ^{0}C by using isophorone diamine thanks to the high rigid C_6 cyclic structure. The latest was also found to be the most thermally stable (up to 287 °C) among the PU coating series. The inherent rigidity of the aromatic groups of DPA-BisCC directly reflected on the surface hardness performances with an excellent pencil strength evolving from 4H to PUs made from ethylene diamine to 5H for the two other formulations. However, PU made from EDA or DETA showed the best crosshatch adhesion value (grade 1).

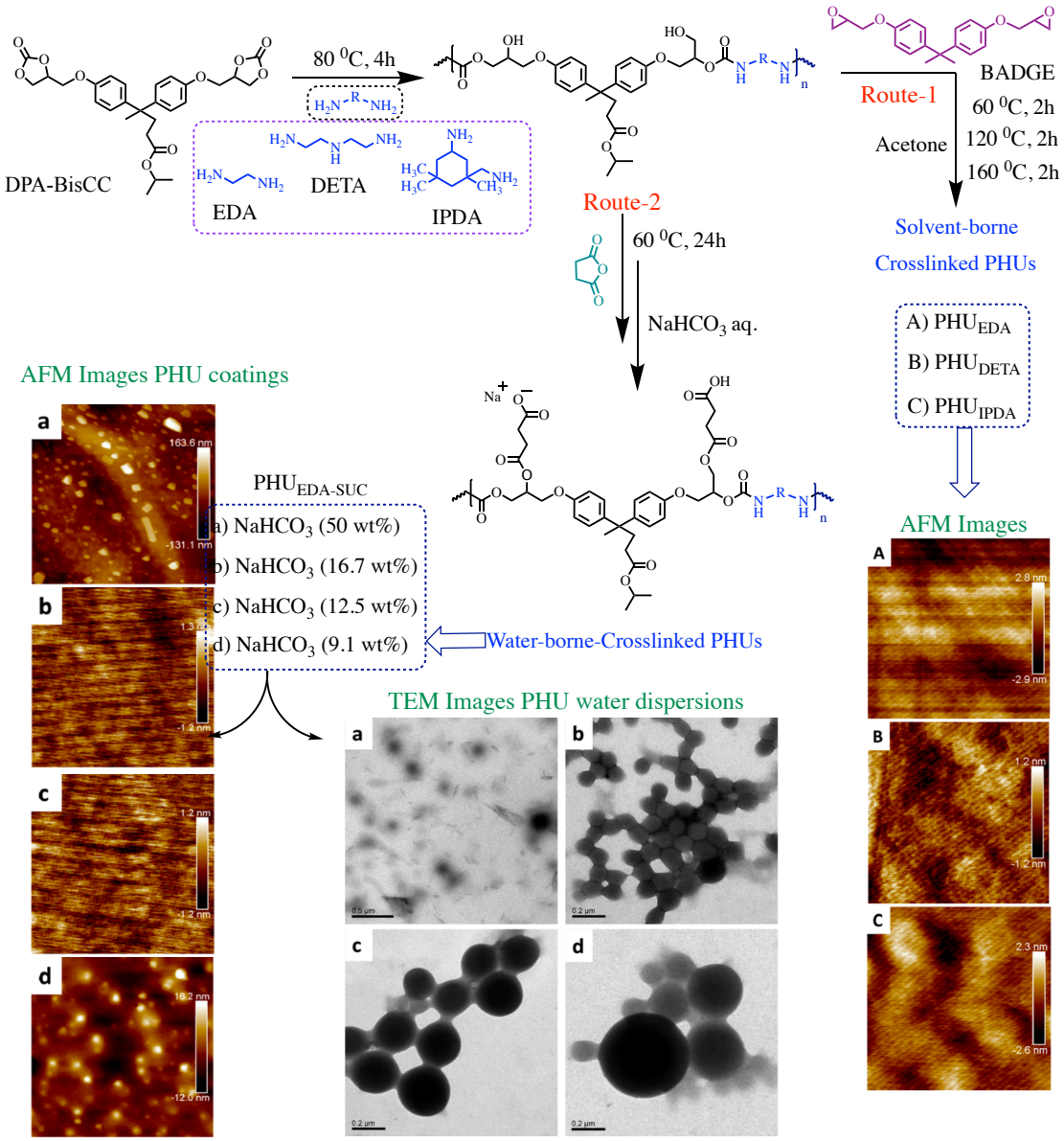

Figure 19. Synthesis of solvent borne (in acetone, route-1) and water borne (in water, route-2) of crosslinked polyhydroxyurethanes from diphenolate acid-based bis-cyclic carbonate (DPA-BisCC). AFM images of PHU solvent-borne coatings (A-C) and water-borne (a-d; $PHU_{EDA\text{-}SUC}$ coatings modified with $NaHCO_3$ (50-9.1 wt%). TEM images of PHU water dispersions of $PHU_{EDA\text{-}SUC}$ coatings modified with $NaHCO_3$ (50-9.1 wt%).[114]

I.5.5 Water-Borne PHU Coatings

Ma *et al*.[114] designed biobased water-borne PHU coatings for aluminum panels, Figure 19, route-2. PHU of Mn ~ 5000 g/mol was first prepared from diphenolic acid-based bis(cyclocarbonate) (DPA-BisCC) and ethylene diamines. Esterification of the hydroxyl groups with succinic anhydride left polymers with carboxylic acids. These acidic groups were easily neutralized with $NaHCO_3$ (from 9.1 wt% to 50 wt%) which enabled the dispersion of the polymer in water as particles with a size ranging from 78 to 321 nm. The water-borne formulation was then mixed with bisphenol A diglycidyl ether-based epoxy resin emulsion and cured by progressive heating at 60 ^{0}C for 2h, at 120 ^{0}C for 2 h and finally at 160 ^{0}C for 2 h after casting on aluminum. All coatings were found hydrophilic, with static contact angle values between 35° and 68° and started to decompose at temperatures between 190 and 230 °C. The pencil hardness and the adhesion properties followed a same trend. By reducing the $NaHCO_3$ content, the hardness increased from 3B to 3H (soft to hard) while the adhesion grade reduced from 4 to 1 (grade ranging from 0-best to 5-worst). However, these water-borne latex-like formulations displayed lower coatings performances than the ones of analogues solvent-based homogeneous hybrid formulations discussed as last example in the previous section.

I.5.6 Composite PHU Coatings

If many strategies and formulations have been developed for designing isocyanate-free PU coatings with good adhesion onto various substrates, none of them really meet the high-level specifications of trademarked products. It's well known that commercial paints and adhesives generally contained series of modifiers, additives and fillers (carbon black, silica, ZnO, clays…)[164–167] which roles are not only to adjust the physico-chemical properties of the formulations and the adhesives/coatings processing conditions (adjustment of the viscosity, curing accelerator…)[166,168] but also to impart novel properties to the final materials (UV-resistance, anti-scratch, anti-corrosion, hydrophobicity…).[169–171] In these complex systems, the key parameters to achieve high performances lie on the proper dispersion of the fillers and its good compatibility with

the matrix. Surface-modification of the fillers by appropriate organic functional groups is one of the best methods for the particles to retain their specific morphology (shape and size) and prevent their agglomeration by generating uniform distribution and improving their compatibility with the polymer matrices (Figure 20). However, other factors may influence the filler dispersion such as their morphology (diameter, size, shape etc), that depends on their production methods (sol-gel, sonication, and mechanical stirring etc), the type of solvent and their synergistic effect. Unlike neat polymers, fillers reinforced composite materials can possess improve crosslinking density and thermal, mechanical (stiffness, strength and toughness) and/or adhesion properties. Kango et al.[172] reviewed the various chemical treatments (organic modification, synthetic polymer grafting…) on the surface of fillers.[173,174]

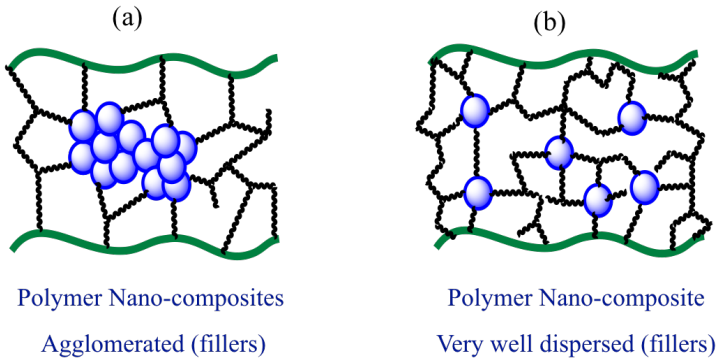

Figure 20: Schematic representation of (a) Agglomerated non-functionalized fillers in the polymer matrix and (b) Well-dispersed functional fillers within a polymer matrix.

I.5.6.1 PHU/Silica Coatings

Turunc *et al.*[175] combined the use of carbonated soybean oils and the nanocomposite technology to design sustainable reinforced coatings (30 µm of thickness) for aluminum panels, Figure 21. Up to 4 wt% of spherical cyclic carbonate functional SiO_2 nanoparticles (diameter = 165 nm, made by a sol-gel process) were dispersed in mixtures composed of CSBO and butanediamine (BDA) as PHU precursors, ethanol as solvent, pyridine as catalyst and a PDMS-based wetting agent (BYK). After deposition onto the substrate using a bar coater, all formulations were cured at 75 °C for 24h. The influence of the fillers addition and their content on the thermal and mechanical properties as well as the adhesion performances of the coatings were investigated. Neat CSBO-based PHU films showed a Tg around -15 °C and an endotherm at ~ 60.7 °C.

Incorporation of the SiO_2 functional fillers (CC-SiO_2) within the PHU had negligible effect on Tg and Tm values. A similar trend pervaded for the evolution of the PHU thermal stability with the fillers content. Neat PHU showed a maximum weight loss at 345 °C that only increased by 5 °C upon addition of up to 4 wt% of functional fillers. The Young's modulus and stress at break values were found maximum at a 2 wt% filler content with values of 9.66 MPa and 6.87 MPa that were twice higher than the ones of the neat PHU system. Further increase in the filler content to 4 wt% clearly weakened the mechanical performances of the nanocomposite PHU as attested by Young's modulus and stress at break values lower or comparable to the ones of CSBO-based PHU. The adhesion performances of the nanocomposites were evaluated onto an Al substrate. After impact tests, no damage of the nanocomposite coatings was observed and all formulations gave rise to a 5B cross-cut adhesion. The benefits of introducing fillers within PHU coatings were highlighted by the MEK rub test showing an increase from 200 rubs for a neat CSBO formulation to more than 400 rubs in the presence of 4 wt% of filler. However, the incorporation of fillers within the PHU coatings had a detrimental effect on the gloss that progressively decreased from 82 to 48 upon addition of 4 wt% of silica. This decrease in gloss was assigned to the phase separation between the hydrophobic PHU coatings and the hydrophilic filler. To prevent to poor dispersion of the silica within the CSBO-based PHU resin and restore surface with high gloss, hydrophilic polypropylene glycol diglycidylcarbonate (CPPG) was added within the PHU formulation (at a 50/50 [CSBO]/[CPPG] weight ratio). The presence of CPPG chains slightly affected the thermo-mechanical properties of the PHU with an increase of the Tg from – 15.2 °C to 13.3 °C and 18.9 °C respectively for neat CSBO-, neat CSBO/CPPG- and nanocomposite CSBO/CPPG-based PHU (containing 4 wt% of fillers) while the Tm remained unchanged. In addition, if the maximum weight loss was 15 °C lower for neat CSBO/CPPG compared to a pure CSBO-based system while addition of 4 wt% of silica significantly improved the thermal stability of the CSBO/CPPG PHU to 370 °C. The addition of CPPG soft segments within the formulation induced a decrease of the Young's modulus and the stress at break at the benefit of the elongation at break. All nanocomposite CSBO/CPPG PHU coatings were found resistant to impact and showed 5B cross-cut adhesion onto Al while the gloss

increased from 51 to 70–76 depending on the filler content. However, these PHU coatings were found less resistant to the solvent with MEK double rub resistance between 100 and 190.

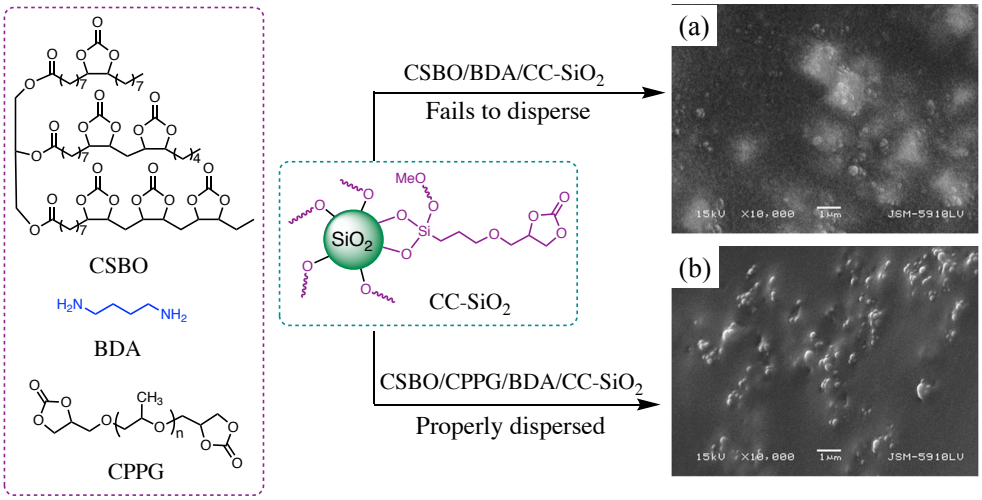

Figure 21: Schematic representation of the formulation composition of monomers and SEM images of (a) CSBO/BDA/CC–SiO_2 (fails to disperse fillers) and (b) CSBO/CPPG/BDA/CC-SiO_2 formulations (properly dispersed fillers).[175]

Upon burning, silica filler may provide thermally insulating chars layers and diffusion barriers to combustible gasses. Besides, phosphorous compounds are known as flame inhibitors thanks to their oxygen scavenger ability. These features were exploited in a synergistic manner by Hosgor *et al.*[176] to potentially design flame retardant PHU coatings. Two silica precursors, i.e. tetramethoxysilane and 4-((3-(trimethoxysilyl)propoxy)methyl)-1,3-dioxalane-2-one phosphorus, were mixed in the presence of water and an acid catalyst for 10 h at pH 4–5. Then, the sol-gel formulation was added with a bis-cyclic carbonate linked by a triphenylphosphine moiety (CBGPPO) and propylene glycol diglycidylcarbonate (CPPG) using methanol. After removal of the solvent under vacuum at 75 °C and addition of HMDA and a BYK-wetting agent, the formulations were applied onto Al (film thickness of 30 µm) and cured at 100 °C for 24h, Figure 22. The Tg of the thermosets evolved from – 28 °C to 1.54 °C for neat PHU formulations respectively made of pure CPPG/HMDA and CPPG/ CBGPPO /HMDA compositions (at a 50/50 CPPG/ CBGPPO content). The addition of the silane precursors induced the in-situ formation of silica upon thermal curing. However, the presence of the fillers within the thermoset PHU had no

significant effect on the Tg values. Whatever the formulation, all coatings were found glossy (132–140 at 60^0), resistant to impacts strength (no damage) and showed an excellent cross-cut adhesion grade of 1. Whatever the CBGPPO content or the presence or not of silica filler, the maximum weight loss was observed at temperature ranging from 331 °C to 346 °C. The authors tentatively tried to demonstrate flame retardant properties by determining i) the residual char content after thermal degradation that was higher (~9% of solid residue) for a 50/50 CPPG/ CBGPPO integrating 20% of in-situ generated silica and ii) the final weight loss temperature that was raised from 527 °C for neat CPPG/HMDA formulations to 716 °C for a 50/50 CPPG/ CBGPPO /silica (20%) formulation. Unfortunately, these tests are clearly insufficient to claim flame retardant PHU coatings and further flame as well as conic calorimetry tests would have been needed to ascertain the fire resistance of the nanocomposite PHU materials.

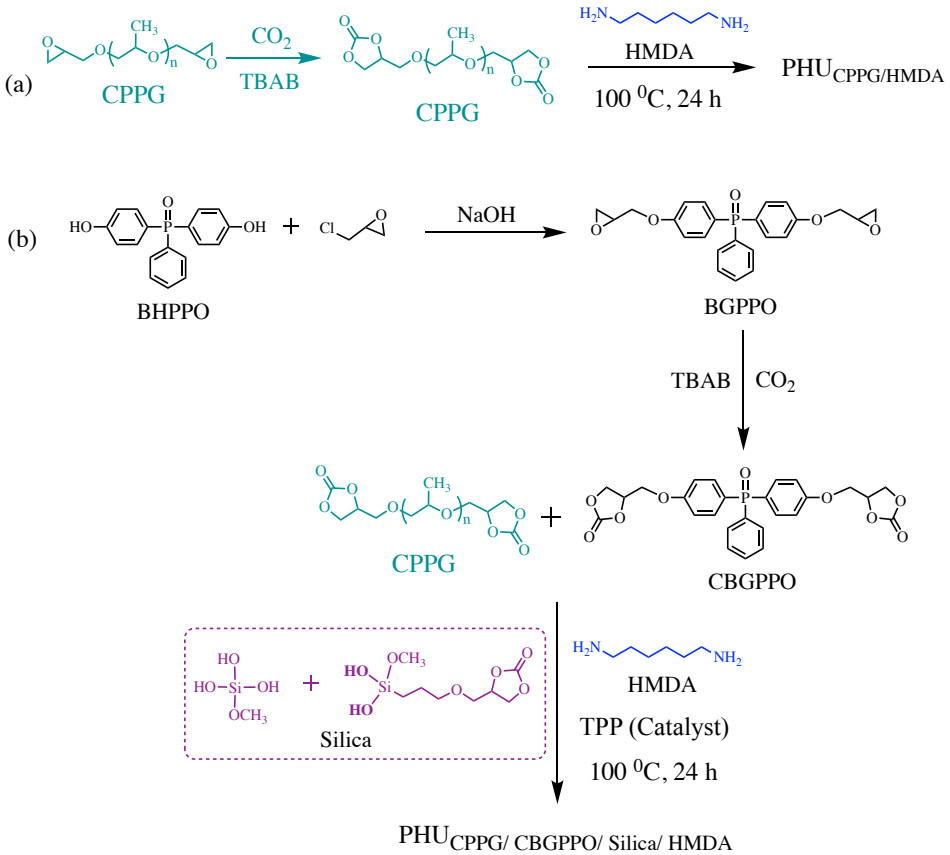

Figure 22. Synthesis of (a) Neat CPPG/HMDA formulations and (b) hybrid 50/50 CPPG/ CBGPPO /silica (20%) formulations.[176]

I.5.6.2 PHU/POSS Coatings

Polyhedral oligomeric silsesquioxane materials (POSS, with an average core diameter in the range of 0.45-0.53 nm)[177–181] have attracted considerable to strengthen the coating thermal and mechanical properties and adhesion performance of various resins such as adhesion, scratch hardness, abrasion resistance, water tolerance, thermal and oxidative stability, chemical, solvent and fire resistance, stiffness, environmental stability...[155,178,182–188] Liu et al. prepared a series of bio-based PHU thermosets and nanocomposite PHU/POSS coatings from rosin[111] or gallic acid[189] based cyclic carbonates, Figure 23. Cyclic carbonate functionalized POSS were dispersed in DMF solutions containing the bis-cyclic carbonate monomers and EDA, HMDA or IPDA as diamines before casting on tin plates and curing at 100 ^{0}C for 8–12 h. The Tg values of the thermoset PHU evolved from 33–41 °C for neat systems made of an aliphatic diamine and gallic acid or rosin to 55–72 °C for analogue formulations made of more rigid IPDA. All PHU systems showed good thermal stability in the range of 335 °C to 384 °C, the highest values being assigned to a formulation made of EDA and rosin monomers. Addition of 20 wt% of cyclic carbonate functional POSS within the PHU formulations had beneficial effect on the thermal properties of the PHU with Tg values that increased to 38-55 °C and 65–82 °C, in line with a higher crosslinking density and the excellent dispersion of the POSS at the nanoscale level that restrict the chain motions, and a thermal resistance up to 388–397 °C (respectively for gallic acid-based cyclic carbonate or rosin /EDA systems) due to the presence of the Si–O–Si cage framework preventing the heat transfer within the matrix and delaying the polymer decomposition. If all PHU coatings, reinforced or not by cyclic carbonate functional POSS, showed similar pencil hardness assigned to 2H or 3H on the hardness scale and resisted to impact, their adhesion behavior onto the tin substrate was strongly affected by the fillers. While all neat and nanocomposite POSS/rosin-based PHU coatings showed an excellent grade 1 adhesion, gallic acid-derived coatings reinforced by 20 wt% of functional POSS poorly adhered to the surface with a adhesion grade from 2 to 6 when aliphatic diamine or rigid IPDA were respectively used as comonomers. Insight on the role of the POSS surface functionality on the coating performances of nanocomposite PHU made from rosin-based formulations was also studied by Liu.

Through benchmarking experiments, he demonstrated that replacing the cyclic carbonates groups of POSS by epoxy ones had only marginal effect on the thermal properties of the coatings (maximum Tg of 58 to 75 °C respectively for rosin/EDA or rosin/IPDA systems, thermal stability up to 385 °C) and the adhesion performances as well as the pencil hardness remained identical to those of analogue coatings made of cyclic carbonate functional POSS.

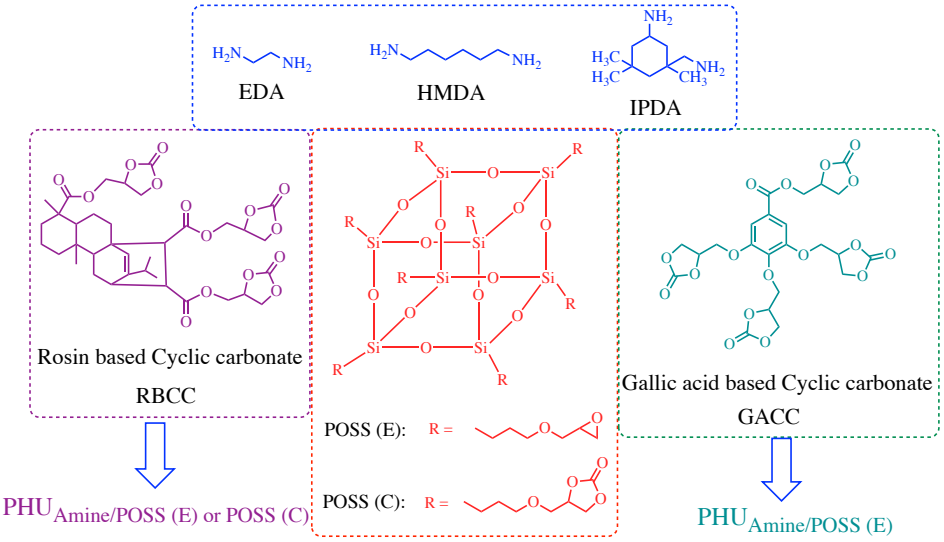

Figure 23. Synthesis of rosin and gallic acid rosin based neat reinforced PHU_{POSS} thermosets.[111,189]

Blattmann *et al.*[178] tailored optically transparent and scratch-resistant nanocomposite PHU coatings for glass from blends of cyclic carbonates-functional polydisperse POSS (mixture of POSS with different cage dimensions), trimethylolpropane glycidyl ether-based cyclic carbonate (TMPGC) and diamines (HMDA or IPDA), Figure 24. The three-component formulation was mixed under solvent-free conditions at 60 °C for 20 to 60 s before deposition of a 0.5 mm thick film onto glass using a bar coater. The formulation was cured for 14h at 80 °C followed by a post-curing treatment for 4h at 100 °C. As generally observed, the Tg of thermosets made from HMDA (Tg ~ 60 °C) were lower than the one of PHU made from rigid IPDA (Tg ~ 95 °C) and further addition of POSS fillers had no significant impact on the Tg values. The Young's moduli of neat PHU thermosets increased from 1600 MPa to 3800 MPa by substituting HMDA for IPDA and further increased to 2800 MPa and 4000 MPa upon addition of POSS. Similar evolution pervaded for the stress at break with values evolving from 44

MPa to 72 MPa for TMPGC/HMDA and TMPGC/HMDA/POSS systems and from 15 MPa and 40 MPa for TMPGC/IPDA and TMPGC/IPDA/POSS formulations, respectively. The scratch resistance of neat and nanocomposite coatings was evaluated by monitoring the surface gloss after 200 double strokes made with an abrasive nonwoven. For reference systems made of TMPGC and HMDA or IPDA, the gloss decreased respectively to 21% and 35% of the initial values. Addition of POSS (cyclic carbonate content of 40 mol%) within the TMPGC/diamine formulation clearly gave rise to coating with scratch resistance that retained 85% (with HMDA) and 56% (with IPDA) of their initial gloss.

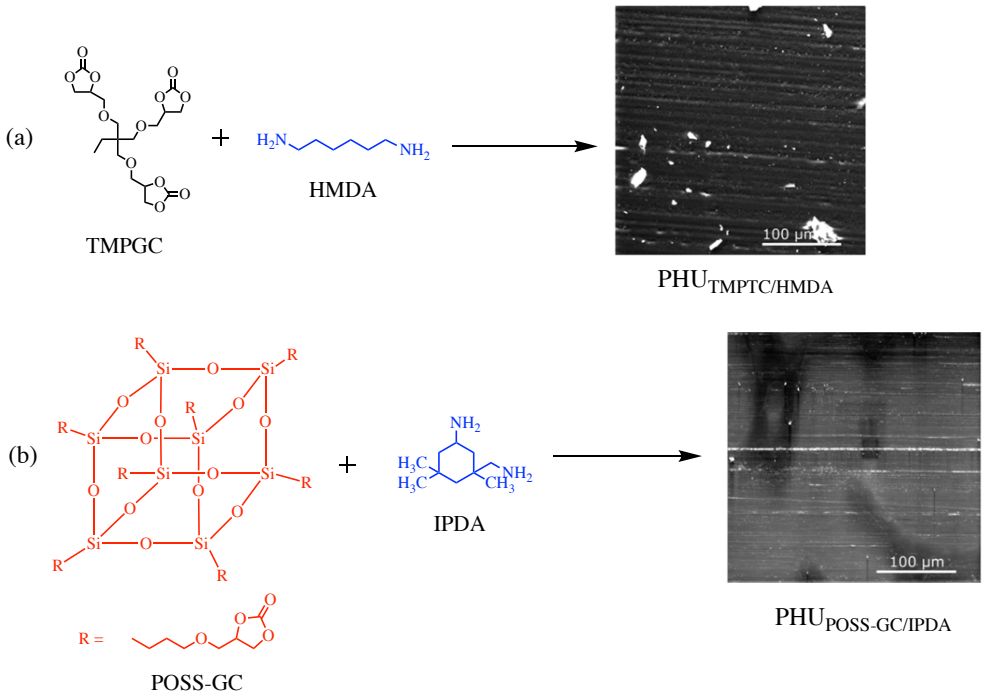

Figure 24: SEM images of scratched PHU/POSS hybrid coatings after scratching stress with 200 double strokes with an abrasive nonwoven: (a) TMPGC/HMDA and (b) POSS-GC/IPDA.[178]

I.5.7 PHU coatings for anticorrosion

PHUs can act as a diffusion barrier to oxygen, H^+ ions or water making them suitable to design corrosion protective coatings. The anticorrosive performance of neat PHUs,[190] nanocomposites PHUs[138,191] or hybrid epoxy-hydroxyurethane resins[192] have been examined on steel. Pathak *et al.*[190] designed 40–55 thick PHUs coatings from cyclic carbonated derived from modified fatty acid (CTEFA) and aliphatic (HMDA), cyclo-aliphatic (IPDA) and aromatic (DDS) diamines. The cyclic carbonate/amine compositions were mixed in a xylene/MEK mixture of solvents and cured for 1 h at 140 ^{0}C. All coatings displayed 100% adhesion, as measured by the tape adhesion method, pencil hardness higher than H, good flexibility (no visible cracks) and impact resistance (70.86 lbs-inch) as well as resistance to acid (5% HCl) with no blistering or loss or gloss. Unlike acidic conditions, the ester bonds of the fatty acid-derived carbonate monomer are susceptible for saponification in alkali medium (5% NaOH), resulting in coatings with blistering and loss of gloss. Detailed anticorrosive performances were investigated by potentio-dynamic polarization studies and electrochemical impedance spectroscopy (EIS). The coating applied onto a metal substrate is usually considered as an insulation layer with good electrical resistance. Upon exposure to 3.5% NaCl solution, the corrosion potential is likely to decrease as the film is swollen by the liquid. The crosslinking density, the film rigidity and hydrophobicity are then key properties to be tuned to tailor effective PHUs anticorrosion coatings. PHU formulations made from the aromatic diamine DDS showed a potential value (E) of – 436.54 mV and a low current corrosion (I_{corr}) value of 0.1197 µA, respectively. Changing the DDS hardener by IPDA or HMDA affected the barrier performances of the coatings with, respectively, a decrease of the E values to – 483.866 and – 488.94 mV and an increase of the I_{corr} to 3.921 and 9.6253 µA. This study highlighted a clear anticorrosion performances/amine hardener structure relationship. While PHU coatings cured with aromatic hardeners were highly rigid and displayed excellent protective barrier to the substrate by limiting the diffusion of the corrosive solution within the polymer layer, systems cured with the aliphatic diamine (HMDA) are less efficient due to the presence of pores within the PHU and the permeable nature of the films.

Wazarkar *et al.*[192] benchmarked the anticorrosion performances of MEK/xylene-based epoxy-hydroxyurethane hybrid coatings to the ones of analogue pure epoxy systems. Hydroxy-urethane adducts made from 1eq. of propylene carbonate and 1 eq. of ethylenediamine were further reacted with an excess of epoxy monomer before blending with different amines (Isophoronediamine-IPDA, Jeffamine®T-403 and diaminodiphenylmethane-DDM) and curing at 120 ^{0}C for 15–20 min. Whatever the diamine hardener, the resultant hybrid coatings showed properties comparable to the ones of pure epoxy-systems with an excellent 5B cross-cut adhesion, pull-off adhesion values above 2.5 MPa (with a maximum for coatings cured with Jeffamine®T-403 with a value of 2.84 MPa), resistance against xylene with double rubs > 200 and pencil hardness between 4H and 6H. But, they were found less flexible than analogue epoxy systems and showed lower resistance against abrasion or MEK solvent. Both hybrid and pure epoxy systems displayed similar and excellent resistance to acidic or alkali media with no visible defects after 24h immersion in 5% HCl or NaOH aqueous solution. The anti-corrosion performances of the coatings were evaluated by the NaCl salt-spray and EIS methods. From comparative experiments, DDM-cured systems showed the best resistance against corrosions after 500 h of immersion in a salt-spray chamber at 35 °C but the corrosion was more pronounced for epoxy-urethane hybrid coatings. Interestingly, unlike epoxy coatings that were easily etched out from the surface after the salt-spray test, IPDA and Jeffamine®T-403-cured hybrid systems still retained 3B and 4B adhesion after the corrosion test thanks to the presence of the extra OH linkages. For both epoxy or hybrid resins, EIS experiments conducted in 5% NaCl solution for 120 h confirmed the previously reported trend suggesting that an aromatic amine hardener should be preferred for designing high performance anti-corrosion coatings. Comparatively, the hybrid coatings clearly displayed superior barrier protection against corrosion than analogue epoxy films with a 140% lower E values (E = – 126.61 mV or –182.52 mV for DDM-cured hybrid or epoxy systems, respectively) and a 29-fold decrease of the corrosion current value (I_{corr} = 0.0008537 µA and 0.00283 µA for DDM-cured hybrid or epoxy systems, respectively) rendering lower corrosion rates

Nanocomposite epoxy-hydroxyurethane hybrid coatings for anticorrosion were designed by Kathalewar *et al.*[193]. Xylene/dimethyl carbonate solvent-based formulations composed of cyclic carbonate modified epoxy resin, 4,9-dioxadodecane-1,12-diamine and 1–3 w% of native or cyclic carbonate-functional ZnO fillers were cured at 70 ^{0}C for 30 min followed by an additional 1 h treatment at 135 ^{0}C. All coatings resisted to acids, base, MEK or boiling water treatments as attested by the absence of defects such as loss of gloss, dissolution/degradation of the polymer film… After 500 h of exposure to 5% NaCl salt spray at 35 °C, bare and all nanocomposite hybrid coatings retained their integrity with no visible damage in the film even if slight hints of corrosion are observed for the exposed surface (cross-cut voluntary made onto the surface prior the test). To highlight the beneficial impact of the filler and the influence of its surface functionalization on the barrier performances of the nanocomposites hybrid coatings, EIS measurements were realized for 120 h in 5% NaCl solution. As general trend, the progressive incorporation of the native filler within the coating increased the corrosion resistance with improved E and I_{corr} values that evolved from -748.45 mV and 0.0023411 µA for bare hybrid PHU to – 349.13 mV and 0.00072382 µA for coatings reinforced by 3w% of native ZnO. Dispersion of functional fillers further improved the anti-corrosion performances of the polymer layer with an increase of the E and I_{corr} values till – 335.16 mV and 0.000052142 µA in line with an improved cross-linking density that limits the diffusion of the solution within the film.

As last exemple, Rossi de Aguiar *et al.*[138] exploited in a synergistic manner the hydrophobic and flexible nature of PDMS in combination with a sol-gel process to construct corrosion resistant silica composite PHU coatings. Biscyclic carbonate PDMS was reacted with pure aminosilane as crosslinker or in blend with IPDA. Addition of phosphotungstic acid promoted i) the silane/silanol condensation and the formation of organo-modified silica at 70 °C within 20 to 40 min and ii) the condensation of the methoxysilane groups with – OH moieties of the substrate (glass, aluminium, steel…). Pull off adhesion from 0.9–1.7 MPa for metallic supports up to 7 MPa were obtained using these composite PHU coatings. The anticorrosive effect of the coating was demonstrated by EIS in basic, acidic and sea water media. The

corrosion potential evolved from – 60mV to – 34 mV and – 46 mV while I_{corr} varied from 0.041 µA to 1.06µA and 0.03µA respectively in acidic, basic or sea water solutions. The anticorrosion performances were drastically improved by adding heteropolyphosphotungstic acid as attested by a significant increase of the E values with concomitant decrease of the I_{corr}.

I.5.8 PHU coatings for antibacterial applications

A decade ago, Moeller exploited the cyclic carbonate/amine chemistry to design coatings with anti-bacterial properties. The two proposed strategies share a similar concept that lied in the post-modification of commercial polymers such as PDMS and poly(ethylene imine) (PEI) with quaternary ammonium moieties either at the polymer chain-ends or within the main backbone. This resulted in the formation of cationic polymers that could be deposited onto negatively charged substrates and provide coatings adherent via ionic interactions.

In the first approach, an α,ω-ammonium telechelic PDMS or a PDMS with quaternary ammonium moieties within the main skeleton were synthesized from α,ω-amino telechelic PDMS, a bis carbonate coupler and respectively a mono- or difunctional primary amine that also contain secondary or tertiary amine for later quaternization.[194] Solutions of the polymers in methanol were then casted by spin-coating onto treated glass. Microscopic studies revealed that the α,ω-ammonium telechelic PDMS self-assembled into layers onto the substrate as a result of the segregation of the hydrophilic cationic groups and the hydrophobic segments of PDMS. Upon water rinsing, the original film is lifted off to a large extend leaving only a PDMS monolayer of 0.7 nm with the cationic moieties oriented towards the surface while the polymer chains are folded such that the PDMS segment were directed outwards. Coatings made from PDMS containing the ammonium within the main chain were found thicker (20.4 nm) as the presence of the NR_4^+ moieties offered multiple anchoring points to the surface resulting in stronger film adhesion. As molecules containing cationic and hydrophobic groups display bacteriostatic and bactericide properties, the PDMS coated surfaces were tested for anti-bacterial effect on Gram-positive (*B.*

Subtilis) and Gram-negative (*E. Coli*) bacteria. α,ω-ammonium telechelic PDMS showed total inhibition effect on bacteria commencing at a 0.01 w% solution for *B. Subtilis* and 0.2 w% solution for *E. Coli.* By using PDMS with ammonium in the main chain, the anti-bacterial effect was much more pronounced with a total inhibition effect observed at 0.04 w% solution for *B. Subtilis* and 0.005 w% solution for *E. Coli*.

In the second approach, antimicrobial polycations were synthesized via a one-step one-pot multi-functionalization of PEI. Primary amines of PEI were reacted with a mixture of quaternary ammonium functionalized ethylene carbonate, Figure 25.[195,196] and benzyl-, C_8- or C_{12}- alkyl and/or allyl- bearing 5-membered cyclic carbonates. Solutions in methanol of series of modified PEI bearing ammonium groups and dodecyl chains in a 8:2 molar ratio, ammonium group and octyl chains in a 1:1 molar ratio or ammonium group or dodecyl chains and cross-linkable allyl moieties in a 1:1:2 were casted on glass (eventually cured with AIBN for 18h for PEI containing allyl groups). All water insoluble coatings show a growth inhibition of Gram-positive and Gram-negative bacteria above 95% that even reached 99% for the crosslinked PEI structure. However, leaching out the polymer from the surface was observed, preventing the authors to tailor highly adherent antibacterial coatings with long lasting properties.

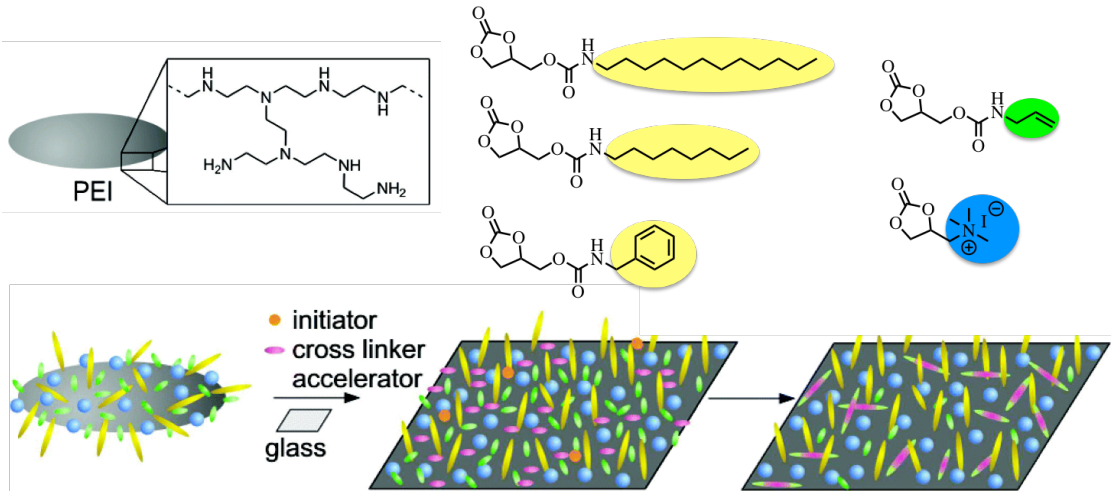

Figure 25. Antibacterial multi-functional PEIs coating bearing crosslinkable allyl groups, quaternary ammonium groups and dodecyl chains.[195,196]

I.5.9 PHU Adhesives

Polymeric adhesives play a vital role in our daily life in post-it notes, packaging, textile, furniture, construction, medical, sports, microelectronics, automotive, airplane assemblies … thanks to their efficient bonding strength, design flexibility, durability and cost effectiveness etc.[197,198] Recent studies revealed that multiple factors influence the bonding performances and includes the proper choice of the monomers and additives, the viscoelastic and flow behaviours, the surface wettability, the curing conditions (time and temperature), the crosslinking density, the frictional and cohesive strength, the thickness, the morphology, the dangling functional groups, the interactions at the molecular level, the load bearing capacity, the dissipative energies of bonded joints ...[71,125,199–201]. Various PHUs formulations have been examined to design isocyanate-free polyurethane adhesives for metal, glass, wood or plastic substrates. The novel interest for these novel adhesives, even at the industrial level, is illustrated by Moeller's patent from Henkel who reported on two-component PHU formulations for adhesives.[202]

In 2016, Caillol [110] engineered series of PHU adhesives of various composition for glass, wood and epoxy-coated Al substrates. The adhesives were synthesized from trimethylolpropane triglycidyl carbonate, polyethyleneglycol diglycidylcarbonate, polypropylene oxide diglycidylcarbonate and EDR-148 diamine or 1,3-cyclohexanebis(methylamine) (CMBA) hardeners. All formulations were pre-cured at 80 ^{0}C for 12 h followed by a post-curing treatment of 30 min at 150 ^{0}C. For Al-Al sticking, all PHU glues showed adhesive failure and lap shear adhesion in the range of 0.5 to 3 MPa. The shear force was increased up to 15 MPa for the sticking of wood substrates with PHU adhesives made from TMPTC/ polypropylene oxide diglycidylcarbonate/CMBA. Increasing the content of flexible chains within the PHU formulation or changing CMBA by EDR-148 induced a lowering of the adhesion strength but all PHU underwent preferable cohesive failure. For glass-glass sticking, the PHU joints were found more resistant than the substrate. The excellent adhesives properties of PHUs for wood and glass were assigned to synergistic Van der Walls interactions between the polymer and the support and hydrogen bond between the –OH

moieties of the PHUs and the Si–O or –OH groups at the surface of glass and wood, respectively. For all substrates, the adhesives performances of PHUs were benchmarked to the ones of isocyanates-based PU and found equal or even superior. Adhesive joint performances of dimethyl succinate-based amide backbone PHUs for wood were briefly examined by Tryznowski et al.[203] They correlated the shear adhesion to the tensile strength and Young modulus of the PHUs and concluded that high tensile strength and Young modulus values disfavoured the tailoring of glues with high adhesion parameters.

Silica composite PHU coatings made by Rossi de Aguiar *et al.*[138] for anti-corrosion application, were also tested for affixing glass-glass or dissimilar glass-Al substrates. The lap shear strength of adhesives reached values up to 3 MPa for Gl-Gl and 1.5 MPa for Gl-Al. For the dissimilar glass-Al substrates, he noted that the shear adhesion increased with the aminosilane content of the PHU formulations and all PHUs retained 50% of their adhesive properties till temperature up to 160 °C.

I.6 CONCLUSION

This chapter summarized the state-of-the art and recent advances in the field of isocyanates-free PU coatings and adhesives made from the cyclic carbonate/amine chemistry. It highlighted the most relevant strategies to design solvent-based, solvent-free, hybrid, latexes or (nano)composites formulations and how to exploit the inherent properties of these new materials to impart additional functionalities to various substrates such as anti-scratches, anti-corrosion or anti-bacterial properties. However, despite the carbonate/amine chemistry for PHU synthesis is known from decades, the scope of application still remains at its infancy and severe hurdles still need to be surpassed to tailor formulations that could compete with commercial PU solutions. The next challenges in PHU adhesives and coatings should address solutions to provide formulations able to cure under ambient conditions in short times and provide colourless materials. The quest for formulations reducing the hydrophilicity of the polymers is a necessity to prevent the PHU delamination from the substrates and provide coating/adhesive long lasting properties. From a fundamental view, in-depth comprehension of the mechanisms and forces entering in the adhesion process of PHUs onto various substrates should facilitate the design of novel marketable formulations. Finally, standard(ized) characterisation procedures for evaluating the PHU performances in coating and adhesive should be established for a proper and easy benchmarking of the PHU performances with commercial and/or existing materials reported in the literature for the envisioned applications.

I.7 REFERENCES

1 K. Dilger, B. Burchardt and M. Frauenhofer, *Automotive Industry*, Springer International Publishing, 2018.

2 U. T. Kreibich and A. F. Marcantonio, *J. Adhes.*, 1987, **22**, 153–165.

3 A. F. Santos, H. Wiebeck, R. M. Souza and C. G. Schön, *Polym. Test.*, 2008, **27**, 632–637.

4 D. Driver, *Adhesive bonding for aerospace applications*, Springer Netherlands, 1995, vol. 4.

5 C. M. Bhuvaneswari, S. S. Kale, G. Gouda, P. Jayapal and K. Tamilmani, *Elastomers and Adhesives for Aerospace Applications*, 2017.

6 J. Bishopp, *Adhesives for Aerospace Structures*, Elsevier, 2011, vol. 1.

7 C. Désagulier, P. Pérés and G. Larnac, *Aerospace Industry*, Springer International Publishing, 2018.

8 C. Severijns, S. T. de Freitas and J. A. Poulis, *Int. J. Adhes. Adhes.*, 2017, **75**, 155–164.

9 E. N. Lopukhina, *Polym. Sci. Ser. D*, 2011, **4**, 50–52.

10 W.-B. Tsai, W.-T. Chen, H.-W. Chien, W.-H. Kuo and M.-J. Wang, *J. Biomater. Appl.*, 2014, **28**, 837–848.

11 W. A. Lees, Springer Berlin Heidelberg, Berlin, Heidelberg, 1984, vol. 211, pp. 307–335.

12 R. Ravichandran, S. Sundarrajan, J. R. Venugopal, S. Mukherjee and S. Ramakrishna, *Macromol. Biosci.*, 2012, **12**, 286–311.

13 A.-D. Bendrea, L. Cianga and I. Cianga, *J. Biomater. Appl.*, 2011, **26**, 3–84.

14 T. J. Deming, *Prog. Polym. Sci.*, 2007, **32**, 858–875.

15 R. L. Mcconnell, M. F. Meyer, F. D. Petke and W. A. Haile, *J. Coat. Fabr.*, 1987, **16**, 199–208.

16 K. N. Ulman and S. R. Shukla, *Adv. Polym. Technol.*, 2016, **35**, 307–325.

17 L. D'Arienzo, G. Gentile, E. Martuscelli, C. Polcaro and L. D'Orazio, *Text. Res. J.*, 2004, **74**, 281–291.

18 J. E. Morris and L. Wang, *Isotropic Conductive Adhesive Interconnect Technology in Electronics Packaging Applications*, John Wiley & Sons, 2014.

19 R. Muthuraj, M. Misra and A. K. Mohanty, *J. Appl. Polym. Sci.*, 2018, **135**, 45726–45761.

20 L. Cao, S. Li, Z. Lai and J. Liu, *J. Electron. Mater.*, 2005, **34**, 1420–1427.

21 S. J. Shaw, *Mater. Sci. Technol.*, 1987, **3**, 589–599.

22 D. Satas, *Pressure-Sensitive Adhesives and Adhesive Products*, CRC Press, 2006.

23 H. G. Schmelzer, *J. Coat. Fabr.*, 1988, **17**, 167–182.

24 B. Richey and M. Burch, *Applications for Decorative and Protective Coatings*, Wiley-VCH, 2002, vol. 7.

25 J. R. Smith and D. A. Lamprou, *Trans. IMF*, 2014, **92**, 9–19.

26 P. C. Briggs and G. L. Jialanella, in *Advances in Structural Adhesive Bonding*, Elsevier, 2010, pp. 132–150.

27 K. J. Abbey, *Advances in epoxy adhesives*, Elsevier, 2010.

28 S. J. Shaw, *Polym. Int.*, 1996, **41**, 193–207.

29 F.-L. Jin, X. Li and S.-J. Park, *J. Ind. Eng. Chem.*, 2015, **29**, 1–11.

30 B. Hussey and J. Wilson, *Epoxy Adhesives*, Springer US, 1996.

31 A. J. Kinloch, *MRS Bull.*, 2003, **28**, 445–448.

32 A. S. Subramanian, J. N. Tey, L. Zhang, B. H. Ng, S. Roy, J. Wei and X. M. Hu, *Polymer (Guildf).*, 2016, **82**, 285–294.

33 L. Ma, E. Zhang and Q. Li, *J. Adhes. Sci. Technol.*, 2000, **14**, 1355–1362.

34 A. M. Motawie and E. M. Sadek, *Polym. Adv. Technol.*, 1999, **10**, 223–228.

35 F. L. Tobiason, *Phenolic Resin Adhesives*, Springer US, 1990.

36 P. Potin and C. Leblanc, *Phenolic-based Adhesives of Marine Brown Algae*, Springer Berlin Heidelberg, 2006.

37 J. L. Paris, F. A. Kamke, R. Mbachu and S. K. Gibson, *J. Mater. Sci.*, 2014, **49**, 580–591.

38 S. Kalami, M. Arefmanesh, E. Master and M. Nejad, *J. Appl. Polym. Sci.*, 2017, **134**, 45124.

39 M. R. Haddon and T. J. Smith, *Int. J. Adhes. Adhes.*, 1991, **11**, 183–186.

40 S. Kawasaki, G. Nakajima, K. Haraga and C. Sato, *J. Adhes.*, 2016, **92**, 517–534.

41 H.-S. Do, S.-E. Kim and H.-J. Kim, *Preparation and Characterization of UV-Crosslinkable Pressure-Sensitive Adhesives*, Wiley-VCH, 2006.

42 Z. Czech, A. Kowalczyk, J. Kabatc and J. Świderska, *Eur. Polym. J.*, 2012, **48**, 1446–1454.

43 S. H. Lee, R. You, Y. Il Yoon and W. H. Park, *Int. J. Adhes. Adhes.*, 2017, **75**, 190–195.

44 B. K. Ahn, J. Sung, N. Rahmani, G. Wang, N. Kim, K. Lease and X. S. Sun, *J. Adhes.*, 2013, **89**, 323–338.

45 C. Strobech, *Constr. Build. Mater.*, 1990, **4**, 214–217.

46 I. V Kochurov and N. V Gubskaya, *Polym. Sci. Ser. D*, 2011, **4**, 292–294.

47 F. Beaud, P. Niemz and A. Pizzi, *J. Appl. Polym. Sci.*, 2006, **101**, 4181–4192.

48 V. Kovačević, I. Šmit, D. Hace, M. Sućeska, I. Mudri and M. Bravar, *Int. J. Adhes. Adhes.*, 1993, **13**, 126–136.

49 S. Clauβ, K. Allenspach, J. Gabriel and P. Niemz, *Wood Sci. Technol.*, 2011, **45**, 383–388.

50 B. Hussey and J. Wilson, *Polyurethane Adhesives*, Springer US, 1996.

51 F. E. Golling, R. Pires, A. Hecking, J. Weikard, F. Richter, K. Danielmeier and D. Dijkstra, *Polym. Int.*, , DOI:10.1002/pi.5665.

52 M. F. Sonnenschein, *Polyurethane Adhesives and Coatings*, John Wiley & Sons, 2014, vol. l.

53 F. Arán-Aís, A. M. Torró-Palau, A. C. Orgilés-Barceló and J. M. Martín-Martínez, *J. Adhes. Sci. Technol.*, 2002, **16**, 1431–1448.

54 J. G. Quini and G. Marinucci, *Mater. Res.*, 2012, **15**, 434–439.

55 D. J. Zalucha and K. J. Abbey, *The Chemistry of Structural Adhesives: Epoxy, Urethane, and Acrylic Adhesives*, Springer US, 2007.

56 B. N. J. Persson and M. Scaraggi, *J. Chem. Phys.*, 2014, **141**, 124701–124716.

57 T. Hata, *J. Adhes.*, 1972, **4**, 161–170.

58 A. J. Kinloch, *Mechanical behaviour of adhesive joints*, Springer Netherlands, 1987.

59 H.-J. Kim, D.-H. Lim, H.-D. Hwang and B.-H. Lee, *Handb. Adhes. Technol.*, 2018, 319–343.

60 L. F. M. da Silva, A. Öchsner and R. D. Adams, *Introduction to Adhesive Bonding Technology*, Springer Berlin Heidelberg, 2011.

61 D. E. Packham, *Handbook of Adhesion*, John Wiley & Sons, 2005.

62 A. Baldan, *J. Mater. Sci.*, 2004, **39**, 1–49.

63 C. Ochoa-Putman and U. K. Vaidya, *Compos. Part A Appl. Sci. Manuf.*, 2011, **42**, 906–915.

64 T. Sugama, L. E. Kukacka, N. Carciello and J. B. Warren, *J. Mater. Sci.*, 1987, **22**, 722–736.

65 L.-H. Lee, *J. Adhes. Sci. Technol.*, 1993, **7**, 583–634.

66 K. W. Allen, *Int. J. Adhes. Adhes.*, 1994, **14**, 69.

67 C. A. Deckert and D. A. Peters, *Adhesion, Wettability, and Surface Chemistry*, Springer US, 1983.

68 D. E. Packham, *J. Adhes.*, 1992, **39**, 137–144.

69 D. . Packham, *Int. J. Adhes. Adhes.*, 2003, **23**, 437–448.

70 A. N. Gent and C. W. Lin, *J. Adhes.*, 1990, **32**, 113–125.

71 J. A. von Fraunhofer, *Int. J. Dent.*, 2012, **2012**, 1–8.

72 G. J. Yang, C. J. Li, C. X. Li, K. Kondoh and A. Ohmori, *J. Therm. Spray Technol.*, 2013, **22**, 36–47.

73 M. Perton, S. Costil, W. Wong, D. Poirier, E. Irissou, J.-G. Legoux, A. Blouin and S. Yue, *J. Therm. Spray Technol.*, 2012, **21**, 1322–1333.

74 J. B. Rosenholm, K.-E. Peiponen and E. Gornov, *Adv. Colloid Interface Sci.*, 2008, **141**, 48–65.

75 B. N. Balzer, M. Gallei, K. Sondergeld, M. Schindler, P. Müller-Buschbaum, M. Rehahn and T. Hugel, *Macromolecules*, 2013, **46**, 7406–7414.

76 S. Vicini, E. Princi, E. Pedemonte and G. Moggi, *Surface Treatment*, Springer Netherlands, 2006.

77 H. K. Tönshoff, A. Mohlfeld, I. Oberbeck-Spintig and C. Marzenell, *Surf. Eng.*, 1998, **14**,

339–345.

78 Z. Sanaee, S. Mohajerzadeh, K. Zand, F. S. Gard and H. Pajouhi, *Appl. Surf. Sci.*, 2011, **257**, 2218–2225.

79 S.-H. Han, B.-J. Kim and J.-S. Park, *Surf. Coatings Technol.*, 2015, **271**, 100–105.

80 L. Ernesto Mendoza-Navarro, A. Diaz-Diaz, R. Castañeda-Balderas, S. Hunkeler and R. Noret, *Int. J. Adhes. Adhes.*, 2013, **44**, 36–47.

81 Z. Suo, *Appl. Mech. Rev.*, 1990, **43**, 276–279.

82 J. Du, F. T. Salmon and A. V. Pocius, *J. Adhes. Sci. Technol.*, 2004, **18**, 287–299.

83 A. D. Crocombe, D. A. Bigwood and G. Richardson, *Int. J. Adhes. Adhes.*, 1990, **10**, 167–178.

84 S. Doley and S. K. Dolui, *Eur. Polym. J.*, 2018, **102**, 161–168.

85 K. Zhang, A. M. Nelson, S. J. Talley, M. Chen, E. Margaretta, A. G. Hudson, R. B. Moore and T. E. Long, *Green Chem.*, 2016, **18**, 4667–4681.

86 M. S. Kathalewar, P. B. Joshi, A. S. Sabnis and V. C. Malshe, *RSC Adv.*, 2013, **3**, 4110–4129.

87 G. Hibert, O. Lamarzelle, L. Maisonneuve, E. Grau and H. Cramail, *Eur. Polym. J.*, 2016, **82**, 114–121.

88 A. Lee and Y. Deng, *Eur. Polym. J.*, 2015, **63**, 67–73.

89 O. Lamarzelle, P.-L. Durand, A.-L. Wirotius, G. Chollet, E. Grau and H. Cramail, *Polym. Chem.*, 2016, **7**, 1439–1451.

90 Z. Karami, M. J. Zohuriaan-Mehr and A. Rostami, *J. CO2 Util.*, 2017, **18**, 294–302.

91 L. Maisonneuve, O. Lamarzelle, E. Rix, E. Grau and H. Cramail, *Chem. Rev.*, 2015, **115**, 12407–12439.

92 V. Froidevaux, C. Negrell, S. Caillol, J.-P. Pascault and B. Boutevin, *Chem. Rev.*, 2016, **116**, 14181–14224.

93 O. Figovsky, A. Leykin and L. Shapovalov, *Altern. Energy Ecol.*, 2016, **4**, 95–108.

94 E. Delebecq, J. Pascault, B. Boutevin and F. Ganachaud, *Chem. Rev.*, 2013, **113**, 80–118.

95 A. Cornille, R. Auvergne, O. Figovsky, B. Boutevin and S. Caillol, *Eur. Polym. J.*, 2017, **87**, 535–552.

96 D. K. Chattopadhyay and K. V. S. N. Raju, *Prog. Polym. Sci.*, 2007, **32**, 352–418.

97 D. Adhikari, A. W. Miller, M.-H. Baik and S. T. Nguyen, *Chem. Sci.*, 2015, **6**, 1293–1300.

98 P. Tascedda and E. Duñach, *Chem. Commun.*, 2000, 449–450.

99 C.-S. Cao, Y. Shi, H. Xu and B. Zhao, *Dalt. Trans.*, 2018, **47**, 4545–4553.

100 H. Matsukizono and T. Endo, *Polym. Chem.*, 2016, **7**, 958–969.

101 B. Liu, H. Tian and L. Zhu, *J. Appl. Polym. Sci.*, 2015, **132**, 42804–42812.

102 N. Kébir, S. Nouigues, P. Moranne and F. Burel, *J. Appl. Polym. Sci.*, 2017, **134**, 44991–

45000.

103 P. Deepa and M. Jayakannan, *J. Polym. Sci. Part A Polym. Chem.*, 2008, **46**, 2445–2458.

104 L. Maisonneuve, O. Lamarzelle, E. Rix, E. Grau and H. Cramail, *Chem. Rev.*, 2015, **115**, 12407–12439.

105 E. Delebecq, J.-P. Pascault, B. Boutevin and F. Ganachaud, *Chem. Rev.*, 2013, **113**, 80–118.

106 L. Poussard, J. Mariage, B. Grignard, C. Detrembleur, C. Jérôme, C. Calberg, B. Heinrichs, J. De Winter, P. Gerbaux, J.-M. Raquez, L. Bonnaud and P. Dubois, *Macromolecules*, 2016, **49**, 2162–2171.

107 B. Grignard, J.-M. Thomassin, S. Gennen, L. Poussard, L. Bonnaud, J.-M. Raquez, P. Dubois, M.-P. Tran, C. B. Park, C. Jerome and C. Detrembleur, *Green Chem.*, 2016, **18**, 2206–2215.

108 A. Salanti, L. Zoia, M. Mauri and M. Orlandi, *RSC Adv.*, 2017, **7**, 25054–25065.

109 A. R. Mahendran, G. Wuzella, N. Aust and U. Müller, *J. Coatings Technol. Res.*, 2014, **11**, 329–339.

110 A. Cornille, G. Michaud, F. Simon, S. Fouquay, R. Auvergne, B. Boutevin and S. Caillol, *Eur. Polym. J.*, 2016, **84**, 404–420.

111 G. Liu, G. Wu, J. Chen and Z. Kong, *Prog. Org. Coatings*, 2016, **101**, 461–467.

112 M. Fleischer, H. Blattmann and R. Mülhaupt, *Green Chem.*, 2013, **15**, 934–942.

113 G. Beniah, X. Chen, B. E. Uno, K. Liu, E. K. Leitsch, J. Jeon, W. H. Heath, K. A. Scheidt and J. M. Torkelson, *Macromolecules*, 2017, **50**, 3193–3203.

114 Z. Ma, C. Li, H. Fan, J. Wan, Y. Luo and B.-G. Li, *Ind. Eng. Chem. Res.*, 2017, **56**, 14089–14100.

115 Z. Wu, W. Cai, R. Chen and J. Qu, *Prog. Org. Coatings*, 2018, **119**, 116–122.

116 V. Besse, F. Camara, F. Méchin, E. Fleury, S. Caillol, J.-P. Pascault and B. Boutevin, *Eur. Polym. J.*, 2015, **71**, 1–11.

117 J. Guan, Y. Song, Y. Lin, X. Yin, M. Zuo, Y. Zhao, X. Tao and Q. Zheng, *Ind. Eng. Chem. Res.*, 2011, **50**, 6517–6527.

118 H. Blattmann, M. Fleischer, M. Bähr and R. Mülhaupt, *Macromol. Rapid Commun.*, 2014, **35**, 1238–1254.

119 S. Schmidt, F. J. Gatti, M. Luitz, B. S. Ritter, B. Bruchmann and R. Mülhaupt, *Macromolecules*, 2017, **50**, 2296–2303.

120 C. Carré, L. Bonnet and L. Avérous, *RSC Adv.*, 2014, **4**, 54018–54025.

121 L. Maisonneuve, A. S. More, S. Foltran, C. Alfos, F. Robert, Y. Landais, T. Tassaing, E. Grau and H. Cramail, *RSC Adv.*, 2014, **4**, 25795–25803.

122 E. Rix, E. Grau, G. Chollet and H. Cramail, *Eur. Polym. J.*, 2016, **84**, 863–872.

123 O. Lamarzelle, G. Hibert, S. Lecommandoux, E. Grau and H. Cramail, *Polym. Chem.*, 2017,

8, 3438–3447.

124 E. Dolci, G. Michaud, F. Simon, B. Boutevin, S. Fouquay and S. Caillol, *Polym. Chem.*, 2015, **6**, 7851–7861.

125 S. Panchireddy, J.-M. Thomassin, B. Grignard, C. Damblon, A. Tatton, C. Jerome and C. Detrembleur, *Polym. Chem.*, 2017, **8**, 5897–5909.

126 S. Schmidt, N. E. Göppert, B. Bruchmann and R. Mülhaupt, *Eur. Polym. J.*, 2017, **94**, 136–142.

127 S. Schmidt, B. S. Ritter, D. Kratzert, B. Bruchmann and R. Mülhaupt, *Macromolecules*, 2016, **49**, 7268–7276.

128 R. Ménard, S. Caillol and F. Allais, *ACS Sustain. Chem. Eng.*, 2017, **5**, 1446–1456.

129 M. Bähr and R. Mülhaupt, *Green Chem.*, 2012, **14**, 483–489.

130 V. Schimpf, B. S. Ritter, P. Weis, K. Parison and R. Mülhaupt, *Macromolecules*, 2017, **50**, 944–955.

131 M. Bähr, A. Bitto and R. Mülhaupt, *Green Chem.*, 2012, **14**, 1447–1454.

132 A. Cornille, C. Guillet, S. Benyahya, C. Negrell, B. Boutevin and S. Caillol, *Eur. Polym. J.*, 2016, **84**, 873–888.

133 A. Cornille, S. Dworakowska, D. Bogdal, B. Boutevin and S. Caillol, *Eur. Polym. J.*, 2015, **66**, 129–138.

134 S. Gennen, B. Grignard, J.-M. Thomassin, B. Gilbert, B. Vertruyen, C. Jerome and C. Detrembleur, *Eur. Polym. J.*, 2016, **84**, 849–862.

135 E. Rix, G. Ceglia, J. Bajt, G. Chollet, V. Heroguez, E. Grau and H. Cramail, *Polym. Chem.*, 2015, **6**, 213–217.

136 L. Meng, X. Wang, M. Ocepek and M. D. Soucek, *Polymer (Guildf).*, 2017, **109**, 146–159.

137 X. Wang and M. D. Soucek, *Prog. Org. Coatings*, 2013, **76**, 1057–1067.

138 K. M. F. Rossi de Aguiar, E. P. Ferreira-Neto, S. Blunk, J. F. Schneider, C. A. Picon, C. M. Lepienski, K. Rischka and U. P. Rodrigues-Filho, *RSC Adv.*, 2016, **6**, 19160–19172.

139 L. Han, J. Dai, L. Zhang, S. Ma, J. Deng, R. Zhang and J. Zhu, *RSC Adv.*, 2014, **4**, 49471–49477.

140 S. Ma, E. P. A. van Heeswijk, B. A. J. Noordover, R. J. Sablong, R. A. T. M. van Benthem and C. E. Koning, *ChemSusChem*, 2018, **11**, 149–158.

141 S. Ma, C. Chen, R. J. Sablong, C. E. Koning and R. A. T. M. van Benthem, *J. Polym. Sci. Part A Polym. Chem.*, 2018, **56**, 1078–1090.

142 S. Doley and S. K. Dolui, *Eur. Polym. J.*, 2018, **102**, 161–168.

143 X. He, X. Xu, Q. Wan, G. Bo and Y. Yan, *Polymers (Basel).*, 2017, **9**, 649.

144 G. A. Phalak, D. M. Patil and S. T. Mhaske, *Eur. Polym. J.*, 2017, **88**, 93–108.

145 M. Wehbi, S. Banerjee, A. Mehdi, A. Alaaeddine, A. Hachem and B. Ameduri,

Macromolecules, 2017, **50**, 9329–9339.

146 G. Liu, G. Wu, J. Chen, S. Huo, C. Jin and Z. Kong, *Polym. Degrad. Stab.*, 2015, **121**, 247–252.

147 S. Panchireddy, J.-M. Thomassin, B. Grignard, C. Damblon, A. Tatton, C. Jerome and C. Detrembleur, *Polym. Chem.*, 2017, **8**, 5897–5909.

148 S. Panchireddy, B. Grignard, J.-M. Thomassin, C. Jerome and C. Detrembleur, *Polym. Chem.*, 2018, **9**, 2650–2659.

149 E. K. Leitsch, W. H. Heath and J. M. Torkelson, *Int. J. Adhes. Adhes.*, 2016, **64**, 1–8.

150 M. Kathalewar and A. Sabnis, *J. Appl. Polym. Sci.*, 2015, **132**, 41391–41401.

151 M. Kathalewar, A. Sabnis and D. D'Mello, *Eur. Polym. J.*, 2014, **57**, 99–108.

152 F. E. Kalinina, D. M. Mognonov and L. D. Radnaeva, *Russ. J. Appl. Chem.*, 2008, **81**, 1302–1304.

153 D. C. Webster and A. L. Crain, *Prog. Org. Coatings*, 2000, **40**, 275–282.

154 S. Schmidt, B. S. Ritter, D. Kratzert, B. Bruchmann and R. Mülhaupt, *Macromolecules*, 2016, **49**, 7268–7276.

155 O. Figovsky, L. Shapovalov and F. Buslov, *Surf. Coatings Int. Part B Coatings Trans.*, 2005, **88**, 67–71.

156 J.-Z. Hwang, S.-C. Wang, P.-C. Chen, C.-Y. Huang, J.-T. Yeh and K.-N. Chen, *J. Polym. Res.*, 2012, **19**, 9900–9910.

157 O. Figovsky, L. Shapovalov and O. Axenov, *Surf. Coatings Int. Part B Coatings Trans.*, 2004, **87**, 83–90.

158 M. U. Kazuyuki Hanada, Kazuya Kimura, Kenichi Takahashi, Osamu Kawakami, *US20120232289 A1*, 2012.

159 J. V. Isabelle Muller-Frischinger, Michel Gianini, *US8263687 B2*, 2012.

160 L. S. Olga Birukov, Dmitry Beilin, Oleg Figovsky, Alexander Leykin, *US2010/0144966 A1*, 2010.

161 L. S. Olga Birukov, Dmitry Beilin, Oleg Figovsky, Alexander Leykin, *US7820779 B2*, 2010.

162 A. Cornille, J. Serres, G. Michaud, F. Simon, S. Fouquay, B. Boutevin and S. Caillol, *Eur. Polym. J.*, 2016, **75**, 175–189.

163 S. Anitha, K. P. Vijayalakshmi, G. Unnikrishnan and K. S. S. Kumar, *J. Mater. Chem. A*, 2017, **5**, 24299–24313.

164 S.-S. Choi, C. Nah and B.-W. Jo, *Polym. Int.*, 2003, **52**, 1382–1389.

165 L. S. A. Leykin, D. Beilin, O. Birukova, O. Figovsky, *J. Sci. Isr. – Technol. Advantages*, 2009, **11**, 160–190.

166 D. L. K. Constantinos D. Diakoumakos, *US8143346 B2*, 2012.

167 D. L. K. Constantinos D. Diakoumakos, *US2012/0149842 A1*, 2012.

168 D. A. Dillard, *Physical Properties of Adhesives*, Springer Berlin Heidelberg, 2011.

169 V. Ambrogi, C. Carfagna, P. Cerruti and V. Marturano, in *Modification of Polymer Properties*, Elsevier, 2017, pp. 87–108.

170 S. Pramanik and N. Karak, in *Properties and Applications of Polymer Nanocomposites*, eds. D. K. Tripathy and B. P. Sahoo, Springer Berlin Heidelberg, Berlin, Heidelberg, 2017, pp. 173–204.

171 C. Wong, J. Xu, L. Zhu, Y. Li, H. Jiang, Y. Sun, J. Lu and H. Dong, in *Conference on High Density Microsystem Design and Packaging and Component Failure Analysis*, IEEE, 2005, vol. 1, pp. 1–16.

172 S. Kango, S. Kalia, A. Celli, J. Njuguna, Y. Habibi and R. Kumar, *Prog. Polym. Sci.*, 2013, **38**, 1232–1261.

173 M. Z. Rong, M. Q. Zhang, Y. X. Zheng, H. M. Zeng, R. Walter and K. Friedrich, *Polymer (Guildf).*, 2001, **42**, 167–183.

174 E. Tang, H. Liu, L. Sun, E. Zheng and G. Cheng, *Eur. Polym. J.*, 2007, **43**, 4210–4218.

175 O. Türünç, N. Kayaman-Apohan, M. V. Kahraman, Y. Menceloğlu and A. Güngör, *J. Sol-Gel Sci. Technol.*, 2008, **47**, 290–299.

176 Z. Hosgor, N. Kayaman-Apohan, S. Karatas, A. Gungor and Y. Menceloglu, *Adv. Polym. Technol.*, 2012, **31**, 390–400.

177 H. Liu, Q. Zhu, L. Feng, B. Yao and S. Feng, *J. Mol. Struct.*, 2013, **1032**, 29–34.

178 H. Blattmann and R. Mülhaupt, *Macromolecules*, 2016, **49**, 742–751.

179 E. Ayandele, B. Sarkar and P. Alexandridis, *Nanomaterials*, 2012, **2**, 445–475.

180 H. Zhou, Q. Ye and J. Xu, *Mater. Chem. Front.*, 2017, **1**, 212–230.

181 W. Zhang, G. Camino and R. Yang, *Prog. Polym. Sci.*, 2017, **67**, 77–125.

182 D. K. Chattopadhyay and D. C. Webster, *Prog. Polym. Sci.*, 2009, **34**, 1068–1133.

183 I. Blanco, L. Abate, F. A. Bottino and P. Bottino, *Polym. Degrad. Stab.*, 2014, **102**, 132–137.

184 H. Yari, M. Mohseni and M. Messori, *RSC Adv.*, 2016, **6**, 76028–76041.

185 R. Sasi and M. Alagar, *RSC Adv.*, 2015, **5**, 33008–33015.

186 K. Tanaka and Y. Chujo, *Polym. J.*, 2013, **45**, 247–254.

187 J. Wu and P. T. Mather, *Polym. Rev.*, 2009, **49**, 25–63.

188 K. Tanaka and Y. Chujo, *J. Mater. Chem.*, 2012, **22**, 1733–1746.

189 G. Liu, G. Wu, J. Chen, S. Huo, C. Jin and Z. Kong, *Polym. Degrad. Stab.*, 2015, **121**, 247–252.

190 R. Pathak, M. Kathalewar, K. Wazarkar and A. Sabnis, *Prog. Org. Coatings*, 2015, **89**, 160–169.

191 M. Kathalewar, A. Sabnis and G. Waghoo, *Prog. Org. Coatings*, 2013, **76**, 1215–1229.

192 K. Wazarkar, M. Kathalewar and A. Sabnis, *Eur. Polym. J.*, 2016, **84**, 812–827.

193 M. Kathalewar, A. Sabnis and G. Waghoo, *Prog. Org. Coatings*, 2013, **76**, 1215–1229.

194 C. Novi, A. Mourran, H. Keul and M. Möller, *Macromol. Chem. Phys.*, 2006, **207**, 273–286.

195 N. Pasquier, H. Keul, E. Heine and M. Moeller, *Biomacromolecules*, 2007, **8**, 2874–2882.

196 N. Pasquier, H. Keul and M. Moeller, *Des. Monomers Polym.*, 2005, **8**, 679–703.

197 H.-W. Engels, H.-G. Pirkl, R. Albers, R. W. Albach, J. Krause, A. Hoffmann, H. Casselmann and J. Dormish, *Angew. Chemie Int. Ed.*, 2013, **52**, 9422–9441.

198 G. Otorgust, H. Dodiuk, S. Kenig and R. Tenne, *Eur. Polym. J.*, 2017, **89**, 281–300.

199 A. Lopez, E. Degrandi-Contraires, E. Canetta, C. Creton, J. L. Keddie and J. M. Asua, *Langmuir*, 2011, **27**, 3878–3888.

200 E. Degrandi-Contraires, A. Lopez, Y. Reyes, J. M. Asua and C. Creton, *Macromol. Mater. Eng.*, 2013, **298**, 612–623.

201 A. Lopez, E. Degrandi, E. Canetta, J. L. Keddie, C. Creton and J. M. Asua, *Polymer (Guildf).*, 2011, **52**, 3021–3030.

202 H.-G. K. Thomas Moeller, *US8118968 B2*.

203 M. Tryznowski, A. Świderska, T. Gołofit and Z. Żołek-Tryznowska, *RSC Adv.*, 2017, **7**, 30385–30391.

Aim of the thesis

The development of isocyanate-free polyurethanes has already inspired new chemistries presenting less toxicity and health issues and has demonstrated the potential of these materials to substitute conventional polyurethanes in various fields. In the recent years, the scope of polyhydroxyurethanes (PHUs) has been drastically increased by developing innovative and high molecular weight polymers for demanding applications. Indeed, the hydroxyl groups present on these PHU is of special interest for the design of novel adhesives and coatings thanks to their ability to bind the numerous surfaces. Nevertheless, only few reports describe PHUs thermoset adhesives and coatings.

The aim of the thesis is to develop well-defined innovative non-isocyanate polyurethanes and new formulations of adhesives that can compete with conventional more toxic ones (see Figure). This objective fits the aim of the FLYCOAT excellence program entitled "Transformation of CO_2 into High Performance Polyhydroxyurethane Adhesives and Coatings". Our strategy is based on the synthesis of a library of cyclic carbonates from CO_2 and biosourced molecules developing an efficient organocatalytic system, followed by the design and optimization of the aminolysis of these cyclic carbonates into polyhydroxyurethanes. This reaction will be investigated by rheology under solvent- and catalyst-free conditions, and the curing conditions will be optimized to obtain high performance thermoset materials including viscoelastic performance, solvent resistance, controlled water uptake, thermo-mechanical properties and adhesion to various substrates. We will also consider the introduction of functional fillers (ZnO and SiO_2) into the formulations to reinforce the material and improve the performance of end products.

The experimental work will be divided into three chapters focused on the synthesis of PHUs and applications. All chapters are written as articles already published (chapters II and III) and revision submitted (chapter IV) in international peer reviewed journals.

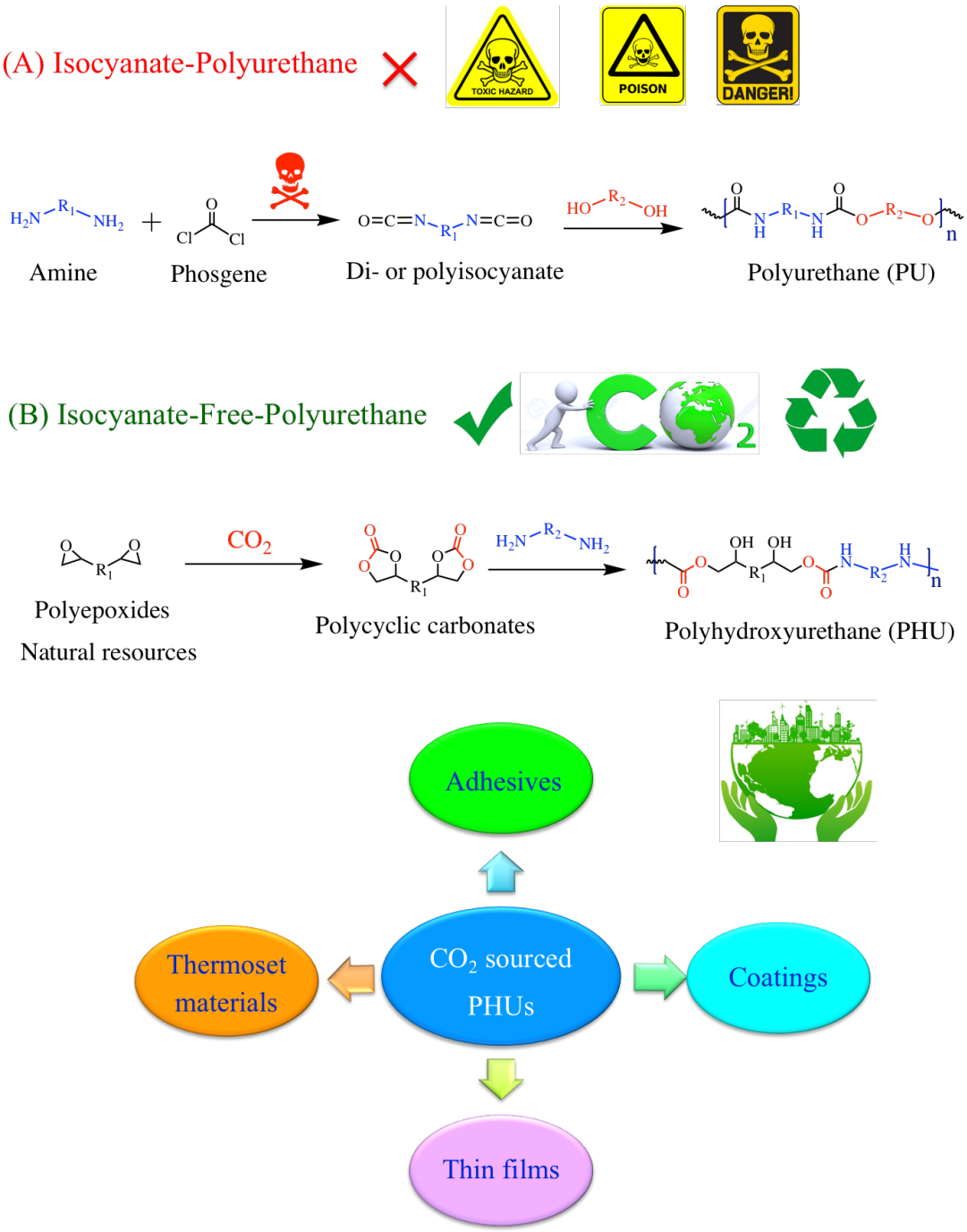

Figure. Thesis Aim to Produce Isocyanate-Free Polyurethanes for day-to-day life applications.

In **chapter-II**, we aim to develop solvent-free reinforced polyhydroxyurethane thermosets as high-performance adhesives and coatings for aluminum substrates. To achieve this goal, we first synthesised CO_2-sourced cyclic carbonates and functional (cyclic carbonate and epoxy) ZnO fillers and then established the curing conditions for the formulation of cyclic carbonates/amine/fillers *via* rheology. Herein, systematic studies of the influence of reinforced functional fillers on crosslinking densities were correlated with solvent resistance, thermomechanical properties and adhesion performances. In this study, we also addressed a limitation of PHU coatings, i.e. their delamination and high-water uptake, by addition of PDMS into the formulations. In order to determine how far we are from the benchmark, adhesive performances of PHUs were compared to commercial PU-adhesives under standard conditions.

Chapter-III is devoted to the development of environmental-friendly novel bio-based thermoset PHU adhesives and coatings that combined hydrophobicity and adhesion to metal surfaces (Al-Al and SS-SS). To achieve this objective, we first synthesised cyclic carbonates bearing vegetable oil (soybean oil) and then investigated the influence of structure of amine (hardener), dispersion of fillers (CC-ZnO/CC-SiO_2) and formulation mixing time on enhancement of final material performances. This work highlights the specific aspects of aim of thesis that are sustainability, solvent-free, toxic-free, cost-effective, environmental-friendly, hydrophobic nature and scale up of end products. The state-of-the-art high-performance adhesives was benchmarked against conventional adhesives. These sustainable adhesives can find most demanding industrial and real-life applications including aerospace, automotive, electronics, surface protection, etc.

In the **Chapter-IV**, our intention is to produce solvent-free innovative mussel-mimetic thermoset PHU adhesives for sticking numerous substrates. To achieve this intention, we first designed polyhydroxyurethane adhesives bearing strongly adherent catechol groups. In this study, we investigated the influence of dopamine content in the PHU on formulations crosslinking, adhesion strength, coatings stability, solvent resistance and thermo-mechanical properties. Finally, these biomimetic adhesives were tested on different surfaces (metals, plastics, glass wood etc) to investigate their ability to withstand load and coating delamination in water.

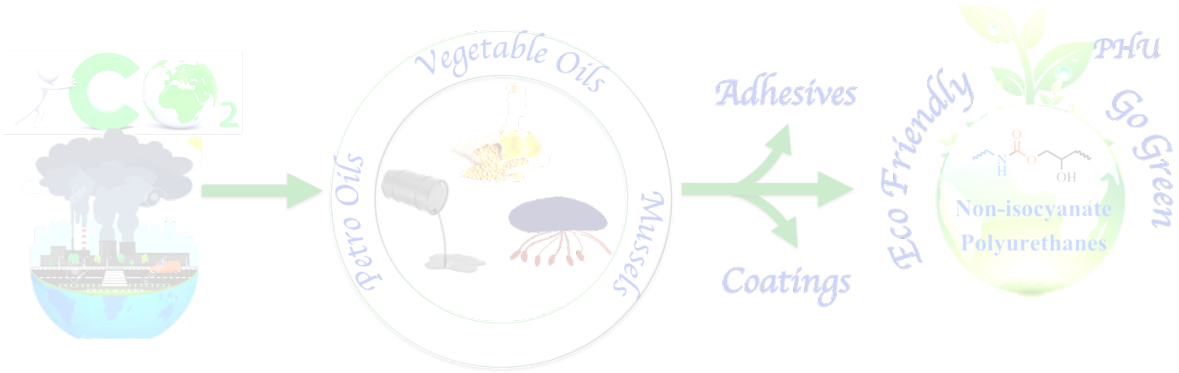
CO2
Vegetable Oils
Petro Oils
Mussels
Adhesives
Coatings
Eco Friendly
PHU
Go Green
Non-isocyanate
Polyurethanes

Chapter-II

Reinforced poly(hydroxyurethane) thermosets as high performance adhesives for aluminum substrates

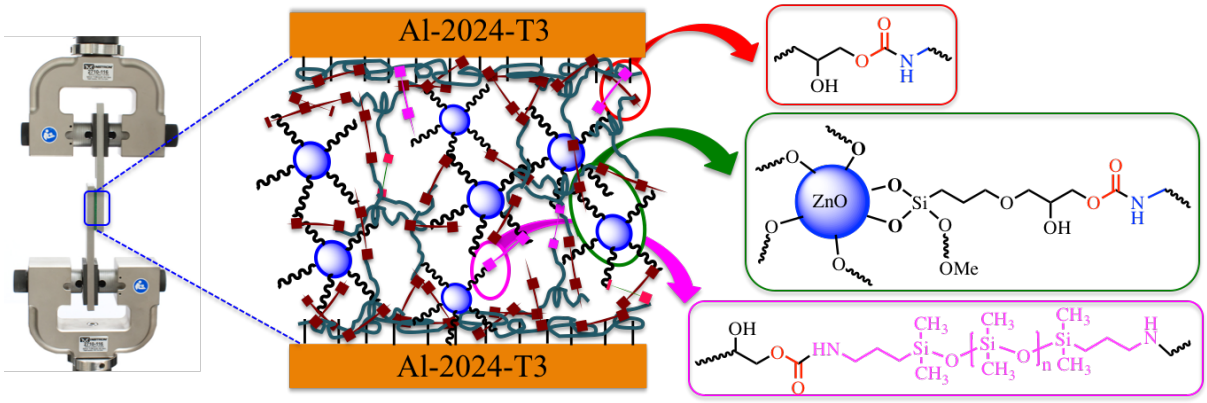

Satyannarayana Panchireddy[a], Jean-Michel Thomassin[a], Bruno Grignard[a], Christian Damblon[b], Andrew Tatton[b], Christine Jerome[a]*, Christophe Detrembleur[a] ***Polym. Chem.***, 2017, **8**, 5897–5909.

ABSTRACT

Poly(hydroxyurethane) (PHU) thermosets reinforced with (functional) nanofillers were developed to design high performance adhesives for bare aluminium. Solvent-free cyclic carbonate/amine/PDMS formulations loaded with native, epoxy- or cyclic carbonate-functionalized ZnO nanofillers were premixed before deposition and thermal curing onto Al. The results highlight that the addition of PDMS prevents PHUs from delamination of the Al surface by increasing the adhesive hydrophobicity and thus limiting the water uptake. The dispersion of functional fillers within PHUs improves their thermal and mechanical properties. Benchmarking of the adhesive performances of the reinforced PHU glues with existing PHU formulations attests for the benefits of dispersing functional fillers and PDMS within the resin and evidences a 270% increase of the shear strength of reinforced PHUs adhesives compared to formulations reported in the literature.

Table of Contents

II.1 INTRODUCTION

Adhesives and glues are widely used in everyday life and largely valorised in various applications from post-it notes to aerospace. The intrinsic properties of polyurethanes (PU) such as flexibility, abrasion resistance, mechanical and thermal properties combined with their excellent adhesion to a wide range of substrates make them polymers of choice for high strength and long lasting adhesives.[1–3] However, due to toxicity issues, and environmental changes in REACH regulations[4] related to the use of isocyanates entering in the PU formulation,[5–8] new synthetic pathways are envisioned for producing isocyanate-free polyurethanes. To date, the synthesis of poly(hydroxyurethane)s (PHUs) by step growth polymerization between five-membered dicyclic carbonates and diamines is one of the most studied and promising route for developing more sustainable PUs.[9–25] PHUs have been exploited, mainly in academic research, for thermoplastics,[26–28] thermoset applications,[18,29,30] foams[20,31] and coatings,[32] but examples of PHUs adhesives are scarce.[33] Torkelson et al.[34] reported on hybrid adhesives produced by curing cyclic carbonates telechelic isocyanate-based PU oligomers and polyamines. The resulting PU/PHU hybrid material showed good adhesion onto polyimide, poly(vinyl chloride) and aluminum, with peel forces of 7.8, 10.5 and 3.4 N mm^{-1}, respectively. These hybrid glues predominantly underwent cohesive failure, a key parameter for high performance adhesives. In 2016, Caillol et al.[35] developed the first promising PHU adhesives for glass, wood and painted Al supports. The envisioned PHU solvent-based formulations showed higher adhesive performances onto wood and glass than PU analogues derived from isocyanates with shear forces up to 15 N mm^{-1}. Interestingly, while PUs underwent adhesive failure, PHUs glues presented a cohesive failure attesting for the positive impact of the pendant hydroxyl groups along the PHU chains on the adhesive performances. However, for painted Al substrate, adhesion performances of PU and PHU were found comparable and low with a shear force around 3 N mm^{-2}, and with an adhesive failure for both glues. However, PHU was never tested for bare aluminum, a substrate that is largely employed in the aeronautic and various fields,[36–39] and is thus of prime importance. Adhesive properties of glues are strongly dependent on the chemical nature of the substrate but also on its morphology. For instance, painted or bare aluminum are totally different substrates because the glue directly interacts with the paint (epoxy resin in the case of Caillol *et al.*[35]) in the first

case, and with aluminum oxide in the second case (considered in this work). Chemical interactions are therefore completely different and adhesion mechanisms and strength are expected to be different when a same glue is used for different substrates.

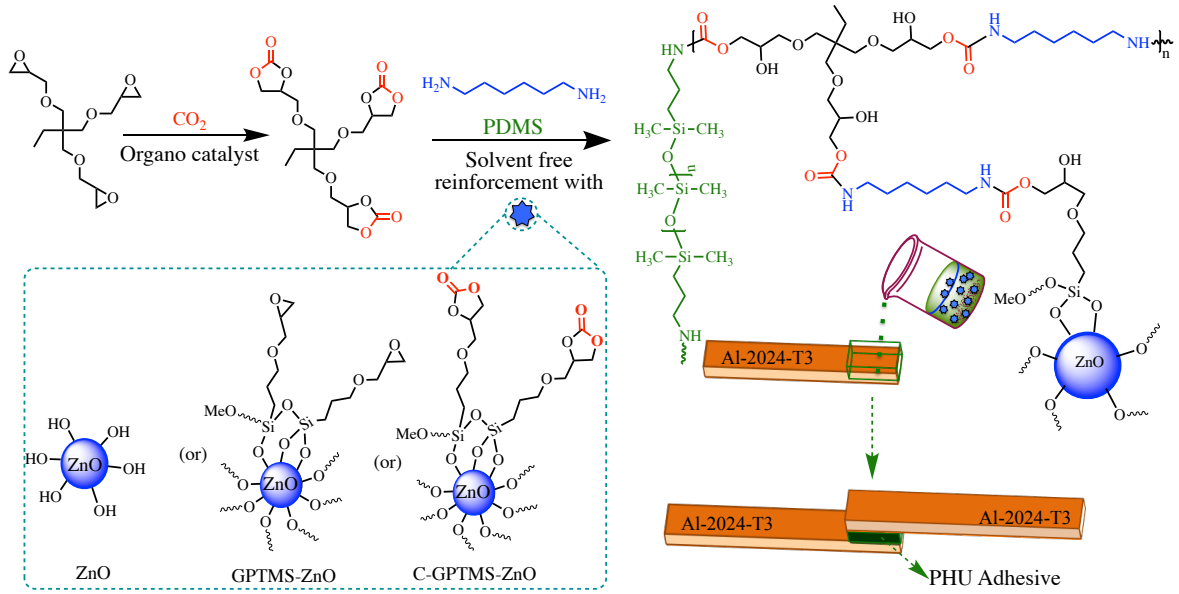

Scheme 1 Synthesis of ZnO-reinforced PHU adhesives metal sticking.

In this work, we develop novel solvent-free PHU thermosets adhesives reinforced with (functional) ZnO nanofillers and evaluate the adhesive performances. These ZnO nanofillers are selected to improve the mechanical and thermal properties of the glues. Reinforced PHU adhesives were prepared from a tricyclic carbonate/diamine/amino-telechelic polydimethylsiloxane formulation containing various amounts of native, epoxy- or cyclic carbonate functional ZnO (Scheme 1). Optimal formulations and curing kinetics were monitored by rheological studies prior evaluating the thermal and mechanical properties of PHUs. The behaviour of PHUs against water was studied by contact angle and water uptake measurements. This study is important to develop optimal formulations for high performance adhesives with limited moisture sensitivity. Finally, the adhesion performances of these PHUs onto Al-2024-T3 substrate were evaluated by standard cross-cut adhesion tests, MEK double rubber tests and lap shear tests, and benchmarking with state-of-the-art PHU adhesives was realized.

II.2 EXPERIMENTAL SECTION

II.2.1 Materials and Methods

Trimethylolpropane triglycidyl ether (TMPTE), tetrabutylammonium iodide (TBAI, purity >99%), (3-glycidoxypropyl)trimethoxysilane (GPTMS, ≥98%), hexamethylenediamine (HMDA), toluene, methanol, dichloromethane were purchased from Sigma Aldrich. Carbon dioxide (CO_2) N45 was supplied by Air Liquid. 1,3-bis(2-hydroxyhexafluoroisopropyl)benzene was purchased from Fluorochem. ZnO®20 (average filler size of 24-71 nm, specific surface area = 15-45 m^2 g^{-1} and density = 5.61 g m^{-3}) was received from Umicore, Belgium. Al-2024-T3 substrates were received from SONACA, Belgium. All chemicals were used as received without any further purification.

II.2.2 Characterization techniques

^{1}H NMR spectroscopy. ^{1}H NMR spectra were recorded with a 400 MHz Bruker AN 400 spectrometer in $CDCl_3$ at 25 °C in the Fourier transform mode. Chemical shifts were referenced to the peak of $CDCl_3$ at 7.24 ppm. NMR samples were prepared by dissolving 15 mg of product in 0.7 ml in deuterated solvents ($CDCl_3$). Cross-polarization magic angle spinning (CP-MAS) solid state NMR spectra were collected with a Bruker Avance DSX-400 instrument (B_0 = 9.04 T). Samples were packed in 4-mm zirconia rotors and spun at 5 KHz. Typical ^{13}C CP-MAS NMR parameters were 10000 scans, a 90° pulse length of 5 ms, and recycle time of 5 s. Typical ^{29}Si CP-MAS NMR parameters were 360 scans, a 90° pulse length of 5.5 µs, and recycle time of 480 s.

Fourier transform infrared spectra (FTIR) measurements. FTIR measurements were carried out on Nicolet IS5 spectrometer (Thermo Fisher Scientific) equipped with a diamond attenuated transmission reflectance (ATR) device, 32 scans were recorded for each sample over the range of 4000-500 cm^{-1} with a normal resolution of 4 cm^{-1} and spectra were analysed with ONIUM™ software.

Rheology measurements. The curing kinetics of PHU formulations were carried out on ARES (Advanced Rheometric Expansion System) Rheometric scientific TA instrument, equipment consists of two parallel plate geometry, frequency (1 Hz), strain (1 %), the measurements were

carried out at 60 °C, the evolution of storage, loss modulus and tan δ was monitored as function of time and the percentage of conversion was recorded on FTIR spectra. Complex viscosity was measured 1 min after the start of the curing kinetic measurement.

Transmission electron microscopy (TEM). The dispersion of ZnO fillers was monitored by transmission electron microscopy (TEM, Philips M100) at an accelerating voltage of 100 kV. Thin samples were prepared by ultramicrotomy (ULTRACUT from REICHERTJUNG) at room temperature. Micrograms were analysed by using the megaview GII (Olympus) software.

Water contact angle measurements. They were obtained on an OCA-20 apparatus (Dataphysics Instrument GmbH) in the sessile drop configuration by deposition of a 5-µL droplet of milli-Q water. Mean contact angle values were determined from at least 6 measurements realized at different locations of each Al coated surfaces.

Water uptake measurements. Water swelling of PHU samples was evaluated by water uptake at room temperature of free-standing films following the procedure reported elsewhere.[19] PHU samples of 0.5 cm length × 0.5 cm thickness × 1 cm width were immersed in 10 mL milli-Q water at 20 °C and the water uptake was measured until the weight of the swollen samples remained constant. Equilibrium water absorption was measured in function of time using *equation*:

$$\text{EWA (\%)} = \left(\frac{W_s - W_d}{W_d}\right) \text{ X } 100 \qquad (1)$$

Where W_s is the weight of swollen sample and W_d is the weight of dried sample.

Thermal characterizations. Thermogravimetric analysis (TGA) of the coatings was evaluated using a Q500 from TA instruments. Thermal degradation of PHUs was measured at heating rate of 20 °C min^{-1} over the temperature range of 0 to 700 °C under nitrogen atmosphere. DSC (Differential scanning calorimetry) analysis was carried out on a Q1000 from TA instruments using standard aluminium pans, calibrated with indium and nitrogen as purge gas. The samples were measured at a heating rate of 10 °C min^{-1} over a temperature range from −80 °C to 200 °C under a flowing nitrogen atmosphere. The glass transition temperature (Tg) was determined using the onset method, defined as the midpoint of the intersection between onset and midpoint with the offset and the midpoint tangent lines, using TA analysis software provided with the instrument.

Tensile properties. They were determined at 298K using an Instron 5594 tensile machine at a speed 10 mm min^{-1} with load capacity of 500 N. E-modulus, tensile strength and elongation at break were estimated by the average values of at least 6 PHU samples. Freestanding reinforced PHU samples were prepared using Teflon molds with the following dimensions: length = 3 cm, length of narrow fraction = 1cm, width = 0.5 cm, width of narrow fraction = 0.2 cm and thickness = 0.05 cm.

Lap-shear tests. They were carried out at 298K using an Instron 5594 equipped with a 10,000 N load cell with displacement rate of 2 mm min^{-1}. Al-metal substrates with dimensions of 50 mm × 10 mm × 0.8 mm were used for single lap-shear measurements and grip length on both sides of test specimens was 25 mm. 10 mg of adhesive polymers were spread on overlapped surface area of 10 mm × 10 mm, thickness was maintained around 0.15 mm and the curing was carried out at 70 °C for 12 h and 100 °C for 3 h. The tests were performed on 3-samples to determine average lap-shear strength of adhesives. The lap shear strength was calculated by the formula.

$$\tau = \frac{P}{A} \qquad (2)$$

Where, τ is lap shear strength (in N mm^{-2} or MPa), P is the force to remove the adhesive (N) and A is the overlapped area (100 mm^2).

Crosscut adhesion tests. They were carried out according to ASTM D3359 standards. The test consists of making six perpendicular cuts with a distance of 3mm onto the PHU coated Al plate with a sharp razor blade followed by the application of a high-pressure sensitive adhesive tape (Intertape tm 51596-ASTM D3359, Gardco). The tape is then removed by rapid pulling off at an angle of 180 degrees. The quality of the coating was visually estimated by comparison with % of area removed from the total surface. Coatings were classified as 5B: 0% of removal, 4B: < 5% of removal, 3B: 5-15% of removal, 2B: 15-35% of removal, 1B: 35-65% of removal, 0B: > 65% detachment.

Solvent resistance of coatings. It was evaluated by the methyl ethyl ketone (MEK) double rub test according to the ASTM D4752 standard. The coated Al surface was rubbed with cheesecloth soaked with MEK until failure or breakthrough of the film occurs. Double rubs were repeated for at least 350 movements or until the substrate becomes visible.

II.2.3 SYNTHESIS PROTOCOLS

II.2.3.1 4-((3-trimethoxysilyl)propoxy)methyl)-1,3-dioxolan-2-one (C-GPTMS)

4-((3-trimethoxysilyl)propoxy)methyl)-1,3-dioxolan-2-one was synthesised by coupling CO_2 with (3-glycidoxypropyl)trimethoxysilane (GPTMS) using the bicomponent catalyst. 30 g (0.135 mol) of GPTMS were introduced in a 80 ml high-pressure cell with 2.5 mol% of TBAI (3.39 mmol, 1.25 g) and 2.5 mol% of 1,3-bis(2-hydroxyhexafluoroisopropyl)benzene (3.39 mmol, 0.843 ml). The coupling reaction was performed at 80 °C and 80 bar. After 18 h, the epoxy groups were completely converted into the corresponding cyclic carbonates. The reactor was depressurized slowly to release unreacted CO_2. The resulting liquid was used without any further purification.

II.2.3.2 Synthesis of epoxy functionalized ZnO nanofillers (GPTMS-ZnO)

ZnO (Zano 20, 3g) were introduced in a two-neck 250 mL round bottom flask equipped with reflux condenser and suspended into 150 mL of dry toluene. The mixture was then heated under reflux and GPTMS (10 mL, 0.042 mol) was added dropwise over a period of 3h and further stirred for 18 h. Epoxy-functional ZnO fillers were then separated from the mixture by centrifugation and the excess of GPTMS was removed by four-cycles of centrifugation (5000 rpm min^{-1}, 10 min, 6 °C) dispersion in toluene and two-cycles in methanol. The functional fillers were then dried under vacuum at 60 °C for 2h prior characterization by ^{13}C and ^{29}Si solid state NMR spectroscopy. The grafting yields were determined by thermogravimetric analysis (TGA) (Fig.1d) using a previously reported method from our group.[40] Weight losses of 2.95 % that corresponds to a grafting of 0.58 epoxy nm^{-2}.

II.2.3.3 Synthesis of cyclic carbonate functionalized ZnO nanofiller (C-GPTMS-ZnO)

ZnO (3g, Zano 20) were introduced in a two-neck 250 mL round bottom flask equipped with reflux condenser and suspended in 150 mL of dry toluene. The mixture was then heated under reflux and C-GPTMS (10 mL, 0.035 mol) was added drop by drop over a period of 3h and further stirred for 18 h. Cyclic carbonate-functional ZnO fillers were then separated from the mixture by centrifugation and the excess of C-GPTMS was removed by four-cycles of centrifugation (5000 rpm, 10 min, 6 °C) dispersion in toluene and two-cycles in methanol. The

functional fillers were then dried under vacuum 60 °C for 2h prior characterization by ^{13}C and ^{29}Si solid state NMR spectroscopy. The grafting yields were determined by thermogravimetric analysis (TGA) (Fig.1d) using a previously reported method from our group.[40] Weight losses of 3.76% that corresponds to a grafting of 0.63 cyclic carbonate nm^{-2}.

Surface treatment of Al-2024. Al-2024-T3 substrates were kindly donated by SONACA (Belgium). Al substrates were cleaned according to a standard procedure typically used in the aerospace industry. The surface treatment consists of degreasing Al plates in a 1/1 v/v acetone/isopropanol mixture, followed by a basic treatment in NaOH (C = 40 g l^{-1}) for 1 min and an acidic treatment in TURCO liquid for few seconds. Between each step, Al substrates were washed with water and wiped with tissue paper. When anodized Al is used, the Al substrates were then immersed into a solution of composed of H_2SO_4 (C = 40 gl^{-1}) and tartaric acid (C = 80 g l^{-1}) and anodised by applying a voltage of 10 V, at 40 °C for 25 min. After anodization, Al plates were washed with water and dried.

II.2.3.4 Synthesis of polyhydroxyurethane (PHU) coatings

In a typical experiment, TMPTC (2 g, 4.6 mmol), HMDA (0.8 g, 6.9 mmol), PDMS (Mn = 27,000 g mol^{-1}, 0.14 g, 5wt%) and 1,3,5 wt% of non-functional, epoxy functional (0.58 epoxide nm^{-2}) or cyclic carbonate-functional (0.63 cyclic carbonate nm^{-2}) ZnO fillers were introduced in a reaction tube equipped with a mechanical stirrer. The reaction mixture was mixed for 3 minutes at 50 °C to obtain homogeneous mixture. Then, the viscous oligomeric solutions were deposited onto bare and anodized Al-2024-T3 surfaces using bar coat applicator to obtain precise control over the coating thickness (in the range of 0.09-0.1mm). The coated substrates were then cured at 70 °C for 12 h and 100 °C for 3h in air circulating oven. It is worth to mention that all coatings were homogeneous, bubbles-free with uniform dispersion of nanofillers. The same procedure was applied for the preparation of all (functional) ZnO-reinforced PHU coatings.

II.2.3.5 Synthesis of poly(hydroxyurethane)s (PHUs) adhesives onto Al substrate

Equimolar amount of TMPTC/HMDA added with 5 wt% of PDMS and 5wt% (compared to TMPTC + HMDA) of non-functional and functional epoxy/cyclic carbonate fillers were mixed at 500 rpm for 3 minutes at 50 °C to obtain homogeneous bubbles-free viscous solutions. The mixture (~ 10 mg) was deposited onto 100 mm^2 Al substrate of 50 mm (l) × 10 mm (w) × 0.8 mm (t) and a second Al substrate was placed on top of deposited mixture (Fig.6a) and then manually pressed with constant force. The overlapped substrates were cured at 70 °C for 12 h, followed by 3 h at 100 °C in air circulating oven.

II.3 RESULTS AND DISCUSSION

II.3.1 Functional fillers synthesis and characterization

Epoxy- and cyclic carbonate functionalized fillers are expected to react with primary amines of the formulation which will improve their dispersion compared to unfunctional fillers. These modified fillers will therefore be strongly anchored to PHU and should increase the crosslinking degree of the polymer matrix. Below, we are first discussing the synthesis of TMPTC and the functionalized fillers, and then describing the formation of reinforced PHU coatings, followed by their characterizations and adhesive properties. First, a tricyclic carbonate monomer, i.e. 4,4'-(((2-ethyl-2-(((2-oxo-1,3-dioxolan-4-yl)methoxy)methyl)propane-1,3-diyl)bis(oxy))bis(methylene))bis(1,3-dioxolan-2-one) (TMPTC), was quantitatively synthesised by coupling CO_2 with trimethylolpropane triglycidyl ether (TMPTE) at 80 °C and 100 bar for 24 h by using a binary organocatalyst composed of tetrabutylammonium iodide (TBAI) and 1,3-bis(2-hydroxyhexafluoroisopropyl)benzene (1,3-bisHFIB) that demonstrated high activity for CO_2/epoxide coupling reaction (Scheme 2; see Supporting Information for details).[41–43]

As primary amines are known to easily react with epoxides and cyclic carbonates, fillers with 2 different functionalities were synthesized. The general strategy for functionalizing commercial ZnO®20 is shown in Scheme 2 and consists in condensing a trimethoxysilyl derivative bearing either an epoxide (GPTMS; (3-glycidoxypropyl)trimethoxysilane) or a cyclic carbonate group (C-GPTMS; 4-((3-trimethoxysilyl)propoxy)methyl)-1,3-dioxolan-2-one) onto the surface of the filler.

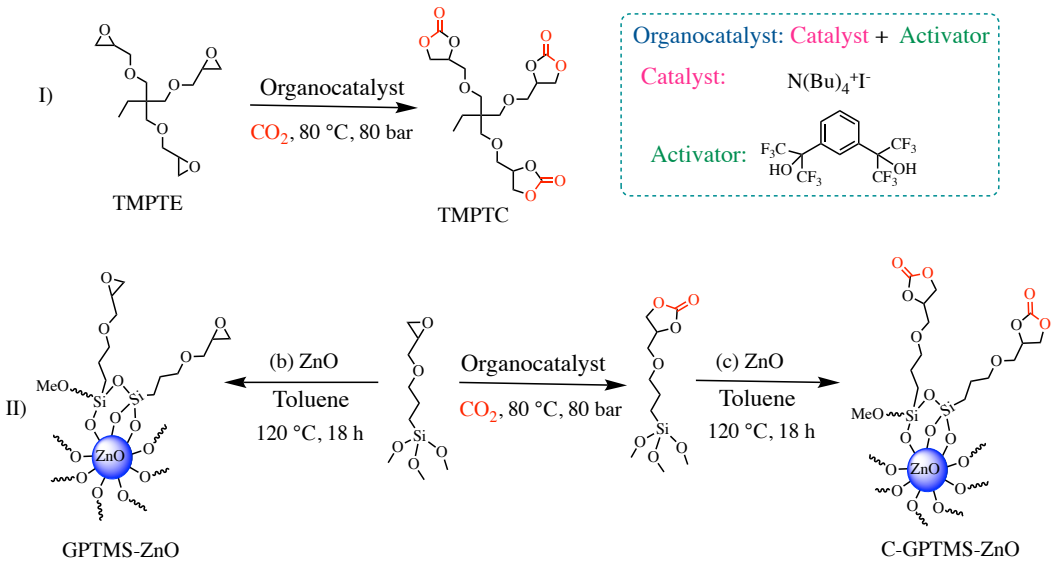

Scheme 2. I) Synthesis of TMPTC by organocatalytic coupling of CO_2 with TMPTE, II) Synthesis of functional ZnO fillers (a) Synthesis of C-GPTMS [4-((3-trimethoxysilyl)propoxy)methyl)-1,3-dioxolan-2-one] by organocatalytic coupling of CO_2 with GPTMS, (b) Synthesis of GPTMS functionalized ZnO fillers (GPTMS-ZnO) and (c) Synthesis of C-GPTMS functionalized ZnO fillers (C-GPTMS-ZnO).

C-GPTMS was synthesized by coupling CO_2 with commercially available GPTMS using 2.5 mol% of bicomponent organocatalyst ([TBAI/1,3-bisHFIB] = 1) at 80 °C and 80 bar for 18 h (Scheme 2). Quantitative conversion of the epoxy rings into the corresponding cyclic carbonates was highlighted by ^{1}H NMR spectroscopy (Fig.S3) by the disappearance of the peaks characteristic of –C*H*–O– and –C*H*$_2$–O– of epoxides at 3.15 and 2.5-2.8 ppm, respectively, and the appearance of new signals of –C*H*–OC(=O)O– and –C*H*$_2$– OC(=O)O– of cyclic carbonates at 4.8 and 4.25-4.6 ppm, respectively. Formation of cyclic carbonate was further confirmed by FTIR (Fig.S4) showing the disappearance of the characteristic band of the epoxy groups of GPTMS at 914 cm^{-1} and the presence of a new band at 1790 cm^{-1} corresponding to the elongation of the carbonyl group of C-GPTMS.

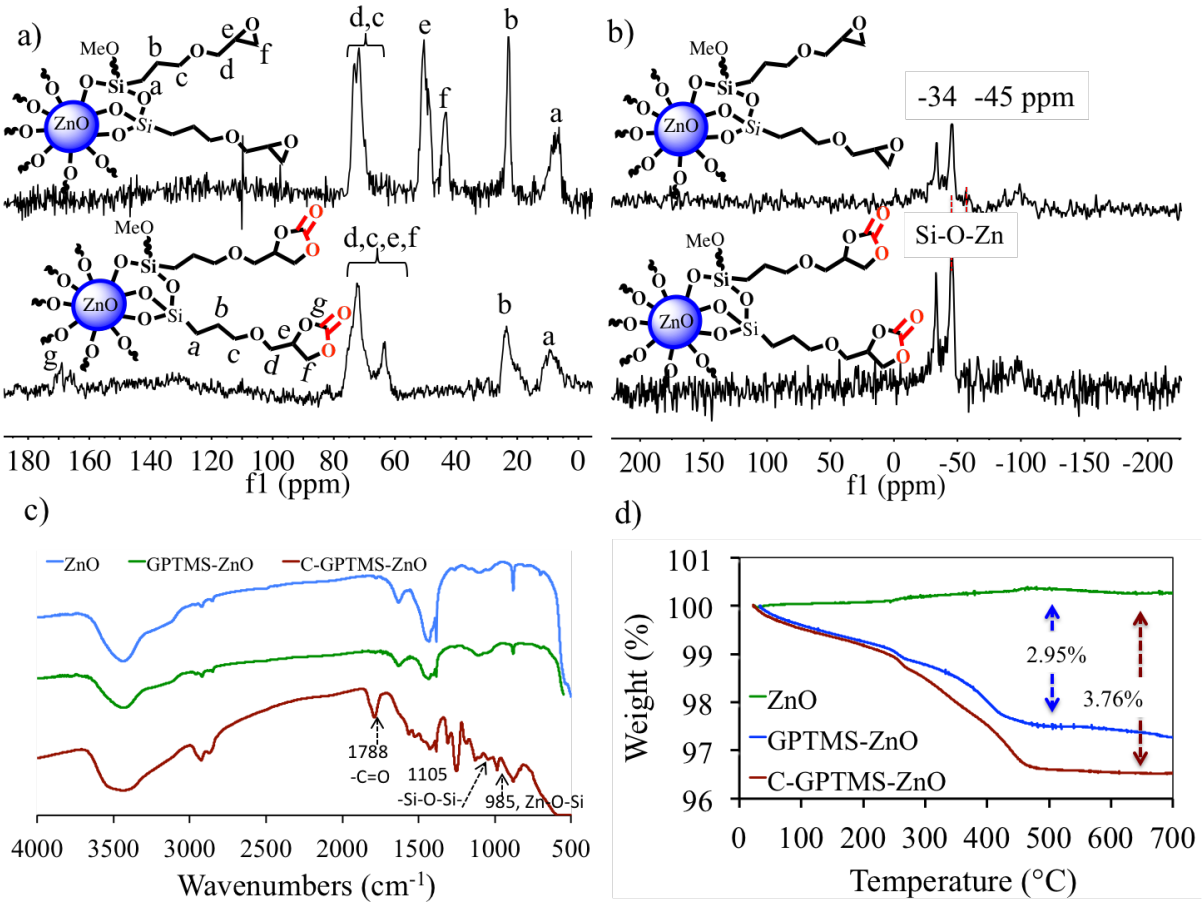

Fig.1 a) Cross-polarized solid-state ^{13}C NMR spectrum of GPTMS-ZnO and C-GPTMS-ZnO fillers, b) ^{29}Si solid state NMR spectra of GPTMS-ZnO and C-GPTMS-ZnO fillers, c) FTIR spectra of ZnO, GPTMS-ZnO and C-GPTMS-ZnO fillers and d) Quantification of the epoxide and cyclic carbonate grafting yields by thermogravimetric analyses: (green) non-functional ZnO, (blue) epoxy-functional ZnO (GPTMS-ZnO) and (red) cyclic carbonate-functional ZnO (C-GPTMS-ZnO).

Epoxy- and cyclic carbonate-functional nanofillers were then prepared by condensing respectively GPTMS or C-GPTMS onto the surface of ZnO in toluene at 120 °C during 18h. After purification by 3 cycles of dispersion/centrifugation in toluene, followed by two 2 cycles in methanol, the functional fillers were characterized by thermogravimetric analysis (TGA, Fig.S5 ESI) to determine the grafting yields of epoxy or cyclic carbonate (Fig.1d) according to a previously reported procedure.[40] Weight losses of 2.95 % and 3.76% were measured for GPTMS-ZnO and C-GPTMS-ZnO, respectively, that corresponds to a grafting of 0.58 epoxide nm^{-2} or 0.63 cyclic carbonate nm^{-2}. Surface functionalization was further confirmed by FTIR spectroscopy (Fig.1c) by the appearance of new absorption bands at 985 cm^{-1} and 1105 cm^{-1} attributed respectively to Si–O–Zn and Si–O–Si linkages and signals at 914 cm^{-1} characteristics

of epoxide (GPTMS-ZnO) and at 1788 cm^{-1} characteristic of C=O of carbonate (C-GPTMS-ZnO). Solid state ^{13}C NMR spectra of the two modified fillers highlight the presence of peaks at 44 and 50 ppm attributed to the carbons of epoxy groups of GPTMS-ZnO and, for C-GPTMS-ZnO, a peak at 165 ppm attributed to the carbonyl group of cyclic carbonate (Fig.1a). Solid state ^{29}Si NMR confirms that silanes were chemically attached to the ZnO surface by the presence of signals at −34 and −45 ppm attributed to Si-O-Zn linkages (Fig.1b). Silanol groups that may originate from hydrolysis of methoxysilyl groups are not observed, with the absence of typical signals of substituted Si-O-Si bonds bonds at −90 to 110 ppm in the ^{29}Si NMR spectrum.

II.3.2 PHU formulations and characterizations

ZnO reinforced PHUs were prepared by mixing equimolar amounts of cyclic carbonates (CC, coming from TMPTC) and primary amines (NH_2, coming from HMDA) with various contents (0 to 5 wt%) of non-functional ZnO or functionalized ZnO fillers at 60 °C under solvent-free conditions. Curing kinetics between TMPTC and HMDA were first monitored by rheology to determine the gelation time and the G″/G′ ratio (tan δ) of the different formulations. Fig.2 shows the increase of G′ and G″ moduli for an CC/NH_2 equimolar formulation (thus, [TMPTC]/[HMDA] = 1/1.5) and highlights that the crossover point (corresponding to gel point) is reached after only 27 min.

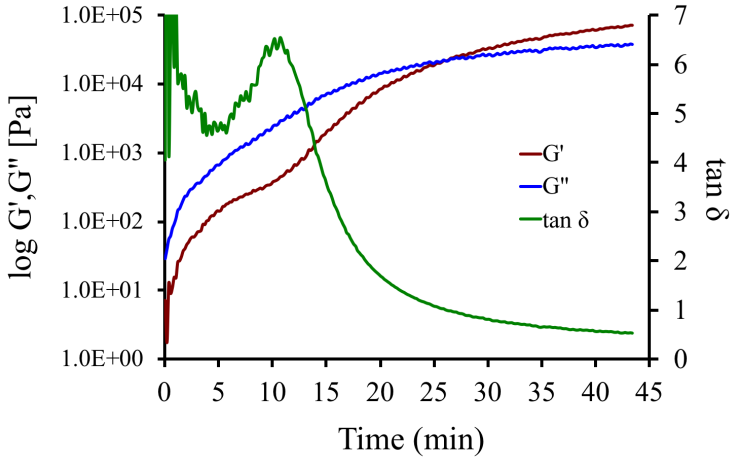

Fig.2 Curing kinetics of TMPTC/HMDA formulation ([CC]/[NH_2] = 1) by rheology under solvent-free conditions. ([TMPTC]/[HMDA] = 1/1.5, T = 60 °C, t = 45 min).

The formulation curing was also monitored in parallel by FTIR spectroscopy under identical conditions. Fig.3 shows a progressive disappearance with time of the elongation typical of the carbonyl group of cyclic carbonate at 1782 cm^{-1} associated to the appearance of new bands characteristic to the β-hydroxyurethane bond at 1690 cm^{-1} (C=O), 1532 cm^{-1} (N–H) and 3300 cm^{-1} (O–H). Cyclic carbonates are fully consumed after 45 minutes of reaction.

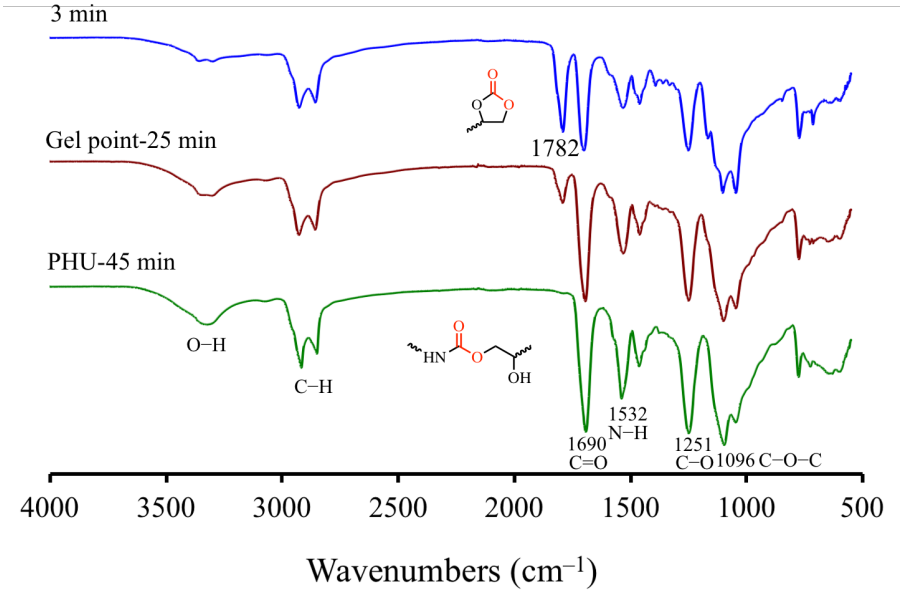

Fig.3 Curing kinetics of TMPTC/HMDA formulation ([CC]/[NH_2] = 1) by FTIR spectra under solvent-free conditions. ([TMPTC]/[HMDA] = 1/1.5, T = 60 °C, t = 45 min).

Similar kinetic studies monitored by rheology were then performed for all PHU formulations reinforced with (functional) ZnO fillers and added with 5 wt% of amino-telechelic PDMS in order to determine and compare gel times, storage modulus (G´) and tan δ values. All results obtained are summarized in Table 1. The addition of 3 or 5 wt% of un-modified or epoxy-modified ZnO fillers did not significantly affect the gelation time neither tan δ values, but improves G' that increased from 56.3 kPa for unfilled PHU (PHU1, Table 1) to 75.4 or 65.5 kPa for reinforced PHU with unmodified (PHU4) or epoxy-modified ZnO (PHU7), respectively. On the other hand, when 5 wt% of cyclic carbonate functional ZnO are added to the TMPTC/HMDA formulation, tan δ decreases from 0.54 to 0.43, G´ increases from 56.3 to 83.7 kPa, and the gelation time decreases from 27 to 24 min. These results show that cyclic carbonates at the surface of ZnO fillers slightly accelerate the formulation curing and improve the crosslinking density of the PHU (lower tan δ value).

Further improvement of the curing rate (gel time) and cross-linking of the network was obtained by using a small excess of HMDA compared to TMPTC ([TMPTC]/[HMDA] = 1/1.6) that compensates amine groups consumed by reaction with cyclic carbonates present at the surface of C-GMPTS-ZnO. Compared to the equimolar formulation, this slight amine excess (for a C-GMPTS-ZnO loading of 3 wt%) enables to decrease the gel time from 26 to 21 min, and to significantly decrease tan δ from 0.48 to 0.39 while increasing G´ from 71.4 to 93.7 kPa (comparison of PHU9 and PHU14). In contrast this amine excess is detrimental to PHU reinforced by unmodified ZnO with an important decrease of both G´ and G˝ moduli, and an increase of tan δ value (comparison of PHU3 and PHU12). Gel time is however not drastically affected. Only very slight improvement in gel time and tan δ is noted when using epoxy-modified ZnO (comparison PHU6 and PHU13). This observation further confirms the beneficial impact of the addition of functional fillers on the cross-linking of the coatings. The optimized solvent-free TMPTC/HMDA formulation reinforced with cyclic carbonate functional ZnO presents a curing time of 21 min at 60 °C with a G´ value of 93.7 kPa (PHU14), compared to 27 min gelation time and G´ of 56.3 kPa for unfilled PHU (PHU1).

Table 1. PHU curing kinetics by rheology, containing 5 wt% of PDMS and reinforced with 1, 3 or 5 wt% of ZnO. N: non-functionalized ZnO, E: Epoxy functional ZnO (GPTMS-ZnO), C: Cyclic carbonate functional ZnO (C-GPTMS-ZnO) fillers. N.d: not determined.

Formulation	[TMPTC]/[HMDA]	ZnO Functionality	Fillers loading (wt%)	Gel time [min]	G´ [kPa]	G˝ [kPa]	Tan δ
PHU1	1/1.5	/	/	27	56.3	30.3	0.54
PHU2 (1N)	1/1.5	/	1	N.d	N.d	N.d	N.d
PHU3 (3N)	1/1.5	/	3	28	60.7	32.4	0.53
PHU4 (5N)	1/1.5	/	5	27	75.4	38.0	0.50
PHU5 (1E)	1/1.5	Epoxide	1	N.d	N.d	N.d	n.d
PHU6 (3E)	1/1.5	Epoxide	3	27	50.4	25.5	0.50
PHU7 (5E)	1/1.5	Epoxide	5	26	65.5	31.7	0.48
PHU8 (1C)	1/1.5	Cyclic carbonate	1	N.d	N.d	N.d	n.d
PHU9 (3C)	1/1.5	Cyclic carbonate	3	26	71.4	34.4	0.48
PHU10 (5C)	1/1.5	Cyclic carbonate	5	24	83.7	36.3	0.43
PHU11	1/1.6	/	/	28	46.6	25.8	0.55
PHU12 (3N)	1/1.6	/	3	27	44.8	26.9	0.60
PHU13 (3E)	1/1.6	Epoxide	3	25	81.5	35.8	0.47
PHU14 (3C)	1/1.6	Cyclic carbonate	3	21	93.7	36.6	0.39

II.3.3 PHU thermal properties

Thermal stability of reference and reinforced PHUs were then evaluated by thermogravimetric analysis (TGA) (Fig.S5 and Fig.4a). The temperatures at 10% degradation ($Td_{10\%}$) are reported in Table 2. $Td_{10\%}$ of reference PHU1 reinforced by non-functional ZnO was around 281 °C. Thermal stability increases to 289 °C and 292 °C with respectively 5 wt% of epoxy or cyclic carbonate functional ZnO fillers. This positive effect is probably relied to the improved cross-linking of these materials, which limits the diffusion of gases during the degradation.

The glass transition temperatures (Tg) of the PHU samples were evaluated by differential scanning calorimetry (DSC) analysis (Fig.S7 and Fig.4b) and are reported in Table 2. For all formulations, no melting/crystallization transitions were observed in the DSC thermograms, evidencing the amorphous nature of the PHUs. The Tg value of the reference PHU produced from a TMPTC/HMDA 1/1.5 molar ratio formulation added with 5 wt% of PDMS was estimated to 51.8 °C and was found to slightly increase for reinforced PHUs by 3 or 4.4 °C upon dispersion of respectively 5 wt% of epoxy or cyclic carbonate functional fillers, in line with an improved polymer network.[35]

II.3.4 Mechanical properties of PHU films

The Young's modulus (E), tensile stress (σ_{Yield}) and the elongation at break (E_{break}) of PHUs and reinforced PHUs films containing 5 wt% of PDMS were investigated by conventional tensile tests (Fig.4c, Table 2). Reference PHU1 has a young's modulus of 325 MPa, a yield stress of 14 MPa and an elongation at break of 0.27 $mm.mm^{-1}$. The addition of unmodified ZnO fillers slightly improves the young's modulus (up to 385 MPa) and yield stress (up to 16 MPa). These improvements are more obvious with the addition of functional ZnO fillers, especially with those containing the cyclic carbonates where the young's modulus and tensile stress are increased by almost 200% upon the addition of 5 wt% of fillers. However, these improvements are associated (as it is usually the case) to the decrease of the elongation at break when increasing the nanofiller content. Again, these observations support the improved network in the presence of the functional ZnO fillers. This hypothesis is further supported by studying the morphology of PHUs with 5 wt% of reinforced bare, epoxy and cyclic carbonate functionalized ZnO fillers by transmission electron microscopy (TEM) (see Fig.S6 in ESI).

The black spots in the images are attributed to the fillers dispersed in the crosslinked networks. This study reveals that the fillers are reasonably well dispersed into all PHU formulations under solvent free conditions. There is no significant difference in the quality of dispersion of the fillers, whether the fillers are functionalized or not. The difference in mechanical properties of the PHU films are therefore assumed to be due to the contribution of the functional fillers to the crosslinking reaction.

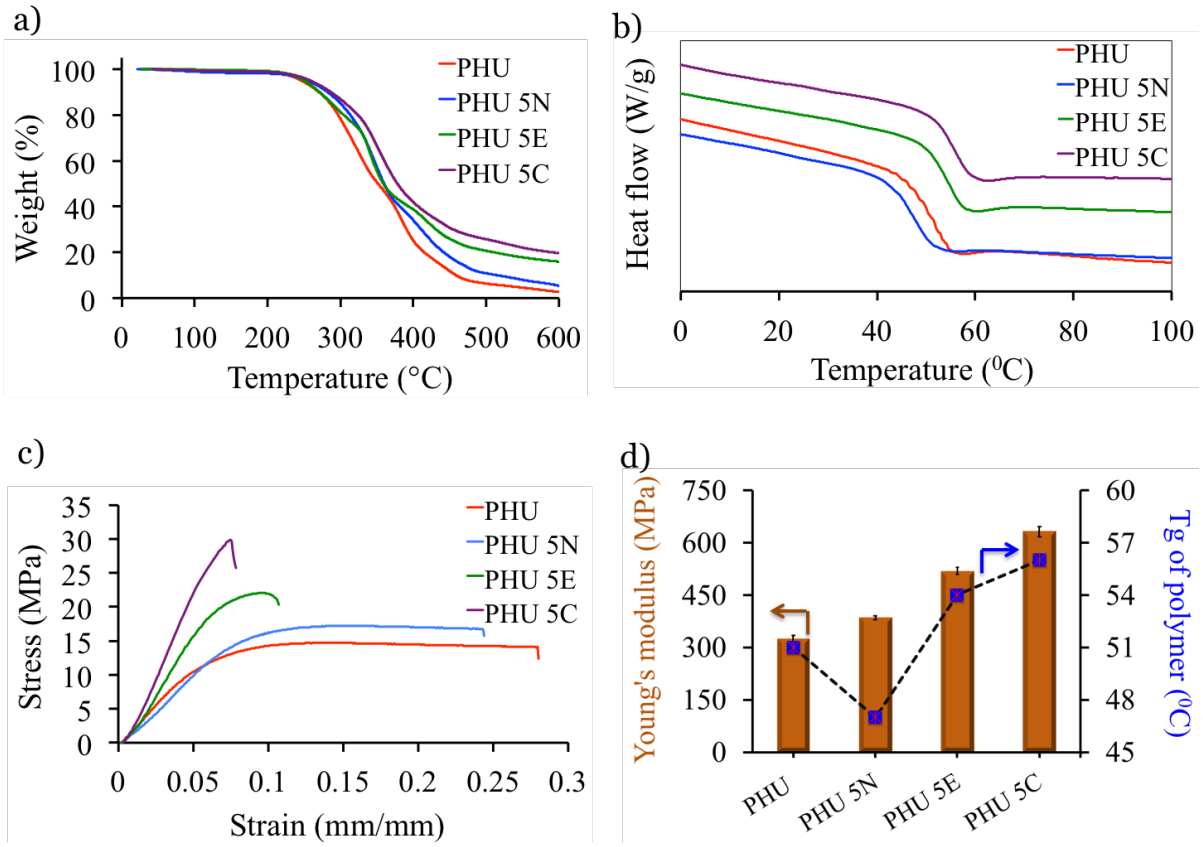

Fig.4 a) TGA b) DSC, c) Stress-strain curves of of PHUs reinforced by 5wt% of ZnO, GPTMS-ZnO and C-GPTMS-ZnO fillers, and d) effect of reinforcement of fillers on thermal and mechanical properties.

II.3.5 Coating hydrophobicity

PHU coatings of 0.09 – 0.1 mm thickness were first deposited onto bare and anodized Al substrate by curing TMPTC/HMDA/(functional) ZnO formulations of different compositions at 100 ^{0}C for 24 h. Prior curing, fillers were dispersed in monomers (without solvent) by mixing for 3 min before deposition of the resulting viscous formulation onto Al plates with a knife coater. After curing, all coatings were homogeneous, bubbles-free, slightly yellow and no visible aggregation of fillers within the PHU coating could be observed by naked eyes. However, all PHU coatings showed poor adhesion upon exposure or immersion of the coated substrate in water and rapidly peeled off the surface within minutes (even by simple deposition of a water droplet). This observation was related to the inherent hydrophilic nature and high-water permeability of PHUs resulting from the presence of dangling OH groups that favour the coating delamination. The high affinity of these PHUs for water was confirmed for a coating prepared from [TMPTC]/[HMDA]= 1/1.5 formulation by water contact angle measurement. A contact angle value of 54° typical of hydrophilic surface was measured after 30 sec and found to evolve to 48° after 4 min.

In order to overcome this important drawback, commercially available α,ω-amino telechelic polydimethylsiloxane (PDMS; Mn = 27,000 g/mol) was added to the formulations. Due to its very low surface energy, hydrophobic PDMS segment is expected to reduce the surface wettability[44,45] and to prevent water permeation of PHUs coatings. Interestingly, introduction of 5 wt% of PDMS (with respect to total mass of the formulation and respecting equimolar amount of CC/NH_2) into the formulations did not affect the curing rate, the gel point and the properties of the cross-linked PHU network. As an example, for a TMPTC/HMDA 1/1.5 molar ratio, gelation still occurred after 27 min and tan δ remained close to 0.54. This observation was assigned to the high molar mass of PDMS that renders negligible the deviation of the amine/carbonate molar ratio from the ideal stoichiometry. Importantly, the water contact angle value of the resulting PHU coating increased from 48 ± 5° to 85 ± 1° upon addition of this PDMS in the formulation. All previous formulations reported in Table 1 were therefore added with 5 wt% of PDMS, and properties of the coatings are summarized in Table 2. Hydrophobicity of the coatings was further improved by dispersing unmodified, epoxy- or cyclic carbonate- functional ZnO fillers within PHUs (Fig.5a, Table 2). This observation is

supported by a systematic increase of the contact angle value of the reinforced coatings with the content of fillers. As a general trend, whatever the filler loading, the hydrophobicity of the coatings is more pronounced for those containing the cyclic carbonate functional fillers and evolves in the order cyclic carbonate functional ZnO > epoxy functional ZnO > unmodified ZnO. The most hydrophobic coatings were obtained for an equimolar amount of CC/NH_2 ([TMPTC]/[HMDA]=1/1.5) formulation containing 5 wt% of PDMS and 5 wt% of C-GMPTS-ZnO as attested by a contact angle that reached a maximum value of 114 ± 3°. As evidence by TEM, there is no significant difference in the quality of dispersion of the different types of nanofillers in PHU (Fig.S6) and can therefore not be responsible for the difference of contact angle noted for the different samples. Moreover, the addition of PDMS does not affect significantly the viscosity of the PHU formulation (Fig.6). Further investigation would therefore be required to understand the origin of the different contact angles measured for the PHUs prepared using the different formulations.

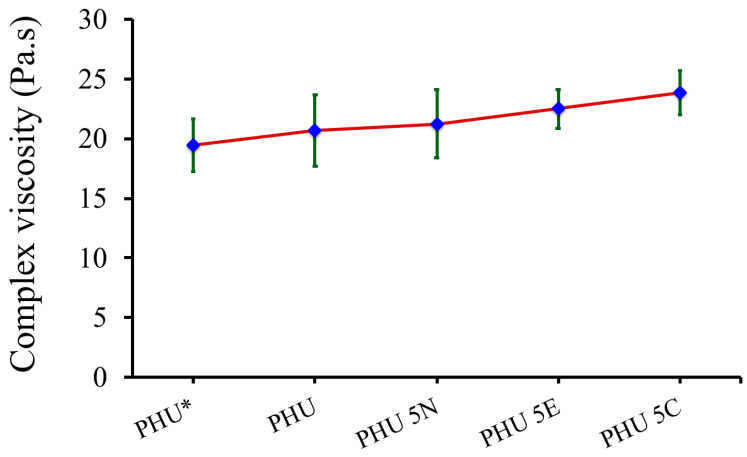

Fig.5 Viscosity properties of reinforced PHU formulations (PHU*-without PDMS and ZnO fillers). Note that we have also investigated PHU formulations with addition of other contents of PDMS, 1 and 10wt%. However, we noticed that 1wt%-PDMS did not show any improvement in the contact angle nor in the viscosity of the formulations compared to formulations without PDMS. The addition of 10wt%-PDMS is detrimental for the homogeneity of the coating (phase separation was observed) and was therefore not investigated further.

II.3.6 Water uptake

The behaviour of PHUs films against water was then evaluated by monitoring the water uptake time evolution after prolonged immersion (Fig. 5b and Table 2). Determination of this parameter is crucial since the diffusion of water within the coating is expected to favour the coating delamination. In the absence of fillers, PHU films produced from [TMPTC]/[HMDA] = 1/1.5 and containing 5 wt% of PDMS showed a water uptake value of ~57% that reached a plateau after 96 h. Addition of 1 to 5 wt% of unmodified ZnO nanofillers to the formulation induced a slight increase of the water uptake from ~57 % to 65% at 1 and 5 wt% of ZnO, respectively, which is related to the hydrophilic nature of ZnO. In contrast, the presence of functional ZnO within the PHU films reduced the water uptake from ~57% to 41% with 5 wt% of epoxy-functional ZnO and to 36% with 5 wt% of cyclic carbonate-grafted ZnO. The significant reduction of this water uptake with 5 wt% of functional ZnO was associated to the higher cross-linking density of PHU that limits the swelling of the films, but also to the hydrophobization of ZnO surface by the silanization process used for their functionalization.

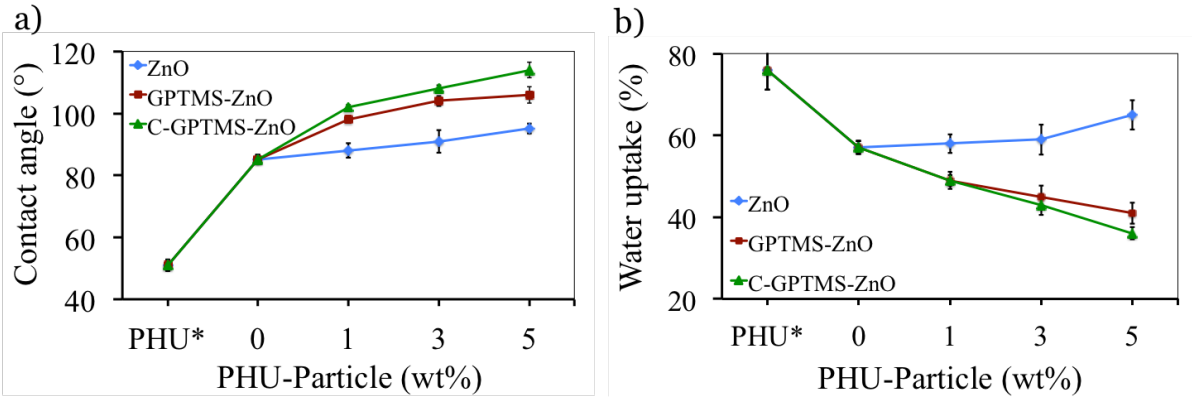

Fig.6 a) Contact angle measurements of PHU coatings and b) Equilibrium water uptake (after 96 h of immersion) of PHU free-standing films (0.5 cm length × 0.5 cm thickness × 1 cm width) synthesized from [TMPTC]/[HMDA] = 1/1.5 formulations containing 5 wt% of PDMS and reinforced with 1, 3 and 5 wt% of ZnO, GPTMS-ZnO and C-GPTMS-ZnO. (PHU*: PHU without PDMS and ZnO).

II.3.7 Coating adhesion properties

The adhesion strength of the PHU coatings on anodized Al surface was evaluated by crosscut test (Fig.8-I) according to ASTM D3359 standards (see experimental section for details). Whatever the formulation, all coatings were classified as 5B-0%, thus were not removed during testing, suggesting that β-hydroxyurethane groups provide strong interaction with anodized aluminum substrate.

To attest for the excellent adhesion of the crosslinked PHU coatings onto anodized Al, complementary solvent resistance tests of reinforced PHUs coatings were investigated by the MEK double rub test according to ASTM D4752 standards. A cheesecloth was soaked in MEK solvent and rubbed back and forth on the surface of the coating with constant force until either the coating was wiped off from the substrate or a maximum number (>350) of double rubs reached. For all TMPTC/HMDA/PDMS/(functional) fillers formulations, the resulting PHU coatings exhibited excellent solvent resistance with more than 350 double rubs without any visible surface defects/wiping off of the coating. All these tests give similar performances when the coating is applied to bare aluminum.

Table 2. Properties of reinforced PHU coatings containing 5wt% PDMS.

Sample	CA[a] (^{0})	EWA[b] %	MEK[c]	Adhesion[d]	$Td^e_{10\%}$	Tg^f (^{0}C)	E^g (MPa)	$\sigma_{Yield}{}^h$ (MPa)	$E_{break}{}^i$ (mm mm^{-1})
PHU1	85 ± 1	57	P	5B	280.6	51.85	325 ± 12	14 ± 0.1	0.27 ± 0.05
PHU2 (1N)	88 ± 1	58	P	5B	280.4	51.86	316 ± 25	12 ± 0.2	0.27 ± 0.03
PHU3 (3N)	91 ± 1	59	P	5B	281.2	49.25	352 ± 17	13 ± 0.1	0.25 ± 0.01
PHU4 (5N)	95 ± 3	65	P	5B	281.7	46.64	385 ± 09	16 ± 0.8	0.24 ± 0.02
PHU5 (1E)	98 ± 2	49	P	5B	283.4	52.26	348 ± 28	13 ± 0.1	0.22 ± 0.01
PHU6 (3E)	104 ± 1	45	P	5B	287.8	53.67	472 ± 21	18 ± 2.3	0.14 ± 0.03
PHU7 (5E)	106 ± 3	41	P	5B	289.3	54.91	519 ± 15	21 ± 0.5	0.10 ± 0.04
PHU8 (1C)	102 ± 1	49	P	5B	286.6	53.30	362 ± 16	18 ± 1.3	0.15 ± 0.04
PHU9 (3C)	108 ± 3	43	P	5B	288.3	54.67	492 ± 32	25 ± 0.2	0.14 ± 0.03
PHU10 (5C)	114 ± 3	36	P	5B	292.7	56.25	632 ± 21	29 ± 0.6	0.07 ± 0.01

[a)] Contact angle measurements, [b)] Equilibrium water uptake of PHU free standing films (0.5 cm length × 0.5 cm thickness × 1 cm width) for 96 h, [c)] Methyl ethyl ketone double rub test (>350; P-passed), [d)] Cross-cut adhesion test (5B-0% coating area removed within crosscut, [e)] TGA- temperatures at 10% degradation ($Td_{10\%}$), heating rate 20 °C min^{-1}, [f)] DSC-glass transition temperature, heating rate 10 °C min^{-1}, [g)] Young's modulus, [h)] Tensile strength, [i)] Elongation at break.

II.3.8 Adhesive properties

Finally, reinforced PHUs containing PDMS were tested as glues for bare Al. The shear adhesion strength of ZnO reinforced PHUs were investigated by lap-shear tests (Fig.7a) and calculated by eq. 2. The unfilled PHU is characterized by an adhesive strength of 11.2 ± 1.2 MPa onto Al. The addition of ZnO fillers improves the adhesion strength, particularly for the cyclic carbonate functionalized ones with lap-shear strength of 16.3 ± 1.4 MPa (Fig.7b and 7c). This 145% improvement of the adhesion strength is explained by a better crosslinking density of PHUs reinforced by cyclic carbonate functional fillers that increases the mechanical resistance of the adhesive. This is in agreement with Sudaryanto *et al*.[46] who showed that adhesive strength of conventional PU glues strongly depend on both the mechanical and surface properties of the support. Indeed, cohesive failure is observed for the unfilled PHU, the PHUs filled with unmodified fillers (PHU 5N) or with epoxy functionalized ZnO fillers (PHU-5E) (Fig.8-II: a-c). This is emphasized by the presence of adhesive on both sides of the substrate after the adhesive rupture. In contrast, sample PHU-5C exhibits adhesive failure, with the adhesive remaining on one side of the Al substrate, which can be related to the high mechanical resistance of the adhesive (Fig.8-II: d).

Benchmarking of the adhesive properties of our PHU formulations with TMPTC/EDR-148 existing ones reported by Caillol or Caillol's formulations processed according to our synthetic method (with and without 5 wt% of PDMS) was then investigated (Fig.7b and 7c). Clearly, unfilled PHU adhesive produced from TMPTC/HMDA/PDMS shows better performances than PHUs made from TMPTC/EDR-148 or TMPTC/EDR-148/PDMS formulations as respectively attested by a 130% and 170% increase of the adhesive shear strength. The best adhesive performances were measured for PHU produced from TMPTC/HMDA/PDMS formulations filled with 5 wt% of cyclic carbonate functional ZnO nanofillers that shows an outstanding 270% increase of the shear strength compared to the reference PHU. All samples are shown cohesive failure.

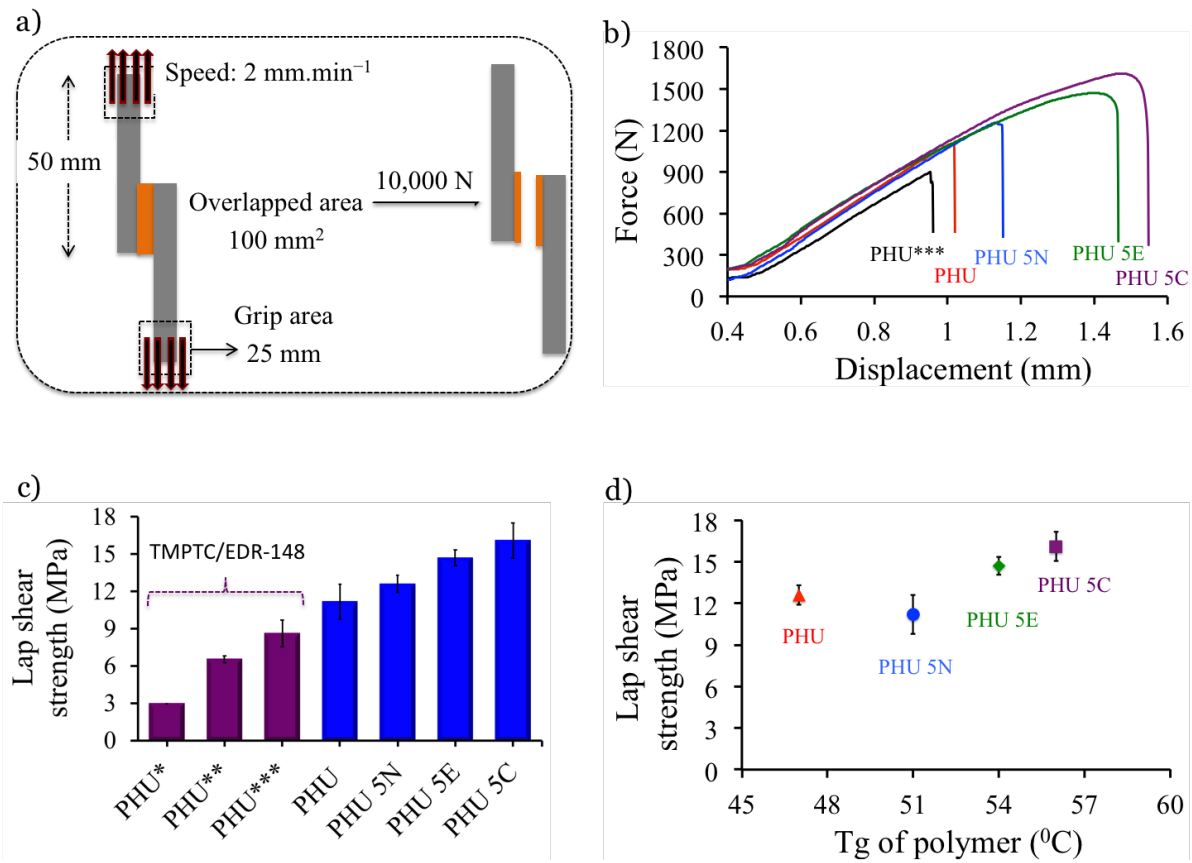

Fig.7 (a) Schematic representation of lap-shear test of PHU glues, (b) Force vs displacement; (c) Benchmarking of lap-shear strength of various state-of-the-art PHUs formulations (calculated from eq. (2)). [PHU*: value of the shear strength of the TMPTC/EDR-148 formulation reported by Caillol onto painted Al[35], PHU** : TMPTC/EDR-148 formulation adapted to our conditions, thus on bare Al and formulation cured at 70 °C 12 h, followed by 3h at 100 °C, PHU***:TMPTC/EDR-148 formulation including 5wt% of PDMS on bare Al using our standard curing conditions; (d) Lap-shear strength evolution with glass transition temperature of PHU.

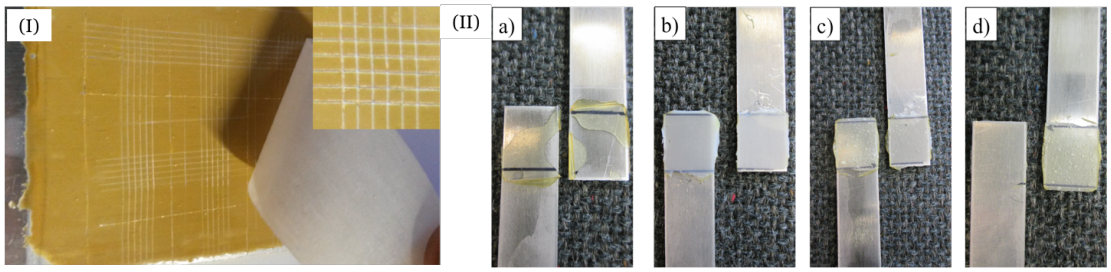

Fig.8 (I) Crosscut adhesion test onto Al-substrate of a PHU coating reinforced with 5 wt% of C-GPTMS-ZnO. (II) Images of reinforced PHU samples after lap-shear measurements a) PHU (50% cohesive failure), b) PHU-5N (cohesive failure), c) PHU-5E (cohesive failure) and d) PHU-5C (adhesive failure).

II.3.9 Bench marking

The adhesion performances of reinforced PHU adhesives were also compared to those of commercial polyurethane (PU) adhesives specifically dedicated for aluminum substrates (Teromix-6700 and Araldite®2000) (Fig.9). The curing of commercial glues was carried out using the recommended protocol by the manufacturer (room temperature) but also by our protocol (70 °C for 12 h and 3 h at 100 °C) for sake of comparison with our sample. The commercial adhesives of PU exhibit highest performance at room temperature cured for 48 h [Araldite and Teromix of lap shear strength 21.7 MPa, 12.5 MPa respectively]. Under these curing conditions, our optimized PHU glue (PHU 5C) presents a low lap shear strength of 3.3 MPa as the result of the low reactivity of the cyclic carbonates with the amines under these conditions, and thus a very slow curing. However, PHU 5C clearly competes the commercial glues when cured under our optimized conditions (70 °C for 12 h and 3 h at 100 °C) with a shear strength of 16.3 MPa. Curing under these conditions is however not appropriate to the commercial glues with a decrease of their lap shear strength to 11.2 MPa for Araldite and 7.2 MPa for Teromix.

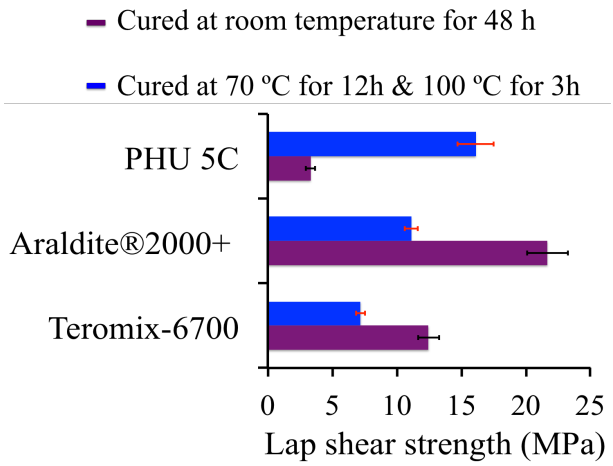

Fig.9 Benchmarking commercial PU and reinforced PHU adhesives.

This benchmarking clearly highlights that well-designed PHU glues can afford a realistic and alternative to conventional glues made of toxic formulations. Thanks to pendent hydroxyl group in PHUs have inherent bonding strength towards different surfaces as compared to conventional PU adhesives without such bonds, where strength of the bonds considerably lower in energy and poorly stands up to the load bearing properties. The bonding strength and interactions in PU substantially set by Vander Waal forces are responsible for physical and mechanical properties.[47] Jalilian *et al.*[48] described that, the functional groups in the networks are ability to increase the domain cohesion through hydrogen bonding and improve adhesion to Varity of substrates.[32]

Finally, Fig.7d illustrates the Tg dependence of the shear strength that increases with the Tg of the various reinforced PHUs (DSC curves are shown in Fig.S7, ESI). This observation is in agreement with Nakamae *et al.*[46] and Caillol *et al.*[35] who assumed that the content of flexible/soft segment in conventional PUs or PHUs (that impacts Tg of polymers) influences their adhesion performances.

II.4 CONCLUSION

We have reported on the preparation of novel highly adhesive reinforced poly(hydroxyurethane) (PHU) glues for Al with a shear strength up to 16.3 MPa. These adhesives consist in cross-linked PHU networks with excellent mechanical properties and thermal stability (up to 290 °C) that were produced from CO_2-sourced tricyclic carbonates and diamine formulations under solvent-free conditions. To prevent water swelling of the PHU films and delamination of the coating from the Al surface, 5 wt% α,ω-amino PDMS was added to the formulation. Introduction of this hydrophobic segment strongly improved the adhesion of the coatings that were classified as 5B according to the ASTM D3359 standard crosscut adhesion test. The coating characteristics and performances were significantly improved by dispersing native, epoxy- or cyclic carbonate-functional ZnO nanofillers. Formulations containing 5 wt% of cyclic carbonate-functional ZnO provided reinforced PHU glues characterized by the best thermal and mechanical properties, and the highest lap-shear adhesion strength to Al. Based on these results, we believe that these PHU glues, prepared from solvent-free formulations, represent promising alternatives to conventional PU glues prepared from toxic isocyanate chemistry.

II.5 REFERENCES

1 D. M. Segura, A. D. Nurse, A. McCourt, R. Phelps and A. Segura, in *Handbook of Adhesives and Sealants*, 2005, vol. 1, pp. 101–162.

2 H.-W. Engels, H.-G. Pirkl, R. Albers, R. W. Albach, J. Krause, A. Hoffmann, H. Casselmann and J. Dormish, *Angew. Chemie Int. Ed.*, 2013, **52**, 9422–9441.

3 G. Otorgust, H. Dodiuk, S. Kenig and R. Tenne, *Eur. Polym. J.*, 2017, **89**, 281–300.

4 S. Merenyi, *Reach Regul. No 1907/2006 Consol. version (June 2012) with an Introd. Futur. Prospect. regarding area Chem. Legis. Vol. 2. GRIN Verlag, 2012.*

5 E. Delebecq, J.-P. Pascault, B. Boutevin and F. Ganachaud, *Chem. Rev.*, 2013, **113**, 80–118.

6 D. K. Chattopadhyay and K. V. S. N. Raju, *Prog. Polym. Sci.*, 2007, **32**, 352–418.

7 O. Kreye, H. Mutlu and M. a. R. Meier, *Green Chem.*, 2013, **15**, 1431–1455.

8 E. Delebecq, J. Pascault, B. Boutevin and F. Ganachaud, *Chem. Rev.*, 2013, **113**, 80–118.

9 O. Figovsky, L. Shapovalov, A. Leykin, O. Birukova and R. Potashnikova, *Int. Lett. Chem. Phys. Astron.*, 2013, **3**, 52–66.

10 M. S. Kathalewar, P. B. Joshi, A. S. Sabnis and V. C. Malshe, *RSC Adv.*, 2013, **3**, 4110.

11 H. Tomita, F. Sanda and T. Endo, *J. Polym. Sci. Part A Polym. Chem.*, 2001, **39**, 851–859.

12 L. Maisonneuve, O. Lamarzelle, E. Rix, E. Grau and H. Cramail, *Chem. Rev.*, 2015, **115**, 12407–12439.

13 B. Nohra, L. Candy, J. F. Blanco, C. Guerin, Y. Raoul and Z. Mouloungui, *Macromolecules*, 2013, **46**, 3771–3792.

14 C. Carré, L. Bonnet and L. Avérous, *RSC Adv.*, 2015, **5**, 100390–100400.

15 G. Rokicki, P. G. Parzuchowski and M. Mazurek, *Polym. Adv. Technol.*, 2015, **26**, 707–761.

16 H. Blattmann, M. Fleischer, M. Bähr and R. Mülhaupt, *Macromol. Rapid Commun.*, 2014, **35**, 1238–1254.

17 M. Bähr, A. Bitto and R. Mülhaupt, *Green Chem.*, 2012, **14**, 1447–1454.

18 L. Poussard, J. Mariage, B. Grignard, C. Detrembleur, C. Jérôme, C. Calberg, B. Heinrichs, J. De Winter, P. Gerbaux, J.-M. Raquez, L. Bonnaud and P. Dubois, *Macromolecules*, 2016, **49**, 2162–2171.

19 S. Gennen, B. Grignard, J.-M. Thomassin, B. Gilbert, B. Vertruyen, C. Jerome and C. Detrembleur, *Eur. Polym. J.*, 2016, **84**, 849–862.

20 B. Grignard, J.-M. Thomassin, S. Gennen, L. Poussard, L. Bonnaud, J.-M. Raquez, P. Dubois, M.-P. Tran, C. B. Park, C. Jerome and C. Detrembleur, *Green Chem.*, 2016, **18**, 2206–2215.

21 S. Gennen, B. Grignard, T. Tassaing, C. Jérôme and C. Detrembleur, *Angew. Chemie Int. Ed.*, 2017, **56**, 10394–10398.

22 V. Besse, F. Camara, F. Méchin, E. Fleury, S. Caillol, J.-P. Pascault and B. Boutevin, *Eur. Polym. J.*, 2015, **71**, 1–11.

23 G. Beniah, X. Chen, B. E. Uno, K. Liu, E. K. Leitsch, J. Jeon, W. H. Heath, K. A. Scheidt and J. M. Torkelson, *Macromolecules*, 2017, **50**, 3193–3203.

24 O. Lamarzelle, P.-L. Durand, A.-L. Wirotius, G. Chollet, E. Grau and H. Cramail, *Polym. Chem.*, 2016, **7**, 1439–1451.

25 J. Guan, Y. Song, Y. Lin, X. Yin, M. Zuo, Y. Zhao, X. Tao and Q. Zheng, *Ind. Eng. Chem. Res.*, 2011, **50**, 6517–6527.

26 S. Schmidt, F. J. Gatti, M. Luitz, B. S. Ritter, B. Bruchmann and R. Mülhaupt, *Macromolecules*, 2017, **50**, 2296–2303.

27 G. Beniah, K. Liu, W. H. Heath, M. D. Miller, K. A. Scheidt and J. M. Torkelson, *Eur. Polym. J.*, 2016, **84**, 770–783.

28 C. Carré, H. Zoccheddu, S. Delalande, P. Pichon and L. Avérous, *Eur. Polym. J.*, 2016, **84**, 759–769.

29 V. Schimpf, B. S. Ritter, P. Weis, K. Parison and R. Mülhaupt, *Macromolecules*, 2017, **50**, 944–955.

30 R. Ménard, S. Caillol and F. Allais, *ACS Sustain. Chem. Eng.*, 2017, **5**, 1446–1456.

31 A. Cornille, C. Guillet, S. Benyahya, C. Negrell, B. Boutevin and S. Caillol, *Eur. Polym. J.*, 2016, **84**, 873–888.

32 O. Figovsky, L. Shapovalov and F. Buslov, *Surf. Coatings Int. Part B Coatings Trans.*, 2005, **88**, 67–71.

33 M. Tryznowski, A. Świderska, T. Gołofit and Z. Żołek-Tryznowska, *RSC Adv.*, 2017, **7**, 30385–30391.

34 E. K. Leitsch, W. H. Heath and J. M. Torkelson, *Int. J. Adhes. Adhes.*, 2016, **64**, 1–8.

35 A. Cornille, G. Michaud, F. Simon, S. Fouquay, R. Auvergne, B. Boutevin and S. Caillol, *Eur. Polym. J.*, 2016, **84**, 404–420.

36 N. E. Prasad, A. Kumar and J. Subramanyam, *Aerospace Materials and Material Technologies*, 2017, vol. 1.

37 T. Monetta, A. Acquesta and F. Bellucci, *Aerospace*, 2015, **2**, 423–434.

38 H. Ni, A. H. Johnson, M. D. Soucek, J. T. Grant and A. J. Vreugdenhil, *Macromol. Mater. Eng.*, 2002, **287**, 470–479.

39 S. Intem, a. E. Hughes, a. K. Neufeld, T. Markley and a. M. Glenn, *J. Coatings Technol. Res.*, 2006, **3**, 313–322.

40 B. Grignard, C. Calberg, C. Jérôme, W. Wang, S. Howdle and C. Detrembleur, *Chem. Commun.*,

2008, **44**, 5803–5805.

41 S. Gennen, M. Alves, R. Méreau, T. Tassaing, B. Gilbert, C. Detrembleur, C. Jerome and B. Grignard, *ChemSusChem*, 2015, **8**, 1845–1849.

42 M. Alves, R. Mereau, B. Grignard, C. Detrembleur, C. Jerome and T. Tassaing, *RSC Adv.*, 2016, **6**, 36327–36335.

43 M. Alves, B. Grignard, A. Boyaval, R. Méreau, J. De Winter, P. Gerbaux, C. Detrembleur, T. Tassaing and C. Jérôme, *ChemSusChem*, 2017, **10**, 1128–1138.

44 J. Zong, Q. Zhang, H. Sun, Y. Yu, S. Wang and Y. Liu, *Polym. Bull.*, 2010, **65**, 477–493.

45 L. J. Matienzo and F. D. Egitto, *J. Mater. Sci.*, 2006, **41**, 6374–6384.

46 K. Nakamae, T. Nishino, S. Asaoka and Sudaryanto, *Int. J. Adhes. Adhes.*, 1996, **16**, 233–239.

47 Thomson, *Polyurethanes as Specialty Chemicals Principles and Applications*, CRC Press, 2005.

48 M. Jalilian, H. Yeganeh and M. N. Haghighi, *Polym. Adv. Technol.*, 2009, **21**, 118–127.

II.6 SUPPORTING INFORMATION

Synthesis of 4,4'-(((2-ethyl-2-(((2-oxo-1,3-dioxolan-4-yl)methoxy) methyl) propane-1,3-diyl) bis(oxy))bis(methylene))bis(1,3-dioxolan-2-one) (TMPTC).

TMPTC was synthesized by coupling CO_2 with epoxide, using a bicomponent organocatalyst that combined tetrabutylammonium iodide (TBAI) as catalyst with 1, 3-bis(2-hydroxyhexafluoroisopropyl)benzene as activator. 34 g (0.112 mol) of trimethylolpropane triglycidyl ether (TMPTE) was introduced in a 80 ml high pressure cell equipped with a mechanical stirrer and prior addition of 2.5 mol% (with respect to the epoxy content) of bicomponent organocatalyst combining TBAI (2.81mmol, 1.0384 g) and 1,3-bis(2-hydroxyhexafluoroisopropyl)benzene (2.81 mmol, 0.698 mL). Then the reaction mixture was heated to 80 ^{0}C prior equilibration of the cell at a CO_2 pressure of 100 bar for 24 h. The reactor was depressurized slowly to release unreacted CO_2. The resulting product was collected as a viscous liquid that was used without any further purification.

The complete conversion of TMPTE into TMPTC was confirmed by ^{1}H NMR spectroscopy with the disappearance of the peaks characteristic of –C*H*–O– and –C*H*$_2$–O– of epoxides at 3.15 and 2.5-2.8 ppm, respectively, and the appearance of new signals of –C*H*–OC(=O)O– and –C*H*$_2$–OC(=O)O– of cyclic carbonates at 4.8 and 4.25–4.6 ppm, respectively (Figure S1). Formation of the cyclic carbonate was further confirmed by FT-IR spectroscopy highlighting the presence of a strong signal at 1789 cm^{-1} corresponding to the elongation of the C=O group (Figure S2).

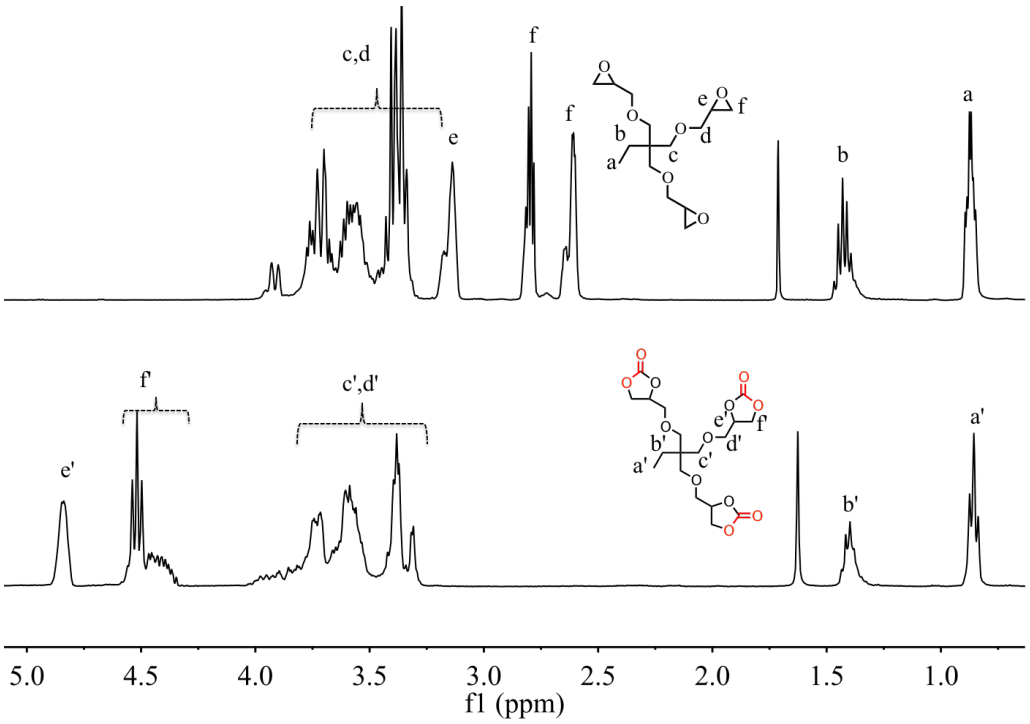

Fig.S1 ^{1}H NMR spectra of TMPTE (top) and TMPTC (bottom).

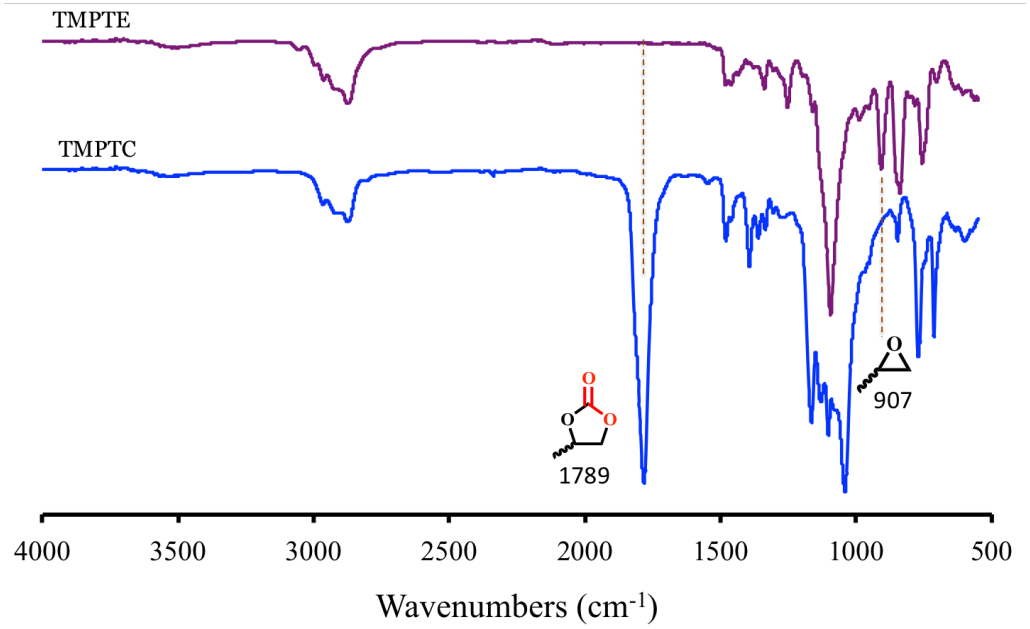

Fig.S2 FTIR spectra of TMPTE and TMPTC

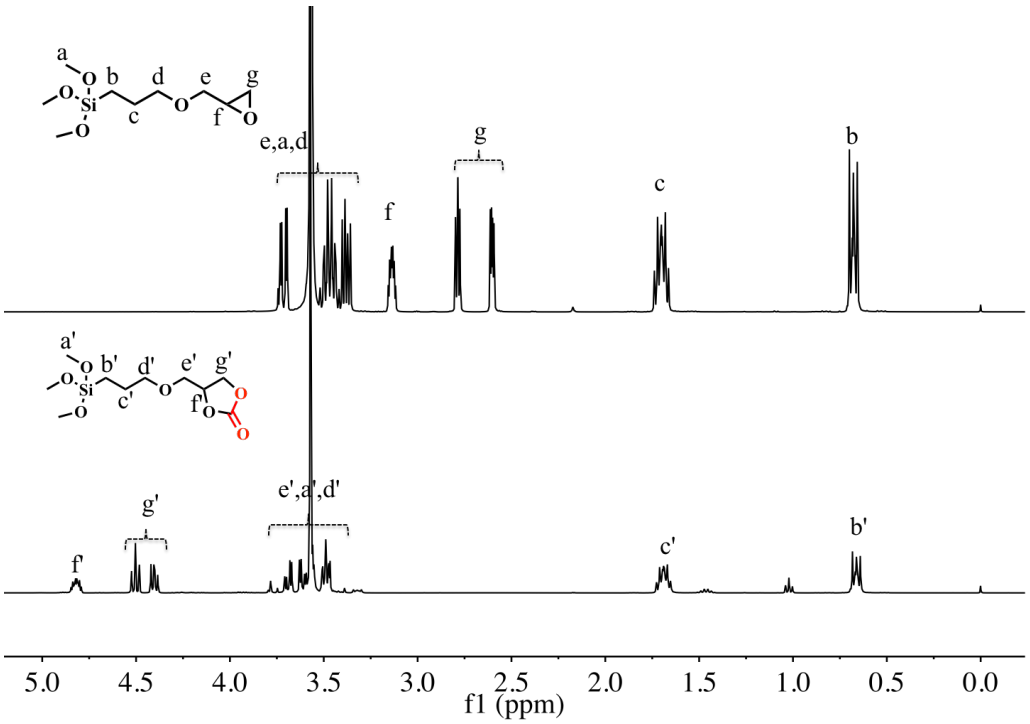

Fig.S3 ^{1}H NMR spectra of GPTMS (top) and C-GPTMS (bottom)

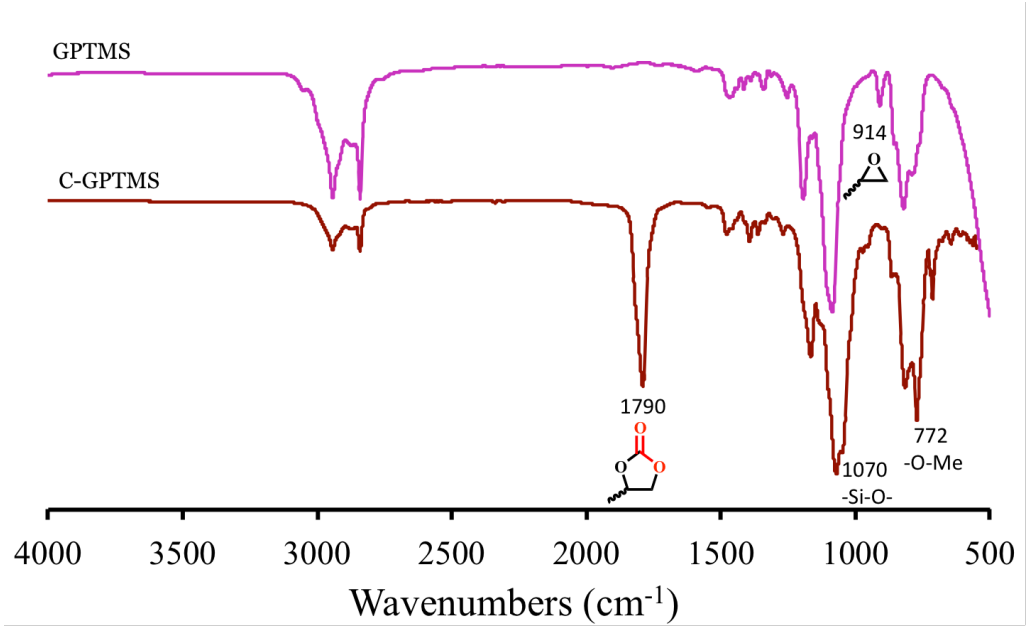

Fig.S4 FTIR spectra of GPTMS and C-GPTMS.

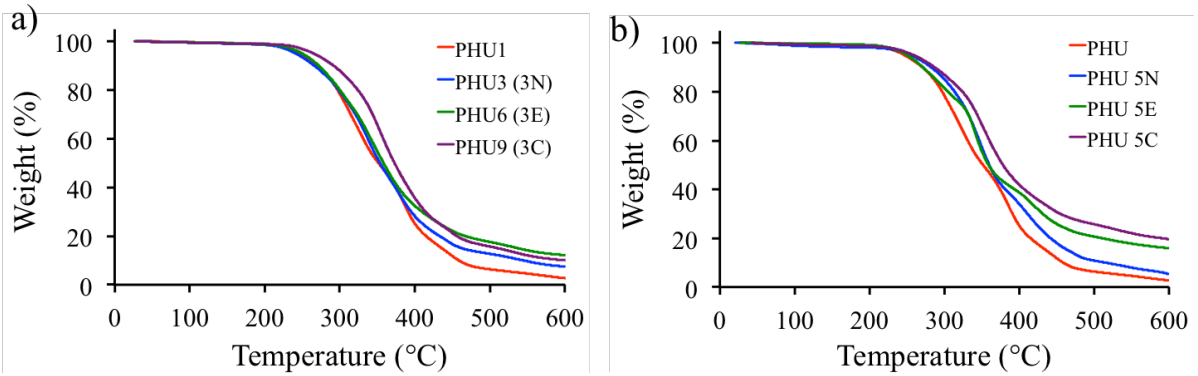

Fig.S5 TGA of a) PHUs reinforced by 3wt% of ZnO, GPTMS-ZnO and C-GPTMS-ZnO fillers. b) PHUs reinforced by 5wt% of ZnO, GPTMS-ZnO and C-GPTMS-ZnO fillers.

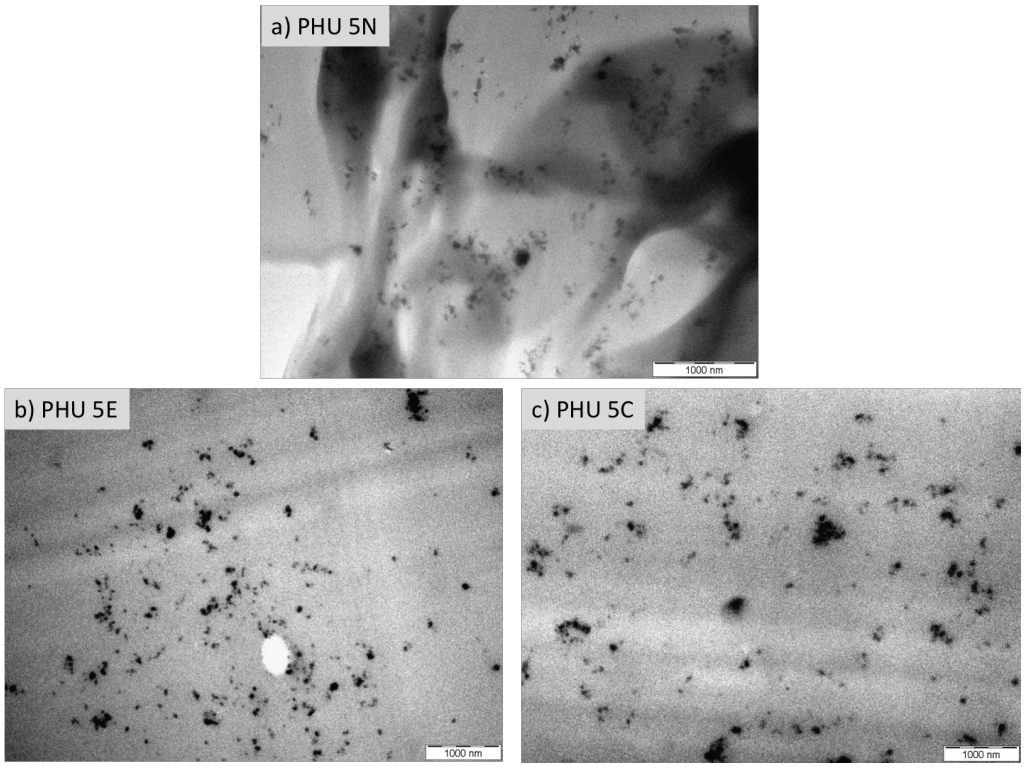

Fig.S6 TEM micrographs of a) reinforced non-functionalized (PHU 5N), b) epoxy functionalized (PHU-5E) and c) cyclic carbonate functionalized (PHU 5C) formulations. (Scale bar = 1µm).

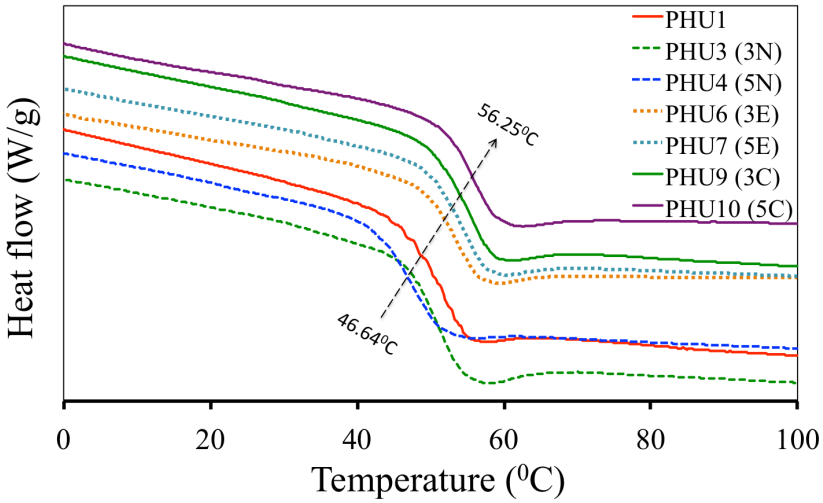

Fig.S7 DSC of PHUs reinforced by 3 and 5 wt% of ZnO, GPTMS-ZnO and C-GPTMS-ZnO fillers.

Chapter-III

Bio-Based Polyhydroxyurethanes Glues for Metal Substrates

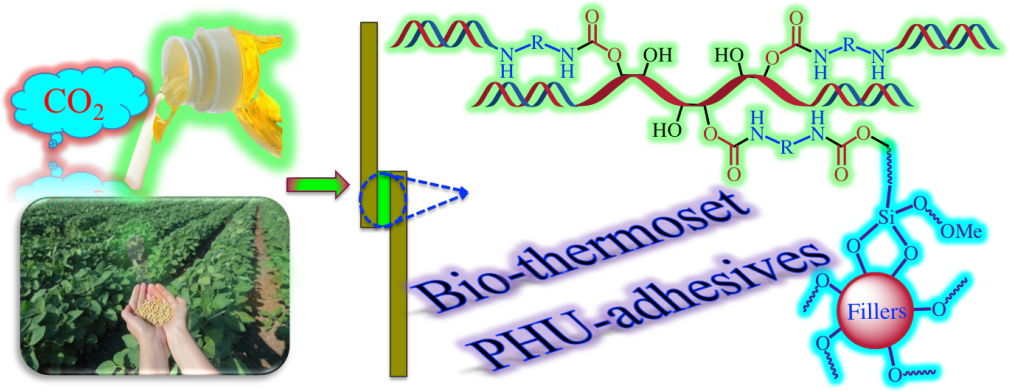

Satyannarayana Panchireddy, Bruno Grignard, Jean-Michel Thomassin, Christine Jerome and Christophe Detrembleur, ***Polym. Chem., 2018***, 9, 2650-2659.

ABSTRACT

Bio- and CO_2-based high performance thermoset poly(hydroxyurethane)s (PHUs) glues were designed from solvent- and isocyanate-free formulations based on cyclocarbonated soybean oil, diamines (aliphatic, cycloaliphatic or aromatic) and functional silica or ZnO fillers. Shear strength values and cohesive or adhesive failure of glues was correlated with the crosslinking, mechanical and thermal properties of the nanocomposite PHU thermosets. The addition of SiO_2 or ZnO fillers bearing cyclic carbonate groups at their surface enabled to strongly improve the adhesion performances of the glues up to 173% compared to the unfilled PHUs. The most performant reinforced PHU adhesives showed a shear strength up to 11.3 MPa for aluminum substrate, and 10.1 MPa for stainless steel with cohesive failure. This study highlights that bio-based nanocomposite PHU thermosets are promising sustainable alternatives to conventional glues made of toxic formulations containing isocyanates.

Table of Contents

III.1 INTRODUCTION

Glues play a vital role in a wide range of industrial applications, including post-it notes, packaging, automotive and airplane assemblies, etc. Due to their intrinsic and tuneable properties such as flexibility, abrasion and chemical resistance, thermal stability and good mechanical performances, polyurethane (PU) materials are widely valorised as coatings, foams, elastomers but also as adhesives.[1–6] They are produced by polyaddition of polyisocyanates[7,8] with diols, but present some limitations such as the involvement of toxic monomers (isocyanates) that are harmful to human health.[9] On the contrary, PU researches focus now on the development of greener routes for their synthesis by polyaddition of (activated) five-membered biscyclic carbonates with diamines.[10–37] The resulting poly(hydroxyurethane)s (PHUs) structurally differ from conventional PUs by the presence in β-position of the urethane bond of primary and/or secondary alcohols.[30,38,39] Inspired by these pendant hydroxyl groups throughout the polymer, our attention shifted to designing materials as high-performance novel glues that may compete the traditional PUs ones by favouring the adhesive/substrate interactions *via* hydrogen bonding. Leitsch *et al.*[40] reported on PU/PHU hybrid adhesives produced by curing low molar mass cyclic carbonates and functional α,ω-telechelic isocyanate-based PU prepolymers with polyamines. The resulting hybrid materials showed good adhesion onto polyimide, poly(vinyl chloride) and aluminium. Additionally, these hybrid polymers predominantly underwent cohesive failure, a key characteristic for developing high performance adhesives. The first solvent-free and isocyanate-free PU adhesives for wood, glass and epoxy painted aluminum supports was reported in 2016 by Cornille *et al.*[41] The bonded adhesives were cured at 80 °C for 12 h and 150 °C for 30 min, and cohesive failure was observed for PHUs (TMPTC/EDR-148) glues on epoxy painted aluminum (shear strength ≈ 3 MPa). Recently, our group designed novel thermoset reinforced PHUs glues for bare aluminum with excellent adhesive performances.[42] Solvent-free multifunctional cyclic carbonate/diamine formulations were added with 5 wt% of cyclic carbonate functional ZnO fillers. These fillers significantly improved the crosslinking, the thermal stability, the mechanical properties but also the adhesion performances of PHU. However, the presence of hydroxyl groups along the polymer backbone rendered the PHUs hydrophilic that favoured the adhesive delamination when the surface was immersed in water. This limitation was overcome

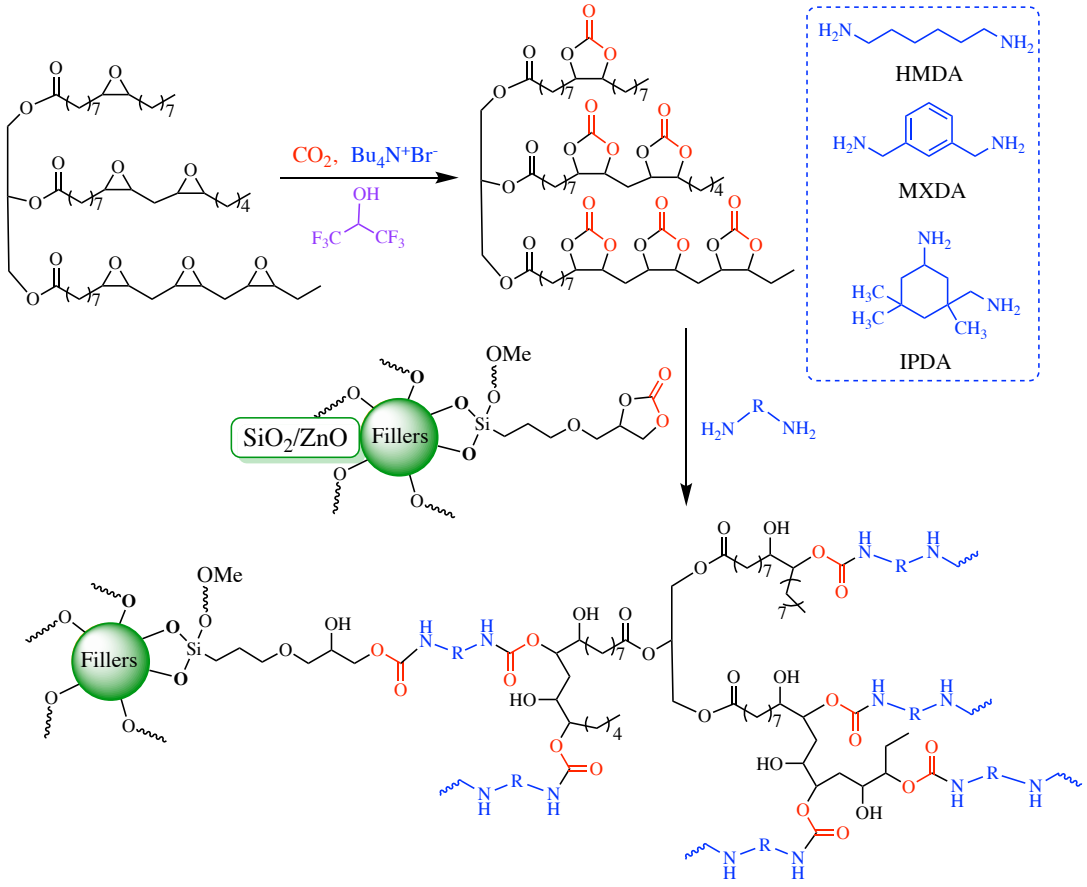

Scheme 1. Synthesis of bio-based nanocomposite thermoset poly(hydroxyurethane) glues for metal sticking (aluminum and/or stainless-steel).

by incorporating hydrophobic PDMS segments within the PHU formulations, which provides high performance PHU glues for Al substrate with shear strength up to 16.3 MPa. However, water uptake was still between 36 and 50 wt% for the best formulations that might limit the applicability of the process, for instance, when the metal substrate has also to be protected from corrosion. Current challenges are to provide high performance environmentally friendly PHU glues with low water absorption, ideally from bio-resourced starting materials (vegetable oils for instance) and by using solvent-free formulations.

In this contribution, we design novel solvent-free nanocomposite thermoset PHU glues with diversified mechanical strength, limited water uptake, and high bonding strength for various metals (aluminum -Al- and stainless steel -SS-). The solvent-free PHU glues were prepared from multicyclic carbonates derived from soybean oil and various amines (aliphatic, cycloaliphatic and aromatic). The cyclocarbonated vegetable oil has been selected to confer a sustainable character to the final PHU glue but also to limit its water uptake and to prevent its

water induced delamination from the surface as the result of the hydrophobicity of the fatty acid aliphatic chain of the triglyceride. No PDMS is here required in the formulation. All bio-based PHUs were reinforced by introducing cyclic carbonate functional silica (CC-SiO_2) or ZnO (CC-ZnO) fillers that increase the thermo-mechanical properties and the adhesive performances of PHU thermosets (Scheme 1). As vegetable oils are typically composed of mixtures of triglycerides with various chain length (up to 18 C atoms), we determine the optimal formulations by rheological studies prior to evaluating water swelling, contact angle, thermo-mechanical performances of neat and nanocomposite PHU thermosets. The ability of PHUs to glue Al substrates is evaluated by ASTM standardized cross-cut adhesion and MEK double rub tests. This work then investigates the influence of the PHU formulation reinforced by CC-SiO_2 or CC-ZnO fillers on the adhesion performances by lap shear measurements on Al and SS substrates.

III.2 EXPERIMENTAL SECTION

III.2.1 Materials and Methods

Epoxidised soybean oil (ESBO) was kindly donated by Vandeputte Oleochemicals (Belgium). Tetrabutylammonium bromide (TBABr, >99%), 3-(glycidoxypropyl) trimethoxysilane (GPTMS, ≥98%), hexamethylenediamine (HMDA), m-xylylenediamine (MXDA) and isophorone diamine (IPDA) were purchased from Aldrich. Carbon dioxide (CO_2, N48) was supplied by Air liquid. Hexafluoroisopropanol was purchased from Fluorochem. ZnO®20 nanoparticles (specific surface area of 15-45 $m^2\ g^{-1}$) was received from Umicore, Belgium. CAB-O-SIL®EH5 (specific surface area of 380 $m^2\ g^{-1}$) was received from Cabot. All chemicals were used as received without any purification. Al-2024-T3 substrates were received from SONACA and 316-stainless steel (AK steel) kindly provided by the mechanical department of ULiege.

Carbonated soybean oils (CSBO),[18] 4-((3-trimethoxysilyl)propoxy)methyl)-1,3-dioxolan-2-one) and cyclic carbonate functional fillers (1.33 cyclic carbonate nm^{-2} for Cab-O-Sil EH5 and 0.63 cyclic carbonate nm^{-2} for ZnO) were synthesized according to our previously optimized procedures.[42,43]

III.2.2 Characterizations techniques

Fourier transform infrared spectra (FTIR) measurements. FTIR measurements were carried out on Nicolet IS5 spectrometer (Thermo Fisher Scientific) equipped with a diamond attenuated transmission reflectance (ATR) device, 32 scans were recorded for each sample over the range of 4000-500 cm^{-1} with a normal resolution of 4 cm^{-1} and spectra were analysed with ONIUM^{TM} software.

Differential scanning calorimetry (DSC) analysis was carried out on a Q1000 TA instruments using standard aluminium pans, calibrated with indium and nitrogen as purge gas. The samples were analysed at a heating rate of 10 °C min^{-1} over a temperature range from –80 °C to 200 °C under N_2 atmosphere.

Thermogravimetric analysis (TGA) was carried out using a Q500 from TA instruments. Thermal degradation of PHUs was measured at heating rate of 20 °C min^{-1} over the temperature range of 0 to 700 °C under nitrogen atmosphere.

Rheology. The curing kinetics of PHU formulations were carried out on ARES (Advanced Rheometric Expansion System) Rheometric scientific rheometer, equipped by two parallel plate geometry at a frequency (1 Hz), a strain (1 %), and the measurements were carried out at 100 ^{0}C. The evolution of storage, loss modulus and tan δ was monitored as function of time.
Tensile properties were determined at 298K using an Instron 5594 tensile machine at a speed 10 mm min^{-1} with load capacity of 10,000 N. E-modulus, tensile strength and elongation at break were estimated by the average values of at least 6 repeated PHU samples. Free-standing dog bone shaped reinforced PHU samples were prepared using Teflon molds with the following dimensions: length of 3 cm, length of narrow fraction of 1cm, width of 0.5 cm, width of narrow fraction of 0.2 cm and thickness of 0.05 cm.

Water swelling of PHU samples was evaluated by water content and absorption measurements at room temperature for free-standing films following the procedure reported elsewhere.[19,42] PHU samples with dimension of 0.5 cm (l) × 0.5 cm (t)× 0.5 cm (w) (0.125 cm^3) were immersed in 10 mL milli-q water at room temperature. The water uptake was measured until the weight of the swollen samples remains constant. The time evolution of the equilibrium water content (EWC) and equilibrium water absorption (EWA) were estimated by using equations (1) and

(2). After swelling measurements, all samples were dried in oven at 70 ^{0}C for 24 h and the gel content was measured using equation (3):

$$EWC\ (\%) = \left(\frac{W_s - W_d}{W_d}\right) X\ 100 \quad (1)$$

$$EWA\ (\%) = \left(\frac{W_s - W_d}{W_s}\right) X\ 100 \quad (2)$$

$$GC\ (\%) = \left(\frac{W_f}{W_i}\right) X\ 100 \quad (3)$$

Where W_s is the weight of swollen sample, W_d is the weight of dried sample, W_i is the initial weight and W_f is the final weight of dried sample.

Water contact angle measurements were performed on an OCA-20 apparatus (Dataphysics Instrument GmbH) in the sessile drop configuration by deposition of a 5-µl droplet of milli-Q water. The mean contact angle values were determined from at least 5 repeated measurements realized at different locations of each PHU coated Al surfaces as well as on both sides of the free-standing films.

Scanning electron microscopy *(SEM).* The morphology of nanocomposite PHU coatings was evaluated by scanning electron microscopy (SEM, JEOL JSM 840-A) apparatus after the metallization of the sample with Pt (30 nm).

Adhesion properties of PHU coatings were investigated by crosscut adhesion tests according to ASTM D3359 standards. The test consists of making six perpendicular cuts with a distance of 3 mm onto coated Al plate with a sharp razor blade followed by the application of a high-pressure sensitive adhesive tape (Intertape tm 51596-ASTM D3359, Gardco). The tape is then removed by rapid pulling off at an angle of 180 degree. The quality of the coating was visually estimated by comparison with % of area removed from the total surface.

Solvent resistance of coatings was evaluated by the methylethylketone (MEK) double rub test according to the ASTM D4752 standard. The coated Al surface was rubbed with cheesecloth soaked with MEK until failure or breakthrough of the film occurred. Double rubs were repeated for at least 200 movements or until the substrate become visible.

Wet adhesion *of the coatings* was investigated by water immersion test. The test consists of making perpendicular cuts with a distance of 10 mm onto coated Al plate with a sharp razor blade followed by immersion in water at room temperature for 5 days. This test is determined by visual appearance of blistering, delamination of the squares at the coating-substrate interface.

Lap-shear adhesion tests were carried out at 298K using an Instron 5594 equipped with a 10,000 N load cell at a displacement rate of 2 mm min^{-1}. Aluminum and stainless-steel metal substrates with dimensions of 50 mm (l) × 10 mm (w) × 0.8 mm (t) were used for single lap-shear measurements and grip length on both sides of test specimens was 25 mm. The tests were performed on at least 5 repeated samples from each type of formulation to determine the average lap-shear strength of adhesives. The lap shear strength was calculated by using the equation.

$$\tau = \frac{P}{A} \qquad (4)$$

Where, τ is lap shear strength (N mm^{-2} or MPa), P is the force to remove the adhesive or load (N) and A is the overlapped or gluing area (100 mm^2).

III.2.3 SYNTHESIS OF PROTOCOLS

III.2.3.1 PHU synthesis (representative protocol)

Prior to the PHUs synthesis, CSBO was degassed by thermal treatment at 60 ^{0}C overnight under vacuum. Solvent-free bio-based thermoset PHUs were prepared by mixing equimolar amounts of CSBO (2.0 g, 1.6 mmol, cyclic carbonate mean content/molecule = 6, molar mass approximated to 1250 g mol^{-1})[17,44–47] and diamine (HMDA, 0.5577 g, 4.8 mmol) at 50 ^{0}C for 3 minutes under stirring (500 rpm). This mixing time was optimized for obtaining an homogenous mixture of the components before curing, and that lead to the complete conversion of the cyclic carbonate after curing (as assessed by FTIR measurement; Figure S2) with the formation of PHU films that did not dissolve in THF or DMF (Figure S3). A lower mixing time did not provide an homogeneous mixture before curing (see ESI for further details, Figure S3). The homogeneous viscous formulation was deposited into Teflon mold to prepare free-standing films (to evaluate swelling measurements and thermo-mechanical properties) or applied on Al-substrates (thickness of 25-30 μm) to measure the contact angle and to perform

the crosscut adhesion and MEK double rub tests. Finally, 10 mg of the formulation was applied onto aluminum and/or stainless steel with contact area of 100 mm^2 for evaluation of shear adhesion strength. Then, all samples were cured at 70 °C for 12 h and 100 °C for 4 h in air circulating oven. Nanocomposite thermoset PHU films based on CSBO and HMDA were prepared following the same protocol but by adding 5wt% of CC-SiO_2/ZnO fillers (0.1278g, compared to CSBO and the diamine). The optimal HMDA content in reinforced formulations (0.6135g or 5.28 mmol and 0.5855g or 5.04 mmol respectively for CC-SiO_2 and CC-ZnO fillers) was determined by identifying the formulation that gives the lowest gel time in rheology (see the Results and Discussion section, Fig. 2).

III.2.3.2 Reaction of cyclic carbonate functionalized silica (CC-SiO_2) with HMDA

The reaction between CC-SiO_2 (0.2 g) and HMDA (0.96 g) was carried out in THF (3 mL) at 60 °C for 30 min. The solvent was then removed under vacuum and cured at 70 °C for 12 h and 100 °C for 4 h. The product was then washed in MeOH to remove unreacted amine and dried in vacuum at 70 °C for 2 h. The reaction was monitored by FTIR, Figure S4.

III.3 RESULTS AND DISCUSSION

III.3.1 Curing kinetics by rheology

Rheology properties play an essential role in material selection and processing of adhesives and coatings, where the determination of gel time could be useful for manufacturing process attributed to phase transition of formulations throughout the time of curing.[48] Before determining the influence of the nature of the amine (hexamethylenediamine (HMDA), isophorone diamine (IPDA) or m-xylylenediamine (MXDA)) on the curing kinetics of CSBO based PHUs thermosets, the optimal CSBO/amine molar ratio was identified by rheology measurements under solvent-free conditions at 100 °C without any catalyst. The molar ratio that gives the shortest gelation time, obtained from the G″/G′ crossover point of the G″/G′ *vs* time plot (see Fig. 1, as typical example) and phase transition due to chemical crosslinking, was selected as the optimal formulation. As a representative example, the evolution of the gelation time for various CSBO/HMDA compositions (PHU-H) is depicted in Figure S5a and Table 1. The curing time was the shortest (27 min) for the optimal CSBO/HMDA molar ratio of 1/3. Similar results were obtained with the other amines (IPDA and MXDA) and this ratio was selected for the following experiments. Table 1 shows that substituting HMDA for the less reactive aromatic amine (MXDA, formulation PHU-M) or cycloaliphatic amine (IPDA, formulation PHU-I) induced an increase of the gelation time from 27 min to 77 min and 463 min, respectively, in line with the decreased reactivity of the amines. FTIR analysis of the starting CSBO and PHU confirms that an almost complete conversion is reached after 50 min of curing at 100 °C, with the disappearance of the typical band of the carbonyl of cyclic carbonate at 1792 cm^{-1} and the appearance of bands of urethane at 1697 cm^{-1} (C=O), 1536 cm^{-1} (N–H), and hydroxyl at 3312 cm^{-1} (Figure S1).

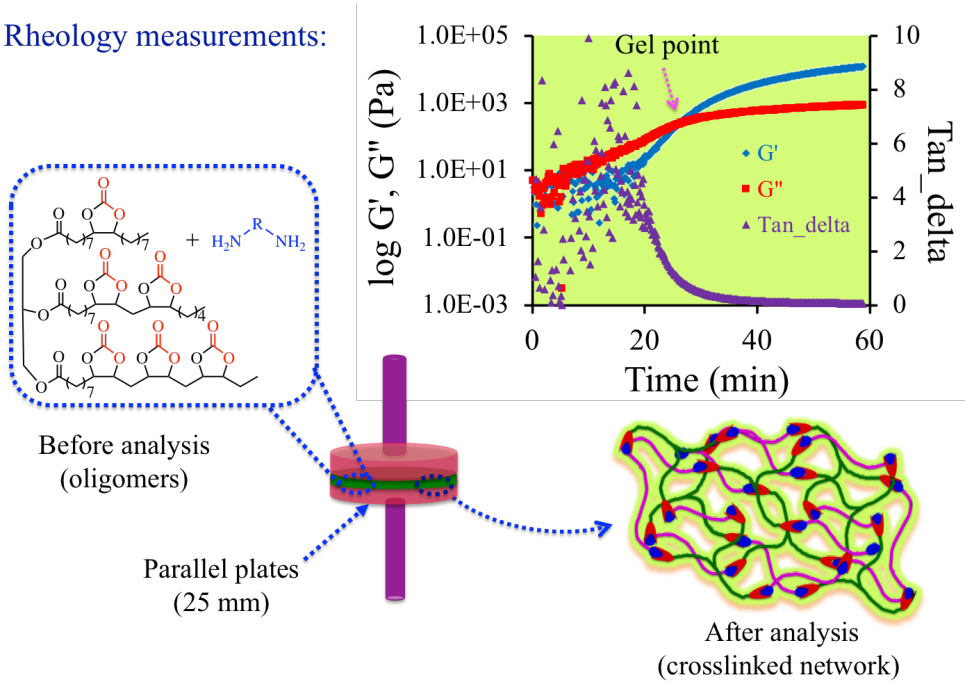

Fig. 1 Curing kinetics and time sweep measurements of CSBO/HMDA formulations by rheology under solvent-free conditions at 100 °C.

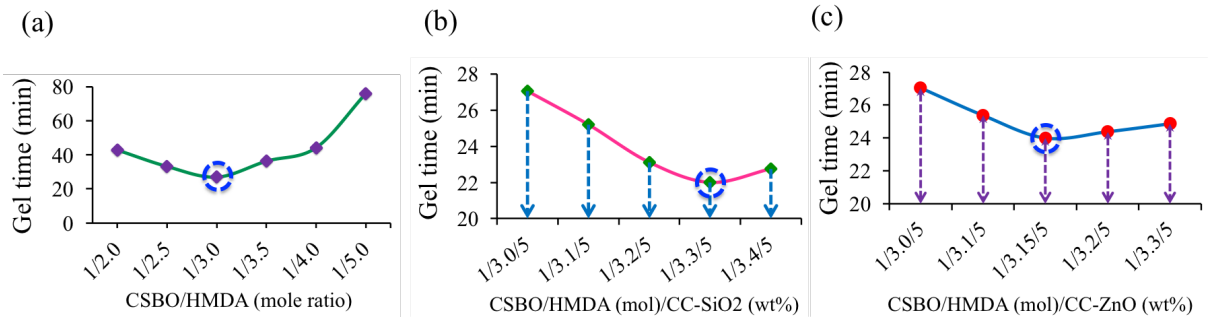

Fig. 2 Optimisation of PHU and analogous nanocomposite formulations. Evolution of the gel time for various (a) CSBO/HMDA (b) CSBO/HMDA/CC-SiO_2 and (c) CSBO/HMDA/CC-ZnO formulations were cured under solvent-free conditions at 100 °C and monitored by rheology. Blue star indicates the shortest gel time and best formulation molar ratios.

The formulations were then reinforced by the addition of 5 wt% of cyclic carbonate functional silica (CC-SiO_2) or ZnO (CC-ZnO) fillers (1.33 or 0.63 cyclic carbonate/nm^2, respectively). Since the presence of terminal cyclic carbonate functional groups on these fillers changes the stoichiometric ratio, compositions were again optimized *via* rheology by determining the gel time for various CSBO/HMDA molar contents. Whatever the filler, the lowest gel time was observed when a slight excess of amine was used (Figure 2 b-c). For each formulation (in the

investigated composition range), the addition of the functional filler slightly accelerated the curing rate as evidenced by a small reduction of the gel time, Fig. 3. The presence of the particles also improved the cross-linking density of the PHU-thermosets as confirmed by a reduction of the tan delta values at 45 min (Figure 3a, Table 1).[49] Indeed, a value of 0.4 was reported for CSBO/HMDA, while lower values of 0.2 for CSBO/HMDA/CC-ZnO and 0.12 for CSBO/HMDA/CC-SiO_2 formulations were measured. This trend might be explained by i) the higher reactivity of the terminal cyclic carbonates present at the surface of the fillers compared to the internal cyclic carbonates in CSBO and ii) the extent of crosslinking density of PHUs in presence of functional fillers.

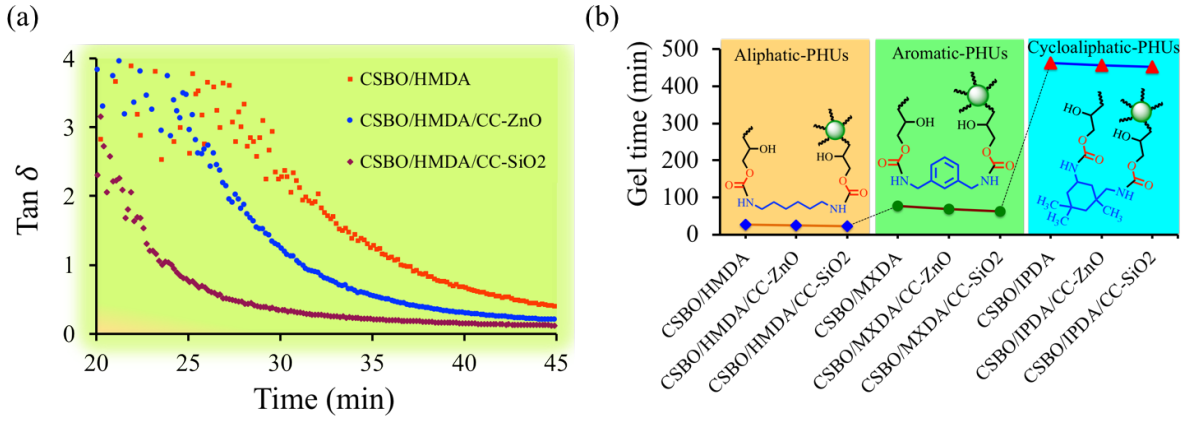

Fig. 3 (a) Evolution of tan delta measure by rheology at 100 °C for 50 min, for neat and reinforced formulations containing 5 wt% of functional (CC-ZnO or CC-SiO_2) fillers and (b) Gel time evolution for neat and reinforced formulations produced from HMDA, MXDA, IPDA using CSBO/diamines 1/3 molar ratio, CSBO/diamines/CC-SiO_2 1/3.3/5 ratio (mol/mol/wt%) and CSBO/diamines/CC-ZnO 1/3.15/5 ratio (mol/mol/wt%). All formulations were cured under solvent-free conditions at 100 °C and monitored by rheology.

In order to demonstrate that the cyclic carbonate-functionalized nanoparticles are able to react with the amine, the reaction between bare and/or cyclic carbonate functionalized fillers and amine was performed in THF at 60 °C for 30 minutes followed by curing at 70 °C for 12 h and 100 °C for 4 h. Fillers were then washed with MeOH to remove unreacted amine and dried in vacuum at 70 °C for 2 h. Figure S4 shows the FT-IR spectra of HMDA, CC-SiO_2, and CC-SiO_2 reacted with HMDA (CC-SiO_2-HMDA). Clearly, the grafting of HMDA to CC-SiO_2 was evidenced by the disappearance of the typical band of the carbonyl of cyclic carbonate at 1792 cm^{-1} and the appearance of the bands of urethane at 1697 cm^{-1} (C=O) and 1536 cm^{-1} (N–H).

III.3.2 Swelling measurement of free-standing PHUs films

Previous studies have shown that the pendant hydroxyl groups of PHUs favoured the interactions with aluminum substrate by hydrogen bonding.[42] However, they also increase the hydrophilicity and water uptake of PHU, which might be detrimental for their wet adhesion by inducing delamination of the glue.[42,50,51] The water uptake is therefore a qualitative information regarding the ability of the PHU glue to delaminate or not in an aqueous environment. The water uptake of our bio-based (nanocomposite) PHUs were evaluated on free-standing PHU films by water absorption experiments. In the absence of fillers, all formulations led to PHUs with low equilibrium water absorption (EWA) values ranging from 7.2% for PHU-H, to 4.8% for PHU-I and 4.0% for PHU-M (Table 1, Figure S6 and Figure S7a). These values are much lower than the ones measured for PHUs based on small multifunctional cyclic carbonate molecules (TMPTC) and charged with 5wt% of PDMS (EWA of 57%).[42] These lower water uptake values arise from the hydrophobic nature of CSBO induced by the long aliphatic chain (up to C_{18}) of the triglyceride. Upon addition of 5 wt% of cyclic carbonate functional silica or ZnO fillers, EWA values significantly decreased compared to unfilled PHU thermosets. For all formulations, the reduction of the water uptake is more prominent with ZnO than with SiO_2 fillers (Table 1). For instance, the addition of CC-ZnO to the CSBO/HMDA formulation drastically decreased the EWA value from 7.2% to 3.6%, compared to 4.3% with CC-SiO_2. The decrease of the water absorption of PHU reinforced by fillers may be correlated to the higher crosslinking density of the nanocomposite materials compared to unfilled PHUs. The same trend is noted for the equilibrium water content (EWC, Table 1). The gel content of the different PHU films is rather similar and high, between 96.2 and 98.9%, with no significant difference between the different formulations (Table 1). This observation indicates a highly crosslinked material in all cases.

III.3.3 Contact angle measurements of PHU coatings

The hydrophobic nature of (reinforced) PHU thermosets was further confirmed by contact angle measurement on PHU coatings on aluminium (thickness: 25-30 µm). Free-flowing solvent-free viscous PHU formulations prepared by mixing CSBO with diamines for 3 min at 50 °C were first deposited onto the metal surface for coating and into teflon molds for free standing films (thickness: 500 µm) *via* a bar-coater. After curing at 70 °C for 12 h and 100 °C

for 4 h, water contact angle of PHU coatings was measured. The coatings produced from unfilled PHU formulations exhibit contact angle values ranging from 95 ± 2° for PHU-H1 to 99 ± 3° for PHU-I1 and 103 ± 1° for PHU-M1 (Figure S7b, Table 1). The coatings are therefore hydrophobic, as expected from the hydrophobic formulation. PHU-M1 prepared from the aromatic diamine (MXDA) presents the higher hydrophobicity. The addition of 5wt% of CC-SiO_2 or CC-ZnO within CSBO/diamine formulations slightly increased the hydrophobicity of coatings with contact angle values up to 112° for PHU prepared from MXDA (PHU-M3, Table 1), which can be due to an increase of the surface roughness in the presence of fillers as evidenced by SEM (Figure S5). Additionally, contact angle measurements were also performed on both sides of free-standing films and similar values were obtained which suggests the homogeneity of the fillers dispersion. Again, CC-ZnO filler has the highest impact on the coating hydrophobicity, in line with the water absorption experiments (Figure S6 and Figure S7, respectively).

Table. 1 Formulation, swelling and adhesion properties of (reinforced) CSBO-derived PHU-thermosets.

Sample code	Formulation		GT [b] (min)	Tan δ [c]	EWC [d] (%)	EWA [e] (%)	GC [f] (%)	CA [g] (⁰)	CCA [h]
	CSBO (mol)/Amine (mol)/filler (wt%) [a]								
PHU-H1	CSBO/HMDA	1/3/0	27	0.40	6.8 ± 0.4	7.2 ± 0.5	96.2	95 ± 2	5B
PHU-H2	CSBO/HMDA/CC-SiO_2	1/3.3/5	22	0.12	4.1 ± 0.2	4.3 ± 0.2	98.5	97 ± 1	5B
PHU-H3	CSBO/HMDA/CC-ZnO	1/3.15/5	24	0.20	3.5 ± 0.1	3.6 ± 0.1	98.1	101 ± 2	5B
PHU-M1	CSBO/MXDA	1/3/0	77	0.56	3.8 ± 0.2	4.0 ± 0.1	98.6	103 ± 1	5B
PHU-M2	CSBO/MXDA/CC-SiO_2	1/3.3/5	68	0.15	3.6 ± 0.1	3.7 ± 0.2	98.8	109 ± 2	5B
PHU-M3	CSBO/MXDA/CC-ZnO	1/3.15/5	72	0.29	2.8 ± 0.1	2.9 ± 0.1	98.9	112 ± 1	5B
PHU-I1	CSBO/IPDA	1/3/0	463	0.92	4.5 ± 0.2	4.8 ± 0.1	97.6	99 ± 3	5B
PHU-I2	CSBO/IPDA/CC-SiO_2	1/3.3/5	455	0.63	3.8 ± 0.1	4.5 ± 0.2	98.1	103 ± 2	5B
PHU-I3	CSBO/IPDA/CC-ZnO	1/3.15/5	452	0.75	3.0 ± 0.4	3.1 ± 0.1	96.4	108 ± 1	5B

[a] Optimum molar compositions determined by rheology (Figure S5, Figure 2a-b) [b] GT-Gel time (determined by rheology at 100 °C), [c] Tan δ values in the plateau region (at 45 min (for PHU-H), at 136 min for (PHU-M) and at 600 min for (PHU-I)). [d] EWC-equilibrium water content, [e] EWA-equilibrium water absorption of free-standing films 0.5 cm (l) × 0.5 cm (t) × 0.5 cm (w) or (0.125 cm^3) for 48 h. [f] GC-gel content, [g] CA-Contact angle and [h] Cross-cut adhesion test (performed *via* maintaining 3 mm space between cuts according to standardised ASTM D3359).

IIII.3.4 Thermal properties

The thermal stability of bio-based thermoset PHU nanocomposites materials was evaluated by thermogravimetric analysis (TGA) (Figure S8). The temperatures at 5% degradation ($Td_{5\%}$) are reported in Table 2 and Figure 4a. In the absence of fillers, polymers started to decompose above 246 °C as attested by $Td_{5\%}$ values of 246.8 °C, 249.5 °C and 270.4 °C for PHUs synthesized respectively from CSBO/HMDA, CSBO/IPDA and CSBO/MXDA formulations. The thermal stability was in the same range for the formulations that were reinforced by 5wt% CC-SiO_2. The addition of functional CC-ZnO fillers has a more pronounced stabilization effect with $Td_{5\%}$ values that increased to 257.3 °C, 259.8 °C and 277.3 °C for CSBO/HMDA, CSBO/IPDA and CSBO/MXDA formulations. Although the thermal stability varied slightly with the nature of the amines, the positive impact of the fillers on this stability probably results from the improved cross-linking of the thermoset PHUs that limits the diffusion of gases during the thermal degradation.

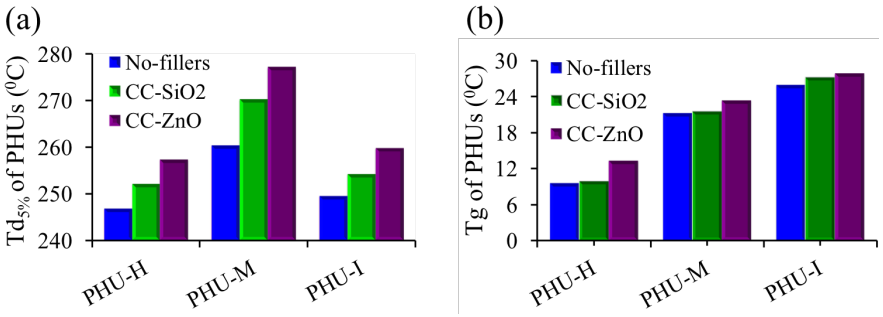

Fig. 4 Evolution of the thermal stability at 5% degradation ($Td_{5\%}$) (a) and glass transition temperature (Tg) (b) as function of the amine structure (H-aliphatic, I-cycloaliphatic and M-aromatic) of the PHU formulation and the filler (CC-SiO_2 or CC-ZnO). (PHU-H: aliphatic, PHU-M: aromatic and PHU-I: cyclic aliphatic thermosets).

The glass transition temperature (Tg) of each PHU was determined by differential scanning calorimetry (DSC) analysis (Table 2, Figure 4b and Figure S9). PHU-H and reinforced PHU-H exhibit a Tg in the range of 9.9 to 13.3 °C, PHU-M and reinforced PHU-M in the range of 21.3 to 24.6 °C, and PHU-I and reinforced PHU-I between 26 and 27.9 °C. As expected, the evolution of this Tg is mainly governed by the nature of the amine and increased in the order aliphatic < aromatic < cycloaliphatic diamine, in line with the expected increased rigidity order of the corresponding polymers.

III.3.5 Mechanical properties

The influence of the amine structure and of CC-silica/ZnO fillers on the mechanical properties of PHU thermosets was investigated by conventional tensile tests (Figure 5a). All results are summarized in Table 2 and Figure 5b. Young's modulus of PHU increased with the PHU rigidity, thus with the nature of the diamine used, i.e. for HMDA ($E_{PHU\text{-}H1}$ = 65 MPa) < MXDA ($E_{PHU\text{-}M1}$ = 94 MPa) < IPDA ($E_{PHU\text{-}I1}$ = 161 MPa), whereas the elongation at break decreased with the PHU rigidity, i.e. for HMDA ($\varepsilon_{PHU\text{-}H1}$ = 308%) > MXDA ($\varepsilon_{PHU\text{-}M1}$ = 227%) > IPDA ($\varepsilon_{PHU\text{-}I1}$ = 177%). For all formulations, the addition of SiO_2 or ZnO particles increased Young's modulus and decreased the elongation at break, as the result of extent of crosslinking density and the formation of a denser network in the presence of the functional particles. Formulations with IPDA and CC-ZnO particles became very brittle, clearly highlighting a transition from elastic (reinforced) PHUs produced from HMDA to rigid and brittle (reinforced) materials by replacing the aliphatic by the cycloaliphatic diamines.

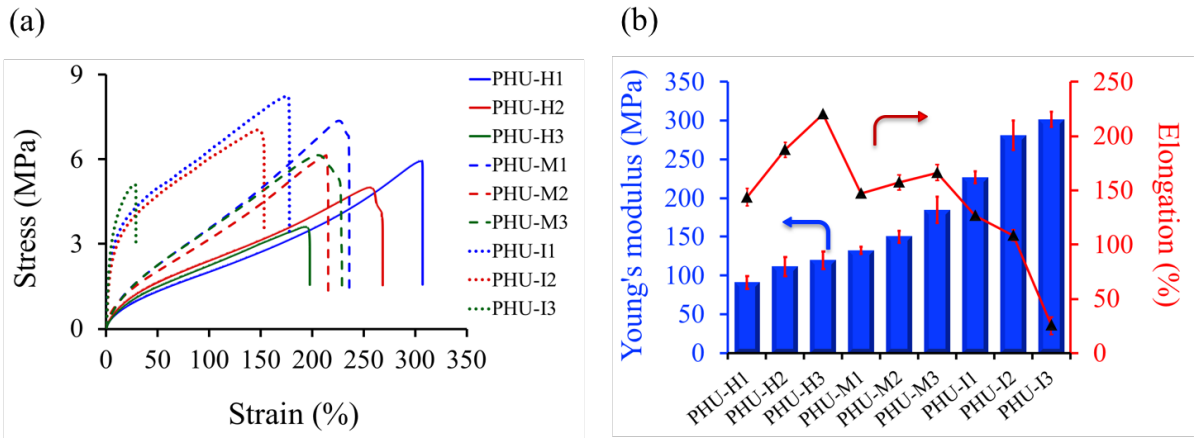

Fig. 5 Evolution of the mechanical properties of PHUs (a) Stress vs strain and (b) Young's modulus & elongation (%) at break vs evolution for the various CSBO/diamine formulations (neat or reinforced with 5wt% CC-SiO2 or CC-ZnO) (PHU-H: aliphatic, PHU-M: aromatic and PHU-I: cyclic aliphatic thermosets).

Table 2. Thermal and mechanical properties of bio and CO_2 sourced neat and nanocomposite thermoset PHU glues.

Sample code	Tg^a (°C)	$Td^b_{5\%}$	E^c (MPa)	σ^d_{Yield} (MPa)	ε^e_{break} (%)	LSS^f (MPa) Al-Al	LSS^g (MPa) SS-SS
PHU-H1	9.9	246.8	65 ± 6	6.1 ± 0.3	308 ± 3	6.5 ± 0.49	4.9 ± 0.12
PHU-H2	9.6	252.1	80 ± 9	5.4 ± 0.6	262 ± 9	8.8 ± 0.35	7.9 ± 0.27
PHU-H3	13.3	257.3	86 ± 8	3.7 ± 0.2	194 ± 2	11.3 ± 0.28	10.1 ± 0.23
PHU-M1	21.3	260.5	94 ± 3	7.5 ± 0.3	227 ± 3	6.4 ± 0.33	6.1 ± 0.49
PHU-M2	21.5	270.4	107 ± 5	6.4 ± 0.4	220 ± 9	6.9 ± 0.26	6.4 ± 0.42
PHU-M3	24.6	277.3	132 ± 12	6.3 ± 0.2	205 ± 2	7.5 ± 0.29	6.9 ± 0.15
PHU-I1	26.0	249.5	161 ± 5	8.3 ± 0.2	177 ± 3	3.7 ± 0.54	3.5 ± 0.04
PHU-I2	27.2	254.2	200 ± 13	7.4 ± 0.5	151 ± 7	4.6 ± 0.36	4.4 ± 0.98
PHU-I3	27.9	259.8	215 ± 7	5.3 ± 0.3	26 ± 1	5.9 ± 0.52	4.6 ± 0.47

Bio-based PHU thermoset glues and analogues PHUs reinforced with 5 wt% CC-SiO_2 or CC-ZnO fillers; [a)] determined by DSC, heating rate 10 °C min^{-1}, [b)] determined by TGA, heating rate 20 °C min^{-1}, [c)] Young's modulus, [d)] Tensile strength, [e)] Elongation at break, [f, g)] Lap shear strength. (PHU-H: aliphatic, PHU-M: aromatic and PHU-I: cyclic aliphatic thermosets). [PHU-H1, PHU-M1 and PHU-I1: unfilled PHUs, PHU-H2, PHU-M2 and PHU-I2: PHUs reinforced with 5 wt% CC-SiO_2; PHU-H3, PHU-M3 and PHU-I3: PHUs reinforced with 5 wt% CC-ZnO].

III.3.6 Adhesive performances

Prior to determine the shear strength of the PHU glues, the adhesion performances of 25-30 µm thick coatings deposited on bare Al surface were qualitatively investigated by the standardized ASTM D3359 cross-cut test (Table 1) performed by maintaining 3 mm space between the cuts. Whatever the PHU formulation, the edges of the cuts were completely smooth and none of the squares of the coatings were removed after tape removal. All PHU coatings were classified as 5B-0%. Such high adhesion properties make the (reinforced) biobased thermoset PHUs good candidates for designing high performances glues. The resistance of coatings against solvents was also investigated by the MEK double rub test in line with ASTM D4752 standards. After 200 double rubs, no visible surface defects and/or wiping off of the coatings from the surface could be detected, confirming the excellent adhesion of all PHU formulations onto Al substrate. Additionally, the wet adhesion performance of thermosets was evaluated by immersing coatings in water at room temperature for 5 days. Figure 6 shows

that unfilled PHU coatings were peeled off after immersion for 5 days. In contrast, the nanocomposite coatings were stable in the same conditions, and no delamination was observed. This study illustrates that reinforced functional fillers significantly improve the films stability in wet environment, in agreement with the water uptake results.

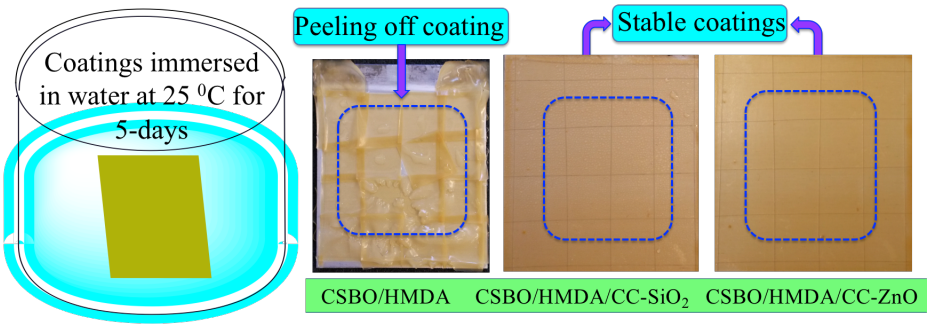

Fig. 6 Evolution of wet adhesion of PHU and analogous nanocomposite thermoset coatings immersed in water at 25 °C for 5 days. The coatings were manually cut into squares (thus, distance of 10 mm between cuts) to visualize peeling off of coating.

Then, the shear adhesion performances of the bio-based nanocomposite PHU glues were evaluated for sticking aluminum to aluminum (Al-Al) (Figure 7a and 7b) and stainless steel to stainless steel (SS-SS) substrates, (Figure 6c and 6d, Table 2). Adhesion values were quantified by lap shear tests using eq-4. For Al substrates, the lap shear strength for bare PHU adhesives varied from about 6.5 MPa for PHU-H and PHU-M, to 3.7 MPa for PHU-I. The lowest adhesive performance of CSBO/IPDA PHU glues was related to the high Tg values and the brittleness of the crosslinked material that are detrimental to the adhesion. Indeed, the presence of flexible/soft segments in conventional PUs or PHUs is most often required for high adhesion performances.[52,41] The addition of functional (CC-SiO_2 or CC-ZnO) fillers increased the adhesion strength of PHU due to extent of crosslinking. The effect is more pronounced with CC-ZnO for PHU-H with a lap shear strength values up to 11.3 MPa, corresponding to 173% increase compared to bare PHU-H. This improvement is explained by a higher crosslinking density of reinforced PHUs that increased the mechanical strength without sacrificing elongation at break of the glue. This trend is further confirmed for PHU-M and PHU-I with a shear strength that increased by 117% (up to 7.5 MPa, PHU-M3) and 160% (up to 5.9 MPa, PHU-I3), respectively, upon addition of 5 wt% of CC-ZnO. All PHU glues underwent cohesive

failure (CF) at the exception of reinforced PHU-I that showed an adhesive failure (AF) mode as the result of a too rigid crosslinked materials that disfavoured adhesive-metal substrate interaction. Interestingly, nanocomposite PHU glues also showed promising adhesion performances to stainless steel (SS) with adhesion strength up to 10.1 MPa for PHU-H reinforced by 5 wt% CC-ZnO. As observed for Al-Al sticking, reinforced formulations made of CSBO and MXDA or IPDA gave glues with significantly lower adhesion performances as attested by shear strength values of 6.9 and 4.6 MPa, respectively.

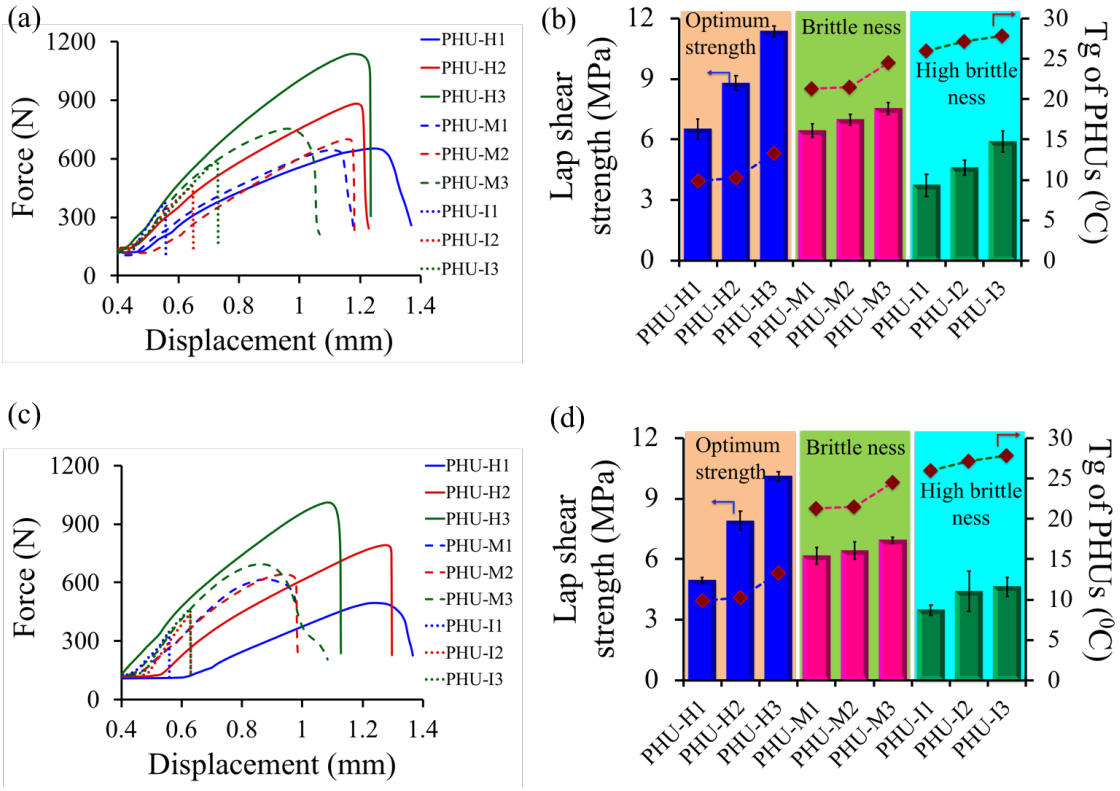

Fig. 7 Influence of the amine structure (H-HMDA, M-MXDA and I-IPDA) and filler (CC-SiO_2 or CC-ZnO) on the adhesive performances of PHUs for Al-Al (a and b) and SS-SS (c and d) substrates sticking. (PHU-H: aliphatic, PHU-M: aromatic and PHU-I: cyclic aliphatic thermosets). Product codes and compositions are summarized in Table 1.

III.3.7 Bench marking

The bio-based PHU with the best adhesion performance (PHU-H3) was then benchmarked against commercial PU adhesives (Teromix-6700 and Araldite®2000) and PHU adhesives (thus, PHU(M-1)[41], PHU-5C[42]). All adhesives are tested on Al under identical conditions, thus with the same amount of glue (10 mg), glue area (100 mm^2) and curing conditions (time and temperature) (70 °C for 12 h and 4 h at 100 °C and/or 48 h at 25 °C). The results are collected in Figure 8 and in Table S1. The commercial PU adhesives exhibited the highest performance when cured at 25 °C for 48 h [Araldite up to 21.7 MPa and Teromix up to 12.5 MPa] whereas PHU adhesives showed a low lap shear strength (PHU(M-1)[41], PHU-5C[42], PHU-H3: 1.9, 3.3 and 2.2 MPa, respectively). This poor adhesion performance for PHUs is the result of their too slow curing due to the low reactivity of cyclic carbonates towards amines at 25 °C. On the other hand, the bio-based glue (PHU-H3) competes with commercial glues (at least with Teromix) when cured under our optimized conditions with a shear strength of 11.3 MPa. Although the adhesion performance is slightly lower compared to our previous PHU-5C[42] and to Araldite, PHU-H3 is formulated from a sustainable bio-sourced cyclic carbonate without any solvent, does not contain any PDMS and does not involve the isocyanate chemistry. This benchmarking clearly highlights that well-designed PHU glues can afford a realistic and alternative to conventional PU glues. These sustainable high-performance bio-nanocomposite PHUs adhesives promising for applications that are compatible to a thermal curing.

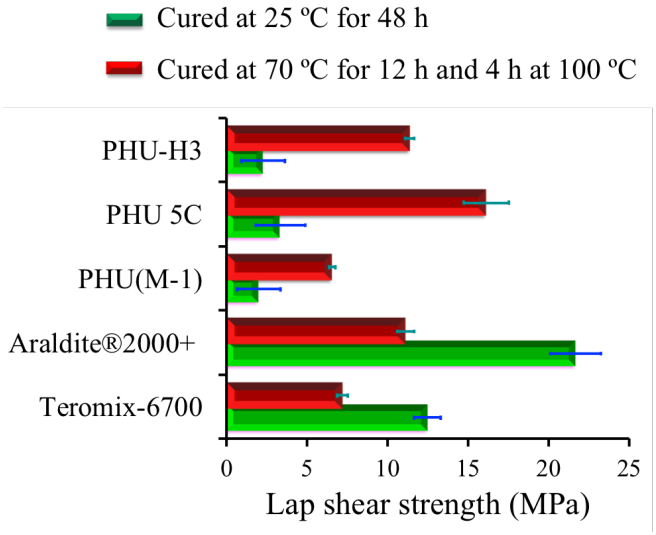

Fig. 8 Adhesive performance of bio-based nanocomposite thermoset PHU glue (PHU-H3) benchmarked against commercial PU and PHU glues were tested on Al, while conditions held constant.

III.4 CONCLUSION

We reported on the preparation of novel bio-based nanocomposite poly(hydroxyurethane) thermoset glues for aluminum and stainless-steel substrates. These glues were formulated by polyaddition of cyclic carbonate bearing vegetable oil (soybean oil) with (cyclo) aliphatic or aromatic diamines under solvent-free conditions. Various formulations reinforced with cyclic carbonate functionalized SiO_2 or ZnO fillers were also designed. Through swelling, contact angle measurements and wet adhesion, we demonstrated that the coating hydrophobicity induced by the long fatty ester chains (up to C_{18}) of soybean oil prevented water swelling of the thermoset PHU films and coating delamination from the surface when immersed in water. All PHU coatings presented good adhesion to Al according to the ASTM D3359 standard crosscut adhesion test and showed excellent mechanical properties and thermal stabilities (up to 277 °C). Formulations composed of aliphatic hexamethylene diamine and CSBO containing 5 wt% of functional ZnO provided reinforced PHU biobased glues offering the best compromise between extent of crosslinking, high thermal and mechanical properties, and the highest lap-shear adhesion strength for Al-Al and/or SS-SS substrates with shear strengths up to 11.3 MPa and 10.1 MPa, respectively. The maximum shear adhesion strength for Al was benchmarked against commercial polyurethane glues (Teromix-6700 and Araldite®2000) and recently reported non-biosourced PHUs (PHU(M-1)[41], PHU-5C[42]). This study has shown that bio-based nanocomposite PHUs thermosets represent attractive sustainable alternatives to conventional glues made of toxic formulations containing isocyanates. Current works investigate routes to cure at room temperature the formulations, while still improving the PHU adhesion strength.

III.5 REFERENCES

1 O. Bayer, *Angew. Chemie*, 1947, **59**, 257–272.

2 R. Auvergne, S. Caillol, G. David, B. Boutevin and J. P. Pascault, *Chem. Rev.*, 2014, **114**, 1082–1115.

3 H.-W. Engels, H.-G. Pirkl, R. Albers, R. W. Albach, J. Krause, A. Hoffmann, H. Casselmann and J. Dormish, *Angew. Chemie Int. Ed.*, 2013, **52**, 9422–9441.

4 C. D. Diakoumakos and D. L. Kotzev, *Macromol. Symp.*, 2004, **216**, 37–46.

5 Thomson, *Polyurethanes as Specialty Chemicals Principles and Applications*, CRC Press, 2005.

6 O. Kreye, H. Mutlu and M. a. R. Meier, *Green Chem.*, 2013, **15**, 1431–1455.

7 S. M. Tarlo and G. M. Liss, *Appl. Occup. Environ. Hyg.*, 2002, **17**, 902–908.

8 M. G. Ott, W. F. Diller and A. T. Jolly, *Crit. Rev. Toxicol.*, 2003, **33**, 1–59.

9 S. Merenyi, *Reach Regul. No 1907/2006 Consol. version (June 2012) with an Introd. Futur. Prospect. regarding area Chem. Legis. Vol. 2. GRIN Verlag, 2012.*

10 W. H. Carothers, *Chem. Rev.*, 1931, **8**, 353–426.

11 T. Sakai, N. Kihara and T. Endo, *Macromolecules*, 1995, **28**, 4701–4706.

12 N. Kihara and T. Endo, *J. Polym. Sci. Part A Polym. Chem.*, 1993, **31**, 2765–2773.

13 H. Tomita, F. Sanda and T. Endo, *J. Polym. Sci. Part A Polym. Chem.*, 2001, **39**, 851–859.

14 L. Maisonneuve, O. Lamarzelle, E. Rix, E. Grau and H. Cramail, *Chem. Rev.*, 2015, **115**, 12407–12439.

15 V. Besse, F. Camara, F. Méchin, E. Fleury, S. Caillol, J.-P. Pascault and B. Boutevin, *Eur. Polym. J.*, 2015, **71**, 1–11.

16 M. Alves, R. Mereau, B. Grignard, C. Detrembleur, C. Jerome and T. Tassaing, *RSC Adv.*, 2016, **6**, 36327–36335.

17 M. Alves, B. Grignard, S. Gennen, C. Detrembleur, C. Jerome and T. Tassaing, *RSC Adv.*, 2015, **5**, 53629–53636.

18 L. Poussard, J. Mariage, B. Grignard, C. Detrembleur, C. Jérôme, C. Calberg, B. Heinrichs, J. De Winter, P. Gerbaux, J.-M. Raquez, L. Bonnaud and P. Dubois, *Macromolecules*, 2016, **49**, 2162–2171.

19 S. Gennen, B. Grignard, J.-M. Thomassin, B. Gilbert, B. Vertruyen, C. Jerome and C. Detrembleur, *Eur. Polym. J.*, 2016, **84**, 849–862.

20 B. Grignard, J.-M. Thomassin, S. Gennen, L. Poussard, L. Bonnaud, J.-M. Raquez, P. Dubois, M.-P. Tran, C. B. Park, C. Jerome and C. Detrembleur, *Green Chem.*, 2016, **18**, 2206–2215.

21 S. Gennen, B. Grignard, T. Tassaing, C. Jérôme and C. Detrembleur, *Angew. Chemie Int. Ed.*,

2017, **56**, 10394–10398.

22 M. Alves, B. Grignard, S. Gennen, R. Mereau, C. Detrembleur, C. Jerome and T. Tassaing, *Catal. Sci. Technol.*, 2015, **5**, 4636–4643.

23 H. Tomita, F. Sanda and T. Endo, *J. Polym. Sci. Part A Polym. Chem.*, 2001, **39**, 3678–3685.

24 P. Anastas and N. Eghbali, *Chem. Soc. Rev.*, 2010, **39**, 301–312.

25 M. Bähr and R. Mülhaupt, *Green Chem.*, 2012, **14**, 483–489.

26 I. Javni, D. P. Hong and Z. S. Petrović, *J. Appl. Polym. Sci.*, 2008, **108**, 3867–3875.

27 A. Lee and Y. Deng, *Eur. Polym. J.*, 2015, **63**, 67–73.

28 O. Figovsky, A. Leykin and L. Shapovalov, *Altern. Energy Ecol.*, 2016, **4**, 95–108.

29 M. S. Kathalewar, P. B. Joshi, A. S. Sabnis and V. C. Malshe, *RSC Adv.*, 2013, **3**, 4110–4129.

30 M. Blain, L. Jean-Gérard, R. Auvergne, D. Benazet, S. Caillol and B. Andrioletti, *Green Chem.*, 2014, **16**, 4286–4291.

31 V. Besse, R. Auvergne, S. Carlotti, G. Boutevin, B. Otazaghine, S. Caillol, J.-P. Pascault and B. Boutevin, *React. Funct. Polym.*, 2013, **73**, 588–594.

32 J. Guan, Y. Song, Y. Lin, X. Yin, M. Zuo, Y. Zhao, X. Tao and Q. Zheng, *Ind. Eng. Chem. Res.*, 2011, **50**, 6517–6527.

33 S. Samanta, S. Selvakumar, J. Bahr, D. S. Wickramaratne, M. Sibi and B. J. Chisholm, *ACS Sustain. Chem. Eng.*, 2016, **4**, 6551–6561.

34 K. M. F. Rossi de Aguiar, U. Specht, J. F. Maass, D. Salz, C. A. Picon, P.-L. M. Noeske, K. Rischka and U. P. Rodrigues-Filho, *RSC Adv.*, 2016, **6**, 47203–47211.

35 M. Tryznowski, A. Świderska, T. Gołofit and Z. Żołek-Tryznowska, *RSC Adv.*, 2017, **7**, 30385–30391.

36 Z. Li, Y. Zhao, S. Yan, X. Wang, M. Kang, J. Wang and H. Xiang, *Catal. Letters*, 2008, **123**, 246–251.

37 L. Annunziata, A. K. Diallo, S. Fouquay, G. Michaud, F. Simon, J.-M. Brusson, J.-F. Carpentier and S. M. Guillaume, *Green Chem.*, 2014, **16**, 1947–1956.

38 B. Ochiai, Y. Satoh and T. Endo, *J. Polym. Sci. Part A Polym. Chem.*, 2009, **47**, 4629–4635.

39 M. V. Zabalov, R. P. Tiger and A. A. Berlin, *Dokl. Chem.*, 2012, **441**, 355–360.

40 E. K. Leitsch, W. H. Heath and J. M. Torkelson, *Int. J. Adhes. Adhes.*, 2016, **64**, 1–8.

41 A. Cornille, G. Michaud, F. Simon, S. Fouquay, R. Auvergne, B. Boutevin and S. Caillol, *Eur. Polym. J.*, 2016, **84**, 404–420.

42 S. Panchireddy, J.-M. Thomassin, B. Grignard, C. Damblon, A. Tatton, C. Jerome and C. Detrembleur, *Polym. Chem.*, 2017, **8**, 5897–5909.

43 B. Grignard, C. Calberg, C. Jérôme, W. Wang, S. Howdle and C. Detrembleur, *Chem.*

Commun., 2008, **44**, 5803–5805.

44 G. Karmakar and P. Ghosh, *ACS Sustain. Chem. Eng.*, 2016, **4**, 775–781.

45 A. Ghosal, O. U. Rahman and S. Ahmad, *Ind. Eng. Chem. Res.*, 2015, **54**, 12770–12787.

46 M. Sacristán, J. C. Ronda, M. Galià and V. Cádiz, *Biomacromolecules*, 2009, **10**, 2678–2685.

47 C. Zhang, Y. Xia, R. Chen, S. Huh, P. A. Johnston and M. R. Kessler, *Green Chem.*, 2013, **15**, 1477–1484.

48 Z. Wu, W. Cai, R. Chen and J. Qu, *Prog. Org. Coatings*, 2018, **119**, 116–122.

49 H. Sardon, L. Irusta, P. Santamaría and M. J. Fernández-Berridi, *J. Polym. Res.*, 2012, **19**, 9956.

50 L. B. Manfredi, A. N. Fraga and A. Vázquez, *J. Appl. Polym. Sci.*, 2006, **102**, 588–597.

51 I. Merdas, A. Tcharkhtchi, F. Thominette, J. Verdu, K. Dean and W. Cook, *Polymer (Guildf).*, 2002, **43**, 4619–4625.

52 K. Nakamae, T. Nishino, S. Asaoka and Sudaryanto, *Int. J. Adhes. Adhes.*, 1996, **16**, 233–239.

III.6 SUPPORTING INFORMATION

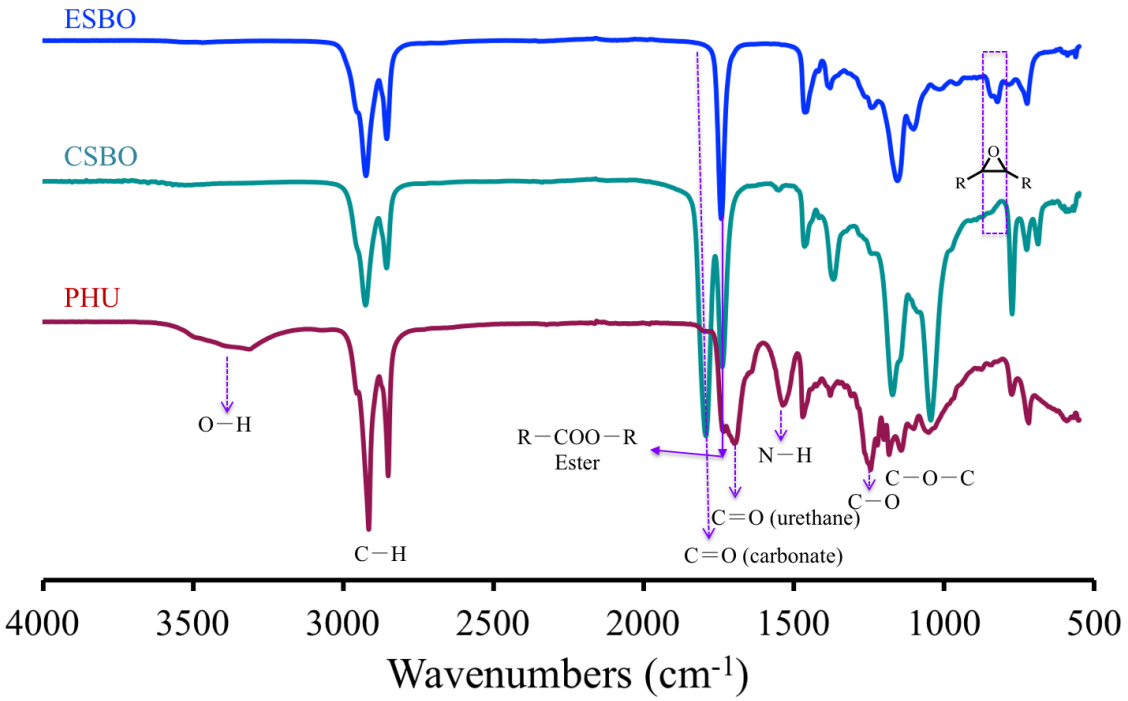

Figure. S1 FTIR spectra of epoxidised soybean oil (ESBO), cyclic carbonated soybean oil (CSBO) and PHU-H (formed from CSBO/HMDA = 1/3 at 100 °C for 50 min).

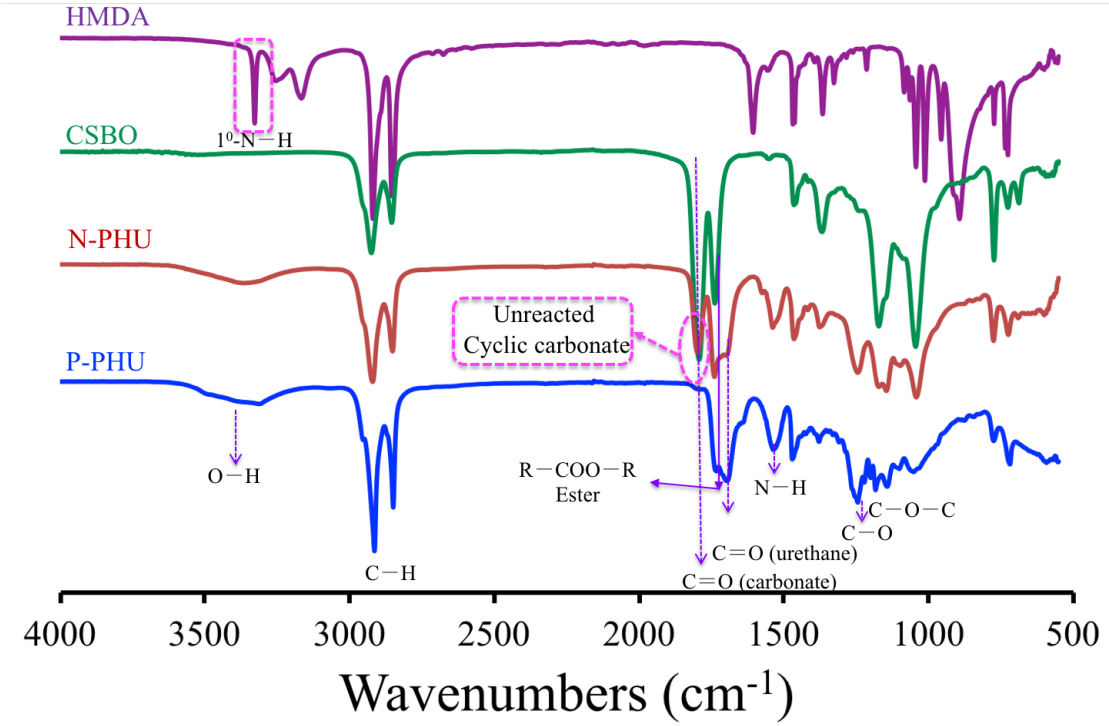

Figure S2. FTIR spectra used to determine the influence of mixing time on the conversion. The spectra of hexamethylene diamine (HMDA), cyclic carbonated soybean oil (CSBO), N-PHU (Not properly mixed polyhydroxyurethanes; mixed for 1 min at 50 ^{0}C) and P-PHU (properly mixed polyhydroxyurethanes; mixed for 3 min at 50 ^{0}C) after curing at 70 °C for 12 h and 100 °C for 4 h.

Effect of formulation mixing time on the stability of thermosets.

We performed the effect of formulation (CSBO/HMDA) mixing time (thus, A: mixed for 3 min at 50 ^{0}C and B: mixed for 1 min at 50 °C) on the stability of the thermosets towards organic solvents (DMF and THF). The samples were prepared by depositing formulations into teflon molds and curing at 70 °C for 12 h and 100 ^{0}C for 4 h. The stability of the PHU-thermoset films was performed by immersion in DMF and THF for 10 to 120 minutes (Figure S3). As can be seen, not properly mixed or inhomogeneous thermosets dissolved/broke into pieces due to insufficient mixing time (1 min) to obtain homogeneous formulations. Whereas properly mixed for 3 min, homogeneous thermosets sustain their structural integrity in organic solvents (THF and DMF). This study showed that, the effectively mixed formulations are crucial to obtain high performance materials.

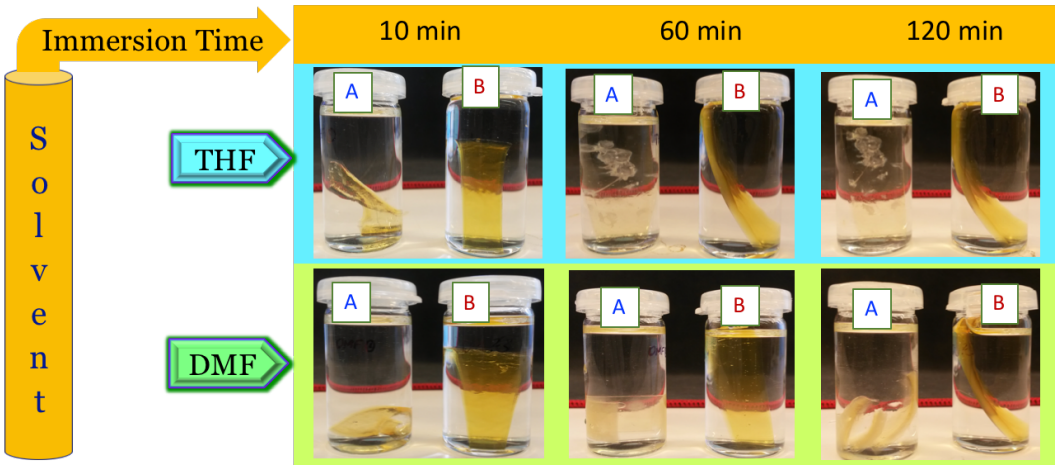

Figure S3. Effect of formulation mixing time on the stability of the PHU thermoset films within organic solvents (THF and DMF). A: on the left, formulation mixed for 1 min at 50 °C, B: on the right, formulation mixed for 3 min at 50 °C. The curing conditions were held constant (at 70 °C for 12 h and 4 h at 100 °C).

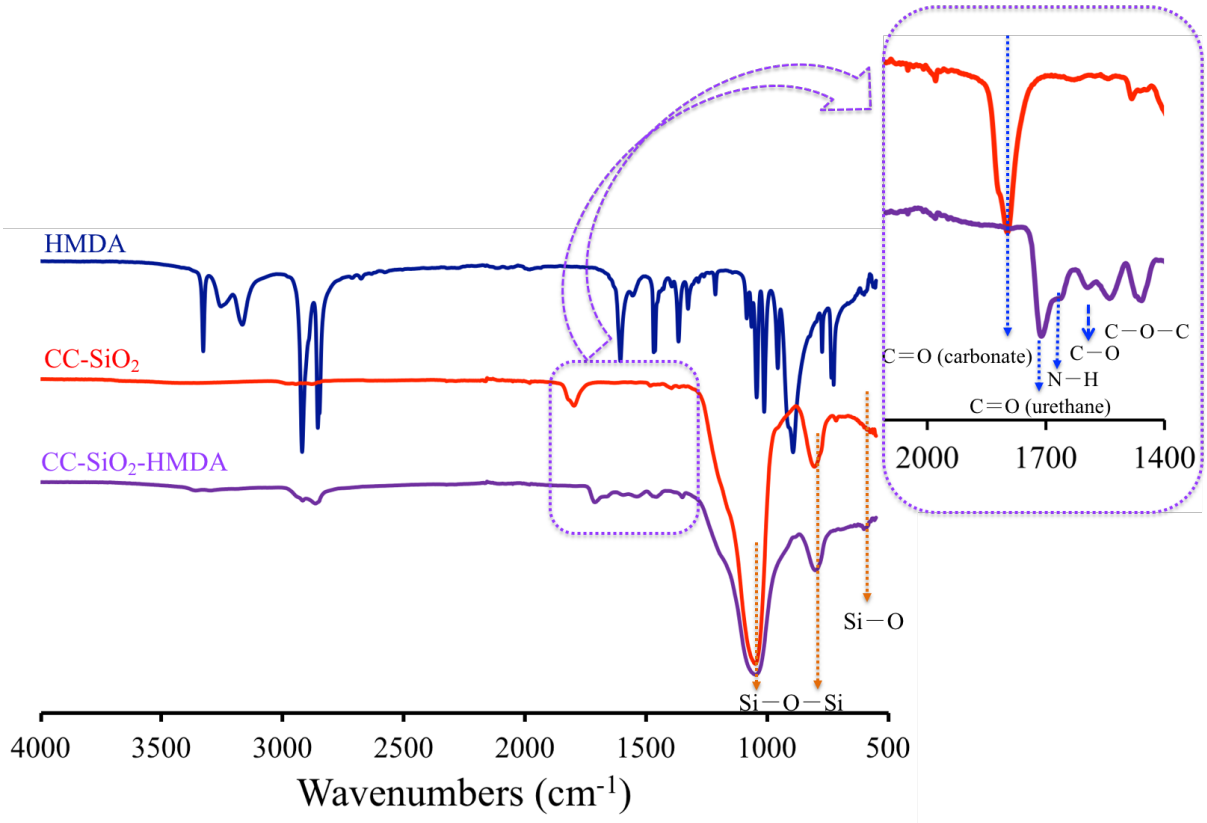

Figure S4. FTIR spectra used to highlight the reaction between cyclic carbonate functional fillers and amines (HMDA). Spectra of HMDA, CC-SiO_2 and spectra after reaction between HMDA and CC-SiO_2 (CC-SiO_2-HMDA) in THF at 60 °C for 30 minutes followed by curing at 70 °C for 12 h and 100 °C for 4 h.

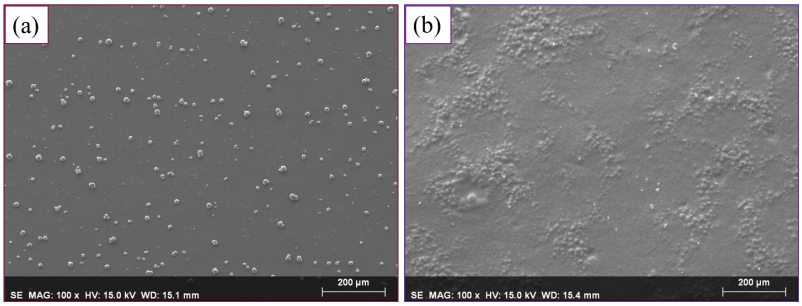

Figure S5. SEM images of PHUs coating reinforced with 5 wt% of (a) cyclic carbonate functional CC-SiO_2 fillers and (b) CC-ZnO fillers.

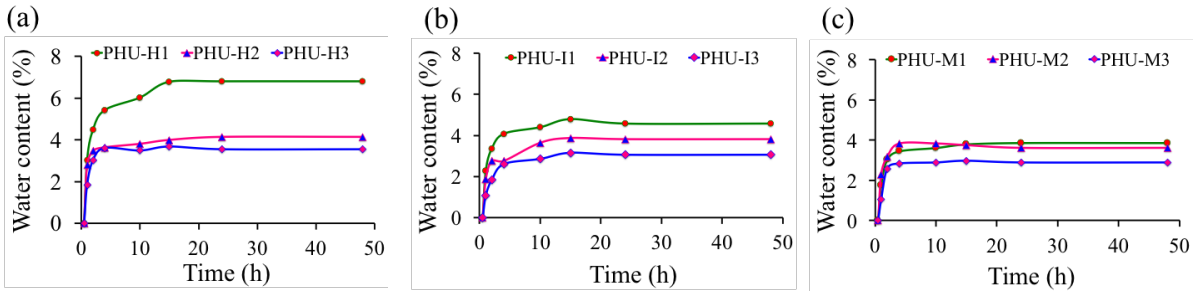

Figure S6. Water content evolution with time evaluated for PHUs and analogue nanocomposite freestanding films [dimensions: 0.5 cm (l) × 0.5 cm (t) × 0.5 cm (w)] prepared from [CSBO]/[diamine] formulations with 5wt% CC-SiO_2 or CC-ZnO. (a) PHU-H (CSBO/HMDA/fillers), (b) PHU-M (CSBO/MXDA/fillers), (c) PHU-I (CSBO/IPDA/fillers) and [PHU-H1, PHU-M1 and PHU-I1: unfilled PHUs, PHU-H2, PHU-M2 and PHU-I2: PHUs reinforced with 5wt% CC-SiO_2; PHU-H3, PHU-M3 and PHU-I3: PHUs reinforced with 5wt% CC-ZnO].

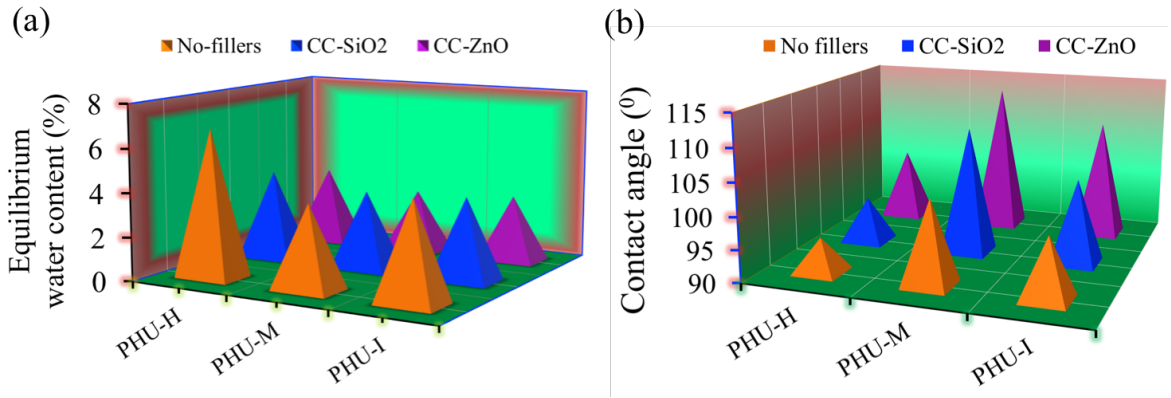

Figure S7. (a) Equilibrium water content (after 48 h of immersion) of PHUs and analogue nanocomposite freestanding films [dimensions: 0.5 cm (l) × 0.5 cm (t) × 0.5 cm (w)] prepared from [CSBO]/[diamine] formulations with 5wt% CC-SiO_2 or CC-ZnO. PHU-H (CSBO/HMDA/fillers), PHU-M (CSBO/MXDA/fillers), and PHU-I (CSBO/IPDA/fillers) and (b) Water contact angle measurements of PHU coatings.

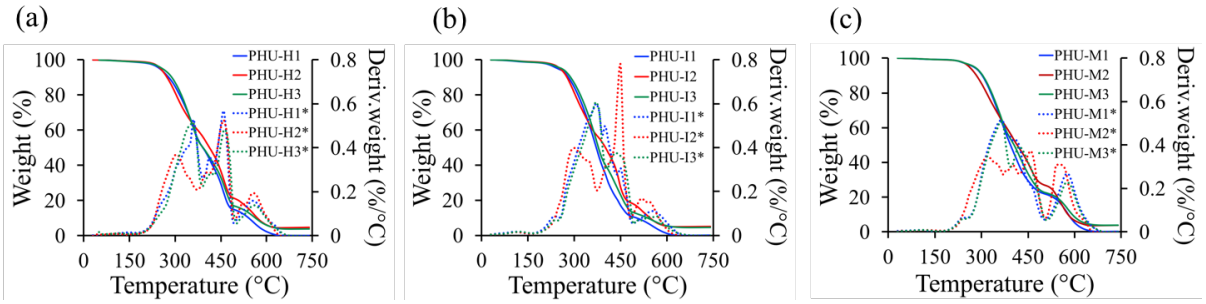

Figure S8. TGA and DTGA of (a) PHU-H (aliphatic), (b) PHU-I (cycloaliphatic) and (c) PHU-M (aromatic) [1: PHUs, 2: PHUs reinforced with 5 wt% CC-SiO_2, 3: PHUs reinforced with 5 wt% CC-ZnO and PHU*-Deriv.weight (%/^{0}C)].

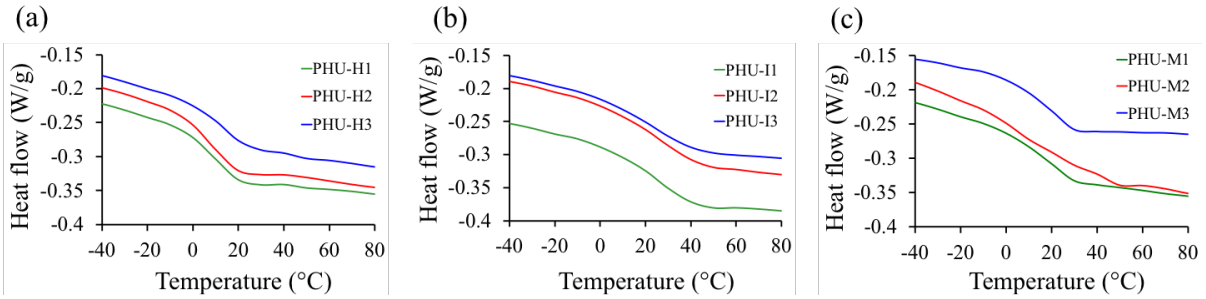

Figure S9. DSC thermograms of (a) PHU-H (from aliphatic amine), (b) PHU-I (from cycloaliphatic amine) and (c) PHU-M (from aromatic amine) and PHUs reinforced with 5 wt% CC-SiO_2 or CC-ZnO [1: PHUs, 2: PHUs reinforced with CC-SiO_2, 3: PHUs reinforced with CC-ZnO].

Table S1. Adhesive performance of bio-based PHU nanocomposite thermoset glues compared with commercial PU as well as with reported PHUs.

Sample code	Cured at 25 °C for 48 h		Cured at 70 °C for 12 h and 100 °C for 4 h	
	Lap shear strength (MPa) Al-Al	Failure mode	Lap shear strength (MPa) Al-Al	Failure mode
Teromix-6700	12.5 ± 0.8	C.F	7.2 ± 0.4	C.F
Araldite®2000+	21.7 ± 0.2	C.F	11,2 ± 0.5	A.F
PHU(M-1)[1]: TMPTC/EDR-148	1.9 ± 0.2	C.F	6.5 ± 0.3	C.F
PHU-5C[2]: TMPTC/HMDA/PDMS/C-GPTMS-ZnO	3.3 ± 0.4	C.F	16.3 ± 1.4	C.F
PHU-H3: CSBO/HMDA/CC-ZnO	2.2 ± 0.9	C.F	11.3 ± 0.28	C.F

C.F: Cohesive failure and A.F: Adhesive failure

REFERENCES:

1. A. Cornille, G. Michaud, F. Simon, S. Fouquay, R. Auvergne, B. Boutevin and S. Caillol, *Eur. Polym. J.*, 2016, **84**, 404 420.

2. S. Panchireddy, J.-M. Thomassin, B. Grignard, C. Damblon, A. Tatton, C. Jerome and C. Detrembleur, *Polym. Chem.* 2017, **8**, 5897–5909.

Chapter-IV

Catechol Containing Polyhydroxyurethanes as High Performance Coatings and Adhesives

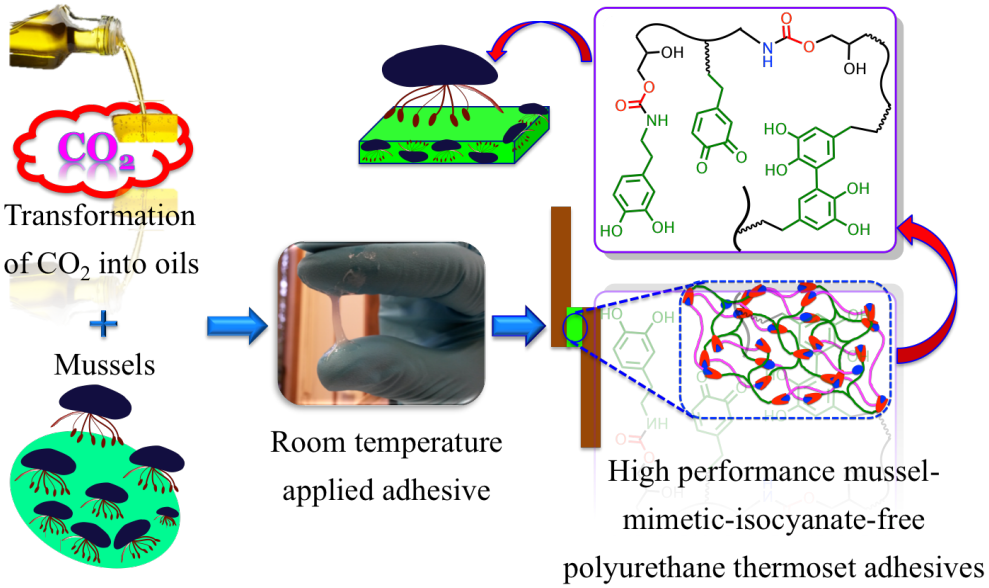

Satyannarayana Panchireddy, Bruno Grignard, Jean-Michel Thomassin, Christine Jerome and Christophe Detrembleur, ACS. *Sustainable Chem.Eng.* 2018, 10.1021/acssuschemeng.8b03429.

ABSTRACT

Green routes for the synthesis of high performant isocyanate-free polyurethane coatings and adhesives are intensively searched for. In this paper, we report a solvent- and isocyanate-free formulation for novel poly(hydroxyurethane) glues bearing strongly adherent catechol groups. These adhesives are prepared by the polyaddition of a CO_2-sourced tricyclic carbonate, hexamethylene diamine and a catecholamine (dopamine). The role of the catechol functions on the PHU curing and on the final PHU properties are investigated. Although the dopamine slows down the curing of the formulation, this catecholamine added at only 3.9 mol% impressively improves the mechanical and adhesion performances of PHU. The lap shear adhesion of our product surpasses those of PHU that do not contain the catechols. We also demonstrate that the catechol-bearing PHU glues are competing with the adhesion performances of commercial PU glues, at least when a thermal curing is implemented to overcome the low reactivity of cyclic carbonate with amines. The use of renewable feedstocks, the solvent-free process, the atom economy polyaddition reaction, and the absence of any toxic reagent benefit to the sustainability of the final product.

Table of Contents

IV.1 INTRODUCTION

Due to their tunable bonding strength, design flexibility, durability and cost effectiveness, polymer-based adhesives are broadly diversified in our daily life with applications ranging from post-it notes to aerospace industry.[1–8] A large palette of adhesives are found on the market place such as those made of cyanoacrylate (Super Glue), epoxy resins, and polyurethane to cite only a few. The main common drawback of many commercial adhesives is that they are produced from some toxic compounds. The production of high performance adhesives by greener routes and eventually from renewable resources is gaining increasing interest.

Polyurethane (PU)-based adhesives are largely used for bonding metal substrates due to their high adhesion strength.[9–14] However, the classical method for their production uses isocyanates that are toxic and so have associated health concerns.[15–18] PUs adhesives prepared by greener alternatives are thus searched for, but their adhesive performances have to compete with those of conventional PUs. The polyaddition of di(poly)cyclic carbonates with di(poly)amines is an attractive strategy for producing poly(hydroxyurethane)s (PHUs), a green variant for conventional PUs.[19,20,29,30,21–28] The presence of an hydroxyl group in the ß-position of the urethane contributes to the improvement of the adhesion with various substrates, the chemical resistance and mechanical properties of the polymer due to multiple hydrogen bondings[31–33] Only few recent reports are describing the potential of PHUs as adhesives. PU/PHU hybrid adhesives produced from cyclic carbonates and functional α,ω-telechelic isocyanate-based PU prepolymers with polyamines achieved good adhesion onto some polymers (polyimide, poly(vinyl chloride)) but also on aluminum.[34] However, these adhesives are still using some conventional PUs in their formulations. Caillol *et al*.[35] recently reported the preparation of all PHU glues with high adhesion strength (≈15 MPa) on wood and glass but their adhesion on painted aluminum was moderate (≈3 MPa). Hybrid poly(dimethyl siloxane) (PDMS)-hydroxyurethanes formulations achieved 7 MPa on glass and 0.9–1.7 MPa on metal (stainless steel, titanium and aluminum).[36,37] Our group recently reported on the solvent-free preparation of PHU thermosets reinforced by ZnO nanoparticles that presented a high shear adhesion strength (up to 16.3 MPa) on aluminum.[32] We highlighted that the reinforcement of PHU with ZnO particles strongly improved the adhesion of PHU by 270%, leading to PHU

adhesives with competitive adhesion strength compared to commercial PU-adhesives. Cyclocarbonated vegetable oils combined to amines and reinforced with ZnO particles provided also more sustainable adhesives.[33] Although high adhesion performances were achieved for these PHUs, the lap shear strength of the commercial PU glues were still higher.

In order to improve adhesion in wet environment, researchers were recently inspired by marine mussels.[38–40] The excellent adhesion of these organisms to any substrates was attributed to the presence of large quantity of 3,4-dihydroxyphenylalanine (DOP) in their surface proteins.[41–47] The catechol of DOP has indeed the ability to form a large diversity of chemical interactions and to self-crosslink, helping the proteins to solidify and to bind tightly to various types of surfaces.[48] Messersmith *et al*.[49–51] demonstrated that polydopamine (PDA) served as a universal surface-modifying agent for virtually any substrates thanks to the presence of covalent and reversible coordination bonds between catechol groups and the surface.[52–55] Recent studies have revealed that PDA-modified-PU can be used as catalytic supports,[56,57] and that PDA modification can enhances the flame retardancy[58] and mechanical properties of the PU.[59–61] The dopamine-containing-PU showed adhesive strength of 5.2 MPa on iron.[62] The design of mussel-inspired isocyanate-free PU adhesive materials may generate a new class of high performance materials competing with conventional PUs. To the best of our knowledge, the development of high-performance adhesives by incorporating pendent catechol groups into the backbone of PHUs has never been reported.

With the main purpose to develop sustainable high performance PHU adhesives, we describe the solvent-free preparation of PHUs thermosets bearing catechols by the addition of a catecholamine, dopamine (DOP), to the formulation of the multifunctional cyclic carbonate and the diamine (Scheme 1). In this study, we systematically study the influence of the addition of DOP on the rate of crosslinking, the thermomechanical and the adhesion properties of the crosslinked PHUs. The best adhesive formulation is then investigated on a large diversity of substrates (aluminum, stainless steel, plexiglass, wood, and polyethylene), and is benchmarked to commercial PU glues and state-of-the-art PHU adhesive.

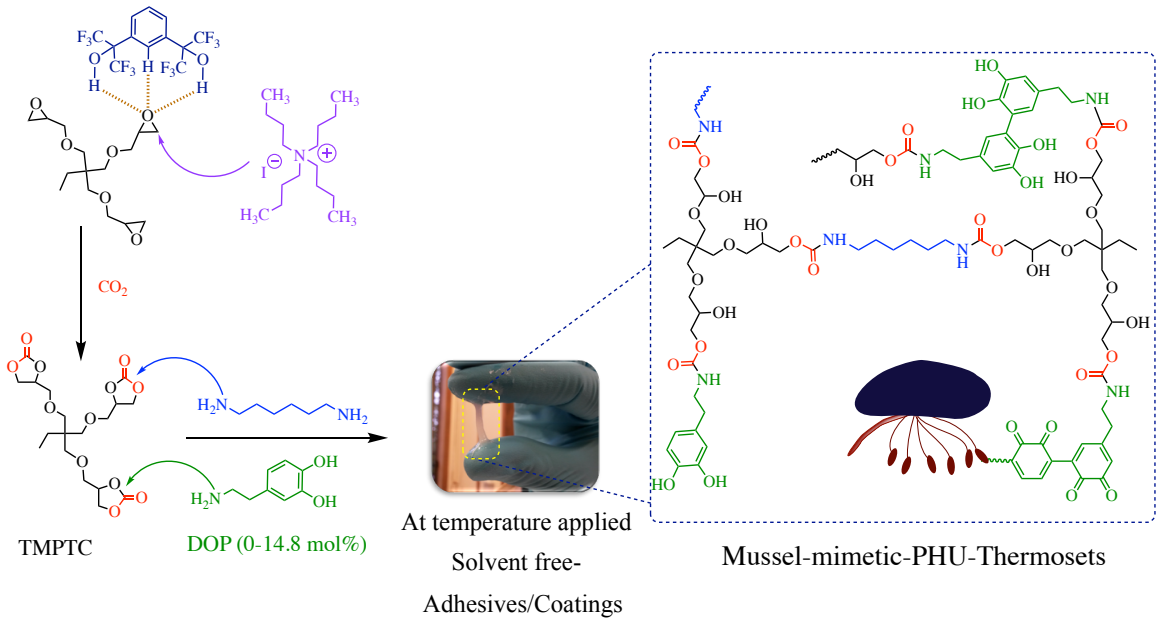

Scheme 1. Design and synthesis of mussel-mimetic-polyhydroxyurethane solvent-free adhesives.

IV.2 EXPERIMENTAL SECTION

IV.2.1 Materials and Methods

Trimethylolpropane triglycidyl ether (TMPTE), tetrabutylammonium iodide (TBAI, purity >99%), hexamethyl diamine (HMDA), dopamine hydrochloride (DOP), pyrocatechol, methanol was purchased from sigma Aldrich. Carbon dioxide (CO_2) N45 was supplied by Air liquid. 1,3-bis (2-hydroxyhexafluroisopropyl)-benzene was purchased from Fluorochem. All chemicals were used as received without any further purification. Al-2024-T3 (thickness of 0.8 mm) substrates were received from SONACA, Belgium. Stainless steel (316-AK steel, thickness of 1 mm), plexiglass (poly(methyl methacrylate) PMMA, thickness of 3 mm) kindly supplied by ULiege. Wood (beech, thickness of 10 mm) substrates was purchased from Brico and plastics (high density polyethylene, HDPE, thickness of 3 mm) developed in the lab.

IV.2.2 Surface Treatments

The substrates surfaces [aluminum (Al), stainless steel (SS), plexiglass (Gl), wood (W) and polyethylene (PE)] were cut into desired dimensions (50 mm × 10 mm) and surfaces were cleaned to degrease the unwanted weak boundary layers such as surface contaminants, oil, grease, oxides etc can physically impair and reduce the formulation adhesion to the substrate. The scrubbing of Al-substrates was adopted to our previously reported method.[32,33] SS, Gl, W and PE substrates were cleaned with an acetone/isopropanol (1/1, v/v) mixture followed by washing with water, repeated the procedure for 3 times then wiped with tissue paper and dried at room temperature for 2 h.

IV.2.3 Preparation of Polymeric Coatings and Films

Prior to prepare solvent free thermoset coatings and films, the required amount of dopamine (Table 1) was dissolved in MeOH (3 mL), added to TMPTC (2.0 g, 4.6 mmol) and heated at 60 °C for 5 min. The reaction mixture was allowed to stir for 20 min at room temperature until an homogeneous solution was obtained, and then solvent was removed under vacuum. Subsequently, a stoichiometric amount of HMDA (compared to cyclic carbonates, see Table 1) was added into the reaction mixture that was then stirred for 1 min at 60 °C and 2 min at room temperature to obtain homogeneous mixture. Then, the viscous mixture was deposited on bare aluminum (Al-2024-T3) by using a bar-coat applicator (ASTM D823) to obtain a coating thickness in the range of 50–60 µm. All coatings were repeated 6 times for evaluating the reproducibility. The coated substrates were cured at 100 °C for 18 h in an oven. These coatings were then evaluated for crosscut adhesion test, and contact angle measurements.

The freestanding films with 5 mm thickness were prepared by pouring the viscous DOP/TMPTC/HMDA mixtures into Teflon mold (3.5 × 3.5 × 0.5) cm^3 for the determination of the water content (EWC), gel content (GC), contact angle and thermal properties. Additionally, dog-bone-shaped samples were made using Teflon molds for the evaluation of the mechanical properties. The samples were cured in oven at 100 °C for 18 h.

IV.2.4 Preparation of Lap-Shear Joints

The adhesive joints were prepared to determine tensile lap shear adhesion strength of the designed thermosets. The viscous oligomeric solutions (~ 10 mg) was deposited onto the cleaned substrates with an overlapped gluing area of 100 mm^2 and the second substrate was placed into contact. Then the samples were then pressed gently with fingers, without formation of defects and/or squeezed out of the adhesive in the joints. The adhesively bonded joints were allowed to cure in an oven at 100 °C for 18 h.

IV.3 CHARACTERIZATION METHODS

Fourier transform infrared spectra (FTIR) measurements. They were carried out on Nicolet IS5 spectrometer (Thermo Fisher Scientific) equipped with a diamond attenuated transmission reflectance (ATR) device, 32 scans were recorded for each sample over the range of 4000-500 cm^{-1} with a normal resolution of 4 cm^{-1} and spectra were analysed with ONIUM™ software.

Rheology measurements. The influence of the content of dopamine on PHU solvent-free formulations (~ 0.5 g) was determined by rheology measurements carried out on ARES from Rheometric scientific TA instrument at 100 °C for 40 min at a frequency of 1 Hz and a strain of 1% using time sweep measurements.

Thermal characterizations. Thermogravimetric analysis (TGA) of the coatings was evaluated using a Q500 from TA instruments at heating rate of 20 °C min^{-1} over the temperature range of 0 to 700 °C under nitrogen atmosphere. DSC (Differential scanning calorimetry) analysis was carried out on a Q1000 from TA instruments using standard aluminum pans, calibrated with indium and nitrogen as purge gas. The samples were measured at a heating rate of 10 °C min^{-1} over a temperature range from –80 °C to 200 °C under a flowing nitrogen atmosphere. The glass transition temperature (Tg) was determined using the onset method, defined as the midpoint of the intersection between onset and midpoint with the offset and the midpoint tangent lines, using TA analysis software provided with the instrument.

Tensile properties. The measurements were performed at room temperature using an Instron 5594 tensile machine at a speed of 10 mm min^{-1} with a load capacity of 10,000 N applied forces perpendicular to the adhesive materials. Young's modulus (E), Ultimate tensile strength (σ_u) and Fracture stress (σ_f) were estimated by the average values of at least 6 repeated flat dog-bone shaped samples with the following dimensions, i.e., length = 3 cm, length of narrow fraction = 1 cm, width = 0.5 cm, width of narrow fraction = 0.2 cm and thickness = 0.05 cm.

Swelling behaviour and gel content. Equilibrium water swelling of PHU samples was evaluated by measuring water content of free-standing films at room temperature.[21] PHU samples of 0.125 cm^3 were immersed in 10 mL of milli-Q water at room temperature for 96 h and the water content was measured until the weight of the swollen samples remains constant. Equilibrium water content (EWC) was measured in function of time using equation (1). After swelling measurements, samples were dried in oven at 70 °C for 24 h. Gel content was measured using equation (2):

$$EWC\ (\%) = \left(\frac{W_s - W_d}{W_d}\right) X\ 100 \qquad (1)$$

$$GC\ (\%) = \left(\frac{W_f}{W_i}\right) X\ 100 \qquad (2)$$

Where W_s is the weight of swollen sample, W_i is the initial weight and W_f is the final weight of the dried sample.

Crosscut adhesion tests. Crosscut adhesion tests were carried out according to ASTM D3359 standards. A cross-hatch cut pattern consisting of six vertical parallel lines and six horizontal lines separated by 3 mm onto series of PHU coated aluminum substrates with a sharp razor blade followed by the application of a high-pressure sensitive adhesive tape (Intertape tm 51596-ASTM D3359, Gardco). The tape is then removed by rapid pulling off at an angle of 180°. The quality of the coating was visually estimated by comparison with percentage (%) of area removed from the total surface. The coatings were classified as 5B: 0% of the coating removed.

Water contact angle measurements. Measurements were obtained on an OCA-20 apparatus (Dataphysics Instrument GmbH) in the sessile drop configuration by depositing a 5-μL droplet of milli-Q water. Mean contact angle values were determined from at least 5 repeated measurements realized at different locations of each Al coated surfaces.

Lap-shear tests. The adhesion properties of thermosets were evaluated at 298K (load or force (N) as function of displacement (mm)] using an Instron 5594 equipped with a 10,000 N load cell and applied force parallel to the adhesive bond with displacement rate of 2 mm min^{-1} until pulling apart the bonded joints. The substrates with dimensions of 50 mm × 10 mm were used for single lap-shear measurements and gripping length on both sides of test specimens was 25 mm. The tests were performed on 5 repeated samples from each type of adhesive to determine average lap-shear adhesion strength of adhesives. The lap shear strength was calculated by the formula.

$$\tau = \frac{P}{A} \qquad (3)$$

Where, τ is lap shear strength (in N mm^{-2} or MPa), P is the maximum loading force to remove & break the adhesive (N) and A is the overlapped or gluing area of adhesive joint (100 mm^2).

IV.4 RESULTS AND DISCUSSION

Modified PHU thermosets were synthesized by reaction between a tri-functional cyclic carbonate, i.e. 4,4'-(((2-ethyl-2-(((2-oxo-1,3-dioxolan-4-yl)methoxy) methyl) propane-1,3-diyl) bis(oxy))bis(methylene))bis(1,3-dioxolan-2-one) (TMPTC), hexamethylene diamine (HMDA) and dopamine (DOP) under equimolar conditions between the cyclic carbonate and the amine groups, Scheme 1. TMPTC was synthesized in kilogram scale using a protocol previously described by the solvent-free organocatalyzed coupling of carbon dioxide with trimethylolpropane triglycidyl ether (TMPTE).[63–67] A pre-mixing of TMPTC and DOP was carried out in methanol in order to obtain an homogeneous solution before removing the solvent under vacuum, followed by the addition of HMDA. The solvent-free formulations were then cured at 100 °C. The influence of the dopamine content on the crosslinking, gel time, the mechanical and thermal properties, and on the adhesive performances of the PHU thermosets was then evaluated and discussed below.

The conversion of cyclic carbonates into PHU was monitored by FTIR spectroscopy (Fig. S1). For PHU, FTIR (ATR): ν_{max} (cm^{-1}) = 3316 (O−H, N−H), 2934-2829 (C−H), 1697 (C=O), 1539 (δ(N−H) + γ(C−N)), 1460, 1257 (C−O), 1103, 1023 (C−O−C). For mussel-mimetic PHU, FTIR (ATR): ν_{max} (cm^{-1}) = 3307 (O−H, N−H), 2935-2840 (C−H), 1695 (C=O), 1531 (δ(N−H) + γ(C−N)), 1607, 1376 (C=C, ph), 1416 (C−C, ph) 1460, 1255 (C−O), 1104, 1022 cm^{-1} (C−O−C), 869 (C−H, ph).

IV.4.1 Curing Kinetics by Rheology

As the addition of mono-functional amines, here dopamine (DOP), in thermosets formulation can adversely affect the formation of the network, the effect of the addition of DOP on the curing kinetics was systematically evaluated by rheology at 100 °C for 40 min (Fig. 1a–b). The measurements were performed on the solvent-free PHU formulations with increasing content of (0, 3.9, 7.7, 14.8 mol%) DOP compared to TMPTC/HMDA (keeping an equimolar content of amine and cyclic carbonate groups for all formulations). All rheological data are summarized in Table S1 (ESI). For all formulations, the loss modulus (G") was initially higher than the storage modulus (G'), confirming that PHU was not crosslinked before the measurement. Fig. 1 illustrates that G' increased faster than G" with the reaction time, and a crossover point was observed that corresponds to the gel point (G′ = G″ and/or tan δ = 1). As expected, the gelation time increased (from about 3 to 30 min) and storage moduli reduced (from 123.2 to 8.5 kPa, at 40 min) with the content in dopamine (0 to 14.8 mol%). These results tend to confirm that part of the dopamine molecules react with the cyclocarbonate functions and are grafted on the resulting PHUs. However, at low dopamine content (10 mol% and below), this effect remains marginal and good PHUs thermosets are expected to be formed in these conditions. Nevertheless, more studies are required to elucidate the complex structure of this crosslinked system.

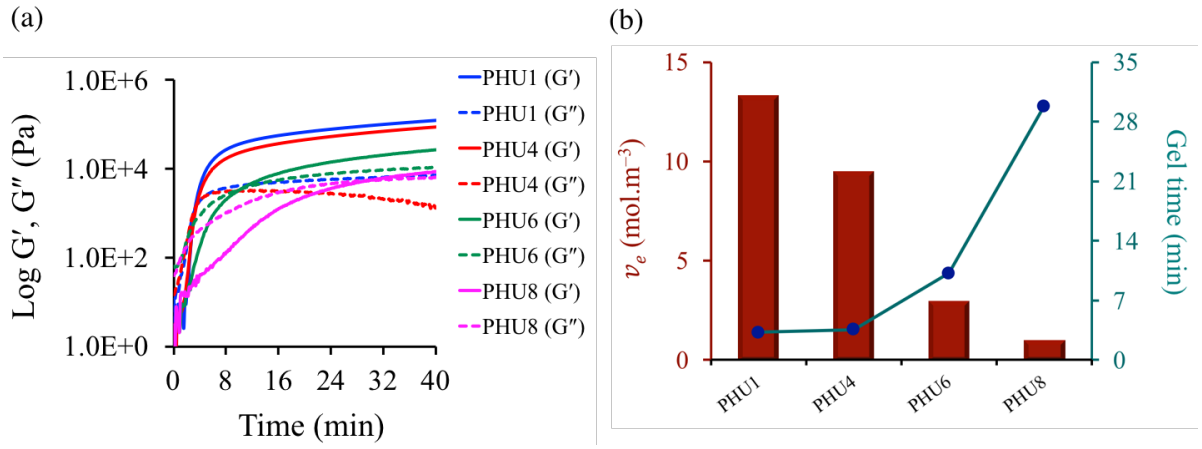

Fig. 1 (a) The influence of dopamine content (DOP, 0-14.8 mol%) on curing kinetics and (b) crosslinking density of PHU (TMPTC/HMDA) formulations was evaluated by dynamic time sweep measurements [storage modulus (G') and loss modulus (G") as a function of gel time, performed at 100 °C for 40 min, frequency (1 Hz), strain (1 %). PHU1 (0 mol% DOP), PHU4 (3.9 mol% DOP), PHU6 (7.7 mol% DOP), PHU8 (14.8 mol% DOP).

IV.4.2 Thermal Properties

The thermal properties of crosslinked PHU with incorporated DOP (0 to 14.8 mol%) was evaluated by thermogravimetric analysis (TGA) and differential scanning calorimetry (DSC) (Fig. S2). The temperature at 50% of degradation ($Td_{50\%}$) and glass transition temperature (Tg) values are reported in Table 1. All PHUs presented a high thermal stability with a $Td_{50\%}$ that increased from 331 °C for PHU1 that did not contain any DOP, to 360 °C for PHU3 that contained only 2 mol% of DOP. At higher DOP content, the $Td_{50\%}$ remained constant around 360 °C. Increased thermal degradation stability of DOP-incorporated-PHUs may be caused by the improvement in internal strength of the networks *via* covalent and non-covalent interactions of auto-polymerized catechols, tends to the formation of dense material that ensure thermal stability. The glass transition temperature (Tg) of PHU-thermosets was progressively increased with the DOP content from 35 °C (neat PHU1) to 45 °C (PHU8 containing 14.8 mol% of DOP). This Tg increase is assumed to be the result of the reduction of the chain mobility owing to presence of dihydroxybenzene functions that form strong H-bond interactions.

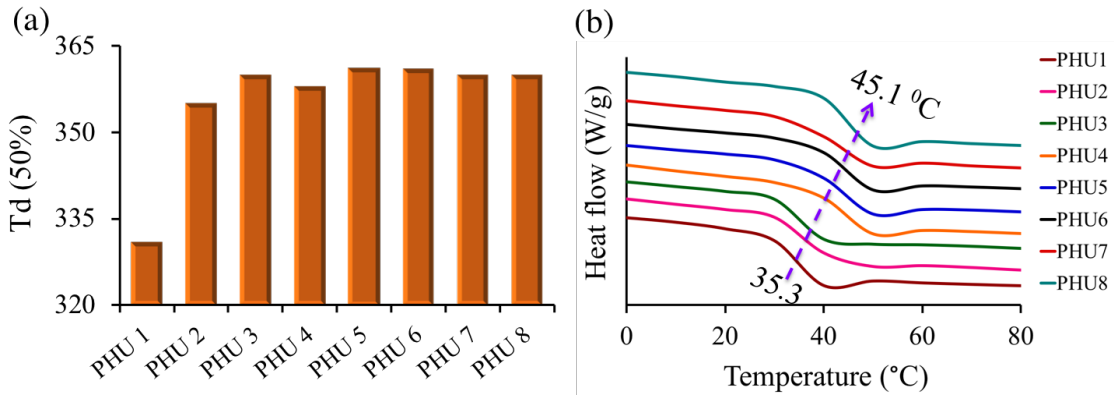

Fig. 2 (a) Evolution of the thermal stability at 50% degradation ($Td_{50\%}$) by Thermogravimetric analysis (TGA) and (b) Glass transition temperature by Differential scanning calorimetry (DSC) curves of neat and series of mussel-mimetic crosslinked PHUs.

IV.4.3 Mechanical Properties

The structure-property relationships of neat and mussel-mimetic PHU thermosets were investigated by conventional tensile tests. Indeed, a variety of network structures were obtained by varying the ratio of formulation (TMPTC/HMDA) composition to DOP content, while processing conditions held constant (see experimental section for details). Fig. 3a shows the tensile test curves (stress *vs* strain) for neat and series of mussel-mimetic PHU thermosets, and Fig. 3b represents the young's modulus and ultimate tensile strength as a function of catechol content for all PHU formulations. All data are also summarized in Table 1. The neat PHU (0% DOP) exhibited young's modulus up to 12.7 MPa, ultimate tensile strength of 17.4 MPa and stress at break of 5.8 %. The presence of low DOP content (3.9 mol%, PHU4) had a remarkable beneficial impact on the young's modulus with a 233% increase, i.e. from 12.7 for neat PHU (PHU1, 0% DOP) to 29.7 MPa for PHU4, and on the ultimate tensile strength with a 196% increase, i.e. from 17.4 to 34.2 MPa. These improvements in the mechanical strength of thermosets are likely attributed to the development of multiple hydrogen bonding interactions between modified PHUs, DOP and eventually self-polymerized catechols. However, when higher DOP content (> 3.9 mol%) were introduced in the formulation, a decrease of the young's modulus and stress at break were observed which demonstrates a transition from a ductile to a brittle material. The presence of a high amount of catechol probably restricts too much the mobility of the chains.

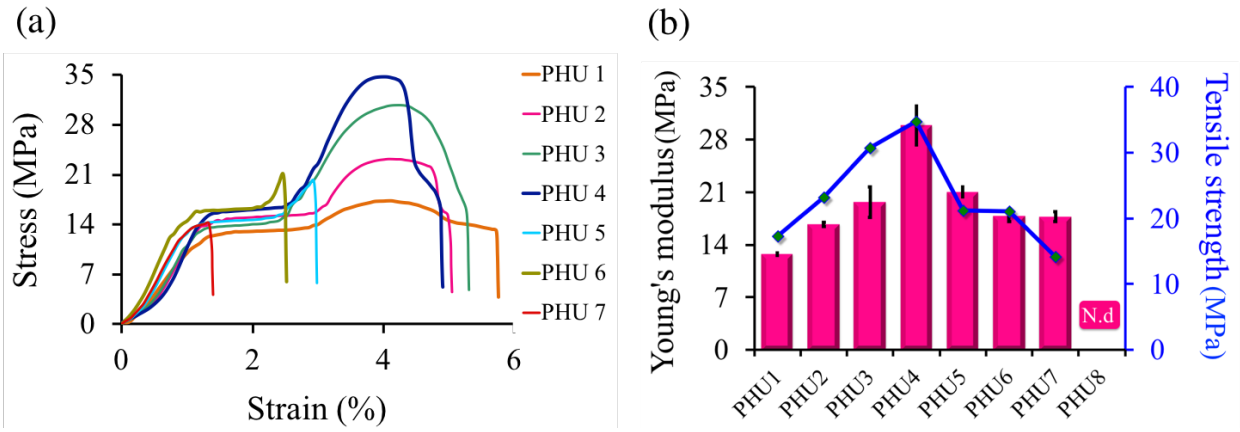

Fig. 3 The influence of incorporation of DOP on adhesive mechanical strength of neat and series of mussel-mimetic PHU thermosets. (a) Tensile test curves (stress *vs* strain) and (b) young's modulus and tensile strength of PHU films containing different amounts of DOP.

IV.4.4 Swelling Measurements

The degree of crosslinking density of PHU thermosets after curing at 100 °C for 18 h was qualitatively studied by measuring the equilibrium water content (EWC-Eq.1) and gel content (GC-Eq.2) with the immersion of their freestanding films (0.125 cm^3) in 10 mL of milli-Q water for 96 h at room temperature. The obtained values are reported in Table 1. EWC slightly increased from 38 ± 4 to 44 ± 5 % (115%) by raising the DOP molar ratio from 0 to 14.8 mol% (PHU1 to PHU8). The improvement of the EWC may be attributed to the presence of polar functional groups (catechol) within the mussel-mimetic-crosslinked PHUs. The gel content was above 94% in all cases demonstrating the formation of highly cross-linked materials and the absence of free dopamine that could be extracted from the samples. The GC slightly increased with the dopamine content to reach a maximum of 98% at 3.9 mol% of dopamine.

IV.4.5 Coating Properties

The solvent-free incorporated DOP containing PHUs were coated on a bare and cleaned aluminum with thickness of ~ 50 – 60 µm (see experimental section for details). Their adhesion strength was then evaluated by performing crosscut tests according to the ASTM D3359 standards. Whatever the coating, the edges of the cuts were completely smooth and none of the squares were removed from the coating. All tested coatings were thus all classified as 5B-0% removal of the coating, thus very adherent to the substrate, Table 1.

The binding ability of the coatings was further evaluated in wet environment after immersing the coated substrate in water. The neat PHU coating was rapidly peeled off (Fig. 4a) from the substrate after 12h of immersion due to the high hydrophilicity of PHU1 (contact angle (CA) = 61°, Table 1. In contrast, the coating containing DOP (PHU4) did not peel off when immersed in water for 48 h (Fig.4b), despite the coating being hydrophilic (Table 1). This comparative study reveals that the incorporation of DOP inside the PHU formulation is beneficial for improving the water resistance of the coating.

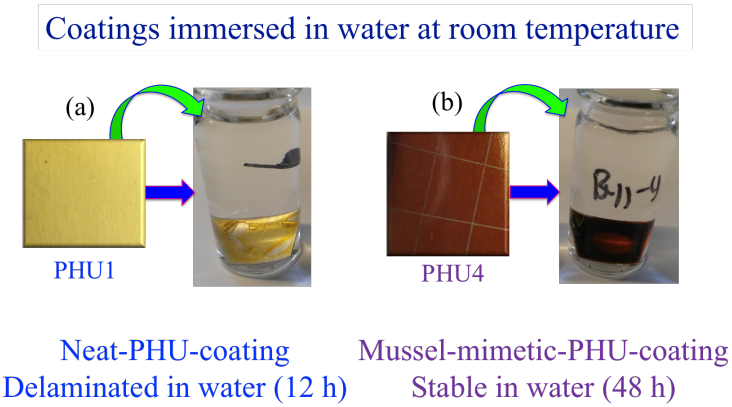

Fig. 4 Photographic images of bare Al-2024-T3 substrates coated with (a) neat PHU (peeling off in water after 12 h) and (b) Mussel-mimetic PHU thermoset (PHU4, 3.9 mol%-DOP, catechol-functionalized PHU) (no peeling off in water after 48 h).

Table 1. Properties of neat and group of mussel-mimetic crosslinked PHUs.

Sample code	TMPTC/HMDA(mol) /DOP (mol%)[a]	EWC[b] (%)	GC[c] (%)	CA[d]	CCA[e]	Tg[f] (°C)	Td[g]$_{50\%}$	E[h](MPa)	σ_u[i](MPa)	σ_f[j] (%)	LSS[k] (MPa)	F.M[l]
PHU 1	1/1.5/0	38 ± 4	95 ± 0.2	61 ± 2°	5B	35.3	331	12.7 ± 0.1	17.4 ± 0.1	5.8 ± 0.2	9.1 ± 3.1	C.F
PHU 2	1/1.485/1.2	40 ± 3	94 ± 0.1	61 ± 3°	5B	38.4	355	16.7 ± 0.2	23.8 ± 0.8	5.2 ± 0.4	13.2 ± 1.9	C.F
PHU 3	1/1.475/2.0	41 ± 4	97 ± 0.5	61 ± 3°	5B	39.3	360	19.6 ± 2.1	31.1 ± 0.3	5.3 ± 0.3	19.9 ± 2.0	C.F
PHU 4	1/1.45/3.9	41 ± 6	98 ± 0.2	59 ± 2°	5B	42.6	359	29.7 ± 2.6	34.2 ± 0.7	4.7 ± 0.3	24.1 ± 1.7	C.F
PHU 5	1/1.425/5.8	42 ± 4	97 ± 0.9	58 ± 3°	5B	42.8	361	21.1 ± 0.6	23.2 ± 1.5	3.1 ± 0.5	18.6 ± 3.3	C.F
PHU 6	1/1.4/7.7	42 ± 7	96 ± 0.4	58 ± 3°	5B	43.2	361	17.6 ± 0.7	20.1 ± 1.3	2.6 ± 0.1	15.7 ± 1.4	C.F
PHU 7	1/1.375/9.5	43 ± 2	97 ± 0.6	57 ± 4°	5B	43.3	360	16.5 ± 0.6	14.6 ± 0.6	1.3 ± 0.3	13.1 ± 3.4	C.F
PHU 8	1/1.3/14.8	44 ± 5	98 ± 0.2	57 ± 3°	5B	45.1	360	N.d	N.d	N.d	3.6 ± 2.1	A.F

[a] Optimum formulation compositions, [b] EWC: Equilibrium water content of self-standing films (0.125 cm^3) immersed in water for 96 h, at room temperature. [c] GC: Gel content, [d] CA: Contact angle measurements, [e] CCA: Cross-cut adhesion test (5B-0% of coating area removed within crosscut), [f] DSC-glass transition temperature, at heating rate 10 °C min^{-1}, [g] TGA- temperatures at 50% degradation ($Td_{50\%}$), at heating rate 20 °C min^{-1}, [h] E: Young's modulus, [i] σ_u: Ultimate tensile strength, [j] σ_f: Fracture stress [k] LSS: Lap shear strength, [l] F.M: Failure mode of adhesive joints, C.F: cohesive failure, A.F: adhesive failure and N.d: not determined

IV.4.6 Adhesion Properties

The influence of catechol on the adhesion performance of crosslinked PHUs was investigated by lap-shear tests (Fig. 5a) on aluminum substrates (Al-2024-T3) that is frequently used in aerospace and aircraft applications. The lap shear bonding strength (MPa and/or $N.mm^{-2}$) was calculated by dividing the maximum load or force (N) by the adhesive surface area (mm^2), using eq3. Fig. 5b shows that neat PHU (PHU1) was characterized by a shear adhesion strength of 9.1 ± 3.1 MPa. The shear strength was strongly improved by the addition of DOP, with a maximum value of 24.1 ± 1.7 MPa with only 3.9 mol% DOP (PHU4), which represents a 264% increase compared to neat PHU1 (Fig. 5b, Table 1). However, when the DOP content was further increased in the formulation, the adhesion performances progressively decreased with an adhesion strength of 13.1 ± 3.4 MPa for PHU7 (9.5 mol% DOP) and 3.6 ± 2.1 MPa for PHU8 (14.8 mol% DOP). This decrease might be explained by the slowing down of the curing kinetics at high DOP content as demonstrated by rheological measurement (Fig. 1), and by the transition from a ductile to a brittle material as evidenced by mechanical measurements (Fig. 3). In addition, for most samples, the adhered metal lap joints failed in a cohesive manner, with both surfaces that remained covered by the adhesive. The cohesive failure is the prominent characteristic to achieve maximum strength of adhesively bonded joints.

The development of an adhesive formulation that is able to efficiently glue a large diversity of substrates is challenging due to their diverse chemical nature, surface energy, wettability and roughness. In this study, the most performant mussel-inspired glue for aluminum (PHU4, 24.1 MPa, Al-Al) was then tested for gluing different substrates such as stainless steel (SS), wood (W), plexiglass (Gl) and polyethylene (PE) (Fig. 5c-f). Interestingly, the highest shear adhesion strength of 28.2 MPa was measured for wood (W-W). It remained high for SS with a value of 22.1 MPa, and slightly decreased to 17.9 MPa for Gl. Although lower, the shear adhesion strength for PE remained satisfactory with a value of 4.76 MPa (Fig. 5c-d, Table 2). This lower value for PE is the result of the low surface roughness and hydrophobic character of the substrate that do not favour the interaction between catechol-hydroxyurethane groups and the substrate.

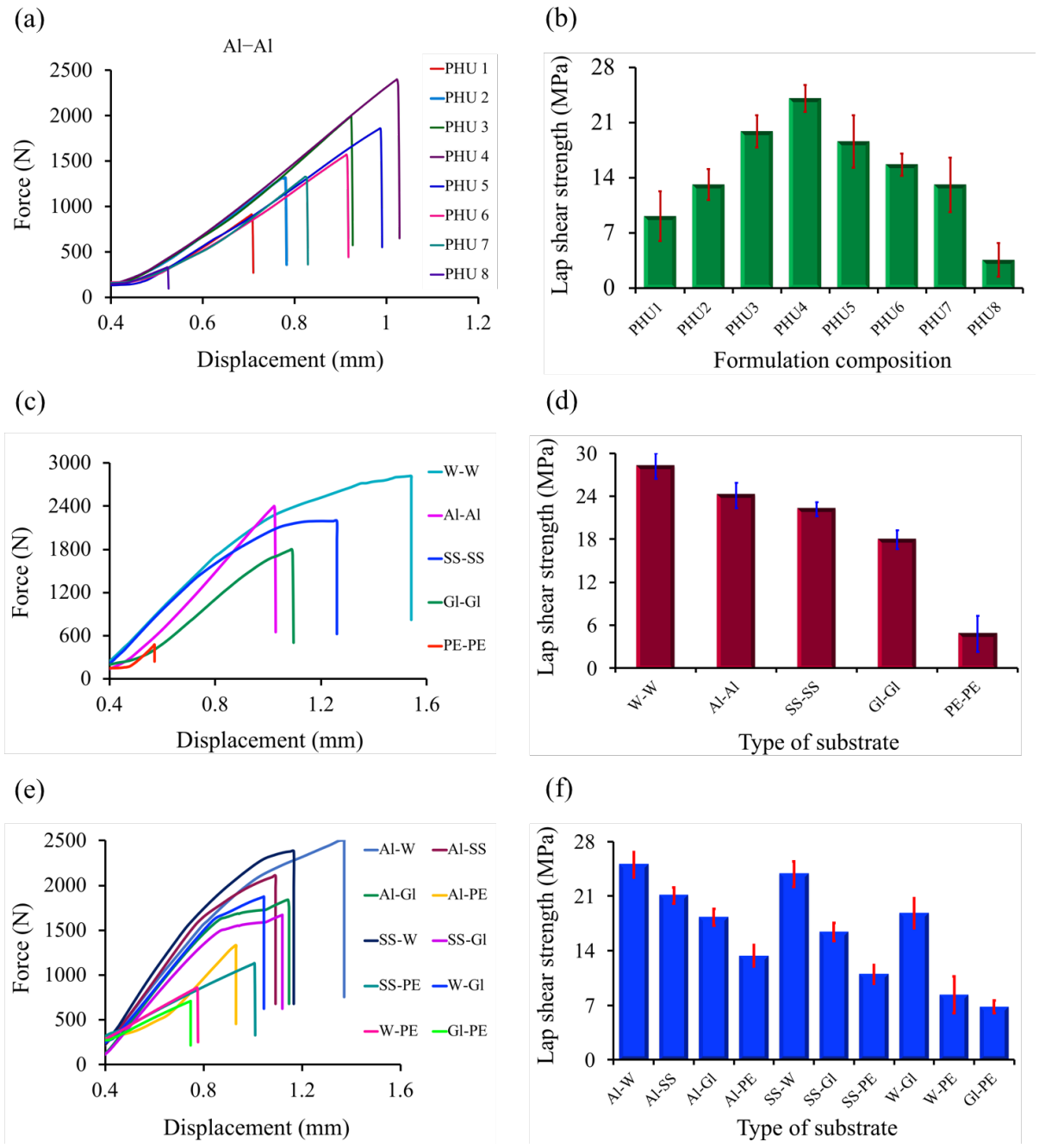

Fig. 5 Influence of DOP content (0 – 14.8 mol%, Table 1) on adhesive bonding strength of crosslinked PHUs was conducted in shear on aluminum substrates. (a) Force *vs* displacement curves, represents the force applied to the adhesively bonded joints (Al-Al) were pulled apart until failure, thereby providing the maximum shear force, (b) Lap shear adhesion strength was calculated by dividing maximum shear load or force (N) per gluing and/or adhesive bonded surface area (mm^2), (c) The highest performing mussel-mimetic adhesive ($PHU4_{3.9\ mol\%\text{-}DOP}$, 24.1 MPa for Al) evaluated for similar substrates (thus, low energy plastics to high energy metal substrates), (d) The adhesion strength comparison of adherently bonded similar substrates, (e) The effect of dissimilar attachment of substrates on shear loading by using highest performing PHU4-adhesive and (f) The adhesion strength correlation between the adherently bonded dissimilar substrates.

In most cases, we noticed a mixture of failure modes (cohesive-C.F.-/adhesive-A.F.-failure modes) in adhered joints. For PE, an adhesive failure is always noted, indicating a low interaction between the hydrophilic glue and the hydrophobic substrate, although the adhesive performances are more than satisfactory. The failure pattern of adhesively bonded joints is summarized in Table 2 and schematically presented in Fig. S2.

The most performant formulation (PHU4) was also tested for affixing dissimilar substrates (Al-W, Al-SS, Al-PE, Al-Gl, SS-PE…etc, Fig. 5e-f, Table 2). PHU4 is highly efficient to glue wood to metals (either to Al and SS) with a remarkable adhesion strength of 25 MPa for Al-W and of 23.8 MPa for SS-W. High adhesive performances are also noted for Al-SS (21.1 MPa). Although slightly lower, the lap shear strengths remained high when PHU4 was used to assemble plexiglass to wood (18.2 MPa), to Al (18.2 MPa) or to SS (16.3 MPa). Importantly, this glue is also efficient to glue the hydrophobic plastic (PE) to the different substrates with lap shear strengths of 13.3 MPa for Al, 10.9 MPa for SS, 8.3 MPa for W and 6.7 MPa for Gl.

Table 2. Adhesion of highest performing mussel-mimetic PHU4 adhesive binding efficiency for various substrates (low energy plastics-to-high energy metals)

Similar joints	LSS (MPa)	Failure mode	Dissimilar joints	LSS (MPa)	Failure mode	Dissimilar joints	LSS (MPa)	Failure mode
W-W	28.2 ± 1.7	C.F/S.F	Al-W	25.0 ± 1.6	C.F/S.F	SS-Gl	16.3 ± 1.1	C.F
Al-Al	24.1 ± 1.7	C.F	Al-SS	21.1 ± 1.1	C.F	SS-PE	10.9 ± 1.2	A.F
SS-SS	22.1 ± 0.9	C.F/A.F	Al-Gl	18.2 ± 1.0	C.F/A.F	W-Gl	18.7 ± 1.9	C.F/A.F
Gl-Gl	17.9 ± 1.3	C.F/A.F	Al-PE	13.3 ± 1.3	A.F	W-PE	8.3 ± 2.3	A.F
PE-PE	4.76 ± 2.5	A.F	SS-W	23.8 ± 1.6	C.F/S.F	Gl-PE	6.7 ± 0.8	A.F

Aluminum (Al), stainless steel (SS), wood (W), polyethylene (PE) and plexiglass (Gl). Amount of adhesive, curing (time and temperature) and experimental conditions (Force-10, 000 N and displacement rate-2 mm min^{-1}) are held constant. Failure modes: [LSS: Lap shear strength, C.F: Cohesive failure, A.F: Adhesive failure, and S.F: Substrate failure].

Iv.4.7 Benchmarking

Finally, the high shear bonding strength of catechol-bearing-PHU thermoset adhesive (PHU4) was benchmarked against commercial (Teromix-6700 and Araldite®2000), petrochemically-based (PHU (M-1),[35] PHU-5C)[32] and bio-based (PHU-H3)[33] polyurethane adhesives (Fig. 6). The processing conditions were held constant for fair comparison. The results are shown in Fig. 6. When cured at 25 °C, the commercial PU adhesives present the best adhesion performance with lap shear strength values up to 21.7 MPa for Araldite®2000 and up to 12.5 MPa for Teromix-6700, whereas PHU adhesives are characterized by a low shear strength (PHU(M-1),[35] PHU-5C,[32] PHU-H3[33] and PHU4: 1.9, 3.3, 2.2 and 3.6 MPa, respectively). The low adhesive performances of PHUs is the result of the slow aminolysis of the cyclic carbonates at room temperature (and thus uncomplete curing), compared to the fast isocyanate/alcohol reaction observed for the conventional PUs. In contrast, our mussel-mimetic PHU adhesives compete the performance of universal commercial-PUs when cured at 100 °C for 18h with a remarkable lap shear strength of 24.1 MPa. These performances surpass those of the state-of-the art PHUs,[32,33,35] even those that have been reinforced by ZnO nanofillers. This benchmarking study clearly highlights that well-designed PHU adhesives are realistic alternatives to commercial PU adhesives, provided that hot curing is permitted.

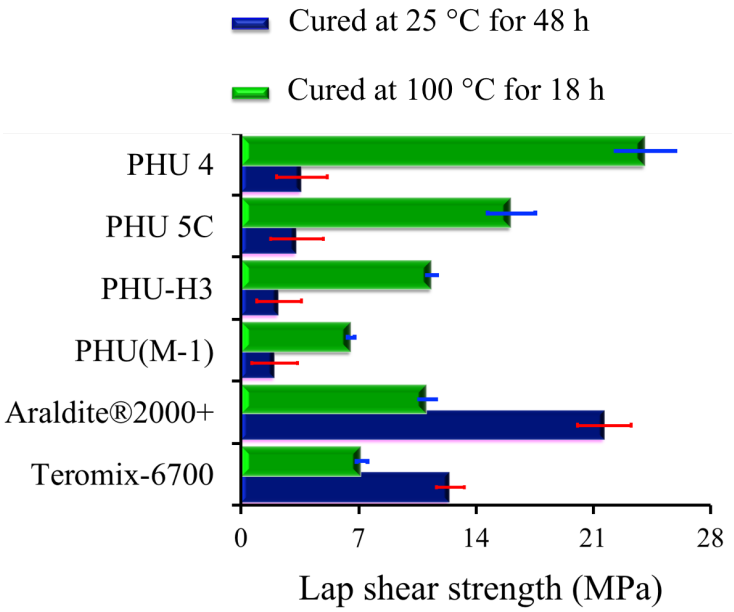

Fig. 6 Highest performing mussel-mimetic PHU thermoset adhesive (PHU4) benchmarked against commercial PU and reported PHU adhesives were evaluated for aluminum substrate.

IV.5 CONCLUSIONS

Novel mussel-mimetic polyhydroxyurethane (PHU) thermoset adhesives were prepared by the solvent-free polyaddition of a tricyclic carbonate (TMPTC), a diamine (HMDA) and dopamine (DOP). We have systematically studied the influence of DOP content on the formulation performances such as the crosslinking, thermomechanical and adhesion properties. We found that the incorporation of only 3.9 mol% DOP to the PHU formulation strongly increased the young's modulus by 233%, and the ultimate tensile strength by 196%, providing a PHU with unprecedented adhesion performances. Indeed, an impressive adhesion strength of 28.2 MPa was noted for wood, and remarkable shear adhesion strengths were measured for metal substrates with values as high as 24.1 MPa for aluminum, 22.1 MPa for stainless steel, but also for organic glass such as plexiglass (17.9 MPa). Importantly, this formulation was also able to efficiently glue substrates of different nature, such as a hydrophobic plastic (polyethylene) with metals (SS or Al), wood or plexiglass. The adhesion performances of our product surpass those of PHU that do not contain the catechol groups. A benchmarking study has demonstrated that the catechol-bearing PHU glues are competing with the adhesion performances of commercial PU glues (Teromix-6700 and Araldite®2000 plus), at least when a thermal curing is implemented to overcome the low reactivity of cyclic carbonate with amines. The valorization of CO_2 in the preparation of the tricyclic carbonate (one of the main component of the formulation), the solvent-free process that does not lead to any release of side products during curing, and the use of dopamine that can be produced from tyrosine[68–70] or phenylalanine[71] amino acids benefit the environment and align with principles of Green Chemistry.[72,73] Current efforts are now dealing with the optimization of the formulations to enable curing at room temperature, and with the use of all bio-sourced products.

IV.6 REFERENCES

1 H. G. Schmelzer, *J. Coat. Fabr.*, 1988, **17**, 167–182.

2 S. J. Shaw, *Polym. Int.*, 1996, **41**, 193–207.

3 A. S. Nasar, G. Srinivasan, R. Mohan and G. Radhakrishnan, *J. Adhes.*, 1998, **68**, 21–29.

4 A. Baldan, *J. Mater. Sci.*, 2004, **39**, 4729–4797.

5 D. J. Zalucha and K. J. Abbey, *The Chemistry of Structural Adhesives: Epoxy, Urethane, and Acrylic Adhesives*, Springer US, 2007.

6 P. Stoyanov, N. Rodriguez, T. Dickinson, D. Huy Nguyen, E. Park, J. Foyos, V. Hernandez, J. Ogren, M. Berg and O. S. Es-Said, *J. Mater. Eng. Perform.*, 2008, **17**, 460–464.

7 F. Awaja, M. Gilbert, G. Kelly, B. Fox and P. J. Pigram, *Prog. Polym. Sci.*, 2009, **34**, 948–968.

8 I. V Kochurov and N. V Gubskaya, *Polym. Sci. Ser. D*, 2011, **4**, 292–294.

9 B. H. Edwards, in *Structural Adhesives*, Springer US, 1986, pp. 181–215.

10 H.-W. Engels, H.-G. Pirkl, R. Albers, R. W. Albach, J. Krause, A. Hoffmann, H. Casselmann and J. Dormish, *Angew. Chemie Int. Ed.*, 2013, **52**, 9422–9441.

11 M. R. Patel, J. M. Shukla, N. K. Patel and K. H. Patel, *Mater. Res.*, 2009, **12**, 385–393.

12 N. Muhammad Zain, S. H. Ahmad, N. A. Ahad and E. S. Ali, *Adv. Mater. Res.*, 2014, **879**, 119–127.

13 J. Weiss, M. Voigt, C. Kunze, J. E. H. Sánchez, W. Possart and G. Grundmeier, *Int. J. Adhes. Adhes.*, 2016, **70**, 167–175.

14 N. M. Zain, S. H. Ahmad and E. S. Ali, *J. Appl. Polym. Sci.*, 2014, **131**, 41151–41159.

15 D. K. Chattopadhyay and K. V. S. N. Raju, *Prog. Polym. Sci.*, 2007, **32**, 352–418.

16 E. Delebecq, J.-P. Pascault, B. Boutevin and F. Ganachaud, *Chem. Rev.*, 2013, **113**, 80–118.

17 O. Kreye, H. Mutlu and M. a. R. Meier, *Green Chem.*, 2013, **15**, 1431–1455.

18 X. Liu, J. Hao and S. Gaan, *RSC Adv.*, 2016, **6**, 74742–74756.

19 H. Tomita, F. Sanda and T. Endo, *J. Polym. Sci. Part A Polym. Chem.*, 2001, **39**, 851–859.

20 H. Tomita, F. Sanda and T. Endo, *J. Polym. Sci. Part A Polym. Chem.*, 2001, **39**, 3678–3685.

21 M. S. Kathalewar, P. B. Joshi, A. S. Sabnis and V. C. Malshe, *RSC Adv.*, 2013, **3**, 4110–4129.

22 B. Grignard, J.-M. Thomassin, S. Gennen, L. Poussard, L. Bonnaud, J.-M. Raquez, P. Dubois, M.-P. Tran, C. B. Park, C. Jerome and C. Detrembleur, *Green Chem.*, 2016, **18**, 2206–2215.

23 L. Poussard, J. Mariage, B. Grignard, C. Detrembleur, C. Jérôme, C. Calberg, B. Heinrichs, J. De Winter, P. Gerbaux, J.-M. Raquez, L. Bonnaud and P. Dubois, *Macromolecules*, 2016, **49**, 2162–2171.

24 S. Gennen, B. Grignard, J.-M. Thomassin, B. Gilbert, B. Vertruyen, C. Jerome and C. Detrembleur, *Eur. Polym. J.*, 2016, **84**, 849–862.

25 O. Figovsky, A. Leykin and L. Shapovalov, *Altern. Energy Ecol.*, 2016, **4**, 95–108.

26 Z. Wang, X. Zhang, L. Zhang, T. Tan and H. Fong, *ACS Sustain. Chem. Eng.*, 2016, **4**, 2762–2770.

27 R. Ménard, S. Caillol and F. Allais, *ACS Sustain. Chem. Eng.*, 2017, **5**, 1446–1456.

28 V. Schimpf, B. S. Ritter, P. Weis, K. Parison and R. Mülhaupt, *Macromolecules*, 2017, **50**, 944–955.

29 R. Jaratrotkamjorn, A. Nourry, P. Pasetto, E. Choppé, W. Panwiriyarat, V. Tanrattanakul and J.-F. Pilard, *J. Appl. Polym. Sci.*, 2017, **134**, 45427–45439.

30 M. Janvier, P.-H. Ducrot and F. Allais, *ACS Sustain. Chem. Eng.*, 2017, **5**, 8648–8656.

31 A. Cornille, R. Auvergne, O. Figovsky, B. Boutevin and S. Caillol, *Eur. Polym. J.*, 2017, **87**, 535–552.

32 S. Panchireddy, J.-M. Thomassin, B. Grignard, C. Damblon, A. Tatton, C. Jerome and C. Detrembleur, *Polym. Chem.*, 2017, **8**, 5897–5909.

33 S. Panchireddy, B. Grignard, J.-M. Thomassin, C. Jerome and C. Detrembleur, *Polym. Chem.*, 2018, **9**, 2650–2659.

34 E. K. Leitsch, W. H. Heath and J. M. Torkelson, *Int. J. Adhes. Adhes.*, 2016, **64**, 1–8.

35 A. Cornille, G. Michaud, F. Simon, S. Fouquay, R. Auvergne, B. Boutevin and S. Caillol, *Eur. Polym. J.*, 2016, **84**, 404–420.

36 K. M. F. Rossi de Aguiar, E. P. Ferreira-Neto, S. Blunk, J. F. Schneider, C. A. Picon, C. M. Lepienski, K. Rischka and U. P. Rodrigues-Filho, *RSC Adv.*, 2016, **6**, 19160–19172.

37 K. M. F. Rossi de Aguiar, U. Specht, J. F. Maass, D. Salz, C. A. Picon, P.-L. M. Noeske, K. Rischka and U. P. Rodrigues-Filho, *RSC Adv.*, 2016, **6**, 47203–47211.

38 D. R. Dreyer, D. J. Miller, B. D. Freeman, D. R. Paul and C. W. Bielawski, *Chem. Sci.*, 2013, **4**, 3796–3802.

39 E. Faure, C. Falentin-Daudré, C. Jérôme, J. Lyskawa, D. Fournier, P. Woisel and C. Detrembleur, *Prog. Polym. Sci.*, 2013, **38**, 236–270.

40 H. Hu, J. C. Dyke, B. A. Bowman, C.-C. Ko and W. You, *Langmuir*, 2016, **32**, 9873–9882.

41 J. Sedó, J. Saiz-Poseu, F. Busqué and D. Ruiz-Molina, *Adv. Mater.*, 2013, **25**, 653–701.

42 T. L. Coombs and P. J. Keller, *Aquat. Toxicol.*, 1981, **1**, 291–300.

43 J. L. Dalsin, B. Hu, B. P. Lee and P. B. Messersmith, *J. Am. Chem. Soc.*, 2003, **125**, 4253–4258.

44 J. L. Dalsin, L. Lin, S. Tosatti, J. Vörös, M. Textor and P. B. Messersmith, *Langmuir*, 2005,

21, 640–646.

45 G. P. Maier and A. Butler, *JBIC J. Biol. Inorg. Chem.*, 2017, **22**, 739–749.

46 T. G. Barclay, H. M. Hegab, S. R. Clarke and M. Ginic-Markovic, *Adv. Mater. Interfaces*, 2017, **4**, 1601192–1601230.

47 S. Kim, J.-M. Moon, J. S. Choi, W. K. Cho and S. M. Kang, *Adv. Funct. Mater.*, 2016, **26**, 4099–4105.

48 N. Patil, C. Jérôme and C. Detrembleur, *Prog. Polym. Sci.*, 2018, **82**, 34–91.

49 X. Fan, L. Lin, J. L. Dalsin and P. B. Messersmith, *J. Am. Chem. Soc.*, 2005, **127**, 15843–15847.

50 J. Kuang and P. B. Messersmith, *Langmuir*, 2012, **28**, 7258–7266.

51 C. E. Brubaker and P. B. Messersmith, *Langmuir*, 2012, **28**, 2200–2205.

52 H. Lee, S. M. Dellatore, W. M. Miller and P. B. Messersmith, *Science (80-.).*, 2007, **318**, 426–430.

53 N. Holten-Andersen, A. Jaishankar, M. J. Harrington, D. E. Fullenkamp, G. DiMarco, L. He, G. H. McKinley, P. B. Messersmith and K. Y. C. Lee, *J. Mater. Chem. B*, 2014, **2**, 2467–2472.

54 Q. Wei, T. Becherer, P.-L. M. Noeske, I. Grunwald and R. Haag, *Adv. Mater.*, 2014, **26**, 2688–2693.

55 J. H. Ryu, P. B. Messersmith and H. Lee, *ACS Appl. Mater. Interfaces*, 2018, **10**, 7523–7540.

56 T. Naresh Kumar, S. Sivabalan, N. Chandrasekaran and K. L. Phani, *Chem. Commun.*, 2015, **51**, 1922–1925.

57 E. Pardieu, N. T. T. Chau, T. Dintzer, T. Romero, D. Favier, T. Roland, D. Edouard, L. Jierry and V. Ritleng, *Chem. Commun.*, 2016, **52**, 4691–4693.

58 J. H. Cho, V. Vasagar, K. Shanmuganathan, A. R. Jones, S. Nazarenko and C. J. Ellison, *Chem. Mater.*, 2015, **27**, 6784–6790.

59 S. L. Phua, L. Yang, S. Huang, G. Ding, R. Zhou, J. H. Lew, S. K. Lau, X. Yuan and X. Lu, *Eur. Polym. J.*, 2014, **57**, 11–21.

60 S. L. Phua, L. Yang, C. L. Toh, S. Huang, Z. Tsakadze, S. K. Lau, Y. Mai and X. Lu, *ACS Appl. Mater. Interfaces*, 2012, **4**, 4571–4578.

61 L. Q. Xu, D. Pranantyo, K.-G. Neoh, E.-T. Kang, S. L.-M. Teo and G. D. Fu, *Polym. Chem.*, 2016, **7**, 493–501.

62 P. SUN, L. TIAN, Z. ZHENG and X. WANG, *Acta Polym. Sin.*, 2009, **009**, 803–808.

63 S. Gennen, M. Alves, R. Méreau, T. Tassaing, B. Gilbert, C. Detrembleur, C. Jerome and B. Grignard, *ChemSusChem*, 2015, **8**, 1845–1849.

64 M. Alves, B. Grignard, S. Gennen, C. Detrembleur, C. Jerome and T. Tassaing, *RSC Adv.*,

2015, **5**, 53629–53636.

65 M. Alves, B. Grignard, S. Gennen, R. Mereau, C. Detrembleur, C. Jerome and T. Tassaing, *Catal. Sci. Technol.*, 2015, **5**, 4636–4643.

66 M. Alves, R. Mereau, B. Grignard, C. Detrembleur, C. Jerome and T. Tassaing, *RSC Adv.*, 2016, **6**, 36327–36335.

67 S. Gennen, B. Grignard, T. Tassaing, C. Jérôme and C. Detrembleur, *Angew. Chemie Int. Ed.*, 2017, **56**, 10394–10398.

68 I. R. Katz, D. Smith and M. H. Makman, *Brain Res.*, 1983, **264**, 173–177.

69 S. C. Daubner, T. Le and S. Wang, *Arch. Biochem. Biophys.*, 2011, **508**, 1–12.

70 K. Min, D.-H. Park and Y. J. Yoo, *J. Biotechnol.*, 2010, **146**, 40–44.

71 G. F. Murphy and T. L. Sourkes, *Arch. Biochem. Biophys.*, 1961, **93**, 338–343.

72 H. J. Cha, D. S. Hwang and S. Lim, *Biotechnol. J.*, 2008, **3**, 631–638.

73 J. H. Waite, *J. Exp. Biol.*, 2017, **220**, 517–530.

IV.7 SUPPORTING INFORMATION

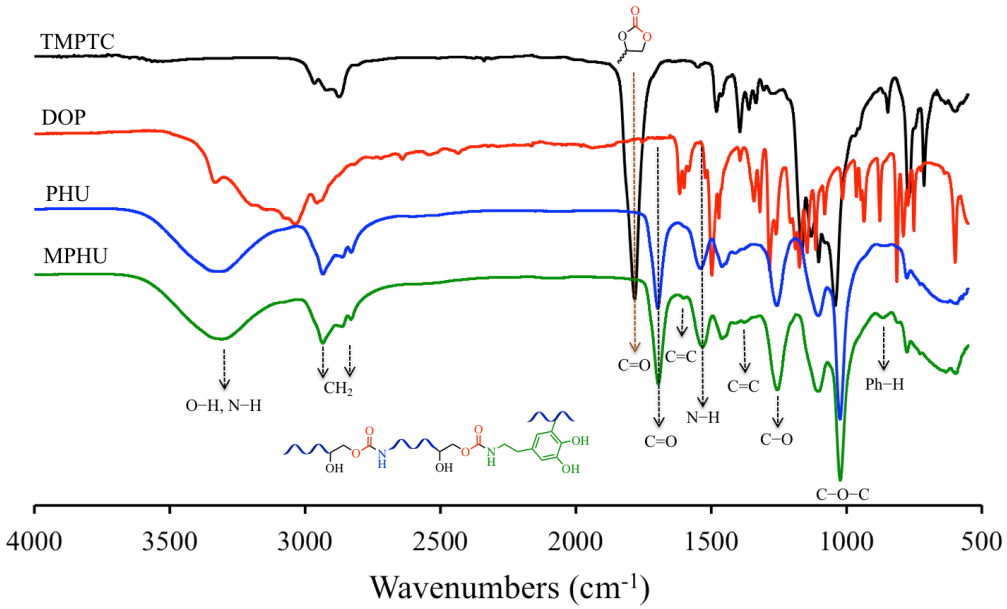

Fig. S1 FTIR spectra of TMPTC, dopamine, neat PHU and mussel-mimetic PHU.

Table S1. Summary of rheology results

Formulation	Gel time (min)	G′ (kPa) at 40 min	Tan δ at 40 min
PHU1	3.21	123.2	0.058
PHU4	3.55	87.4	0.015
PHU6	10.2	26.7	0.399
PHU8	29.8	8.5	0.727

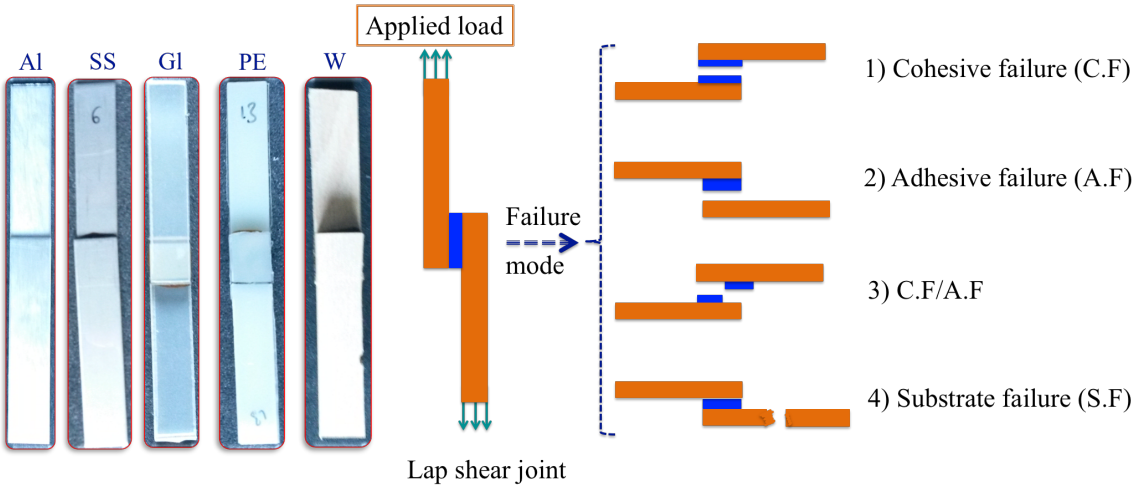

Fig. S2 Photographic images of affixed numerous substrates (thus, Al-Aluminum, SS-Stainless steel, Gl-Plexiglass, PE-Polyethylene and W-Wood) by bio-mimetic polyhydroxyurethane adhesives. Schematic representation of applied shear load to the adhesively bonded joints and their failure pattern.

General conclusions and future Research

General Conclusions and Future Research

Much progress has been made in academic research on the synthesis of polyhydroxyurethanes (PHU), enabling the replacement of conventional polyurethanes (PU) in various applications as an answer to the increasing stringency of toxicity regulations. In addition, PHU is triggering enormous interest for the design of novel adhesives and coatings due to their ability to bind to numerous surfaces from low energy plastics to high energy metals, thanks to the pendant hydroxyl groups along the polymer chains. Nevertheless, several challenges are still remaining that include the development of new methods and the efficient production of novel sustainable PHU-thermoset, notably to improve the molar masses limited by the low reactivity of aminolysis of cyclic carbonates. The appearance of air bubbles due to excess of CO_2 solubilized in the cyclic carbonates, the delamination due to high-water uptake of coatings and adhesives are also limitations to the end-use applications, and is an issue for industrialization. It should be noted that the complete elimination of bubbles is practically impossible without a thermal treatment of the cyclic carbonates. Nowadays, the judicious exploitation of the well-designed high-performance PHU adhesives and coatings starts to appear in the literature.

The design of the PHUs in this thesis was driven by the current trends in the global market, and target to tackle multiple challenges including sustainability, non-hazardous, non-volatile compounds, adhesion to multiple substrates, high performance under extreme conditions, durability, cost-effective to compete with commercial materials. Therefore, this thesis was devoted to meet industrial demand *via* the design and implementation of highly efficient sustainable formulations in a green approach, i.e. by transformation of CO_2 and biosourced compounds into PHU in the absence of solvent and catalyst. In this thesis also considerable efforts have been made to improve the performance and extend the application of the materials by designing sustainable PHU nanocomposites.

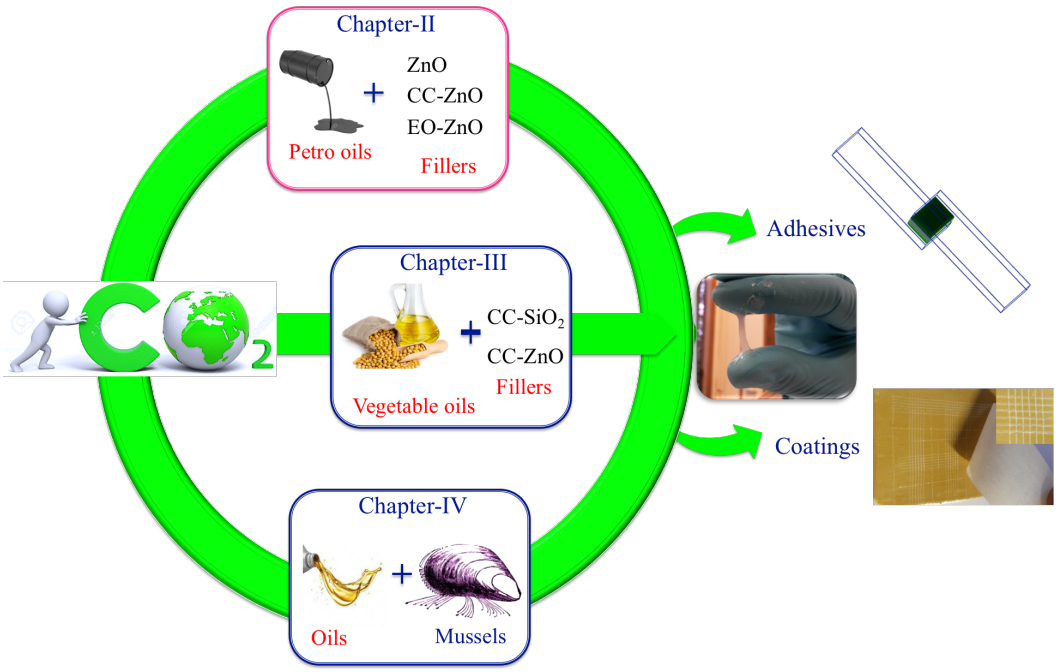

Figure 1. Schematic representation of transformation of CO_2 into natural resources to produce sustainable adhesives and coatings.

Figure 1 summarizes the three main strategies followed in this work whom results are reported and discussed in detailed in the previous chapters II to IV. Briefly, in **chapter II,** eco-friendly adhesives which allows binding especially aluminum surfaces from low–to–high adhesion strength have been targeted. To achieve this, we designed novel reinforced PHU thermosets as an alternative to toxic polyurethanes commonly used in aerospace and automotive industries. The use of ZnO fillers, modified or not, to reinforced the PHU has been investigated so as its impact on the adhesive properties of the PHU coatings. By this strategy, we could prevent delamination of coatings which is often a limitation of such PHU material. In addition, we could solve the problem of appearance of air bubbles and defects in the coating originating from CO_2 solubilisation in the formulation. By following our optimized processing conditions, novel cost-effective high performance adhesives produced *via* consumption of petroleum waste oils and CO_2 in the absence of solvent-/catalyst, were obtained as valuable alternative products for the market.

In **chapter III,** our intention was to produce bio-adhesives in order to improve the sustainability as an answer to the current and future trends of the chemical engineering industries. Therefore, vegetable oils, rather than petro based oils, have been used as starting materials for the synthesis of PHU. To reach high performance adhesives, we reinforced them

by various fillers in the light of the results of the previous chapter. So, two-component formulations were optimized and processed without hazardous or toxic solvent emission, to reach high-performance bio-PHU-adhesives, bonding in both dry and wet environments, resistant to chemicals, heat and high load.

In **Chapter IV**, we aimed to design PHU adhesive able to bind to numerous substrates, i.e. from plastics to metals. Therefore, we designed PHU bearing catechol moieties prone to promote adhesion in mussels glue. Mimicking nature, PHU adhesives containing dopamine have been synthesized and the effect of their content on the coating cohesive strength, crosslinking, thermomechanical properties, and adhesion to numerous substrates was investigated. The developed fully-biobased adhesives and the easy method to produce them are beyond the state-of-the-art and leads to adhesives that can compete with trends in the market. These adhesives are especially eco-friendly (non-hazardous and catalyst/solvent-free) withstand high load (10 mg of adhesive can withstand 15 kg weight) and exhibit prolong stability under water for diversified substrates, i.e. plastics, glass, plexiglass, wood, aluminum and stainless-steel. They can find applications in packaging, pharmaceutical, automotive, aerospace, consumer goods etc.

Overall, this thesis successfully achieved the goal of current challenges in the global market by the design and implementation of novel sustainable thermoset PHU adhesives. The produced crosslinked PHU adhesives were characterised by an adhesion strength up to 24.1 MPa on aluminum and up to 28.2 MPa on wood substrates and coatings adhesion of 5B (0% area removed from coated surfaces). Moreover, the benchmarking study illustrates that the well-designed PHU adhesives have the ability to compete even surpass the performances of commercial polyurethane adhesives such as Teromix-6700 and Araldite®2000 (Figure 2). Nevertheless, additional efforts are required to push this concept even further in order to develop even more sustainable process and to fasten the curing.

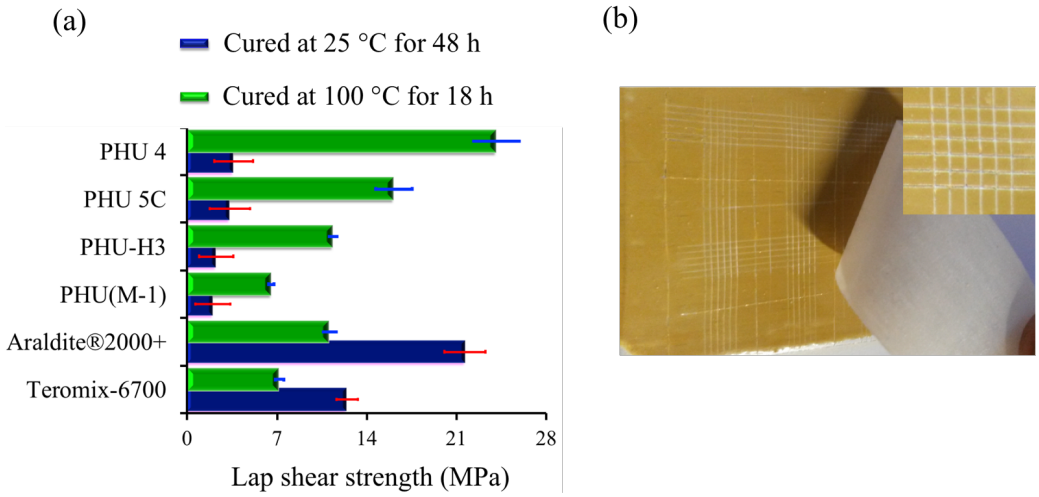

Figure 2. (a) Benchmarking of polyhydroxyurethane adhesives [PHU(M-1): TMPTC/EDR-148, PHU5C: TMPTC/HMDA/PDMS/CC-ZnO), PHU-H3: CSBO/HMDA/CC-ZnO) and PHU 4: TMPTC/HMDA/DOP] against conventional polyurethane adhesives and (b) Cross-cut adhesion strength of coatings (5B; 0% area of squares removed from coated surfaces)

FUTURE RESEARCH.

What is clear from our research is that PHUs are capable to bind to quite dissimilar substrates. The load bearing properties and strength of the materials can be improved by modifying formulations with functional fillers. However, the role of fillers (SiO_2 and/or ZnO) in formulation crosslinking and mechanism is not clear and further research should be perform to address better their roles.

In the future, PHUs able to be cured at ambient temperature should be developed, for example by using activated cyclocarbonates exhibiting a faster reaction towards aminolysis.

Besides, due to the high water-uptake of PHU networks, the adhesion strength under water remains a weakness. Therefore, the concept of developing superhydrophobic coatings should be exploited further with PHUs.

If the hydroxy groups of PHUs appear favourable towards adhesion, the mechanism of adhesion and failure pattern of adhesive joints is not fully understood and remains to be addressed.

Our research efforts illustrate that vegetable oil based PHU thermoset composite adhesives offer green materials reducing VOC, cost-effective, scalable and are attractive alternatives to petroleum-based adhesives. Fully bio-based PHU in a green approach and establishing recycling process still remains challenging. Moreover, this work provides new insights into the reduction of environmental impact by transforming CO_2 into profitable sustainable materials as adhesives. Future research will continue to produce adhesives and coatings from fully renewable feedstocks that could replace conventional materials in the global market. However, scalable and industrialization of PHUs still remain an issue up to date.